CONTRIBUTIONS TO
GUIDED WAVE THEORY

A thesis presented for the degree of
Doctor of Philosophy
in Electrical Engineering,
in the University of Canterbury,
Christchurch, New Zealand,

by

Ng Fook Loy, B.E.(Hons.)

1972

ACKNOWLEDGEMENTS

I am especially indebted to my supervisor, Mr R.H.T. Bates, for his guidance, encouragement and interest throughout this research.

I am grateful to Heng, my wife, for her patience and understanding.

I thank the External Aid Division, Ministry of Foreign Affairs, New Zealand, for the award of a Colombo Plan Scholarship.

GLOSSARY

Symbols, notations and abbreviations

The number in brackets indicates the chapter where the symbol as defined is first used. Some of the symbols listed here (and others not listed) are also used to represent other quantities and are defined at the appropriate places in the text.

$\vec{A}$	magnetic vector potential (1)
$A_{mn}(k)$	elements of determinant in null field method (2)
$\vec{B}$	magnetic flux density (1)
c	speed of light in vacuo (4)
C	cross-section of waveguide (1)
$C_{\ell m}$	continuous curve which lies in $\Lambda_\ell \cap \Lambda_m \cap \Omega_-$ (3)
$d_{mn}(k)$	elements of determinant in point-matching methods (3)
$\vec{D}$	electric flux density (1)
exp	exponential function (1)
eqn	equation
$\vec{E}$	electric field intensity (1)
$\vec{f}$	general field = $\begin{bmatrix} \vec{E} \\ \vec{H} \end{bmatrix}$ (4)
$\vec{f}_0$	incident field (4)
$\vec{f}_p$	reradiated field (4)
$\vec{f}_d$	field radiated from polarization sources in v_d (4)
$\vec{f}_\sigma$	field radiated from polarization sources on σ (4)

$\vec{f}_s$	field radiated by charges and currents on s (4)
F	z-component of surface current density (1)
G	component of surface current density directed along C (1)
$\vec{H}$	magnetic field intensity (1)
$H_\nu^{(2)}(z)$	Hankel function of second kind of order ν and argument z (1)
j	$j^2 = -1$ (1)
$\vec{J}$	electric current density (1)
$J_\nu(z)$	Bessel function of first kind of order ν and argument z (1)
k	free space propagation constant, cutoff wave-number (1)
$\vec{K}$	surface current density (1)
$K_1(x)$	modified Bessel function of order 1 and argument x (6)
L	differential operator (1); total length of curve C (2)
M	order of determinant (2)
n	outward normal to contour C (1); refractive index of dielectric, $n^2 = \varepsilon_r$ (7)
O	origin of coordinates (1)
P	arbitrary point in space (1); Poynting vector (6)
q	electric charge density (1)
q_s	surface charge density (1)
Q	point on waveguide wall (1)
r	largest circle centred at O which is enclosed by C (3)

r_+ smallest circle centred at O which encloses C (3)

r_0 radius of convergence of R.H.S. of eqn (3.4) (3)

R distance between points P and Q (1); radius of azimuthal guiding surface (6)

$R_{p,\nu}$ Lommel polynomial (6)

s surface of perfect conductor (4)

S waveguide region enclosed by C (1); point either on or outside C where R.H.S. of eqn (3.4) ceases to be analytic (3)

T arbitrary point in v_p(4); trapping factor (7)

T_1 centre of curvature for an arc of C (3)

U scalar potential function satisfying the Helmholtz equation (1)

$\bar{U}$ trial function in variational method (1)

v all space (4)

v_0 space containing $\vec{f}_0$ (4)

v_d space containing media which is well behaved (4)

v_p space containing polarization sources (4)

V scalar potential (1)

$\vec{w}$ polarization source density (4)

W thickness of dielectric coating (7)

$Y_n(z)$ Bessel function of second kind (2)

$Z_{\ell,q}$ members of a set of functions (3)

$Z_\mu(\mathcal{C},\mathcal{D},\alpha)$ see eqn (5.9) (5)

α angle between radius vector and outward normal at a point Q on C (1)

β exterior angle of sharp corner of sector waveguide (2)

γ constitutive parameter of medium, ε or μ (4)

Γ_ℓ curve in Λ_ℓ (3)

$\Gamma(\nu)$ Gamma function (7)

$\delta(x)$ Dirac delta function (1)

ε permittivity (1)

ε_r relative dielectric constant (4)

ζ refractive index, $\zeta^2 = \varepsilon_r$ (5); surface impedance = $(\xi + j\eta)$ (6)

ζ_0 intrinsic impedance of free space (6)

η interior angle of sharp corner of sector waveguide (2)

$\vec{\eta}$ polarization source density of abrupt surfaces

λ wavelength (1)

Λ square matrix, $\vec{\eta} = \Lambda\vec{f}$ (4)

Λ_ℓ ℓ^{th} region in EPM (3)

μ permeability (1)

ν outward normal to surface (4); propagation constant = $(\beta - j\alpha)R$ (6)

$\vec{E}$ $= \vec{f}_d + \vec{f}_\sigma + \vec{f}_s = \vec{f}_p$ (4)

σ abrupt boundary between two media (4); conductivity (6)

ϕ included angle of any sharp corner possessed by C (3)

Φ_n members of a set of functions

Ψ arbitrary point on σ

ω	angular frequency
Ω	all space in xy-plan (3); square matrix $\vec{w} = \Omega\vec{f}$ (4)
Ω_-	space interior to C (3)
Ω_+	space exterior to C (3)
$\mathcal{A}$	$\{z_{\ell,q}\}$ is of the class $\mathcal{A}$ if all its members satisfy the appropriate boundary condition on a curve Γ_ℓ (3)
$\mathcal{L}$, $\overline{\mathcal{L}}$	if $\Gamma_\ell \not\subset C$ but $\Gamma_\ell \cap C \neq 0$ then Γ_ℓ belong to the class $\mathcal{L}$ if there are no extra constraints on the wavefunction, and to $\overline{\mathcal{L}}$ if there are (3)
$\cup$	union of sets (3)
$\cap$	intersection of sets (3)
Δ	small spatial interval (4)
∇	vector gradient operator (1)
∇_t^2	transverse Laplacian operator (1)
$\hat{x}$	unit vector in x-direction (4)
$\dot{X}$	time derivative of X, $\partial X/\partial t$ (1)
$\vec{X}$	vector of magnitude X (1)
$\nabla\times$	vector curl operator (1)
$\nabla\cdot$	vector divergence operator
(x,y,z)	Cartesian coordinates (1)
(r,θ,z) (ρ,φ,z) (τ,ϕ,z)	cylindrical polar coordinates (1,3)
(r_n,θ_n)	polar coordinates of matching point on C (1)

APM	Alternative point-matching method (1)
CPM	Complete point-matching method (1)
EPM	Extended point-matching method (1)
IRH	Internal Rayleigh hypothesis (3)
RHS	Right hand side (1)
SPM	Straightforward point-matching method (1)

TABLE OF CONTENTS

PREFACE

There are many forms of structure for the guiding of electromagnetic waves. A review of these forms is given by Barlow (1964). He describes the well established parallel-wire and coaxial lines, and hollow uniform waveguides. He also considers waveguides containing solid materials and gaseous plasmas, and beam and surface waveguides.

This thesis is a report on investigations into the numerical computations of the propagation characteristics of three types of guiding structures namely, the hollow waveguide, dielectric loaded waveguide and the dielectric clad azimuthal surface waveguide.

The numerical solution of the hollow waveguide problem is considered in Part 1. Chapter 1 contains a comprehensive review of the methods used for the solution of the waveguide problem. This complements the only presently available review, given by Davies (1972) who compares and discusses the relative merits of some current methods (finite difference, finite element, point-matching, integral formulations and conformal transformation). Some useful criteria established by Davies in his review for the comparison of methods are used in Chap. 1 (Sec. 1.3).

Chapter 2 is concerned with the numerical solution of waveguides of arbitrary cross-section by the null field method which was developed by Bates (1969b). Accurate results are obtained and it is demonstrated that for shapes possessing sharp reentrant corners, the

computational accuracy is improved by explicitly satisfying the edge conditions at these corners. The detailed numerical investigation provides the supporting evidence for the computational viability of the null field method.

The complete point-matching method is derived from the null field method and it provides an insight into the straightforward point-matching method (Bates 1969b). Chapter 3 considers point-matching methods of solution. Results obtained using the complete point-matching method show that accuracies of about 0.1% are obtainable for waveguide cross-sections which are convex. Less accurate results are obtained for cross-sections that are strongly reentrant.

The alternative point-matching method (Bates 1969b) is also briefly considered. By comparing results for a rectangular waveguide, the alternative point-matching method is shown to be more error sensitive than the complete point matching method.

When the straightforward point-matching method (Yee and Audeh 1965, 1966b; Bates 1969b) was proposed and used by Yee and Audeh for waveguide problems, doubts were raised as to its universal applicability (Harrington 1965; Bates 1967, 1969b; Millar and Bates 1970; Lewin 1970) and an example of its failure was given by Davies and Nagenthiram (1971). The detailed investigations in chapter 3 show conclusively that the straightforward point-matching method does sometimes break down and give erroneous wavefunctions. Chapter 3

also relates the applicability of the straightforward point-matching method to the validity or otherwise of an internal Rayleigh hypothesis which is introduced; and shows that the straightforward point-matching method is unlikely to produce correct results when the waveguide cross-section has reentrant parts.

An extended point-matching method is next introduced in chapter 3 and is employed to obtain accurate results for some cases for which the straightforward point-matching method fails. The success of the extended point-matching method is further illustrated by the prediction of a particular mode for the ridge waveguide (Sec. 3.5.1.4) which seems to have been missed by a previous analysis (Beaubien and Wexler 1970) using a high-order finite difference method.

Part 2 is concerned with the cutoff characteristics of dielectric loaded waveguides. A specialised form of a general polarization source formulation (Bates 1970) is given in Chapter 4 and is used in Chapter 5 to obtain formulas for the cutoff characteristics of a waveguide of arbitrary cross-section loaded with a circularly cylindrical dielectric tube. The significance of the derivation given in chapter 5 is that the unknown field in the dielectric is eliminated and formulas are obtained that are line integral equations for the surface current densities on the waveguide wall alone. The computational convenience of the formulas is illustrated by results for a square waveguide loaded with a dielectric rod. Confirmatory experimental results are also reported.

The numerical computation of the propagation of an azimuthal surface wave is presented in Part 3. In previous analyses of the azimuthal surface wave the attenuation is assumed to be small. This assumption is generally only satisfactory for very small curvatures. An investigation without such assumptions is given in Part 3. The general external field for any circular cylindrical guiding surface is considered in chapter 6 and universal tables for the surface impedance are given. These results are used in chapter 7 to obtain the accurate dependence upon curvature of the propagation characteristics of a dielectric clad circular cylindrical guiding surface.

General conclusions are drawn in Part 4 which also gives some suggestions for further research. The results of chapters 2 and 3, for the null field method and point-matching methods, are new. The formulation and results of chapter 5 (dielectric loaded waveguides) are also new, as are the derivations and results of chapters 6 and 7 (azimuthal surface wave).

All the computer programs used, except for one subroutine, were written by the author, in Fortran IV with 8-byte (64 bit) words, and run on the University of Canterbury IBM 360/44 machine which has 128 Kbytes of core memory. The Bessel functions of the first and second kind used were computed from the ascending series (Abramowitz and Stegun 1965, formulas 9.1.10 and 9.1.11). The Lommel polynomials required in Part 3 were computed using the recurrence relation given in Watson (1968, sec. 9.63) and a standard IBM subroutine (IBM System 360,

Scientific Subroutine Package 1968, p.367), modified to double precision by the author, was used to generate the modified Bessel function K_1.

The following papers, relevant to this thesis, have been produced:

Bates, R.H.T. and Ng, F.L. (1971), "Contributions to the theory of the azimuthal surface wave", Alta Frequenza, 40, 658-666.

Ng, F.L. and Bates, R.H.T. (1972), "Null field method for waveguides of arbitrary cross-section", IEEE Trans., Microwave Theory Tech., in press.

Bates, R.H.T. and Ng, F.L. (1972), "Point matching computation of transverse resonances", submitted to: Int. Jour. for Numerical Methods in Engineering.

Bates, R.H.T. and Ng, F.L. (1972), "Polarization source formulation of electromagnetism and dielectric loaded waveguides", submitted to: Proc. IEE (London).

PART 1: Characteristics of Hollow Waveguides of Arbitrary Cross-Section

CHAPTER 1: SOLUTION OF THE WAVEGUIDE PROBLEM

'.....
Of shoes - and ships - and sealing wax -
Of cabbages - and kings -
And why the sea is boiling hot -
And whether pigs have wings.'
Lewis Carroll

A survey of the various methods used for the solution of the empty waveguide problem is presented and comparisons are made between the methods. The various waveguide shapes that have been used in the literature are listed in a table for handy reference.

1.1 INTRODUCTION

Maxwell's equations provide a rigorous description of electromagnetic behaviour in nature. The equations are

$$\nabla \times \vec{E} = -\dot{\vec{B}}, \qquad \nabla \times \vec{H} = \dot{\vec{D}} + \vec{J},$$

$$\nabla \cdot \vec{D} = q, \qquad \nabla \cdot \vec{B} = 0. \tag{1.1}$$

Consider a uniform waveguide with perfectly conducting walls and which is embedded in free space. For the propagation of monochromatic electromagnetic waves inside the waveguide, Maxwell's equations (1.1) reduce to the two-dimensional Helmholtz equation (Harrington 1961, sec. 8.1):

$$(\nabla_t^2 + k^2)\, U = 0, \tag{1.2}$$

where

$$k^2 = \omega^2 \mu_0 \varepsilon_0 - k_z^2, \qquad k_z = 2\pi/\lambda_g. \tag{1.3}$$

k is the cutoff wavenumber, λ_g is the guide wavelength and ∇_t^2 is the two-dimensional Laplacian operator. The factor $\exp(j\omega t)$ is suppressed and the wave propagation is in the z-direction. At cutoff, $k_z = 0$. The scalar potential function U is E_z for E (TM) modes and H_z for H (TE) modes.

All analyses of the hollow waveguide problem are attempts at solving, exactly or approximately, the Helmholtz equation (1.2) subject to the imposed boundary conditions:

$$\text{Dirichlet:} \quad U = 0 \text{ on } C \text{ (E modes)};$$

$$\text{Neumann} : \frac{\partial U}{\partial n} = 0 \text{ on } C \text{ (H modes)}; \qquad (1.4)$$

where the waveguide cross-section is bounded by the curve C and n is the outward normal to C at any point Q on C (Fig. 1.1).

A solution of the waveguide problem for various cross-sectional shapes is important for considerations of power handling capacity, bandwidth requirements, mode stability, waveguide discontinuity analysis and manufacturing and handling facility. In addition, the waveguide problem is, in itself, a mathematical and numerical challenge.

The more tractable, straightforward waveguide shapes can be solved analytically. However, all other shapes are not amenable to exact analysis and approximate methods have to be employed. The various methods are considered in the following section.

1.2 REVIEW OF METHODS FOR SOLUTION OF THE WAVEGUIDE PROBLEM

Many techniques have been proposed and used to analyse the propagation of electromagnetic fields in waveguides. The classical method of separation of variables can only be applied to certain separable coordinate systems and recourse to approximate methods has to be made for the analysis of other shapes.

A general introduction to numerical techniques and a review of finite-difference and variational techniques for electromagnetic problems has been given by Wexler (1969). Green (1965) has discussed the finite-difference solution of field problems satisfying Laplace's equation. A review of the current numerical methods for the solution of the waveguide problem is given by Davies (1972) and he has established certain criteria as a basis for comparison of the various methods. In connection with numerical methods it should be mentioned that most matrix methods can be cast in the useful generalised moment method formalsim of Harrington (1967, 1968).

A review of the methods proposed and used for the solution of the waveguide problem is presented in this section. It is hoped that the review will complement that of Davies. Detailed consideration is given to a simply-connected region but the methods discussed apply or can be modified to apply to multiply-connected regions. The methods are described in this section and a comparison of the more important methods is given in

Section 1.3. A Table given in Section 1.4 lists the waveguide shapes that have been considered in the literature. This is provided as a handy reference of shapes that can be used for the testing of any numerical method.

1.2.1 Separation of Variables and Analytic Solutions

Where the cross-section C of a waveguide coincides with coordinate surfaces of a separable coordinate system (Morse and Feshbach 1953, sec. 5.1), the classical method of separation of variables (Harrington 1961, sec. 4.1) can be employed. The rectangular and circular - including other shapes related to the cylindrical polar coordinates, e.g. the circular with a radial baffle (Schelkunoff 1943, p.392) - waveguides have been analysed by this method. The elliptical waveguide was first studied by Chu (1938) and by several others since then (Kretzschmar 1970; Rayevskiy and Smorgonskiy 1970). In particular, more accurate numerical computations for the cutoff wavenumbers and corrections to the lowest order E-mode have been made by Kretzschmar (1970, 1971). The only other waveguide shape that is solvable by the separation of variables method is that of the parabolic waveguide. This has been considered by Zagrodzinski (1968) and Horiuchi et al. (1968).

Apart from the above waveguide shapes, a few others are amenable to exact analysis. By the introduction of trilinear coordinates, exact solutions can be found for a waveguide whose cross-section is an equilaterial

triangle (Schelkunoff 1943, sec. 10.8). The cutoff wavenumbers are given by

$$k = \frac{4\pi}{3a} (m^2 + mn + n^2)^{\frac{1}{2}}, \qquad (1.5)$$

where a is the side of the equilaterial triangle and m and n are any integers, which cannot be zero for E-modes.

The isoceles right-angled triangle shaped waveguide can also be solved exactly (Schelkunoff 1943, sec. 10.8; Morse and Feshbach 1953, pp. 753-757). An expansion which satisfies the Helmholtz equation (1.2) for this shape is made up of a combination of eigenfunctions for the square waveguide such that the combination satisfies the appropriate boundary condition (1.4) along a diagonal of the square cross-section. For example (Schelkunoff 1943, sec. 10.8), the first H-mode is given by $U = (\cos \pi x - \cos \pi y)/2$ where the (x,y) coordinates are referred to the right-angled vertex. Its cutoff wavenumber ka is 4.43, where a is the length of the longest side.

1.2.2 Variational Techniques and Functional Approximation

The function U that minimises the functional defined by (Kantorovich and Krylov 1958, sec.4.1)

$$F = \tfrac{1}{2} \iint_S [(\nabla \phi)^2 - k^2 \phi^2] ds, \qquad (1.6)$$

where S is the region enclosed by C, satisfies a Euler equation which corresponds exactly to the Helmholtz equation (1.2). The Neumann boundary condition (1.4) is satisfied automatically ("natural boundary constraint" of (1.6)) by the solution U but the Dirichlet boundary

condition (1.4) will have to be imposed on U. An equivalent problem to equation (1.6) is that of the minimisation of the functional (Forsythe and Wasow 1960, sec. 19.2)

$$\Lambda = \frac{\iint_S (\nabla\phi)^2 \, ds}{\iint_S \phi^2 \, ds} \quad . \tag{1.7}$$

Λ is called the Rayleigh quotient and equals k^2 for any physically possible solution U. The variational technique thus attempts to minimise an integral expression (1.6) or (1.7), the function that produces this minimal value being the solution of the field problem, instead of solving the Helmholtz equation (1.2) directly. The minimisation can be achieved in various ways.

1.2.2.1 Rayleigh-Ritz method

In the Rayleigh-Ritz method (Kantorovich and Krylov 1958, chap. 4; Forsythe and Wasow 1960, chap. 19) the function U is represented by a trial function

$$\bar{U} = \sum_{i=1}^{N} \alpha_i \, \Phi_i(x,y), \tag{1.8}$$

where the Φ_i are members of a set of functions and the α_i are unknown parameters to be determined. The minimisation of F or Λ is effected by setting

$$\frac{\partial F}{\partial \alpha_i} \quad \text{or} \quad \frac{\partial \Lambda}{\partial \alpha_i} = 0, \quad i = 1, N. \tag{1.9}$$

This results in a standard matrix eigenvalue problem (Davies 1972). The trial functions $\bar{U}$ that have been chosen and used in practice are described in sec. 1.2.2.3; after the Galerkin's method, which is closely related

to the Rayleigh-Ritz method, is described in the next section.

1.2.2.2 Galerkin's Method

For the Galerkin's method of solution (Kantorovich and Krylov 1958, sec. 4.2; Jones 1964, sec. 5.12) the trial function $\overline{U}$ (1.8) is again used. It has to satisfy the Helmholtz equation (1.2), thus

$$L(\overline{U}) = 0, \tag{1.10}$$

where the operator $L = (\nabla_t^2 + k^2)$. Equation (1.10) is equivalent to a requirement of orthogonality of $L(\overline{U})$ to all the functions of the system in (1.8); i.e. the N conditions of orthogonality

$$\iint_S L(\overline{U})\, \Phi_i \, ds = 0 \tag{1.11}$$

have to be satisfied. Equation (1.11) gives again the standard matrix eigenvalue problem (Davies 1972).

In general, for problems where a variational functional can be defined and solved by the Rayleigh-Ritz method (sec. 1.2.2.1), the matrix eigenvalue problem obtained from Galerkin's method (eqn (1.11)) is identical with that of the Rayleigh-Ritz method (eqn 1.9)) (Kantorovich and Krylov 1958, sec. 4.2). However, the Galerkin approach is a more general method of solution than the Rayleigh-Ritz method and can be applied to various types of differential equations without the necessity of an auxiliary variational formulation (Kantorovich and Krylov 1958, sec. 4.2).

1.2.2.3 Functional approximations

The variational technique depends on a choice for the trial function (1.8). The continuous polynomial set

$$\bar{U} = \sum_m \sum_n \alpha_{mn} x^m y^n \qquad (1.12)$$

has been chosen by Bulley and Davies (1969) for the solution of H-modes in arbitrary shaped waveguides. For E-modes the polynomial set (1.12) is modified to (Bulley 1970)

$$\bar{U} = g(x,y) \sum_m \sum_n \alpha_{mn} x^m y^n \qquad (1.13)$$

where

$$g(x,y) = 0 \text{ on } C, \qquad (1.14)$$

so that the trial function $\bar{U}$ satisfies the Dirichlet boundary condition (1.4). Equations (1.12) and (1.13) are substituted into (1.7) and the resulting matrix eigenvalue equation (1.9) is solved (Bulley and Davies 1969, Bulley 1970). A similar approach, with the trial function given by equation (1.12) simplified by taking $n \equiv 0$, was used by Valenzuela (1961) for a specific waveguide with flat top and bottom and semicircular side walls.

Thomas (1969) chooses a trial function in terms of cylindrical polar coordinates (ρ,φ),

$$\bar{U} = \sum_m \sum_n \alpha_{mn} \rho^m \cos n\varphi. \qquad (1.15)$$

E-modes are solved by incorporating the Dirichlet boundary condition (1.4) into the functional by introducing a Lagrange multiplier μ and defining an augmented

functional

$$F^* = F + \mu B(\bar{U}) \qquad (1.16)$$

which satisfies the additional boundary condition $B(\bar{U}) = 0$.

As mentioned in Sec. 1.2.2.2 the Rayleigh-Ritz and Galerkin's methods are essentially identical, and hence the method of solution adopted by Thomas (1969) is similar to that of Bulley and Davies (1969), the two methods differing only in the choice of trial functions (Davies 1972). Bulley and Davies use an expansion set in Cartesian coordinates while Thomas chooses one in polar coordinates.

It should be noted that in the above methods a complicated region can be broken into several smaller regions with corresponding piecewise polynomials. This is discussed by Bulley and Davies (1969) who state that implementation of this idea has proved to be difficult and has given only poor results.

Other sets of trial functions can be used. Harrington (1968, sec. 8.3), for example, uses a trial solution made up of pyramid expansion functions and obtains a solution by Galerkin's method. Because of the discontinuous expansion functions used this method is less accurate than that of Bulley and Davies (1969) which uses the expansion set defined by eqn (1.12).

1.2.2.4 Finite-element method

The finite-element method was first used for structural analyses in Civil Engineering (Zienkiewicz

and Cheung 1967) and was later applied to the solution of the Helmholtz equation for waveguide problems (Arlett et al. 1968; Silvester 1969a,b,c; Ahmed and Daly 1969b). The finite-element method is essentially a variational technique and again attempts to minimise the functional F (1.6). The waveguide cross-section is divided into elemental regions (usually triangular) and a set of trial functions (1.8) is defined over each region. In this case, the α_i's are taken as the unknown field values at the nodes of the elemental regions, hence the trial solution is expressed as a function of the nodal values. In the simplest case, the trial functions are chosen to be piecewise linear functions of x and y (Ahmed and Daly 1969b; Arlett et al. 1968; Silvester 1969b). This is the simple finite-element approach (Davies 1972). Higher-order polynomial approximations can be chosen to improve the convergence over the simple finite-element method. An approximation equivalent to (1.12) has been used by Silvester (1969c, d). This approach is then similar to that of Bulley and Davies (1969) and differs only in the way that the trial functions straddle the elemental regions (Wexler 1969).

The variational and finite-element techniques can be applied to general shaped waveguides and involve dense (of order 30 to 90) matrices of block diagonal form. Convergence is slower when reentrant corners exist. The main complication in programming is in the definition of the elements in data input (and in the

further subdivisions of the regions in the finite-element method). Silvester (1969a) reports an asymptotic convergence rate of M^{-2D} for a 2.25:1 rectangular waveguide where M is the matrix size and D is the order of the polynomial (anywhere from 1 to 4 in Silvester's work). In the approximation for the cross-section, higher order boundary fitting can also be employed. This is discussed by Richards and Wexler (1972) who apply the finite-element method to Poisson's equation and show that a higher order secondary fitting yields more accurate results than a method with a coarser polygonal boundary fitting.

1.2.3 Finite-Difference Method

This method solves the Helmholtz equation by defining unknown field values U_n at the vertices of a mesh erected over the waveguide cross-section. The differential operator in the Helmholtz equation (1.2) is then approximated in terms of the U_n's by the first few terms of some series expansion; e.g. a Taylor expansion is used to obtain the five-point formula at any point P

$$(\nabla_t^2 U)_P = -k^2 U_P = ((\sum_{n=1}^{4} U_n) - 4U_P)/h^2, \qquad (1.17)$$

where h is the width of the square mesh (Collins and Daly 1963).

The rate of convergence of the finite-difference method can be increased by the introduction of an "accelerating factor" β and the modification of the five-point formula (eqn (1.17)) to (Davies and Muilwyk 1966)

$$U_P = \beta \frac{U_1 + U_2 + U_3 + U_4}{4 - h^2k^2} - (\beta-1)\, U_P. \qquad (1.18)$$

When β equals 1, eqn (1.18) reduces to eqn (1.17). A discussion on the estimation of the optimum accelerating factor is given by Sinnott (1968).

The first general automatic computer algorithm employing the five-point finite-difference scheme was drawn up by Davies and Muilwyk (1966). This finite-difference scheme is essentially similar to the simple finite-element method (Davies 1972). A different algorithm employing the five-point formula is given by Steele (1968).

A disadvantage of the above finite-difference scheme is the slow convergence rate with curved boundaries. In addition, the algorithms as defined (Davies and Muilwyk 1966; Steele 1968) only yield the lowest order E and H modes. These disadvantages have been overcome by various techniques (Davies 1972). In Pontoppidan's method (1969) a higher order mode is obtained by requiring the solution to be orthogonal to all the lower order modes. Convergence rate is improved by using a first order boundary fitting. Beaubien and Wexler (1968) proposed an alternative algorithm that employs a thirteen-point finite-difference operator. This gives a resulting matrix that yields all higher-order modes (in contrast to the algorithms of Davies and Muilwyk (1966) and Steele (1968) which give only the first E and H modes). The algorithm was improved by taking unequal-arm operators (Beaubien and Wexler 1970)

so that good boundary fitting was obtained. Silvester (1970a) gives a discussion on the general discretization of biharmonic operators and shows that the thirteen-point finite-difference operator of Beaubien and Wexler's is one such particular discretized operator. Silvester (1970b) also gives an algorithm for the automatic generation of finite-difference operators. It should be noted that instead of obtaining finite-difference formulas from a discretization process, an alternative procedure is to use the variational expression (1.6) for the formulation of the finite-difference formulas (Davies 1972). This is discussed by Sinnott (1970).

The original finite-difference scheme (Davies and Muilwyk 1966) suffers from the disadvantage that only the dominant E and H modes are predicted. However, this point is overcome by the later improvements and these can be used to yield accurate results. The method of Beaubien and Wexler's is especially well documented (1968, 1970, 1971). This method however requires good "starts" for the iteration process. Finite-difference methods in general involve sparse matrices. The whole matrix therefore need not be stored and the bulk of the storage space may be used for the field values U_n at the node points. This makes it possible to define 5,000 to 20,000 node points, which represents effective matrix sizes of the same orders (Beaubien and Wexler 1968). In general, accurate results are obtained with the finite-difference method because large matrix sizes are (effectively) used.

1.2.4 Integral Operator Formulations

The $\vec{E}$ and $\vec{H}$ fields at any point can be expressed, in terms of the vector potential $\vec{A}$ and scalar potential V, as (Jones 1964, sec. 1.16)

$$\vec{E} = - j\omega\vec{A} - \nabla V \; ; \tag{1.19}$$

$$\vec{H} = (\nabla \times \vec{A})/\mu \; , \tag{1.20}$$

where $\vec{A}$ and V respectively are given by

$$\vec{A} = - j\mu_0/4 \int_C \vec{K}(C)\, H_0^{(2)}(kR)\, dC; \tag{1.21}$$

$$V = - j/(4\varepsilon_0) \int_C q_s(C)\, H_0^{(2)}(kR)\, dC. \tag{1.22}$$

$\vec{K}$ and q_s are the surface current and charge densities respectively and are related by the equation of continuity

$$\nabla \cdot \vec{K} = - j\omega q_s. \tag{1.23}$$

$H_0^{(2)}$ is the Hankel function of the second kind. R is the distance between any arbitrary point P in the xy-plane with coordinates (ρ,φ) and any point Q with coordinates (r,θ) on C (Fig. 1.1). Equations (1.19) and (1.20) are line integral equations for the surface current density and surface charge density respectively, and these integral operator formulations can be used as a basis for the solution of the waveguide problem. Equation (1.19) is used directly by Harrington (1968, sec. 8.8) and Spielman and Harrington (1972), together with the boundary condition that the tangential component of $\vec{E}$ at any point Q on C is zero. The unknown functions $\vec{K}$ and q_s are represented by some expansion set and the

cutoff wavenumber and unknown coefficients of this set can be solved for from the resulting homogeneous set of non-linear integral equations. Spielman and Harrington (1972) use a moment method of solution (Harrington 1967, 1968) by representing $\vec{K}$ (and hence q_s from (1.23)) by triangle functions over subsections of C.

Hashimoto and Fujisawa (1970) use the integral equation

$$U(P) = -j/4 \int_C U(Q) \frac{\partial}{\partial n} H_0^{(2)}(kR)\, dC + j/4 \int_C \frac{\partial U}{\partial n} H_0^{(2)}(kR)\, dC \qquad (1.24)$$

which can be derived from Green's Theorem, and is equivalent to equations (1.19) and (1.20) when $\vec{K}$ and q_s are substituted from the surface fields (Silver 1965, sec. 4.1). By considering limiting procedures when P tends to an arbitrary point on C, an integral equation is obtained and the expression can be specialised to waveguides (Hashimoto and Fujisawa 1970). However, the numerical solution for waveguide problems is not well documented by them and they have only shown a set of results for the circular waveguide.

1.2.4.1 Null field method

In this method equations (1.19) and (1.20) are again used. However, instead of taking the conventional boundary conditions (1.4) on C, the 'extended boundary condition' of Waterman (1965) is employed. The extended boundary condition, in the waveguide case, recognizes that the field is completely zero outside C, providing

the waveguide wall is perfectly conducting (sec. 5.2). By the application of the Addition theorem for Bessel functions (Watson 1968, chap. 11) to $H_0^{(2)}$ in equations (1.19) and (1.20) and setting the fields equal to zero outside C leads to the null field equations (Bates 1969b)

$$\int_C F(C)\, J_m(kr)\, \exp(-jm\theta)\, dC = 0, \quad \text{E-modes} \tag{1.25}$$

$$\int_C G(C)\, [J_{m-1}(kr)\, \exp(j\alpha) - J_{m+1}(kr)\, \exp(-j\alpha)]$$

$$\exp(-jm\theta)\, dC = 0, \quad \text{H-modes}, \tag{1.26}$$

where F(C) is the z-directed surface current density, G(C) is the surface current density directed along C and α is the angle that OQ makes with the coordinate n at Q (Fig. 1.1). When the surface current densities F(C) and G(C) are represented by expansions with finite numbers of terms, equations (1.25) and (1.26) lead to sets of homogeneous equations which can be solved for the cutoff wavenumber. The investigation of the computational implementation of (1.25) and (1.26) forms part of the work of this thesis (Chap. 2).

It should be noted that in the first two integral operator methods (Spielman and Harrington 1972; Hashimoto and Fujisawa 1970) singular integrands (associated with the Green's function $H_0^{(2)}$) are obtained because of the use of boundary conditions on C. Special consideration has therefore to be given to the integration in the neighbourhood of the singular points. The use of the extended boundary condition in the null field method

however circumvents this complication and in general, produces integral equations (1.25) and (1.26) with non-singular integrands.

In all the integral operator methods the cutoff wavenumber k appears as a non-linear parameter and hence the determination of the cutoff wavenumbers requires a search procedure (e.g. a 'regula falsi' method (Abramowitz and Stegun 1965, formula 3.9.3)). Generally, integral operator methods involve dense matrices of order 10-30 and provide accurate results. Reentrant corners of C can be handled by the choice of appropriate expansion functions which have the correct analytic behaviour in the neighbourhood of the corners (Ng and Bates 1972). This point is considered in detail in this thesis (Chapter 2). For the null field method, the convergence rate for the error is typically M^{-10} where M is the size of the determinant.

1.2.5 Point-Matching Methods

These include the straightforward point-matching method (Yee and Audeh 1965, 1966b; Audeh and Fuller 1968; Bates 1969b), the complete point-matching and alternative point-matching techniques (Bates 1969b). The extended point-matching method, which is a modification of the straightforward point-matching method, is introduced here. An investigation of these point-matching methods is presented in this thesis (Chapter 3).

1.2.5.1 Straightforward point-matching method

The straightforward point-matching method (Bates 1969b) was first applied to the calculation of the characteristics of electromagnetic waveguides by Yee and Audeh (1965, 1966a,b). There are also point-matching treatments of mechanical vibration (Conway 1960, 1961), acoustics (William et al. 1964) and heat conduction (Ojalvo and Linzer 1965) problems. Point-matching approaches to electromagnetic scattering have recently been discussed by Bolle and Fye (1971). The method has also been used for the calculation of the propagation characteristics in dielectric rod waveguides (Cullen and Özkan 1971).

A general solution of equation (1.2) valid in at least a neighbourhood of the origin O is

$$U(\rho,\varphi) = \sum_{m=-\infty}^{\infty} A_m J_m(k\rho) \exp(-jm\varphi). \qquad (1.27)$$

In the straightforward point-matching method (SPM) the right hand side (RHS) of (1.27) is made to satisfy the boundary conditions (1.4) at a finite number of points on C. In order to get numerical solutions it is further assumed that the summation on the RHS of (1.27) can be truncated without introducing unacceptable error. So the SPM equations are

$$\sum_{m=-N}^{N} A_m J_m(kr_n) \exp(-jm\theta_n) = 0, \quad \text{E-modes}; \qquad (1.28)$$

$$\sum_{m=-N}^{N} A_m [J_{m-1}(kr_n) \exp(j\alpha_n) - J_{m+1}(kr_n) \exp(-j\alpha)]$$

$$\exp(-jm\theta_n) = 0, \quad \text{H-modes}; \qquad (1.29)$$

where, in (1.28) and (1.29), $1 \leqslant n \leqslant 2N+1$, (r_n,θ_n) is the set of coordinates for the points on C and α_n is the value of α at (r_n,θ_n). It was early pointed out that the SPM appeared to contradict expressions derived on a rigorous basis (Harrington 1965; Bates 1967) even though Yee and Audeh had obtained some accurate results. Similar doubts about the non-universal applicability of the SPM were raised by Laura (1965, 1966b; also Yee 1966). Fuller and Audeh (1969) demonstrated by example that the contradictions might only be apparent, at least for cross-sectional shapes which are convex, when viewed from the outside. It was then shown that the SPM could be rigorously justified, by what was called the complete point-matching method, as far as the computation of cutoff wavenumbers was concerned, but appeared in general to give incorrect values for the wavefunction (Bates 1969b).

In the derivation of (1.28) and (1.29) from (1.27) the SPM implicitly assumes that the expansion (1.27) is valid for the whole waveguide region. The validity of this assumption, which is closely related to the Rayleigh hypothesis, was the subject of much discussion (Burrows 1969a,b; Bates 1969a; Millar and Bates 1970; Lewin 1970). Davies and Nagenthiram (1971) showed by example that the SPM fails when the cross-section of the waveguide is L-shaped. An attempt to synthesize concrete conclusions from the aforementioned work together with the introduction of the internal Rayleigh hypothesis is undertaken in this thesis (Chapter 3).

The SPM loses its effectiveness for complicated shapes and is unlikely to produce accurate results when the wall is strongly nonconvex when viewed from the outside. No sharp theorem however has yet been found to establish the validity or otherwise of using the SPM for any given shape, although the trenchant but difficult analysis given by Millar (1969, 1970, 1971) (which is developed for the scattering or external case) is a useful contribution. He considers mainly the location of singularities of the assumed solution when C is an analytic curve. This is further discussed in secs 3.4.1 and 3.4.2.

1.2.5.2 Extended point-matching method

In an attempt to extend the usefulness of the SPM, a modification of the method was developed. This is the extended point-matching method (EPM). In this method, the region S of the waveguide is divided into a number of overlapping subregions and in each of these subregions an expansion similar to (1.27) is employed. However, for a subregion which contains a reentrant corner a different representation must be used. The representation is chosen so that the singular behaviour of the wavefunction at the corner can be accommodated (Hunter and Bates 1970, 1972; Hunter 1972; Davies and Nagenthiram 1971). The representations for all the subregions are made to satisfy the boundary conditions (at discrete points) on their respective parts of C. Continuity of U throughout the cross-section is ensured by matching the representations and their normal

derivatives at points along a line in the common area between overlapping subregions. The extended point matching method is described in detail in sec. 3.5. It is applied successfully to several waveguides and is shown to yield accurate results.

The EPM is reminescent of mode matching techniques (Lewin 1970; Read 1969). The actual subregions and representations to be used depend on the detailed shape of C. In certain cases it may be difficult to find useful representations. However, it is often possible to use the EPM when the SPM fails and to do this without introducing undue complication. It should also be mentioned that where the SPM fails, its usefulness can also be extended by an analytic process similar to that of Mittra and Wilton (1969). This is described in the next section.

1.2.5.3 Analytic continuation method

A procedure which makes use of analytic continuation can also be used to extend the usefulness of the straightforward point-matching method. This method is an alternative to that of the extended point-matching method. It is essentially an adaptation to the waveguide case of a method described by Mittra and Wilton (1969; see also Imbriale and Mittra 1970) for the scattering or exterior problem.

It is known (Bates 1969b; Millar and Bates 1970; also sec. 3.4) that the right hand side of eqn (1.27) is absolutely convergent in at least the region defined by the largest circle, centred on O, which is enclosed

by C (Fig. 1.2). The right hand side of (1.27) is hence made to satisfy the boundary condition (1.4) at the points Q_1 and Q_2 (Fig. 1.2) to obtain either eqn (1.28) or (1.29) for the E or H modes. This procedure has not assumed that the representation (1.27) must be valid for the whole region enclosed by C.

By using the addition theorem for Bessel functions (Watson 1968, chap. 11) the expansion (1.27) can be analytically continued to a different region with a new origin O' (Fig. 1.2) such that the smallest possible region of convergence of the analytically continued representation about O' intersects the original region of convergence. The representation for the field about the point O' is

$$U(\rho',\varphi') = \sum_{n=-\infty}^{\infty} B_n \, J_n(k\rho') \exp(-jn\varphi'); \qquad (1.30)$$

$$B_n = \sum_{m=-\infty}^{\infty} A_m \, J_{m-n}(k\rho_0) \exp(-j[m-n]\varphi_0), \qquad (1.31)$$

where (ρ',φ') are the cylindrical polar coordinates of a point P with respect to the origin O' and (ρ_0,φ_0) are the coordinates of O' with respect to the origin O. The right hand side of (1.30) can be used immediately to satisfy the appropriate boundary condition at the point Q_3 (Fig. 1.2). Note that the right hand side of eqn (1.30) contains a double summation.

The representation (1.30) can be continued analytically to another region with origin O" by the same process. The representation for the new region centred about O" will contain three summations and can

be used to satisfy the boundary condition at points Q_4 and Q_5. Similarly the original representation (1.27) can be continued analytically to the region centred about O_1. By a judicious choice of a sufficient number of regions, the contour C may be adequately covered, and the resulting set of homogeneous equations is solved for the wavenumber. The method as described above for the waveguide case is as yet untested. However, a limitation on the method is the increasing number of terms introduced by each additional continuation step.

1.2.5.4 Complete point-matching and alternative point-matching

The complete point-matching method (Bates 1969b) is derived from the null field equations (1.25) and (1.26) by taking $F(C) = \sum_n F_n \, \delta(C-C_n)$, where δ denotes the Dirac delta function and F_n is proportional to the surface current density at the point C_n, with the polar coordinates (r_n, θ_n) on C. A similar expansion is taken for G(C). The complete point-matching method (CPM) equations are

$$\sum_{n=1}^{2N+1} F_n \, J_m(kr_n) \exp(-jm\theta_n) = 0, \quad \text{E-modes;} \qquad (1.32)$$

$$\sum_{n=1}^{2N+1} G_n \, [J_{m-1}(kr_n) \exp(j\alpha_n) - J_{m+1}(kr_n) \exp(-j\alpha_n)]$$

$$\exp(-jm\theta_n) = 0, \quad \text{H-modes;} \qquad (1.33)$$

where $-N \leqslant m \leqslant N$ in (1.32) and (1.33). In the calculation of the cutoff wavenumber the CPM involves a

determinant which is the transpose of that of the SPM (Bates 1969b). Thus the CPM and SPM predict the same cutoff wavenumber for any given shape and the CPM is hence no more accurate in the determination of the cut-off wavenumbers than the SPM. However, the wavefunction solution given by the CPM is in general valid as the CPM is derived from a rigorous basis, while that assumed by the SPM is not in general valid. This difference is borne out by the fact that although the determinants are the same for both methods, their generating equations, (1.32) and (1.33) as opposed to (1.28) and (1.29), differ in the summation indices.

By multiplying eqns (1.32) and (1.33) by $j^m \exp(jm\phi_p)$ and summing over the interval $-\infty < m < \infty$ (Bates 1969b), the simplified alternative point-matching formulas are obtained:

$$\sum_{n=1}^{2N+1} F_n \exp(jkr_n \cos(\phi_p-\theta_n)) = 0, \text{ E-modes;} \quad (1.34)$$

$$\sum_{n=1}^{2N+1} G_n \exp(jkr_n \cos(\phi_p-\theta_n)) \cos(\alpha_n-\theta_n+\phi_p) = 0, \text{ H-modes;} \quad (1.35)$$

where $1 \leqslant p \leqslant 2N+1$ and $0 \leqslant \phi_p \leqslant 2\pi$ in (1.34) and (1.35). It is found that the alternative point-matching method (APM) is significantly more error sensitive than the CPM and it exhibits appreciably greater error than the CPM when C is asymmetrical (sec. 3.3).

In general, the SPM, CPM and APM are unlikely to produce accurate results for strongly nonconvex shapes (when viewed from the outside). The CPM however, can often give usable estimates of the eigenfunction. Where

suitable representations can be found, the EPM is useful and can be applied even for strongly nonconvex shapes. The main feature of point-matching methods is their inherent simplicity. Small dense determinants (order 10-30) with simple elements are involved; thus making only small demands on computer storage and times. The wavenumber k is again a non-linear parameter (cf. section 1.2.4) and a search routine is required in the determination of the cutoff wavenumbers.

1.2.6 Conformal Transformation Method

The basis of this method lies in the mapping of the given region into a simpler region (usually a rectangle or circle) where the boundary condition can be easily satisfied.

It is convenient in this section to consider the given waveguide region to be in the ξ plane and the transformed region (rectangle or circle) to be in the z plane ($z = x + jy$). The conformal mapping of the region in the ξ plane into the region in the z plane is effected by a transformation function

$$\xi = f(z). \tag{1.36}$$

This results in a transformed Helmholtz equation

$$\nabla_t^2 U + k^2 \left|\frac{d\xi}{dz}\right|^2 U = 0 \tag{1.37}$$

which has now to be solved. The factor $|d\xi/dz|$ is known as the scale factor of the transformation and equation (1.37) is equivalent to the description of a field in the transformed waveguide filled with an anisotropic dielectric medium. The first application

of the conformal transformation method to wave fields was made by Meinke in 1949 (Meinke and Baier 1968) and since then the method has been exploited to obtain solutions for various waveguide shapes (Meinke et al. 1963; Tischer 1963; Laura 1967; Laura et al. 1967, 1972; Meinke and Baier 1968; Abaka and Baier 1969). An early survey on conformal transformation methods is given by Meinke (1963).

The transformed equation (1.37) can be solved by a numerical method. Meinke (Meinke et al. 1963; Meinke and Baier 1968) considers the transformation of the given region to a rectangular region in the z-plane. A solution for U in the transformed region can then be written straightforwardly as (Meinke et al. 1963)

$$U = \sum_m \sum_n A_{mn} \exp(m\pi x/a + n\pi y/b), \qquad (1.38)$$

where a and b are the sides of the rectangle and the A_{mn} are unknown coefficients to be determined. The scale factor (see eqn (1.37)) is also written as a Fourier series

$$\left|\frac{d\xi}{dz}\right|^2 = \sum_p \sum_q f_{pq} \exp(p\pi x/a + q\pi y/b), \qquad (1.39)$$

where the coefficients f_{pq} can be determined from a Fourier analysis (Meinke et al. 1963). Eqns (1.38) and (1.39) are substituted into eqn (1.37) when a matrix eigenvalue problem is obtained (Meinke et al. 1963; Meinke and Baier 1968).

Laura (1964, 1967; Laura et al. 1972) transforms the waveguide region into a circular or an annular region

in the z-plane. An expansion (1.8) is taken as a general solution to eqn (1.37). The actual forms of the expressions for Φ_i (eqn (1.8)) used by Laura are a Bessel function term, $J_i(k_i\rho)$ (Laura 1964) and a polynomial expansion term, $\rho^{2i}(\rho^2/(2i+2) - 1/2i)$ (Laura 1967). Eqn (1.8) is substituted into (1.37) to give an equation similar to eqn (1.10) where the operator L is now equal to $(\nabla_t^2 + |(d\xi/dz)|^2k^2)$. A solution is then obtained by Galerkin's method (sec. 1.2.2.2) (Laura 1967, Laura et al. 1972).

In general, the conformal transformation method satisfies the boundary condition exactly but satisfies the partial differential equation (1.37) approximately. This is in contrast to the straightforward point-matching method which satisfies the partial differential equation (1.2) exactly but the boundary condition approximately. The conformal transformation is restricted by the choice of a suitable transformation function. Approximate transformation functions can be constructed for general shapes (Laura 1966c) but the increased complexity causes a fall in accuracy (Meinke and Baier 1968).

1.2.7 Method of Partial Regions

The waveguide region is divided into smaller (partial) regions which are usually rectangular such that adjacent regions are separated by a common boundary or line of continuity. For example, as in Fig. 1.3 the L-shaped waveguide can be divided into two regions, I : ABCD and II : DEGH, with a common boundary AD.

The field in each partial region is expressed as a Fourier series in terms of the fundamental solutions of the wave equation appropriate to the region which satisfy the boundary conditions on the waveguide wall except along the line of continuity, e.g. DAH in Fig. 1.3 (Collins and Daly 1964). The unknown coefficients in the expansion together with the cutoff wavenumbers can then be determined from the homogeneous system of equations obtained by forcing the representations to satisfy the remaining boundary conditions and continuity requirements along the lines of continuity. This method of partial regions has been used by several authors (Gruner 1967; Veselov and Platonov 1969; Veselov and Semenov 1970; Veselov and Gaydar 1970) and has also been called the orthogonal mode (Collins and Daly 1964) and segment matching (Laura 1966a) methods.

A modification of the method to produce an iterative procedure has been used by Gal'chenko and Mikhalevskiy (1970) who call the technique the alternating Schwartz's method. In this method the (rectangular) partial regions are chosen so that they overlap. For example, in Fig. 1.3 region I is now taken to be BCEF while region II is DEGH; the two regions thus intersecting in DEFA. The wave expansions are then solved for their unknowns for each region in succession. For example, the current solution for region I (Fig. 1.3) involves the matching along the line AD of its representation to the values given by a previous iteration solution for region II. With this updated solution

for region I, a new solution for region II is then obtained by a similar matching along the line AD.

The method of partial regions can only be applied to a limited number of waveguide shapes, especially those that can be decomposed into rectangular partial regions. For waveguide shapes that have reentrant corners the method is liable to give poor convergence (Collins and Daly 1964; Gal'chenko and Mikhalevskiy 1970). One suspects that the main reason for this is that the edge conditions (Jones 1964, Chap. 9) are not generally satisfied.

The method of partial regions bears resemblances to the extended point-matching method (sec. 1.2.5.2). The extended point-matching method however, unlike the partial regions method which is best applied to the restricted waveguide shapes mentioned above, can handle more general shapes. In addition, the extended point-matching method can account for the analytic behaviour of the field around reentrant parts of C, thus maintaining a good convergence rate.

1.2.8 Transverse Resonance Method

As with the method of partial regions, the transverse resonance method can only be applied to a limited class of waveguide shapes. At cutoff, there is no variation in the z-direction, and the wave may be considered to be propagating in the transverse direction inside the waveguide. The waveguide can be divided into sections and each section may be considered to be a transmission line. The impedance of the fields in the transmission line sections may then be matched to obtain

the conditions for transverse resonance which then corresponds to a cutoff mode.

The ridge waveguide was considered by Cohn (1947) as a three-section cascaded parallel plate transmission line with two of the lines terminated at the ends by metallic planes. Fig. 1.4a shows a ridge waveguide. Consider, for example, the TE_{10} mode. The admittance at the centre (dashed line in Fig. 1.4a) of the cross-section is zero (Cohn 1947) and the equivalent circuit is shown in Fig. 1.4b, where Y_1 and Y_2 are the admittances of the transmission lines (region 1 and 2 respectively). Equating admittance across the line X-X (Fig. 1.4b) gives the following condition for k (Cohn 1947):

$$\frac{b_1}{b_2} = \frac{\cot(ka_1/2) - B/Y_1}{\tan(ka_2/2)} , \qquad (1.40)$$

where B is the equivalent susceptance introduced by the discontuity in the cross-section. The computed and experimental results obtained by Cohn agree to about 0.5%.

Cohn's results for the ridge waveguide were extended by Hopfer (1955) and Pyle (1966) who introduced a first order correction to the gap discontinuity susceptance.

A somewhat similar, but comparatively crude, approach using the generalized telegraphist's equations has been developed by Schlosser (1968).

1.2.9 Perturbation Techniques

Perturbation methods of solution (Harrington 1961, sec. 7.4) can be used when the problem under consideration differs only slightly from a problem which can be solved exactly or which can be

more easily solved by some accurate numerical method.

For the case where an exact solution is known for the second shape, this exact solution can then be used as a basis for the solution to the actual problem. The change in the cutoff wavenumber Δk, effected by a small change in the waveguide wall can be calculated approximately from (Harrington 1961, sec. 7.4)

$$\frac{\Delta k}{k} = \frac{\iint_{\Delta S} \mu|H_0|^2 - \varepsilon|E_0|^2 \, ds}{\iint_{S} \mu|H_0|^2 - \varepsilon|E_0|^2 \, ds} \tag{1.41}$$

where S is the cross-section of the unperturbed guide, and ΔS is the perturbation in cross-section and the fields are those of the unperturbed guide.

This boundary perturbation technique was used long ago by Schelkunoff (1943, sec. 10.9) to obtain the characteristics of waveguides which are slightly non-circular. It has been used recently to obtain accurate characteristics of elliptical waveguides (Davies and Kretzschmar 1972), by perturbing solutions (obtained by a Rayleigh-Ritz method) for inscribed polygons.

When the perturbations are small, the solution (using some approximate method) to the perturbed shape is sometimes taken to be the required solution to the actual problem. This technique is sometimes referred to as geometrical approximation. Uptain and Audeh (1966) solve the trapezoidal waveguide by approximating the area by vertical rectangular strips. The problem is then solved by the transverse resonance method by

considering the perturbed guide to be made up of cascaded parallel plate lines. Essentially the same method is used by Pyle and Angley (1964) for a circular waveguide with straight side walls. Geometrical approximation is used by Hu (Hu and Ishimaru 1961, 1963; Hu Wang 1964) to break up the lunar waveguide and T-septate waveguide cross-sections into segments of a circle and solution is effected by the method of partial regions on the perturbed problem. The numerical and experimental results given by Hu agree to within 10%.

The success of the geometrical approximation technique depends on the possibility of dividing the cross-section into standard subregions. Both the number of regions and the perturbation should be small.

A useful point borne out by the perturbation technique is that since an inward or outward perturbation may result in an increase or decrease in the cutoff wavenumber (Harrington 1961, sec. 7.4) the geometrical deformations used in some of the techniques considered (e.g. variational, finite-element and finite-difference) should be made alternatively inwards and outwards around C so that the resultant area is neither the inscribed nor escribed polygon of the region but one in between these (Bulley 1970). This procedure would introduce the least overall change in the cutoff wavenumber.

1.2.10 First Order Coupled Equations

Helmholtz's equation can be reduced (Harrington 1968, sec. 8.5) to a system of coupled first order equations

$$\left.\begin{aligned} -\frac{\partial U}{\partial x} &= k\varphi \\ -\frac{\partial U}{\partial y} &= k\phi \\ \frac{\partial \varphi}{\partial x} + \frac{\partial \phi}{\partial y} &= kU \end{aligned}\right\} \qquad (1.42)$$

where φ and ϕ are the transverse fields. The operators in the above system (1.42) contain only first derivatives as opposed to the second order derivatives in the Helmholtz equation. However, because of the coupled system, the matrices tend to be larger. The method is not yet well documented in the literature although convergence is claimed to be faster (see Davies 1972) than for straightforward methods of solution of the Helmholtz equation (e.g. the finite difference method).

1.2.11 Other Methods

Besides the techniques already discussed there are several others which are either of very limited application or have not been much exploited yet.

The solution of the Helmholtz equation by a network impedance analogue method (Vine 1966; Kron 1944; Whinnery and Ramo 1944) is of limited applicability due to the great complexity of the electrical network needed.

The Monte Carlo method (Hammersley and Handscomb 1964) has been applied to Laplace's equation (Royer 1971) and can be extended to solve the Helmholtz equation (Wasow 1951) although the method requires excessive computing time in the simulation of a sufficient number of random walks.

Analog/hybrid computation techniques may possibly be employed, although these methods are in their infancy at the moment (Wexler 1969). A discussion of analogue techniques for partial differential equations is also given by Fifer (1961, chap. 20) where an electronic analog computer solution for the eigenvalues of a one-dimensional wave equation is given.

1.3 COMPARISON OF METHODS

Waveguide shapes can be classified (Bulley and Davies 1969) into three basic types (Fig. 1.5):

Type 1: Polygonal or curved, convex when viewed from the outside

Type 2: Nonconvex, with smooth reentrant part(s)

Type 3: Nonconvex, with sharp reentrant corner(s).

In general, Type 3 is the most troublesome computationally because of the singular behaviour of the field at the reentrant corners (Jones 1964, sec. 9.2) and most of the methods either suffer from a slower convergence rate or do not produce reliable results for this type of shape.

There is, of course, no best method but the variational, finite-elements, finite-difference, integral operator, null field and coupled first order differential methods are of wide applicability and can be used with all three types of shapes with suitable modifications where necessary for a type 3 shape. For example, in the variational techniques the region around the reentrant corner may be divided into a larger number of element areas while for the finite-difference method a

finer mesh may be used or an expansion with the correct analytic behaviour may be used in the neighbourhood of the reentrant corner (Motz 1946; Reid and Walsh 1965; Whiting 1968; Whiteman 1971; Fox 1971). In the null field method, the current in the region of the corner may also be represented by an expansion which behaves in the same analytic way as the currents on a wedge of the same angle (Ng and Bates 1972; Jones 1964, sec. 9.2). This technique is discussed in detail in chapter 2 of this thesis. Similar representations of surface currents have recently been used successfully in scattering problems (Hunter and Bates 1972, Hunter 1972).

Point-matching methods are attractively economic techniques, from the points of view of programming effort and computer time, but they lose their effectiveness with complicated shapes. The straightforward point-matching method is generally invalid for Type 3 shapes. However, a representation for the field which satisfies the correct analytic behaviour around the corner can again be used to extend the usefulness of the SPM (Davies and Nagenthiram 1971). This technique is a special case of the extended point-matching method which is discussed in detail in chapter 3.

The other techniques are not of general applicability and lend themselves well to particular classes of shapes only, although the conformal transformation method can handle a relatively wide class of shapes.

The distinction made between some of the methods in section 1.2 is not rigid. Some methods are in fact closely related. For example, the finite-element and

variational technique are equivalent in the sense that both methods attempt to minimise the same functional. The conformal transformation method employs some subsidiary method, like the Galerkin's method, in its solution; while a transverse resonance or partial regions technique is used in the perturbation method.

The methods discussed above are compared in Table 1.1. Davies (1972) has established some criteria for the comparison of methods and these points are incorporated into columns 3, 5 and 8 and the "Remarks" column of Table 1.1. The properties of the matrix (column 4) and CPU time (column 7) quoted are those required to give results accurate to 0.1% in general, unless otherwise stated. The storage requirements quoted are for programs with 8-byte (64 bit) words. All the methods listed in Table 1.1, except for an earlier finite-difference scheme (Davies and Muilwyk 1966; Steele 1968), are capable of predicting higher order modes in addition to the first E and H modes.

No comprehensive comparison of the methods on a single computer is available at present, and different machines have been used in the various methods listed in Table 1.1. A useful comparison of the characteristics of digital computers can be found in Computers and Automation (1969).

At present, programs for the finite-element (Silvester 1969c, Konrad and Silvester 1971) and the finite-difference scheme of Beaubien and Wexler (1971) have been documented and are available. Programs for

the variation Rayleigh-Ritz and integral operator methods although not documented in the literature have been mentioned by Bulley (EHPOL program, see Bulley 1970) and Spielman and Harrington (1970) respectively.

1.4 TABLE OF WAVEGUIDE SHAPES

Many waveguide shapes have now been used as examples for the solution of the waveguide problem in the literature. These range from the more straightforward trapezoidal to the more exotic club shape of Davies and Muilwyk (1966). Recently, attention has been focused on the fairly challenging and more practical ridge waveguide (a Type 3 shape) and this trend will probably increase. To this end it would be useful to determine accurately the cutoff wavenumbers of this waveguide by experiment in order that the results can be used in comparison with numerical ones.

Because of the profusion of shapes that have been used at one time or another, it is felt that Table 1.2, which lists these shapes, will prove useful.

Table 1.1: Comparison of methods for the numerical solution of the hollow waveguide problem. (The properties of the matrix (Column 4) and CPU time (Column 7) quoted are those required to give results accurate to 0.1% in general, unless otherwise stated. All the methods, except for an earlier finite-difference scheme, are capable of predicting the higher order modes in addition to the first E and H modes.)

Method	Reference	Cross-sectional shapes (see Fig. 1.5)	Properties of Matrix/ determinant, and orders needed for k accurate to 0.1% for appropriate shapes	Computer program/ solution for wavenumber, k	Program Storage Requirements (8-byte words)	CPU time	Asymptotic convergence rate of the error	Remarks
Variational Rayleigh-Ritz	Bulley (1970), Bulley and Davies (1969)	General, except type 3 cannot be handled for E modes	Dense, Order 30-40	Versatile. Prog. EHPOL mentioned in reference Standard eigenvalue matrix problem	70 Kbytes	30-70 secs (IBM 360/50)	Not well defined with polynomial order	Types 2 and 3 slower convergence. Good for curved type 1 shapes. Similar method by Thomas (1969)
Finite-element	Silvester (1969a,c)	General	Dense, block diagonal. Order 30-100	Versatile. Progs. documented: Silvester (1969c), Konrad and Silvester (1971). Standard eigenvalue matrix problem	about 200 Kbytes	40 secs/ mode (IBM 7094)	M^{-2D}, M = matrix size D = order of polynomial	Types 2 and 3 slower convergence. D = 1 in the simple finite-element method (Silvester 1969b).

Finite-difference (PDSOR)	Beaubien and Wexler (1970)	General	Sparse, large matrix. Order 5000 - 20000	Versatile. Prog. documented: (Beaubien and Wexler 1971). Eigenvalue matrix problem. Estimate of k required to start iteration	140-220 Kbytes	8 mins/ mode (IBM 360/65)	About h^{-1} to h^{-2}, h = mesh size	See also Pontoppidan (1969) for an alternative algorithm. An earlier five-point finite-difference scheme (Davies and Muilwyk 1966) gives only the lowest order modes.
Integral operator formulation	Spielman and Harrington (1972)	General	Dense, Order 10-30	Versatile, zeros of determinant give values of k, search routine required	Not given (probably around 100 K bytes)	Not given but stated as "substantial"	-	A moment method (Harrington 1968) using triangle functions is used. Field values close to waveguide wall are computed less accurately.
Null field method (NFM)	Chap. 2 of this thesis, Ng and Bates (1972)	General	Dense, Order 8-12	Versatile, zeros of determinant give values of k, search routine required	70 K bytes	25 secs per evaluation of determinant (10-15 required per mode)	about M^{-12}, M = order of determinant	See also Bates (1969b). A representation for the surface current density satisfying the requirements of the corner is needed for a type 3 shape. A representation by pulses gives the CPM.

Straight-forward point-matching method (SPM)	Chapter 3 Yee and Audeh (1965, 1966b); Bates (1969b)	Not universally applicable	Dense, order 8-12	Versatile, zeros of determinant give values of k, search routine required	13 K bytes	1.5 secs per evaluation of determinant (10-15 required per mode)	M^{-15} or better (before levelling off) for appropriate shapes. Oscillates with increasing M when the method is not valid.	Not always valid for Types 2 and 3 shapes.
Extended point-matching method (EPM)	Chapter 3	Extends usefulness of SPM	As for SPM	Depends on detailed shape of C (the rest as for SPM)	16 K bytes	2.3 secs per evaluation (the rest as for SPM)	As for SPM	Produces accurate results for Type 2 and 3 shapes, if suitable representations can be found.
Complete point-matching method (CPM)	Chapter 3, Bates (1969b)	General	As for SPM	As for SPM	As for SPM	As for SPM	As for SPM, Generally oscillates for increasing M for types 2 and 3 shapes	Errors may be large (10-20%) for types 2 and 3 shapes.

Conformal transformation	Meinke & Baier (1968), Meinke et al.(1963)	Best suited to shapes for which simple transformation functions can be found	Dense, order 80-90 for accuracies to 1%	Versatile. Eigenvalue matrix problem.	-	12 mins/ mode (TR4)for a complete calculation (including the field)	-	For shapes requiring complicated mapping functions or for higher order modes, the large number of terms which have to be taken into account causes a fall in accuracy.
Perturbation (geometrical approximation)	Uptain & Audeh (1966), Pyle and Angley (1964), Hu and Ishimaru(1961)	Limited shapes	Dense	Each waveguide becomes a separate problem. See individual references.	-	-	-	See also Pyle (1966) for transverse resonance method and Collins & Daly (1964) and Veselov (1969,1970) for partial regions method
Coupled first order operators	Harrington(1968, sec. 8.5) (see also Davies 1972)	General	Dense	Versatile,zeros of determinant give values of k	-	-	-	Convergence should be better than a second order differential operator method but the matrix size will be larger (Davies 1972)

Table 1.2: Table of Waveguide Shapes

Shape	Dimensions: cutoff wavenumber ka, of lowest order mode given in reference		Reference	Method used in Reference
	H mode	E-mode		
Rectangle 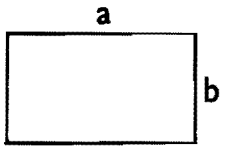	b = a/2		Standard shape e.g. Jordan and Balmain (1968, chap. 8)	Separation of Variables
	3.1416	7.0248		
Truncated Square 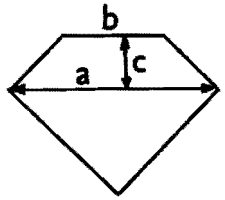	b=0.55a, c=0.225a		Bulley and Davies (1969)	Variational Rayleigh-Ritz
	4.215			
Trapezoid 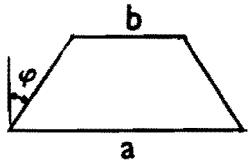	b/a=0.25, φ = 0°(10°)60°. Table of ka values		Uptain and Audeh (1966). See also Audeh & Fuller (1968), Veselov & Platonov (1968), Chopra & Durvasula (1971,1972)	Transverse resonance

"Rounded" Rectangle 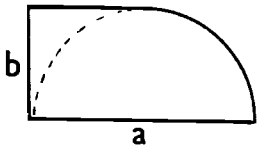	No ka listed. Field plots given.		Bulley (1970)	Variational Rayleigh-Ritz
Rectangle with Semi-circular sides 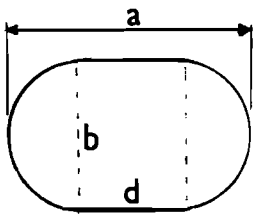	b/a = 0 to 1.0. H-mode. Graph of ka values		Valenzuela (1961)	Variational Rayleigh-Ritz
L-shape 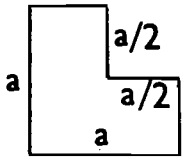		4.819	Reid and Walsh (1965). See also Davies and Nagen-thiram (1971)	Finite-difference

Single Ridge 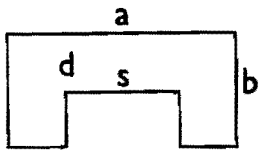	b/a=s/a=d/b=1/2.			
	2.2566	12.164	Spielman and Harrington (1972)	Integral Operator
	2.412	12.1416	Beaubien and Wexler (1970)	Finite-difference PDSOR
	2.2627		Bulley and Davies (1969)	Variational Rayleigh-Ritz
	2.250	12.134	Chapter 3	Extended point-matching
	b/a = 0.45; d/b,s/a=0.05(0.05) 0.95. Table of ka values.		Pyle (1966)	Transverse resonance
Ridge, with unequal ridge depths 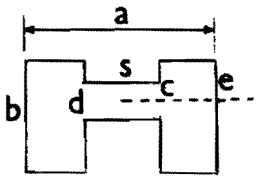	a = 0.5,b = 0.4, s = 0.1,c = 0.055,e = 0.02, 0.13, 0.17; d/b = 0.225 to 0.325. H-mode. Graph of ka values.		Montgomery (1971) See also Beaubien and Wexler (1968)	Ritz-Galerkin
Rectangle, with trapezoidal ridges 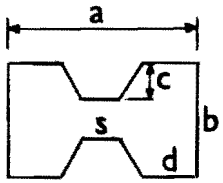	b/a = 0.75, s/a = d/a = 0.15, c/a = 0.2		Meinke et al.(1963)	Conformal transformation
	2.53	7.61		

Meinke guide	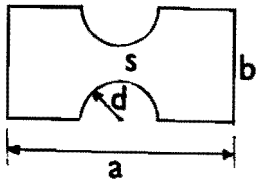	a/b=1.29, d/b=0.3	Bulley and Davies (1969)	Variational Rayleigh-Ritz
		2.267		
		2.268	Chapter 3	Extended point-matching
		b/a = 0.775, s/a = 0 to 1.0 Graph of ka values	Meinke and Baier (1968)	Conformal transformation
Vaned rectangle	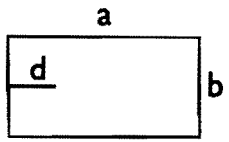	b/a = 0.25 (0.25) 1.0, d/a = 0 to 0.8. Graph of ka values	Silvester (1969a)	Finite-element
T-septate rectangle	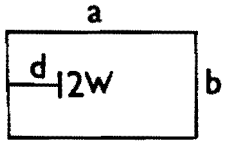	b/a = 4W, d/a = 0.26, W/a = 0.311/2.744	Beaubien and Wexler (1970) See also Silvester (1969a)	Finite-difference PDSOR
		2.9682 8.1181		
Square outer, eccentric circular inner	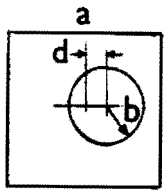	2a = 0.125, 0.250, 0.375 d/(a-b) = 0 to 1.0 Graphs of ka values	Audeh and Fuller (1968)	(Extended) point-matching

n-sided polygonal outer, co-axial circular inner. 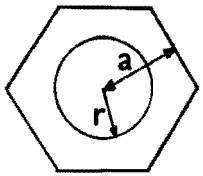	n = 4,5,6,7 and 8 r/a = 0 to 1.0 Lowest order E mode. Graphs of ka values		Laura et al.(1972)	Conformal transformation
Coaxial rectangles 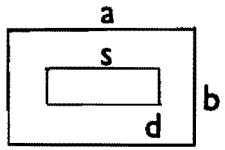	b/a = 0.8, 2d/b = 0.6 s/a = 0 to 1.0 Graph of ka values		Gruner (1967)	Partial regions
Equilat-eral triangle 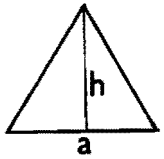	$4\pi/3$	$2\pi a/h$	Schelkunoff (1943, sec. 10.8). See also Thomas (1969). E mode.	Analytic solution
Isosceles right-angled triangle 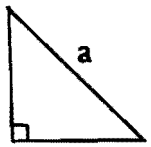	4.43	9.96	Schelkunoff (1943, sec. 10.8) and Morse and Feshbach (1953, p.756).	Analytic solution

Regular pentagon		2.285	Laura (1967)	Conformal transformation
Regular hexagon		2.317	" "	" "
Regular heptagon		2.339	" "	" "
Regular octagon		2.355	" "	" "
Hexagon 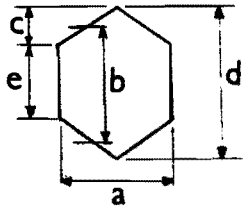	b/a = 0.9, d/b = 1.0 to 1.15 Graph of ka values		Meinke and Baier (1968)	Conformal transformation
	c/a = 0 to 5.0, for several values of cross-sectional area. Graph of ka values.		Schlosser (1968)	Transverse resonance
Star shaped 	Dimensions not given, see figure in reference		Thomas (1969)	Variational Galerkin's
		k = 4.087		
Circle 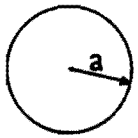	1.8412	2.4048	Standard shape e.g. Jordan and Balmain (1968, Chap. 8)	Separation of variables

Sector	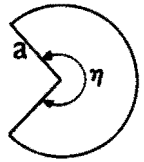	$\eta = \pi/2$ 3.0542 5.1356 $\eta = 3\pi/2$ 1.4012 3.3756	Chapter 2 see also Ng and Bates (1972)	Separation of variables
"Rounded" sector	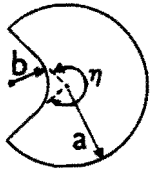	$\eta = 3\pi/2$, $b/a = 0.35$ 3.2015	Chapter 2	Null field method
Truncated circle	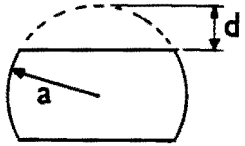	d/a = 0 to 0.3 E mode. Graph of ka values.	Pyle and Angley (1964). See also Sinnott (1970) and Schlosser (1968)	Perturbation and transverse resonance
Segment	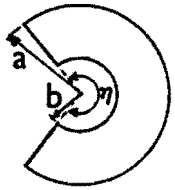	$\eta = \pi/2$, $b/a = 0.2$ 5.2218 $\eta = 3\pi/2$, $b/a = 0.3$ 4.5457	Chapter 3	Separation of variables

Circular outer, eccentric circular inner 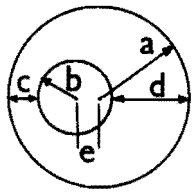	b/a = 0.25, 0.5; e/b = 0 to 3.0 Graphs of ka values	Yee and Audeh (1966b)	(Extended) point-matching
	b/a = 0.434, c/d = 0.1 to 1.0 Graphs of ka values	Abaka and Baier (1965). See also Veselov and Semenov (1970), and Dwight (1948)	Conformal transformation
Lunar shape 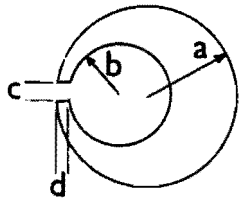	a = 13, b = 7.435, c = 1.0, d = 1.43 0.990 | 4.605	Beaubien and Wexler (1970). See also Meinke and Baier (1968), Hu and Ishimaru (1961), Arlett et al.(1968).	Finite-difference PDSOR
Inverted lunar 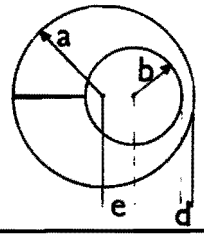	a = 34, d = 3.74, e = 38.9 0.770	Meinke et al.(1963). See also Meinke and Baier (1968)	Conformal transformation
Circle, with central cross 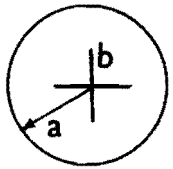	b/a = 0 to 1.0 Graph of ka values	Veselov and Gaydar (1970)	Partial regions

T-septate circle 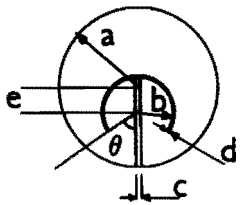	a = 13, b = 6.875, c = 1.125, d = 0.5, e = 3.375, θ = 22.5° 0.517 | 4.903	Beaubien and Wexler (1970). See also Hu Wang (1964), Arlett et al. (1968)	Finite-difference PDOSR
Ellipse 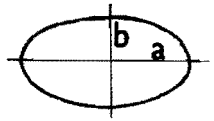	$(x/a)^2 + (y/b)^2 = 1$, $e^2 = 1 - b^2/a^2$. e = 0.0 to 1.0. E and H modes. Graphs of ka values	Krestzschmar (1970). See also Rayevskiy and Smorgonskiy (1970), Davies and Kretzschmar (1972)	Separation of variables
Super-ellipse 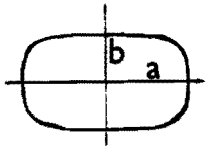	$(x/a)^n + (y/b)^n = 1$ b/a = 0.3 to 1.0, n = 2 to ∞. H-mode. Graph of ka values.	Larsen (1969)	Finite-difference
Parabolic 	see reference	Horiuchi et al. (1968) and Zagrodzinski (1968)	Separation of variables

"Star" shape	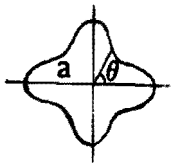	$\rho = 1 + b \cos 4\theta$, b = 0 to 0.3 H mode. Graph of ka values	Laura (1964)	Conformal transformation
Club shape		See reference 3.32	Davies and Muilwyk (1966)	Finite-difference

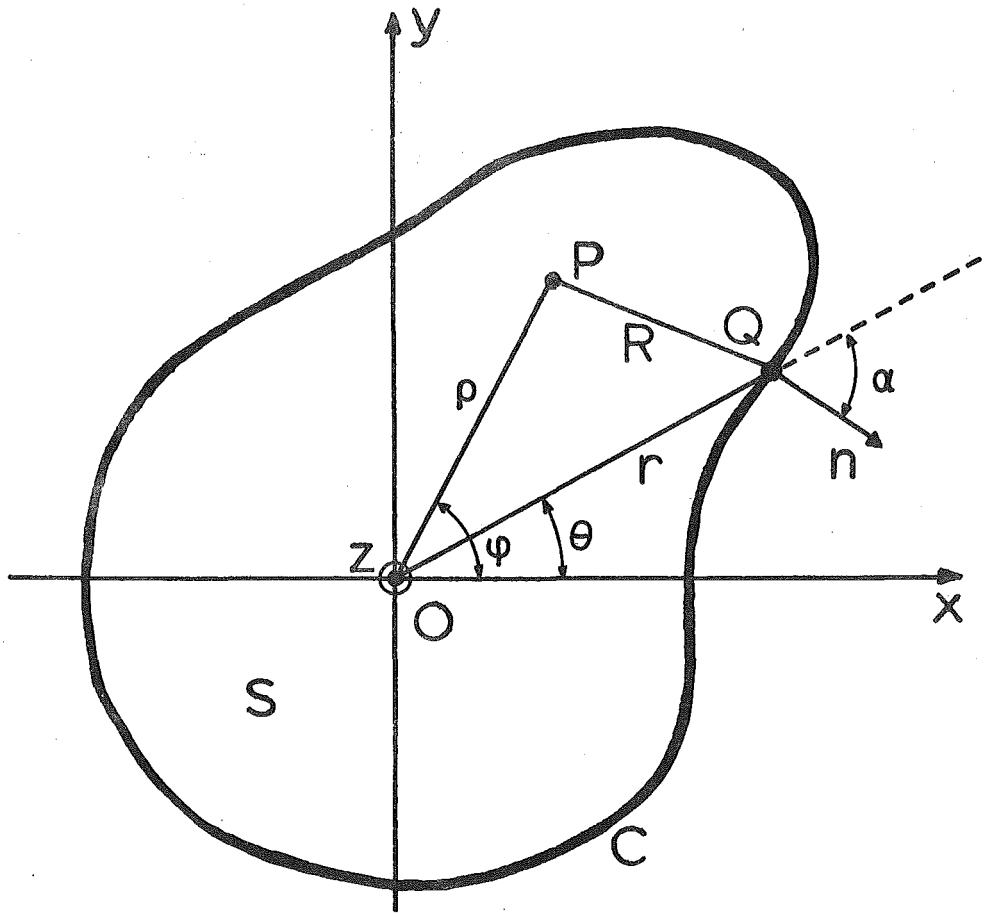

Fig. 1.1 Waveguide cross-section and coordinate system. z-coordinate perpendicular to paper.

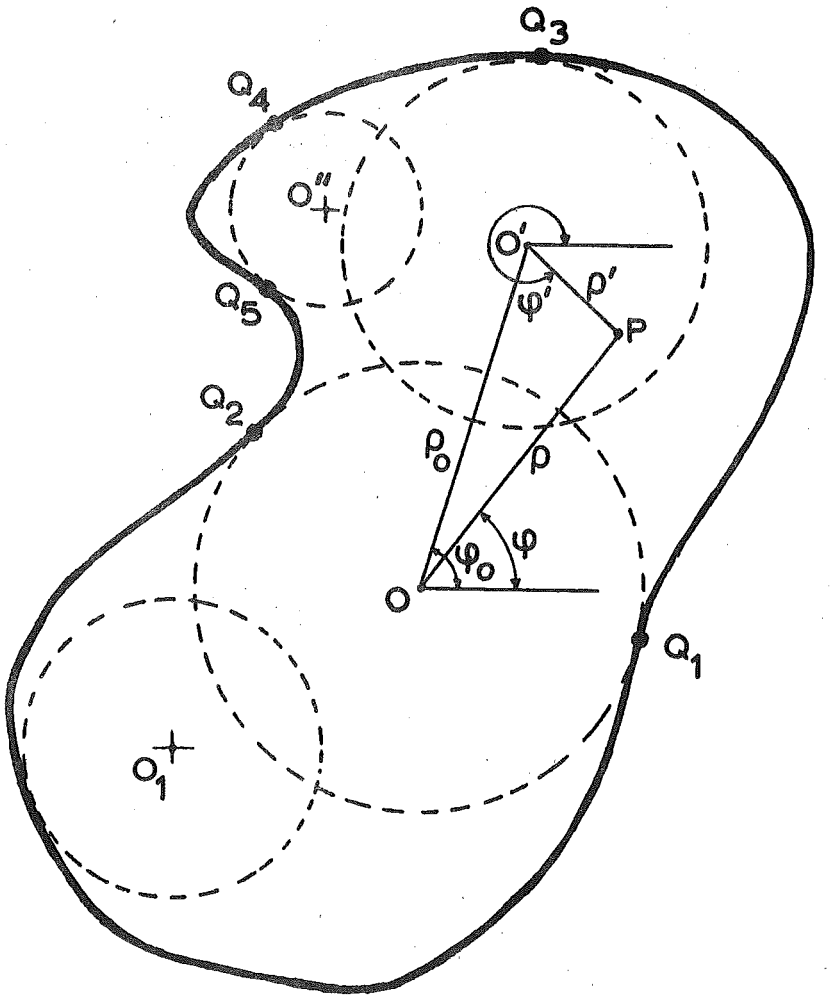

Fig. 1.2 Coordinate system for analytic continuation method.

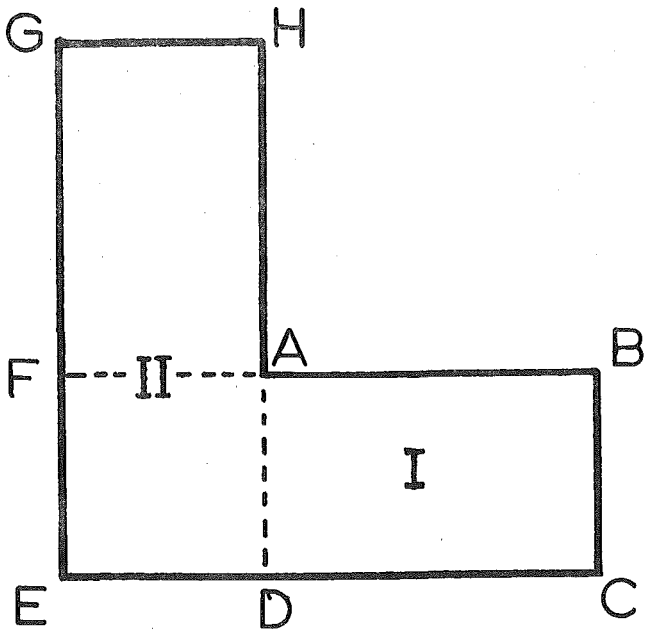

Fig. 1.3 Division of L-shaped waveguide into partial regions.

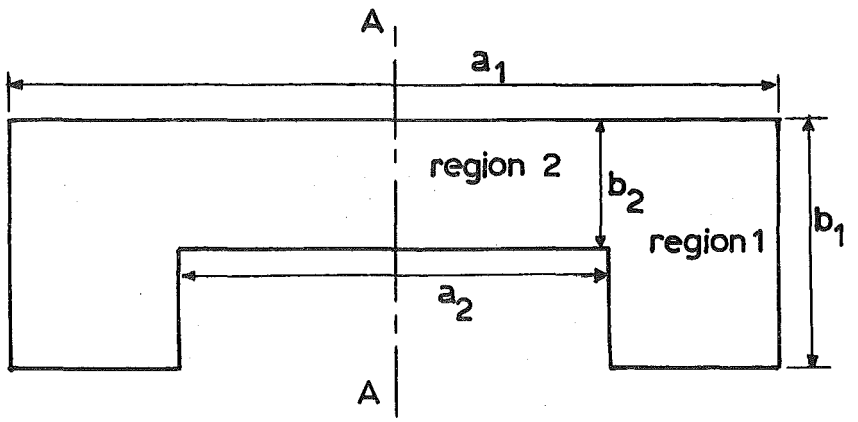

(a) Ridge waveguide

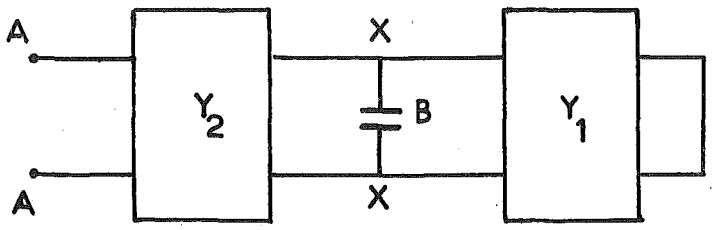

(b) Equivalent circuit

Fig. 1.4 Ridge waveguide and equivalent circuit for transverse resonance method.

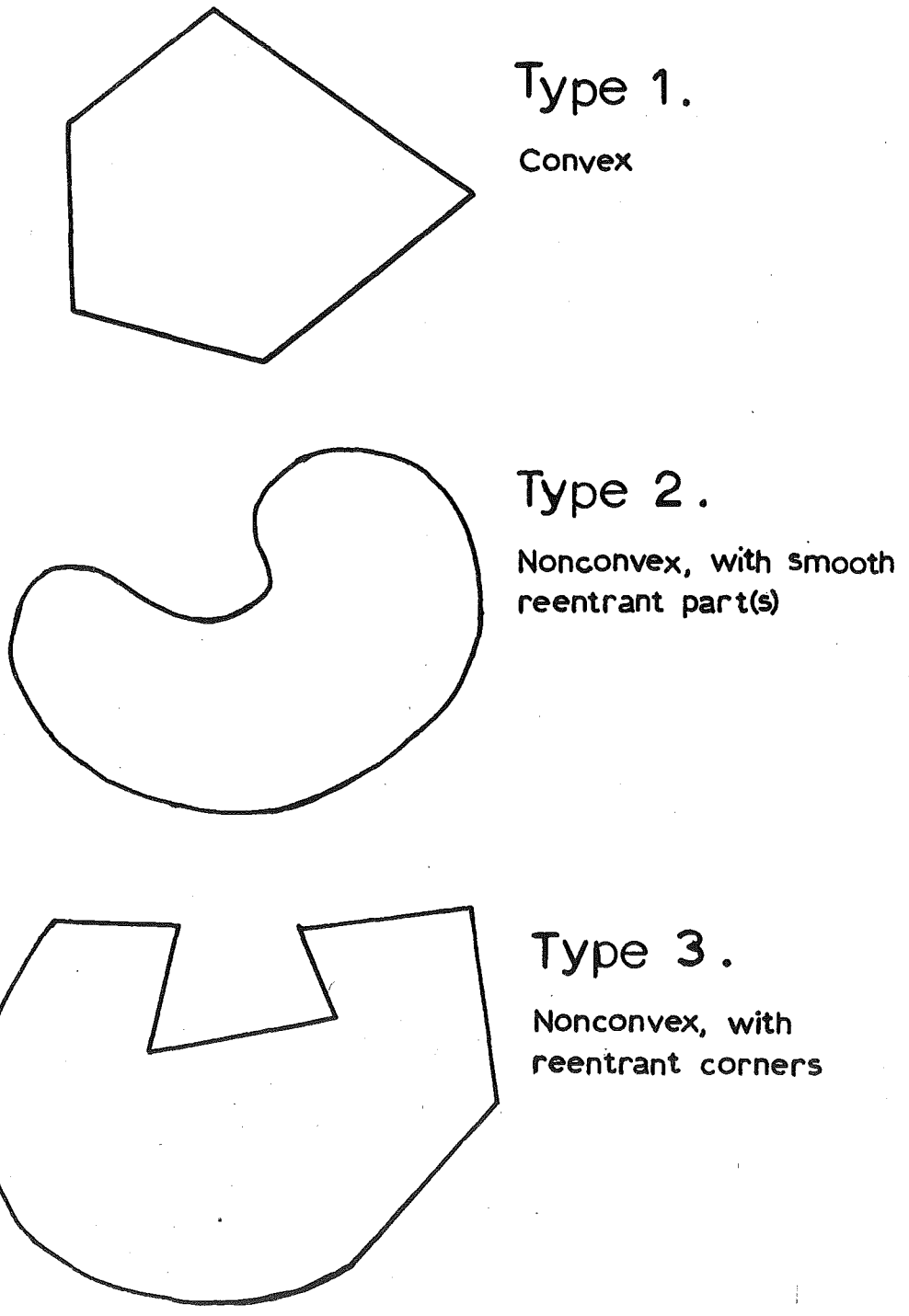

Fig. 1.5 Classification of waveguide shapes

CHAPTER 2: NULL FIELD METHOD

'Does your watch tell you what year it is?'
'Of course not,' Alice replied very readily:
'but that's because it stays the same year
for such a long time together.'
'Which is just the same with mine,' replied
the Hatter.

Lewis Carroll

The numerical solution of the waveguide problem by the null field method is considered. Computational results are presented for several waveguides. It is demonstrated that where a reentrant corner exists, explicitly satisfying the edge conditions at this corner significantly improves the computational accuracy. The cutoff wavenumbers computed by the null field method are generally accurate to 0.1% or better.

2.1 INTRODUCTION

A null field method has been developed by Bates (1969b), for uniform waveguides and transmission lines, from Waterman's (1965) extended boundary condition. The formal expression of the method is an infinite set of nonsingular integral equations for the surface current densities in the waveguide wall. The null field method provides a rigorous basis (Bates 1969b) for Yee and Audeh's (1965, 1966b) computations of cutoff wavenumbers by point-matching. The method has also been applied to two-dimensional scatterers (Bates 1968; Hunter and Bates 1970, 1972; Hunter 1972).

The computational implementation of the null field method is presented in this chapter. The numerical results obtained show that the characteristics of arbitrarily shaped waveguides can be computed from the null field equations with an accuracy and computational economy at least comparable with that of other proven methods (see chapter 1 and Davies (1972) for reviews). One of the waveguides considered is the sector waveguide (Fig. 2.1) with $\beta = \pi/2$. This is a Type 3 shape (Fig. 1.5) and the corner can cause difficulties because of the singular fields and currents in its neighbourhood (Jones 1964, chap. 9). The usefulness of the technique is confirmed by accurate results being obtained in spite of the sharp reentrant corner exhibited by the cross-section of this sector waveguide.

A paper (Ng and Bates 1972) on the results of this chapter is in press.

2.2 NULL FIELD METHOD

2.2.1 Null Field Equations

Consider a uniform, perfectly conducting waveguide embedded in free space supporting an E or H mode at cutoff. Denote by C the closed planar curve representing the cross section of the waveguide wall. Take the z-direction to be perpendicular to the plane of C. At any point P in this plane, the field intensity is given by (Bates 1969b)

$$E_z(\rho,\varphi) = -\frac{\omega\mu_0}{4}\int_C F(C)\, H_0^{(2)}(kR)\, dC, \quad \text{E-modes;} \tag{2.1}$$

$$H_z(\rho,\varphi) = \frac{j}{4}\int_C G(C)\left[\frac{\sin(\alpha+\varphi-\theta)}{\rho}\frac{\partial}{\partial\varphi}\right.$$

$$\left. - \cos(\alpha+\varphi-\theta)\frac{\partial}{\partial\rho}\right] H_0^{(2)}(kR)dC, \quad \text{H-modes,} \qquad (2.2)$$

where ω is the angular frequency of the field (the time factor $\exp(j\omega t)$ is suppressed), k is the free space wavenumber corresponding to the angular frequency ω, and F(C) is the z-component (only component) of the surface current density in the waveguide wall for E-modes while G(C) is the component (only component) of the surface current density directed along C for H-modes. C is used to denote arc length along the curve C, measured from any convenient point on C. Fig. 1.1 shows an arbitrary shape for C. The point P has cylindrical polar coordinates (ρ,φ). An arbitrary point Q on C has coordinates (r,θ) and the distance between P and Q is denoted by R. α is the angle that OQ makes with the coordinate n normal to C at Q.

Equation (2.1) for E-modes is obtained from equation (1.19) where at cutoff the electric field intensity $\vec{E}$ and surface current density are completely z-directed and the charge density q_s is equal to zero (eqn (1.23)). The expression for H_z for H-modes (equation (2.2)) is derived from equation (1.20) by substituting for $\vec{A}$ from eqn (1.21). The surface current density is now directed completely along C.

The field outside C must be completely zero. This extended boundary condition (Waterman 1965) yields, after applying the addition theorem for Bessel functions (Watson 1968, chap. 11) to $H_0^{(2)}$ in eqns (2.1) and (2.2)

and after some further manipulations, the null field equations (Bates 1969b)

$$\int_C F(C)\, J_m(kr)\, \exp(-jm\theta)\, dC = 0, \quad \text{E-modes;} \qquad (2.3)$$

$$\int_C G(C)\, [J_{m-1}(kr)\, \exp(j\alpha) - J_{m+1}(kr)\, \exp(-j\alpha)]$$

$$\exp(-jm\theta)\, dC = 0, \quad \text{H-modes,} \qquad (2.4)$$

for all integers m within $-\infty < m < \infty$, where J_m is the Bessel function of the first kind of order m. The line integrals are seen to contain nonsingular integrands in general. The surface current densities F(C) and G(C) can be represented approximately by

$$\begin{matrix} F(C) \\ G(C) \end{matrix} = \sum_{n=0}^{N} a_n \Phi_n(C), \quad -L/2 \leqslant C < L/2 \qquad (2.5)$$

where the a_n are constants, the $\Phi_n(C)$ are some suitable functions, N is a positive integer and L is the total length of the curve C.

2.2.2 Symmetries of C

For all practicable waveguide shapes that are actually used and all not-so-practicable shapes that appear in the literature (see Table 1.2) it is possible to choose the origin of C such that the curve is symmetrical about C = 0. Consequently, for a particular mode, F(C) (or G(C)) is either an even or an odd function of C. If the left hand side of equation (2.3) (and (2.4)), with m replaced by -m, is multiplied by $(-1)^m$ and is then added to, or subtracted from, (2.3) itself then (2.3) is recovered, for $m \geqslant 0$ with exp replaced by cos or -sin. It is therefore convenient to define

$$A^{\pm}_{mn}(k) = \int_C \Phi_n(C)\, J_m(kr) \begin{matrix}\cos\\ \sin\end{matrix}(m\theta)\, dC, \quad \text{E-modes;} \tag{2.6}$$

$$A^{\pm}_{mn}(k) = \int_C \Phi_n(C) \left[J_{m-1}(kr) \begin{matrix}\cos\\ \sin\end{matrix}(\alpha - m\theta) \mp J_{m+1}(kr) \begin{matrix}\cos\\ \sin\end{matrix}(\alpha + m\theta)\right] dC, \quad \text{H-modes.} \tag{2.7}$$

Note that for modes with even or odd symmetry, A^{-}_{mn} and A^{+}_{mn} respectively are identically zero. To obtain numerical solutions, eqn (2.5) is substituted into equations (2.3) and (2.4), for $0 \leqslant m \leqslant N$, giving

$$\sum_{n=0}^{N} a_n\, A^{\pm}_{mn}(k) = 0 \tag{2.8}$$

where $\pm$ applies to modes with even or odd symmetry respectively.

In some cases, e.g. a rectangular waveguide, the cross-section C may be symmetrical about both the lines $\varphi = 0$ and $\varphi = \pi/2$. For this two-fold symmetry case the surface current densities may be either odd or even functions about the two lines of symmetry. Thus the surface current density is one of four possible combinations: even-even, even-odd, odd-even, odd-odd; where, for example, the set "even-odd" means that the surface current density is even about the line $\varphi = 0$ and odd about the line $\varphi = \pi/2$. For both the even-even and odd-odd cases, m in eqns (2.6) and (2.7) is replaced by 2m because the integrals in eqns (2.6) and (2.7) are identically zero when m is an odd integer. Similarly m is replaced by (2m+1) for the even-odd and odd-even cases.

The computed cutoff wavenumbers are those values of k which bring to zero the determinant formed from the $A^{\pm}_{mn}(k)$. (For a cross-section which possesses no symmetry of C the cutoff wavenumbers are those values of k which bring to zero the modulus of the determinant $|\det A_{mn}|$ where A_{mn} is given by eqns (2.6) and (2.7) with exp instead of the cos or sin terms). For each cutoff wavenumber, the computed surface current density can be evaluated by giving a convenient constant value to one of the a_n in eqn (2.5) and then solving for the remaining members by pivotal elimination (Goodwin 1961, chap.1).

2.2.3 Other integral formulations

Multiply eqns (2.3) and (2.4) by $J_m(k\rho)\exp(jm\varphi)$ and sum over the interval $-\infty < m < \infty$. Thus, (using the addition theorem for Bessel functions (Watson 1968, chap. 11))

$$\int_C F(C)\, J_0(kR)\, dC = 0, \quad \text{E-modes;} \tag{2.9}$$

$$\int_C G(C) \left[\frac{\sin(\alpha+\varphi-\theta)}{\rho} \frac{\partial}{\partial \varphi} - \cos(\alpha+\varphi-\theta) \frac{\partial}{\partial \rho} \right] J_0(kR)\, dC = 0, \quad \text{H-modes.} \tag{2.10}$$

Substituting eqn (2.9) in eqn (2.1) and (2.10) in (2.2) we obtain

$$E_z(\rho,\varphi) = \frac{j\omega\mu_0}{4} \int_C F(C)\, Y_0(kR)\, dC, \quad \text{E-modes;} \tag{2.11}$$

$$H_z(\rho,\varphi) = \tfrac{1}{4}\int_C F(C)\left[\frac{\sin(\alpha+\varphi-\theta)}{\rho}\frac{\partial}{\partial\varphi} - \cos(\alpha+\varphi-\theta)\frac{\partial}{\partial\rho}\right]$$

$$\cdot Y_0(kR)\, dC, \quad \text{H-modes,} \qquad (2.12)$$

where Y_0 is the Bessel function of the second kind of zero order. Note that either eqns (2.11) and (2.12) (or the equivalent eqns (2.1) and (2.2)) or the eqns (2.9) and (2.10) can be used as a method of solution. These methods involve satisfying the equations at a number of isolated points (for (2.9) and (2.10) the points can be anywhere in the x-y plane, for (2.11) and (2.12) the points have to be outside C where E_z and H_z are set to zero, or on C where E_z and $\partial H_z/\partial n$ are zero. The null field method adopted here however satisfies the extended boundary condition for all points outside C.

A description of a method using eqns (2.11) and (2.12) as a basis is given by Harrington (1968, sec. 8.8). The conventional boundary conditions (eqn (1.4)) are used. Care has to be exercised as the integrand now has a singular behaviour. This singularity can be avoided if the points are chosen outside C and not on C itself. The derivation of equations (2.9) and (2.10) presented here confirms the assumption made by Harrington (1968, sec. 8.8) that equations (2.11) and (2.12) can be used instead of (2.1) and (2.2). Equations (2.11) and (2.12) do not satisfy the radiation condition but this is unnecessary as the field is zero outside C (Harrington 1968, sec. 8.8). An integral equation formulation equivalent to eqns (2.1) and (2.2) together with the boundary condition that the tangential E field is

zero on C has recently been used by Spielman and Harrington (1972, see also sec. 1.2.4).

2.3 SURFACE CURRENT DENSITY REPRESENTATION

A set $\{C_n\}$ of (N+1) points on C is chosen and $\Phi_n(C)$ is taken to be $\delta(C-C_n)$, where δ denotes the Dirac delta function. This is the complete point-matching solution (Bates 1969b) and is only a crude method of evaluating the integral on the left hand sides of equations (2.3) and (2.4), and it only gives accurate results if C has no reentrant parts. (A detailed consideration of this point is presented in Chapter 3).

Better accuracy is obtainable if $\Phi_n(C)$ is taken to be the n^{th} trigonometric Fourier component, $\cos(2n\pi C/L)$ or $\sin(2n\pi C/L)$. This gives accurate results when C belongs to a type 1 or 2 shape (Fig. 1.5). If C has reentrant parts that exhibit sharp corners, accurate results are only obtained if in the neighbourhood of each such corner, at least one of the $\Phi_n(C)$ behaves in the same analytic way as the currents on a wedge of the same angle (Jones 1964, chap. 9). Similar representations of surface currents have recently been used successfully in scattering problems (Hunter and Bates 1972, Hunter 1972). Numerical results of the application of the null field method method are presented in the next section.

2.4 NUMERICAL RESULTS

In the computations, an extended Simpson's rule (Abramowitz and Stegun 1965, formula 25.4.6) is

employed for the numerical integration. This provides results which are generally accurate to 0.1% or better. Higher order quadrature methods, e.g. Gaussian, have not been used. Because of the oscillatory nature of the integrands in equations (2.6) and (2.7) (owing to the cos and sin terms) the use of higher order quadrature methods does not necessarily lead to an improvement in the convergence rate (Davies and Rabinowitz 1967, pp 31, 37 and 58). The important point is to ensure that there are sufficient integration points for the oscillations (about 8 or more per oscillation).

The wavenumber k appears as a non-linear parameter in eqn (2.8). Thus a search procedure has to be employed to find the values of k which null the determinant formed from the $A^{\pm}_{mn}(k)$. A 'regula falsi' method (Abramowitz and Stegun 1965, formula 3.9.3) is employed. The slope for the values of the determinant computed for successive increments of k is also monitored to ensure that multiple roots corresponding to degenerate modes are not missed. This, however, occurs only rarely.

The computer program for the null field method requires about 70 K bytes of storage, with 8-byte words. This includes the storage required for a maximum determinant order of 10 and 199 (maximum) integration points for each of the 100 (maximum) integrals for the $A^{\pm}_{mn}(k)$, given by eqn (2.8). To evaluate a determinant of order 8 using 199 integration points takes about 27 secs (CPU time for IBM 360/44). Between 10 and 15 determinants are needed to evaluate each cutoff wavenumber to an accuracy of better than 0.1%.

2.4.1 Rectangular waveguides

Consider the rectangular waveguide shown in Fig. 2.2. A trigonometric Fourier series representation for the surface current density F(C) or G(C) was used in the null field method. Table 2.1 gives results for the computed cutoff wavenumbers truncated to two decimal places for the E-modes of a rectangular waveguide with an aspect ratio of 2 : 1 (i.e. a = 2b, see Fig. 2.2). The 'exact' values are those given by the standard theory (Jordan and Balmain 1968, chap. 8). The integrals in eqns (2.3) and (2.4) were evaluated using a 29-point extended Simpson's rule. The results show that small displacements of the origin O from the central point (d = 0, Fig. 2.2) do not affect the accuracy of the results. Table 2.1 indicates that accurate results are obtained with a determinant order (which corresponds to the number of Fourier components used) of about 8. Results for the H-modes of the rectangular waveguide, using 69 integration points and a determinant order of 8, are shown in Table 2.2. The computed cutoff wavenumbers obtained are truncated to the third decimal place. Fig. 2.3 is a plot of the typical behaviour of the determinant value, $\mathrm{Det}(A^{\pm}_{mn}(k))$ as a function of the wavenumber ka. The H_{40} and H_{02} modes for the rectangular waveguide (b/a = $\frac{1}{2}$) are degenerate and have the same cutoff wavenumber. This behaviour is reflected in the presence of the double root at ka = 12.57 in Fig. 2.3. The presence of this double root is detected by a change in the slope of the

determinant values computed for incremental values of k. The cutoff wavenumber k corresponding to the double root is determined by a process of halving the incremental steps for k. The value of k giving the smallest determinant value is taken as the cutoff wavenumber. Because of the sharp cusp (Fig. 2.3) the double root can be determined to an accuracy of better than 0.1%.

2.4.1.1 Rate of convergence

The H_{31}-mode in a rectangular waveguide having an aspect ratio of 2.25 : 1 has been examined. This allows a direct comparison to be made of the null field method and the high-order finite-element method (Silvester 1969a). The accuracy of the computation of cutoff wavenumbers depends upon the order of the determinants and matrices used in the respective methods. A trigonometric Fourier series representation for the surface current density was used in the null field method, the integrals in equation (2.4) being evaluated using a 69-point extended Simpson's rule (Abramowitz and Stegun 1965, formula 25.4.6). The actual integration was over only a quarter of C because of the two-fold symmetry of the waveguide cross-section. Silvester used finite element polynomials up to order 4. The number of Fourier terms (the order of the determinant) in the null field method was varied. The results obtained are shown in Fig. 2.4. The cutoff wavenumber ka of the H_{31}-mode in the rectangular waveguide (a/b = 2.25) given by standard theory (see e.g. Jordan and Balmain 1968, Chap. 8) to

ten significant figures is 11.78097245. The cutoff wavenumber using the null field method for a determinant order of 8 has been computed to 9 significant figures. The error in the computed wavenumber was proportional to M^{-10} for the null field method (Fig. 2.4) and M^{-8} for Silvester's method, when he used a polynomial of order 4. (M denotes the order of the determinant in the null field method and the order of Silvester's matrix). The same error, of 0.02%, was obtained with M = 3 for the null field method and M = 70 for the high order finite-element method of Silvester (1969a). The error dependence on the number of integration points p is about p^{-2} (e.g. with M = 4, the errors for 29 and 49 points are 0.0017% and 0.00057% respectively).

2.4.2 Sector Waveguides

The lowest order E-modes of two sector waveguides (with $\beta = 3\pi/2$ and $\pi/2$, Fig. 2.1) were examined in detail. The 'exact' cutoff wavenumbers for these waveguides have been calculated from equation (A3) given in Appendix A. For the sector waveguide with $\beta = 3\pi/2$, the exact cutoff wavenumber ka for the lowest order E-mode is 5.13562. The null field method gives a calculated value 5.1356, for the cutoff wavenumber which is correct to at least five significant figures (with a trigonometric Fourier series, 69 integration points and M = 8). The surface current density computed by the null field method for this mode together with the surface current density computed from the exact expression given in Appendix B2 are shown in Fig. 2.5. It is

seen that the surface current density computed by the null field method follows closely the exact current density except at the points Y and Z on C where the exact current density is zero.

The sector waveguide with $\beta = \pi/2$ (Fig. 2.1) has a sharp reentrant corner and the surface current density is singular at the corner for the lowest-order E-mode (Appendix B2, see Fig. 2.6). Two representations for the surface current density (eqn (2.5)) are used - a trigonometric Fourier series only and a trigonometric Fourier series together with a component which satisfies the edge conditions (Jones 1964, chap.9; Appendix B1) explicitly. The details of these two representations are given in Table 2.3. (Details for the point-matching method are also given to facilitate comparison when the method is discussed in Chapter 3.) The origin of C is chosen as the point on C which intersects the line $\varphi = 0$ (Fig. 2.1). Table 2.3 shows that the accuracy of the computed wavenumber increases markedly as the representation for the surface current density is improved. This is emphasized by Fig. 2.6 which shows the surface current densities computed from the exact expression (Appendix B2) and using the representations 2 and 3 of Table 2.3. Lewin (1970) has pointed out that when a waveguide cross-section has reentrant parts, the representation of the surface current used in the null field method must be very accurate if the right hand side of equation (2.11) (or eqn (2.1)) is to be close to zero just outside the reentrant parts. This is clearly confirmed by Table 2.4 which shows how the exact

field (Appendix B2), and the fields computed from equation (2.11) using representations 2 and 3, vary with ρ for $\varphi = \pi$ (see Fig. 2.3).

Table 2.5 compares, at a number of points on C, the fields computed by the null field method. The boundary condition for E-modes requires the exact field to be zero on C. The fields computed by the null field method are seen to be very small on C, except near the reentrant corner. Of the two representations for the surface current density used with the null field method, the second (representation 3 of Table 2.3) gives somewhat better results, as it should since it satisfies the edge conditions (Jones 1964, chap. 9) explicitly.

2.4.3 Ridge Waveguide

The improvement in accuracy of the computed results obtained with a surface current density representation which has the correct analytic behaviour at the reentrant corner for the sector waveguide ($\beta = \pi/2$) above is again evident for the ridge waveguide. The first H-mode of a single-ridge waveguide is considered. The dimensions used are a : b : w : d = 4 : 2 : 2 : 1 (Fig. 2.7). Two representations of the surface current density are again considered. The first (representation 1) is a trigonometric Fourier series only. The other (representation 2) is a trigonometric Fourier series together with the first two terms of a representation which satisfies the edge conditions at the reentrant corners. These functions are (see Appendix B1) given by

$$\Phi_n^{(1)} = (-1)^{n+1} J_{2n/3}(kx), \quad n = 0, 1; \tag{2.13}$$

$$\Phi_n^{(2)} = f_n(x) - f_n(w-x), \quad n = 0, 1 \tag{2.14}$$

where

$$f_n(x) = \tfrac{1}{2}\left[1 + \tanh \frac{w/2-x}{(w/2)^2-(w/2-x)^2}\right] J_{2n/3}(kx). \tag{2.15}$$

Equation (2.13) is used for the part of C labelled 1 in Fig. 2.7 where x is measured along 1 from the point X. Eqn (2.14) is used along the ridge (part 2 of C, Fig. 2.7) where x is again measured from the point X. The expression (2.14) is chosen so that it has the correct analytic behaviour at the reentrant corners. It also has to be an odd function about the line of symmetry of C (see Fig. 2.7) so as to account for the odd symmetry of the surface current density for the first H-mode (see e.g. Bulley and Davies 1969).

The above two representations are used in the null field method. The results obtained with M = 6 are summarised in Table 2.6. Bulley and Davies (1969) using a variational technique give ka = 2.263. As expected, the second representation for the surface current density gives better results. The value ka = 2.283 (given by representation 2 and with 199 integration points) differs by about 1% from that of Bulley and Davies and could be improved with increased integration accuracy (this was not done because of direct-access storage limitations). The error dependence on the number of integration points was about p^{-1} in both cases.

Table 2.1: Cutoff wavenumbers ka for E-modes in a rectangular waveguide by the null field method. b/a = 1/2 (Fig. 2.2). M = order of determinant. Number of integration points = 29.

Mode (E)		11	21	31	12	41	22	32
Exact ka		7.02	8.89	11.33	12.95	14.05	14.05	15.71
M	d/a							
8	0.0	7.02	8.89	11.33	12.94	14.05	14.05	15.52
	0.1	7.02	8.89	11.33	12.94	14.05	14.05	15.52
	0.2	7.02	8.89	11.33	12.94	14.05	14.05	15.52
6	0.0	7.02	8.87	10.80	12.90	13.54	13.88	15.42
7		7.02	8.89	11.33	12.94	13.54	13.88	15.54
8		7.02	8.89	11.33	12.94	14.05	14.05	15.53
9		7.02	8.89	11.33	12.95	14.05	14.05	15.76

Table 2.2: Cutoff wavenumbers ka of H-modes in a rectangular waveguide by the null field method. b/a = 1/2 (Fig. 2.2). M = 8, number of integration points = 69.

Symmetry of wavefunction about $\varphi = 0$ and $\varphi = \pi/2$	ka					
Even-even	Mode	20	40, 02	22	42	60
	Exact	6.28319	12.5664	14.0496	17.7715	18.8496
	Computed	6.2832	12.566	14.050	17.772	18.850
Even-odd	Mode	10	30	12	50,32	
	Exact	3.14159	9.42478	12.9531	15.7080	
	Computed	3.1416	9.4248	12.953	15.708	
Odd-odd	Mode	11	31	51	13	
	Exact	7.02481	11.3272	16.9180	19.1096	
	Computed	7.0248	11.327	16.918	19.110	
Odd-even	Mode	01	21	41	03	61,23
	Exact	6.28319	8.88577	14.0496	18.8496	19.8692
	Computed	6.2832	8.8858	14.050	18.850	19.869

Table 2.3: Lowest order E-mode in sector waveguide, $\beta = \pi/2$.

Representation of surface current density			ka, for M=8	% error in ka	Dependence of error on M	Remarks
Number	Name	$\Phi_n(C)$				
1	point matching method (CPM and SPM)	$\delta(C-C_n)$	3.3078	2%	oscillates with increasing M	M = order of determinant k = cutoff wavenumber Accurate value of ka, obtained from (A3) is 3.3756 Number of integration points used with representations 2 and 3 is 169.
2	null field method, trigonometric Fourier representation for F(C).	$\cos(2n\pi C/L)$	3.3254	1.5%	M^{-2}	
3	null field method, representation for F(C) explicitly satisfying edge conditions (Jones 1964, chap.9) at sharp re-entrant bend.	$\left.\begin{array}{l}[(\frac{L}{2}-C)(\frac{L}{2}+C)]^{-\frac{1}{3}},\ 0\ll C\ll\frac{L}{2}\\ [(C-\frac{L}{2})(\frac{3L}{2}-C)]^{-\frac{1}{3}},\ \frac{L}{2}\ll C\ll L\end{array}\right\}n=0$ $\cos(2[n-1]\pi C/L),\quad n>0$	3.3730	0.08%	M^{-14}	

Table 2.4: Values of the field E_z, for lowest order E-mode in sector waveguide at points along $\varphi = \pi$. $\beta = \pi/2$, $d/a = 0.5$. Field normalised to 1.0 at $\rho/a = 0$. The numbers in parentheses denote powers of ten. The two null field representations are defined in Table 2.3.

ρ/a	Method			
	Exact E_z; given by (B7) for $\rho < d$; $E_z = 0$, $\rho > d$.	Straightforward point matching	Null field method, representation 2	Null field method, representation 3
0.1	1.031	1.036	1.042	1.032
0.2	0.969	1.003	0.997	0.972
0.3	0.809	0.891	0.860	0.814
0.4	0.537	0.701	0.624	0.545
0.5	0.0	0.441	0.216	(-1) 0.405
0.6	0.0	-	(-1) 0.86	(-2) 0.32
0.8	0.0	-	(-1) 0.15	(-2)-0.85
1.0	0.0	-	(-2) 0.14	(-2)-0.52
2.0	0.0	-	(-4)-0.22	(-4)-0.65

Table 2.5: Values of the field E_z, for lowest order E-mode in sector waveguide at points along C, where C is measured from the point on C at which $\varphi = 0$. Details are given in Table 2.4. The exact field E_z is zero on C. The numbers in parentheses denote powers of ten.

C/a	Method		
	Straightforward point matching	Null field method, representation 2 of Table 2.3	Null field method, representation 3 of Table 2.3
0.0	(1) 0.23	(-2)-0.23	(-2)-0.49
0.2	0.17	(-2)-0.22	(-3)-0.91
0.4	(1)-0.22	(-2)-0.18	(-2) 0.28
0.6	-0.49	(-2)-0.15	(-3) 0.90
0.8	(1) 0.21	(-3)-0.81	(-3) 0.35
1.0	0.80	(-3)-0.48	(-3) 0.87
1.2	(1)-0.20	(-4)-0.43	(-2)-0.53
1.4	(1)-0.11	(-3) 0.56	(-4)-0.72
1.6	(1) 0.19	(-3) 0.41	(-2)-0.56
1.8	(1) 0.15	(-3) 0.23	(-2) 0.13
2.0	(1)-0.20	(-3) 0.89	(-2) 0.26
2.2	(1)-0.22	(-3) 0.52	(-2) 0.17
2.4	(1) 0.12	(-3)-0.12	(-2)-0.16
2.6	0.42	(-2) 0.62	(-1) 0.11
2.8	-0.15	(-2)-0.89	(-2) 0.37
3.0	-0.21	(-1)-0.16	(-1)-0.10
3.2	0.11	(-1) 0.48	(-2) 0.45

Table 2.6: Lowest order H-mode in ridge waveguide by the null field method with M = 6. a : b : w : d = 4 : 2 : 2 : 1 (Fig. 2.7). ka obtained from Rayleigh-Ritz method = 2.263 (Bulley and Davies 1969).

Representation of surface current density	ka	
	79 integration points	199 integration points
1. trigonometric Fourier series	2.48	2.36
2. trigonometric Fourier series plus representation (eqns (2.13) and (2.14)) satisfying edge conditions.	2.313	2.283

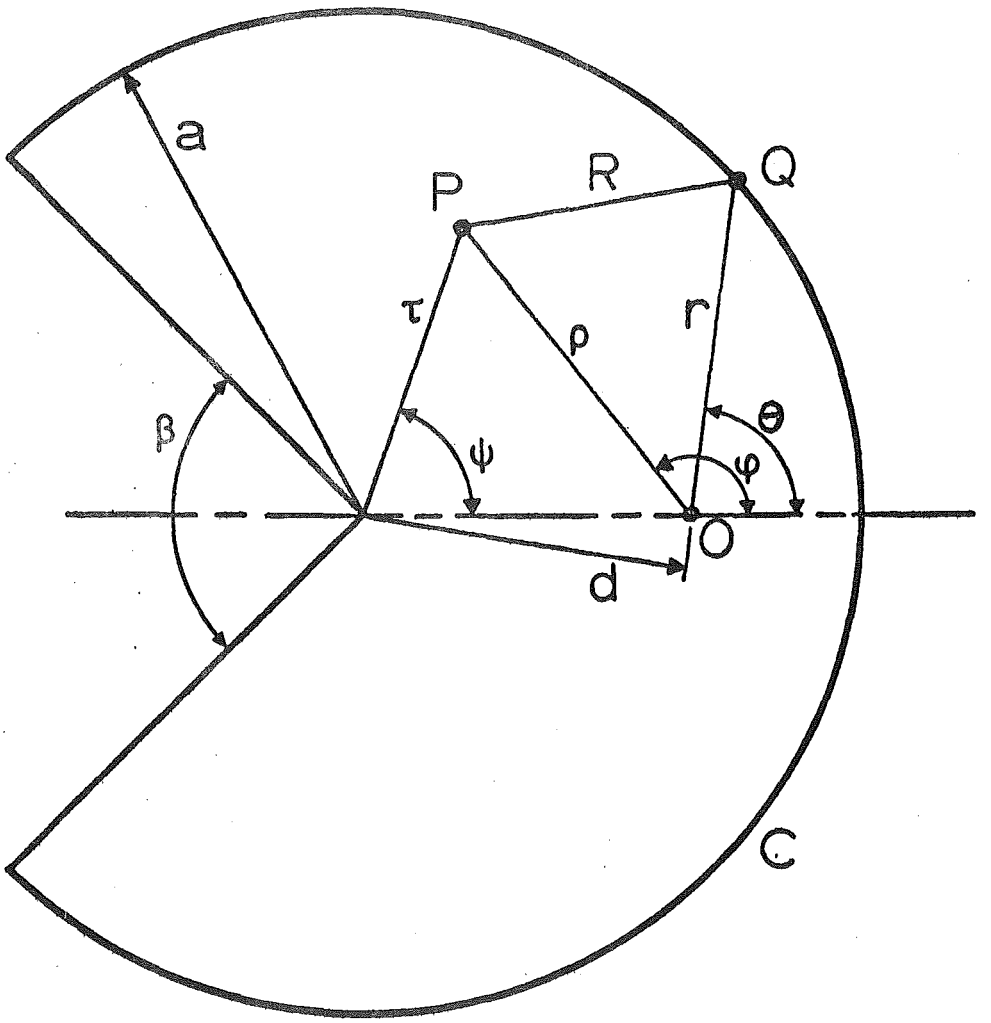

Fig.2.1 Waveguide cross-section. Sector waveguide. $\eta = 2\pi - \beta$.

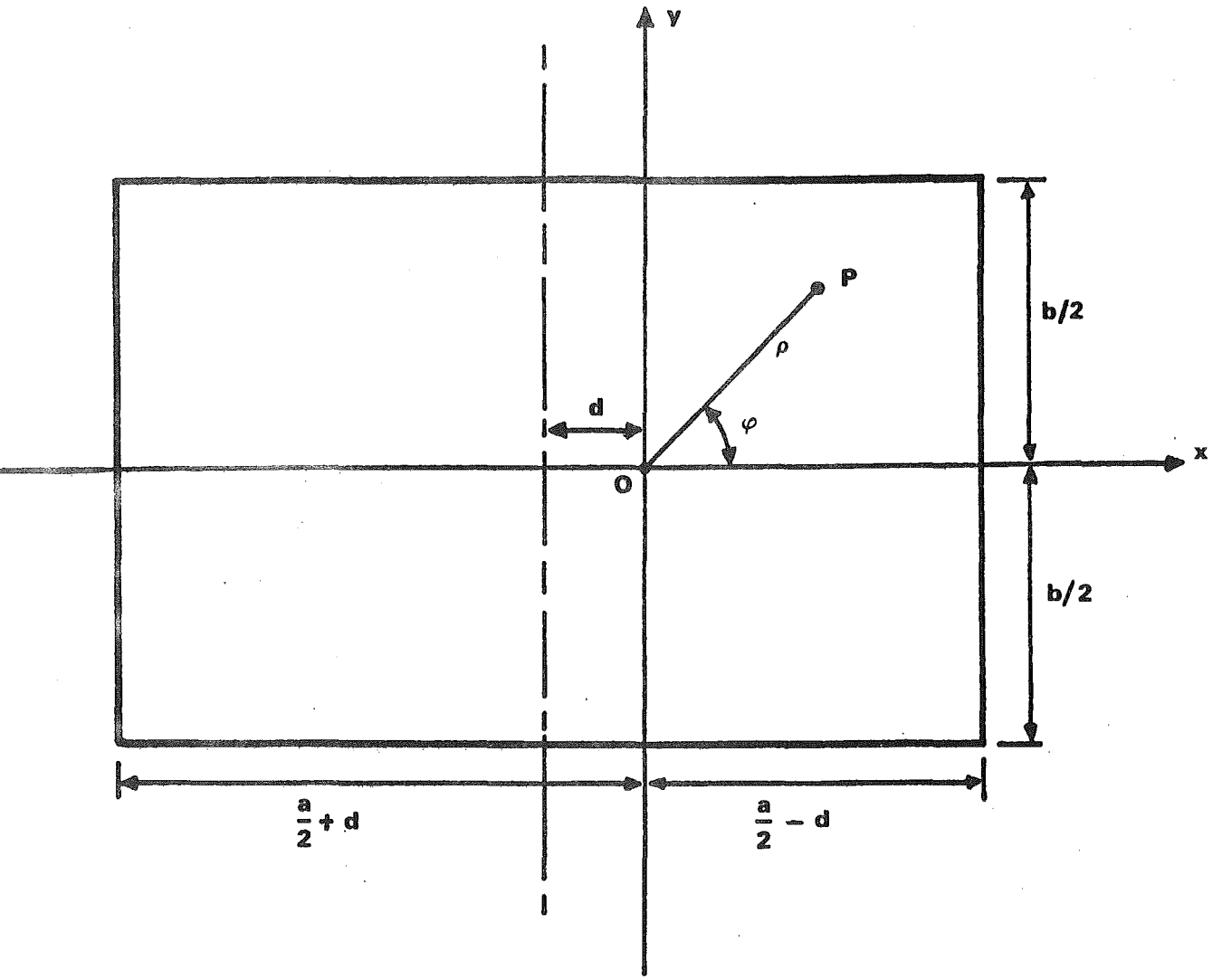

Figure 2.2 Rectangular waveguide.

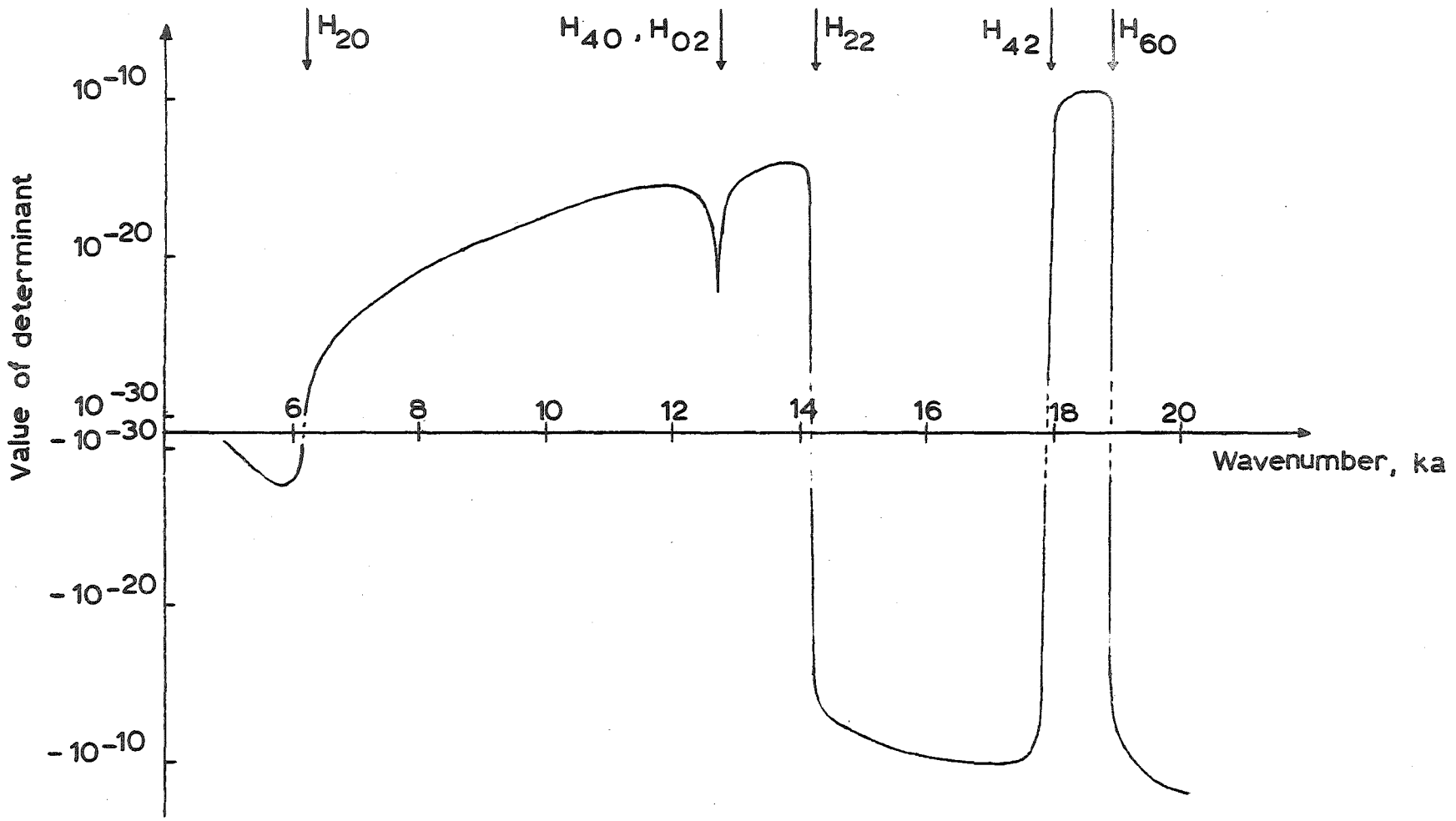

Fig. 2.3: Behaviour of determinant value, $\mathrm{Det}(A^{+}_{mn}(k))$, as a function of the wavenumber ka for the H-modes with even symmetry about both $\varphi = 0$ and $\varphi = \pi/2$ in a rectangular waveguide (b/a = 1/2).

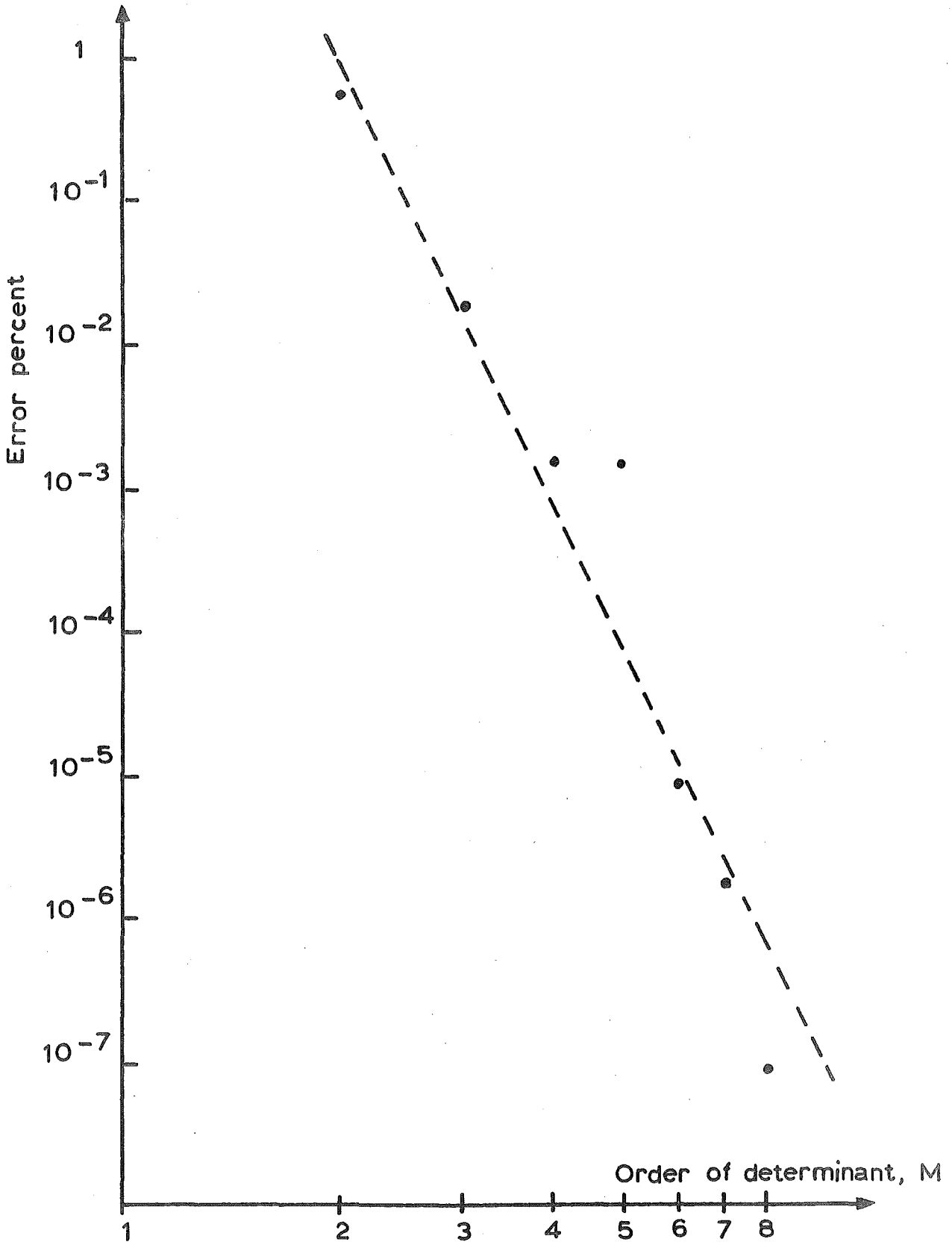

Fig. 2.4: Error in calculating the cutoff wavenumber of the H_{31} mode of a 2.25 : 1 rectangular waveguide by the null field method as a function of the determinant order. Number of integration points = 69.

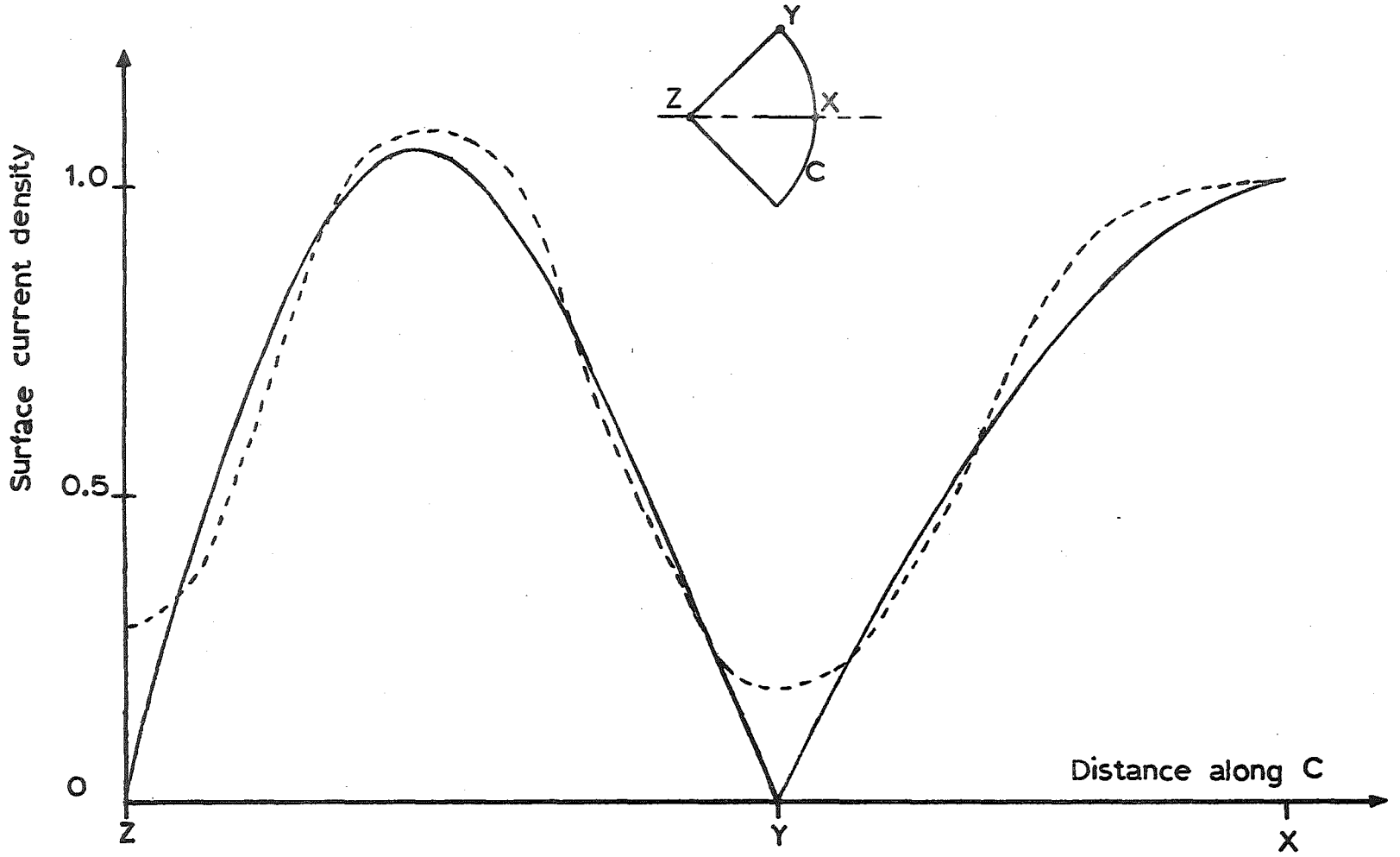

Fig. 2.5: Surface current density for lowest order E-mode in sector waveguide ($\beta = 3\pi/2$). F(C) normalised to 1.0 at the point X. Full line denotes surface current density computed from exact expression, equations (B8) and (B9). --- computed F(C) using null field method.

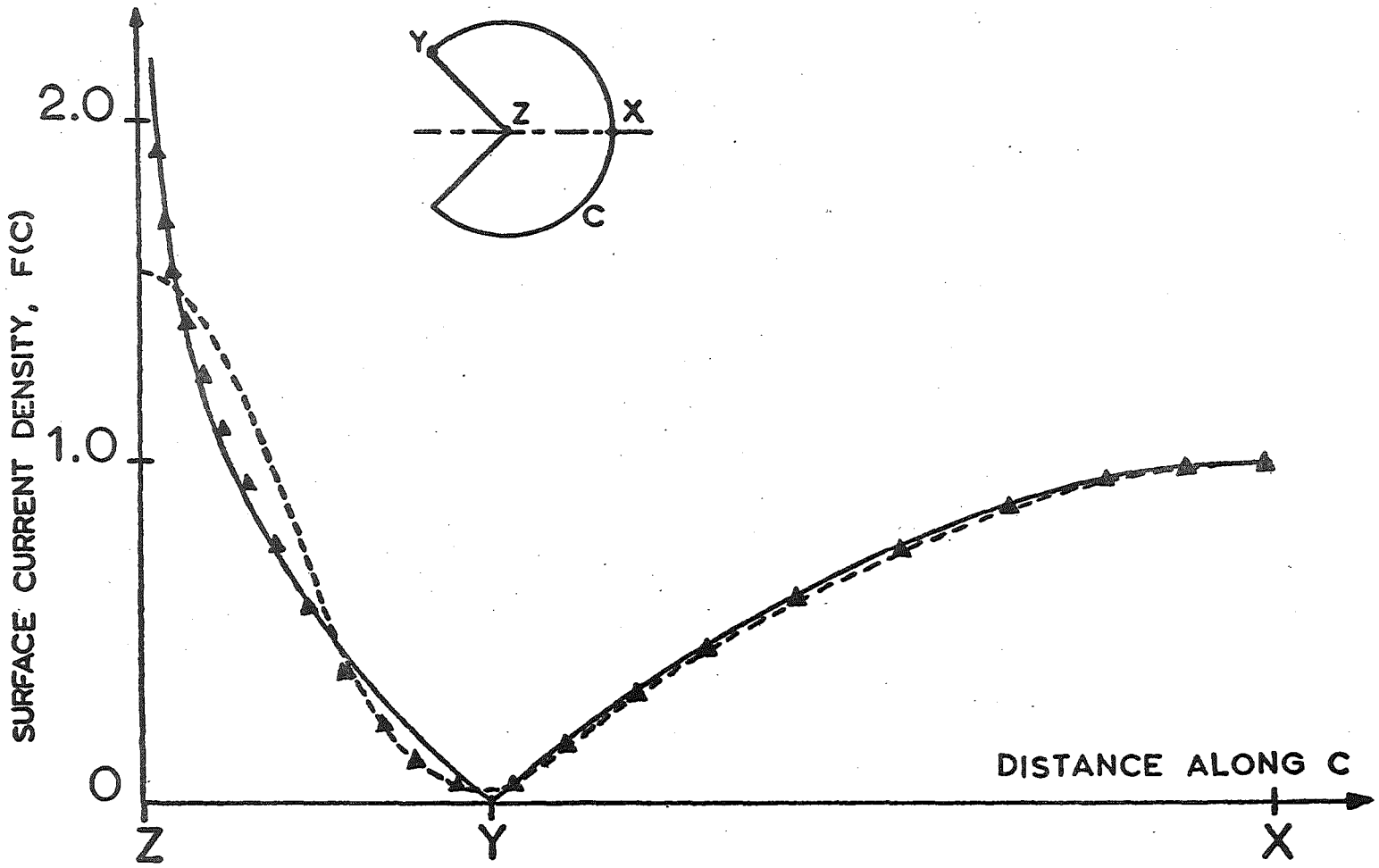

Fig. 2.6: Surface current density for lowest order E mode in sector waveguide ($\beta = \pi/2$).
F(C) normalised to 1.0 at the point X.
Full line denotes surface current density computed from exact expression, equations (B8) and (B9).
--- computed F(C) using representation 2 of Table 2.3.
▲▲▲ computed F(C) using representation 3 of Table 2.3.

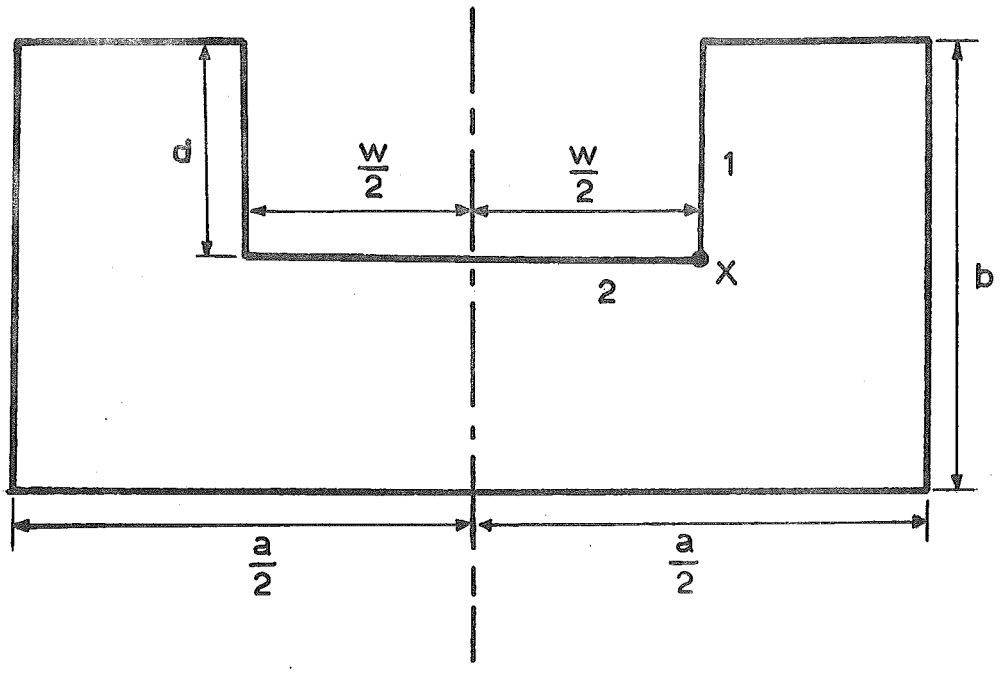

Fig. 2.7: Single-ridge waveguide.

CHAPTER 3: POINT-MATCHING METHODS

'I told you butter wouldn't suit the works!' the Hatter added, looking angrily at the March Hare.
'It was the best butter,' the March Hare meekly replied.

Lewis Carroll

An investigation of the numerical solution of the waveguide problem by point-matching methods is presented in this chapter. Results obtained show that the complete point-matching method is less accurate for shapes with reentrant parts. The alternative point-matching method is found to be more error sensitive than the complete point-matching method. The straightforward point-matching method does not always give the correct wavefunctions and its validity is related to an internal Rayleigh hypothesis. An extended point-matching method is introduced to handle cases for which previous methods fail.

3.1 INTRODUCTION

A review of point-matching methods is given in section 1.2.5 where the equations for the complete, alternative and straightforward point-matching methods are given. The chief advantage of the point-matching methods is that they do not require the time-consuming and storage-consuming ancillary computations which are usually necessary with other techniques (chapter 1). A summary of the equations for the point-matching methods is given in Tables 3.1 and 3.2. As with the null field

method (sec. 2.2), where one-fold symmetry of C exists, the wavefunction for the straightforward point-matching method or the surface current densities for the complete or alternative point-matching methods are either even or odd functions about the line of symmetry. In this case each "m" term in the summation in the respective equations (sec. 1.2.5, see Tables 3.1 and 3.2) can be added to or subtracted from the "-m" term to produce the same summation expressions but with the exp term replaced by cos or -sin (see Tables 3.1 and 3.2). Where two-fold symmetry of C exists, the expressions can be separated into four distinct cases (Tables 3.1 and 3.2). When one or two-fold symmetry of C is present, points distributed along a half or a quarter of C need only be taken.

The cutoff wavenumbers are those values of k which null the determinant formed from the $d_{mn}(k)$ of Tables 3.1 and 3.2. For each cutoff wavenumber, the wavefunction (for the straightforward point-matching method) or surface current density (for the complete and alternative point-matching methods) is evaluated approximately by giving a convenient constant value to one of the A_m or F_n (and G_n) and then solving for the remaining members by pivotal elimination (Goodwin 1961, chap.1).

The complete point-matching method, being derived from the null field equations (2.3) and (2.4), is a rigorously based method (Bates 1969b) but it is less effective for shapes with reentrant parts for which the errors in the computed cutoff wavenumbers are larger.

The straightforward point-matching method has the same determinant as the complete point-matching method (Bates 1969b; see also tables 3.1 and 3.2) and hence give the same computed wavenumbers. However, the two methods differ in the index over which the summation is made (Tables 3.1 and 3.2) and the wavefunctions computed by them differ in general. The straightforward point-matching method can give erroneous wavefunctions.

A combined theoretical and computational study of the practical applicability of the point-matching methods and the reasons for their frequent failure is given in the following sections. An extended point-matching method is introduced and illustrated by a number of computational examples, which demonstrate the increased usefulness of the method.

3.2 COMPLETE POINT-MATCHING

Divide the curve C into a number of parts of equal arc length. The complete point-matching method (CPM) is derived from the null field equations (2.3) and (2.4) (Bates 1969b) by considering the surface current densities F(C) and G(C) to be constant over each part. The equations are given in Tables 3.1 and 3.2.

Table 3.3 gives the computed cutoff wavenumbers (truncated to the second decimal place) for the first four E-modes in a rectangular waveguide (Fig. 2.2) for three values of d/a. The order of the determinant used is denoted by M. The results obtained are accurate to at least three significant figures and are not significantly affected by small displacements of the origin.

(Refer to the next section for a discussion of the results given for the alternative point-matching method.) A more detailed examination of the computed wavenumber for the lowest order E-mode in a rectangular waveguide (with a = 2.25 and b = 1) is given in Table 3.4. It is seen that the computed value is accurate to at least seven significant figures for M = 6, where M is the order of the determinant used. Results for the H-modes in a rectangular waveguide (b/a = 1/2) are given in Table 3.5. A plot of the typical behaviour of the determinant as a function of the wavenumber k is shown in Fig. 3.1. The behaviour resembles that for the null field method (Fig. 2.3) and degenerate modes again produce the sharp cusp of the double root.

Table 3.4 shows that the error in the computed wavenumber is proportional to M^{-25} before it settles down to the more accurate value at about M = 7. This initial asymptotic convergence rate is more rapid than that (M^{-10} to M^{-14}) of the null field method. Fig. 3.2 shows the wavenumbers computed using the CPM as a function of M for the first four E-modes in a sector waveguide with $\beta = 3\pi/2$ (Fig. 2.1). The results show that there is an initial rapid convergence rate of about M^{-20}. The computed cutoff wavenumbers then undergo very small oscillations about the steady values (from M about 6 onwards). The computed cutoff wavenumbers (at the steady values) are accurate to at least four significant figures. The computed cutoff wavenumbers, truncated to the third decimal place, for E and H-modes are given in Table 3.6.

Fig. 3.3 shows the computed F_n given by the CPM (with M = 8) for the lowest order E-mode in the sector waveguide ($\beta = 3\pi/2$). The computed cutoff wavenumber ka, accurate to five significant figures, is 5.1356. The computed F_n are seen to agree reasonably well with the exact surface current density computed from eqns (B8) and (B9) given in Appendix B2.

For a sector waveguide (Fig. 2.1) with $\beta = \pi/2$ (a Type 3 shape, Fig. 1.5) the complete point-matching method produces less accurate results. The computed cutoff wavenumber with M = 8 for the lowest order E-mode is ka = 3.3078 (see Table 2.3). This differs by 2% from the accurate value of 3.3756. A plot of the computed surface current density for this case is shown in Fig. 3.4. It is seen that the computed surface current density agrees reasonably well with the accurate current density for the part XY of the curve C and the agreement is poorest in the part YZ of the curve C where the exact surface current density is singular at the corner Z.

The results obtained show that, in general, the CPM gives accurate results if the waveguide cross-section is convex and is less accurate for shapes with reentrant parts and especially reentrant corners. The decrease in accuracy is due to the fact that the CPM formulas are derived by evaluating the integrals in eqn (2.3) and (2.4) using a trapezoidal integration rule. Because of the limited number of integration points considered in the numerical integration process, inaccurate results are obtained if the integrands of the integrals vary too rapidly.

3.3 ALTERNATIVE POINT-MATCHING

The simplified, alternative point-matching formulas (Bates 1969b) are derived from the CPM (or null field) formulas (sec. 1.2.5.4). The formulas, which are given in Tables 3.1 and 3.2, are relatively simpler than the CPM formulas as they contain only exponential or trigonometric functions. This simplicity however is achieved with a loss in sensitivity. This property is made clear by the following analysis.

The field E_z for an E-mode in a waveguide at cutoff is given by eqn (2.1). Consider a point P outside C such that $R \gg r$ (see Fig. 1.1). Then

$$R \simeq \rho - r\cos(\theta-\varphi) \tag{3.1}$$

and equation (2.1) becomes, using the asymptotic expansion for $H_0^{(2)}$ (Abramowitz and Stegun 1965, sec. 9.2)

$$E_z \simeq (z/(\pi k\rho))^{\frac{1}{2}} \exp(j[\pi/4-k\rho]) \cdot \int_C F(C) \exp(jkr\cos(\theta-\varphi))\, dC, \tag{3.2}$$

which is an expression for E_z in the 'far field' region. But the field is completely zero outside the waveguide (extended boundary condition) and this results in the condition (using (3.2))

$$\int_C F(C) \exp(jkr\cos(\theta-\varphi))\, dC = 0. \tag{3.3}$$

By taking (2N+1) values of φ and denoting these by ψ_m and using a trapezoidal integration rule we obtain the alternative point-matching equation for E-modes (Table 3.1). A similar analysis using eqn (2.2) leads to the

H-mode formula. The alternative point-matching method (APM) thus explicitly satisfies the null field condition only in the 'far field' region and as a consequence is significantly more error sensitive than the CPM. Tables 3.3 and 3.4 compare results for the APM and CPM used in computing the cutoff wavenumbers in a rectangular waveguide (Fig. 2.2). The APM gives results almost as accurate as the CPM when d = 0, but the accuracy of the APM falls off rapidly as d increases (Table 3.3). Because of this little effort has been expended on the APM. Fig. 3.5 shows the typical behaviour for the determinant formed from the $d_{mn}(k)$ (Tables 3.1 and 3.2) for the APM. The oscillatory behaviour, on comparison with Fig. 3.1, is seen to be similar to that of the CPM.

3.4 STRAIGHTFORWARD POINT-MATCHING AND THE INTERNAL RAYLEIGH HYPOTHESIS

Refer to Fig. 3.6. The closed curve C is the cross-sectional shape of a waveguide and lies in the plane Ω. The interior and exterior of C are denoted by Ω_- and Ω_+ respectively. The largest circle which is enclosed by C and the smallest circle which encloses C, both circles centred at O, have radii r_- and r_+ respectively. A general solution of the Helmholtz equation (1.2) valid in at least a neighbourhood of O, is (see sec. 1.2.5.1)

$$U(\rho,\varphi) = \sum_{m=-\infty}^{\infty} A_m J_m(k\rho) \exp(-jm\varphi). \qquad (3.4)$$

The uniqueness of analytical continuation (Bochner and

Martin 1948, pp 33-35) ensures that the right hand side (R.H.S.) of equation (3.4) is a complete representation of U at all points $P \in \Omega_-$ for which the (R.H.S.) of equation (3.4) is uniformly convergent. Also, at all points $P \in \Omega_+$ for which the R.H.S. of equation (3.4) is uniformly convergent, the R.H.S. of equation (3.4) is the analytic continuation of U from Ω_- into Ω_+. Define

r_0 = <u>radius of convergence of the R.H.S. of equation (3.4)</u>.

The exact field at any point P (for the E-mode) given by equation (2.1) can be rewritten (Bates 1967, Millar and Bates 1970) as (using the addition theorem for Bessel functions (Watson 1968, chap. 11))

$$E_z(\rho,\varphi) = \sum_{m=-\infty}^{\infty} [A_m J_m(k\rho) + B_m(k\rho)] \exp(-jm\varphi), \quad (3.5)$$

where

$$\left.\begin{aligned} A_m &= -j \int_C F(C)\, Y_m(kr) \exp(jm\theta)\, dC, \\ B_m(k\rho) &= j \int_{\alpha(\rho)} [J_m(k\rho)\, Y_m(kr) \\ &\quad - Y_m(k\rho)\, J_m(kr)]\, F(C) \exp(jm\theta)\, dC. \end{aligned}\right\} \quad (3.6)$$

$\alpha(\rho)$ is that part of C which is enclosed by the circle with centre O and radius ρ (i.e. OP). When $\rho < r_-$, $\alpha(\rho)$ is identically zero and hence

$$B_m(k\rho) \equiv 0, \quad \rho < r_-. \quad (3.7)$$

The exact eqn (3.5) then corresponds to eqn (3.4). This analysis shows that for equation (3.4), $r_0 \geqslant r_-$. However, unless the R.H.S. of equation (3.4) is absolutely convergent there must be a point S (see Fig. 3.6)

either on or outside C, at which the R.H.S. of eqn (3.4) ceases to be analytic. Millar (1969, 1970, 1971) has investigated in great depth the conventional Rayleigh hypothesis, which is the assumption that the field scattered from a body may be expressed everywhere outside the body as a single series of outward travelling waves. The analysis (which is quite involved) attempts to locate the region of convergence by finding out when analytic continuation cannot be made.

An internal Rayleigh hypothesis (IRH) is introduced here, which is the assumption that the R.H.S. of equation (3.4) is valid everywhere in Ω_-, which can be stated concisely as

The IRH assumes that $r_0 \geq r_+$.

In the straightforward point-matching method (SPM), the R.H.S. of equation (3.4) is made to satisfy the boundary condition, eqn (1.4), at a finite number of points (see sec. 1.2.5.1). Consequently, the SPM assumes that the IRH holds. The SPM equations are given in Tables 3.1 and 3.2 and the computed wavefunction is

$$U(\rho,\varphi) = \sum_{m=-N}^{N} A_m J_m(k\rho) \exp(jm\theta). \qquad (3.8)$$

(To avoid confusion, the limits of the summation in (3.8) are denoted by N and not M as M is used to denote the order of the determinant used.)

3.4.1 Rectangular Waveguide

Millar's (1969, 1970, 1971) analysis is given for the case when C is an analytic curve and he concludes

(or at least appears to conclude) that unless C is analytic the assumed solution will always have singularities on C. This suggests that S cannot be any further from O than the nearest sharp corner of C. The following example shows however that this is not necessarily so.

Denote by ϕ the included angle of any sharp corner possessed by C. If

$$\pi/\phi = I = \text{a positive integer} \tag{3.9}$$

then U is analytic in the neighbourhood of the corner (Jones 1964, sec. 9.2). For instance, consider an E-mode in the rectangular waveguide shown in Figure 2.2. All four corners satisfy the condition (3.9). For a mode with even symmetry U has the form (see e.g. Jordan and Balmain 1968, chap. 8), when d = 0,

$$U(\rho,\varphi) = \cos(p\pi x/a)\cos(q\pi y/b) \tag{3.10}$$

where p and q are odd integers. Expressing the rectangular coordinates on the R.H.S. of equation (3.10) in their polar form, using formulas based on the generating functions for Bessel functions (Abramowitz and Stegun 1965, p.361) and rearranging the resulting expressions gives

$$U(\rho,\varphi) = \sum_{m=-\infty}^{\infty} (-)^m J_{2m}(\pi R\rho)\cos(2m\beta)\exp(j2m\varphi) \tag{3.11}$$

where $R^2 = (p/a)^2 + (q/b)^2$ and $\cos(\beta) = p/aR$. The R.H.S. of equation (3.11) is found to be valid for all ρ

so that $r_0 = \infty$ for even E-modes (and, as is easily established, all modes) in the rectangular waveguide. However, if $\bar{Q}$ is the point on C of the sharp corner (if one exists) closest to O for which

$$\pi/\bar{\phi} \neq I \tag{3.12}$$

where $\bar{\phi}$ is the included angle of the corner, then (Jones 1964, sec. 9.2) U is almost always not analytic at $\bar{Q}$, so that almost always

$$r_0 \leqslant \bar{r} \tag{3.13}$$

where $\bar{r}$ is the radial coordinate of $\bar{Q}$. If $\pi/\bar{\phi}$ is irrational, U is never analytic at $\bar{Q}$. If $\pi/\bar{\phi}$ is rational, U can be analytic at $\bar{Q}$ under special circumstances, as is discussed later in sec. 3.4.3.

3.4.2 Effect of Concave Curvature of C

This section is concerned with estimating the position of singular points (such as the point S of Figure 3.6) when C has one or more parts which are strongly concave, when viewed from outside the waveguide.

Figure 3.7 shows arbitrary waveguides with walls that are in part strongly concave when viewed from outside. Consider a point Q_0, with centre of curvature T_1, on a concave part of C. It is natural to represent the wavefunction, in the neighbourhood of that part of the extension of the line T_1Q_0 which lies in Ω_-, by a series such as

$$U = \sum_q D_q Z_q(\tau,\psi) \tag{3.14}$$

where each $Z_q(\tau,\psi)$ satisfies both the Helmholtz equation (1.2) and the appropriate boundary condition on C and $\{D_q\}$ is a particular set of constants. The origin of the (τ,ψ) coordinates is taken at some convenient point T_0 on the line T_1Q_0 or its extension. For instance, in Figure 3.7(a), if the inner part of C is a circle of radius b centred on T_0 (which is the same as T_1 in this case) then

$$Z_q(\tau,\psi) = [J_q(k\tau) - d_q\, Y_q(k\tau)]\cos(q\psi+\theta_q) \qquad (3.15)$$

where each θ_q is a real constant and

$$\left.\begin{aligned} d_q &= J_q(kb)/Y_q(kb), \quad \text{E-modes} \\ d_q &= J'_q(kb)/Y'_q(kb), \quad \text{H-modes} \end{aligned}\right\} \qquad (3.16)$$

Yee and Audeh (1966b) have obtained accurate results by developing, from equations (3.15) and (3.16), formulas which are special cases of what is later introduced as extended point matching. Their work confirms that T_0 corresponds to the point S of Figure 3.6, since each Z_q when given by equation (3.15) is singular at T_0. So, the R.H.S. of equation (3.4) can only be used as a representation of U for $\rho < r_0 = OT_0$.

If the inner part of C in Figure 3.7(a) is an ellipse centred at T_0 with semi-major-axis T_0Q_0 and focus (nearest Q_0) at T_2, then as Millar (Millar and Burrows 1969) has pointed out the analytic continuation of U from Ω_- into Ω_+ becomes singular at T_2, which then corresponds to the point S of Figure 3.6, because the Z_q of equation (3.14) are Mathieu functions singular at

T_2. So, $r_0 = OT_2$, which will usually be less than OT_1, where T_1 is the centre of curvature for Q_0. For an ellipse of eccentricity e

$$Q_0T_1/Q_0T_2 = 1 + e \qquad (3.17)$$

Millar (1971) has examined the wavefunction above a periodic sinusoidal surface, having the form $y = b \cos(x/a)$ where a and b are constants and (x,y) are rectangular coordinates. Denote the point (x = 0, y = b) by Q_0. When b/a = 0.448, Millar (1971) has shown that the point T_2 at which the analytic continuation of the wavefunction becomes singular is closer to Q_0 than is the centre of curvature T_1. In fact, $Q_0T_1/Q_0T_2 = 2.49$.

3.4.2.1 Rounded sector waveguide

Figure 3.8 shows the rounded sector waveguide for which there is no closed form expression for the wavefunction. The origin of the (τ,ϕ) coordinates is denoted by T, not S, because the analytic continuation of the field becomes singular closer to C, as is shown below. The centre of the larger circular arc, of radius a, is denoted by R.

The density of equivalent surface sources on the rounded sector waveguide has been computed by the null field method (chapter 2) together with the A_m (computed from (3.6)) required for the R.H.S. of eqn (3.8). Table 3.7 shows the convergence of the R.H.S. of equation (3.8) with M, for particular values of the parameters shown in Fig. 3.8. It is seen that the convergence is

poor for $\rho/a > 0.4$, suggesting that the R.H.S. of equation (3.8) is the truncated form of a summation, such as the R.H.S. of equation (3.4), having a finite radius of convergence r_0, which is less than OT ($OT/a = 0.645$). Consequently, in Figure 3.8 the point S, at which it is conjectured that the analytic continuation of the wavefunction becomes singular, is shown closer to O than is T.

It is tempting to try and find an estimate of Q_0T_1/Q_0T_2 in terms of the rate of change of curvature at Q_0. The examples of the ellipse and the periodic surface suggest that this might be possible. However, the curvature is constant on the rounded parts of the rounded sector waveguide and yet S appears to be closer to C than is T (see Figure 3.8).

Refer to Figure 3.7(b). Suppose that, when C has a concave part, Q_0 is the point on the concave part for which the radius of curvature T_1 is closest to O. The above results suggest strongly that the IRH will fail unless Q_0T_1/Q_0T_+ is about 2 or more, where T_+ is the intersection of Q_0T_1 with the circle having centre O and radius r_+.

3.4.3 Consequences of Failure of IRH

3.4.3.1 Segment waveguide

Fig. 3.9 shows the segment waveguide for which the wavefunctions are known in closed form (see Appendix A). The cutoff wavenumbers are those values of k which satisfy either of the conditions (A2). Eqn (A1) shows that U is singular at $\tau = 0$, and in keeping with the

notation illustrated in Fig. 3.6, the origin of the (τ,ϕ) coordinates has been designated by S in Fig. 3.9.

Detailed computations have been made for a segment waveguide (Figure 3.9) for which $\eta = 3\pi/2$ and $b/a = 0.3$. It is apparent that the position of O cannot be chosen such that $OS \geqslant r_+$ (see Figure 3.6), which means that the IRH must fail in general because U is always singular at S. For the two lowest order E-modes at cutoff, the exact expression (A2) gives, for $q = 1$ and 2 respectively, $ka = 4.5457$ and 4.9189. With a determinant order M of 13 and the origin O of the (ρ,φ) coordinate being chosen such that $d/a = 0.5$, the SPM predicts 3.6078 for the first of these values and fails to predict the second. The members of $\{A_m\}$ for the SPM have been computed for $M = 13$ for the lowest mode $(q = 1)$. Fig. 3.10(a) show where the SPM wavefunction (R.H.S. of eqn (3.8)) becomes zero. The results indicate that the SPM wavefunction satisfies the proper E-mode boundary condition (1.4) on curves in Ω different from C. The dotted line in Figure 3.10(b) is a complete version of one of these curves.

3.4.3.2 Sector waveguide, $\eta = 109^\circ$

Consider the sector waveguide (Fig. 2.1). The wavefunction is given in eqn (A1) of Appendix A (with $B_q = 0$). The wavefunction is singular at S, unless π/η is an integer or, in certain special cases π/η is rational.

In a sector waveguide for which $\eta = 109^\circ$, the position of O can be chosen such that $OS = r_+$, so that

the IRH is valid. The SPM wavefunction for the lowest order E-mode has been computed with M = 9, and Figure 3.11 shows that it is zero on C, except close to S (U is non-analytic at S, even though the IRH is valid, so that one cannot expect the SPM wavefunction to behave properly close to S). However, the exact wavefunction is itself small in the vicinity of S so that this discrepancy has little effect on the cutoff wavenumber computed using the SPM (e.g. the computed SPM cutoff wavenumbers ka for the four lowest order E-modes of 4.6896, 6.7491, 7.9364 and 8.7177 are all accurate to the fifth significant figure).

The results of Figs 3.10 and 3.11 show that when the IRH holds, the SPM computations are accurate; and when the IRH fails, the SPM computations converge, although usually more slowly, but the results apply to cross-sectional shapes different from the ones being investigated. The computations suggest that the IRH is valid for these new cross-sectional shapes. For instance, C in Figure 3.10(b) is strongly concave when viewed from outside (this is way the IRH fails), but the dotted curve is smoothly convex.

3.4.3.3 Sector waveguide, $\eta = 3\pi/2$

Table 3.8 shows cutoff wavenumbers for a sector waveguide for which $\eta = 3\pi/2$, which means that $OS < r_+$ necessarily. The results emphasize both that the SPM sometimes predict spurious wavenumbers and that it rests on the IRH. Note that the order $q\mu$ of the Bessel functions in (A1) is an integer for certain values of

q, when $\eta = 3\pi/2$. $B_q = 0$ for the sector waveguide, so that when $q\mu$ is an integer, U is regular at S, and the IRH holds. In Table 3.8, asterisks mark the exact cutoff wavenumbers of modes for which the IRH holds. It is seen that the SPM is accurate for these modes, but is generally inaccurate and more slowly convergent for other modes. The relation of the SPM and the IRH is borne out clearly in Figs 3.12 and 3.13 which give the fields computed from the SPM wavefunction for the first two E-modes. The IRH does not hold for the lowest E-mode and Fig. 3.12 shows that the field given by the SPM (with M = 8 and ka = 3.3078, see also Table 2.3) does not satisfy the required E-mode boundary condition on C, except at the matching points. This is further illustrated by Tables 2.4 and 2.5 which give values for the SPM wavefunction at various points along $\varphi = \pi$ and on C respectively. The IRH holds for the second E-mode and the field shown in Fig. 3.13 is correct (M = 8 and ka = 5.1356 in the SPM).

The results of Table 3.8 show that when the IRH fails, actual wavenumbers may not be predicted at all, even inaccurately, and spurious ones can appear (see the first E-mode in Table 3.8).

The SPM and the CPM both lead to the same determinant, whose vanishing gives the modal cutoff wavenumbers. The CPM does not depend on the IRH and is always rigorously based. Yet the CPM does not predict accurate wavenumbers when the IRH fails. The explanation for this is that the CPM formulas are derived by

evaluating the integrals in eqn (2.3) and (2.4) using a trapezoidal integration rule (sec. 3.2). When the IRH fails, the integrands of these integrals vary too rapidly for the trapezoidal rule to give accurate results.

3.5 EXTENDED POINT-MATCHING

The R.H.S. of equation (3.4) can be thought of as a two-dimensional Taylor series. The wavefunction U, or its analytic continuation from Ω_- into Ω_+, often has singular points. So, the R.H.S. of equation (3.4) is not valid for values of ρ greater than the distance from O of the closest singular point. Consequently, the R.H.S. of equation (3.8) cannot be used for values of ρ greater than this.

An extended point-matching method (EPM) is introduced here. Series representations for U are still used in order to maintain computational simplicity.

In general, it is impossible to find a single series for U which is valid throughout Ω_-. So, take a region $\Lambda_\ell \subset \Omega$ in which U can be written as (see Figure (3.14))

$$U(\rho,\varphi) = \sum_q D_{\ell,q}\, Z_{\ell,q}(\tau,\psi), \qquad P \in \Lambda_\ell \tag{3.18}$$

where the origin of the (τ,ψ) coordinates is a point O_ℓ, which may or may not lie in Λ_ℓ. The functional forms of the members of $\{Z_{\ell,q}\}$ must accommodate any singularities which exist in Λ_ℓ. There must be sufficient regions, say L of them, such that

$$\Omega_- \subset \Lambda_1 \cup \Lambda_2 \cup \ldots \cup \Lambda_L \tag{3.19}$$

Denote by $C_{\ell m}$ a continuous curve which lies in $\Lambda_\ell \cap \Lambda_m \cap \Omega_-$. For each of the L values of ℓ, the R.H.S. of equation (3.18) is made to satisfy the appropriate boundary condition at a number of points which lie on $C \cap \Lambda_\ell$. Also, the R.H.S. of equation (3.18) for $\ell = m$ and its derivative normal to C_{mn} respectively is matched at a number of points on C_{mn} to the R.H.S. of equation (3.18) for $\ell = n$ and its derivative normal to C_{mn}. This ensures proper continuity of U throughout Ω_-.

The set $\{\Lambda_\ell\}$ is not unique. Ingenuity is always needed in choosing both it and $\{Z_{\ell,q}\}$. However, the examples examined in the following section show that the EPM is often convenient and accurate.

Let $\{Z_{\ell,q}\}$ be of the class $\mathcal{A}$(on Γ_ℓ), if all its members satisfy the appropriate boundary condition on a curve Γ_ℓ. The size of the parts of C, on which point matching is required, is reduced if $\Gamma_\ell \cap C$ is not empty. Usually there are parts of Γ_ℓ not on C, which means that there are extra (beyond the physical requirements of the problem) constraints on the wavefunction, unless symmetry ensures that, either U must satisfy the appropriate boundary condition on the parts of Γ_ℓ not on C, or that the wavefunction satisfies Dirichlet or Neumann boundary conditions at all points, for all ℓ and m, where Γ_ℓ intersects $C_{\ell m}$. The latter condition occurs when $C_{\ell m}$ is part of a line of symmetry of the wavefunction U. The wavefunction is then either odd or even about $C_{\ell m}$. Let Γ_ℓ belong to the class $\mathcal{L}_0$ if $\Gamma_\ell \subset C$. If $\Gamma_\ell \not\subset C$ but $\Gamma_\ell \cap C$ is not empty, then Γ_ℓ is defined as

belonging to the class $\mathcal{L}$, or $\bar{\mathcal{L}}$, if there are not, or are, extra constraints on the wavefunction.

3.5.1 Some Applications of the EPM

3.5.1.1 Two conductor waveguides with circular inner conductor

A simple example of the EPM is Yee and Audeh's (1966b) treatment of two-conductor waveguides (Figure 3.7(a)) for which the inner part (call it Γ_1) of C is a circle. They assume L = 1 with $O_1 = T_0$. Their $\{Z_{1,q}\}$ is $\{Z_q\}$ as defined by equation (3.15), so that $\{Z_{1,q}\} \in \mathcal{A}$ (on $\Gamma_1 \in \mathcal{L}_0$).

3.5.1.2 Rounded sector waveguide

When $\eta = 3\pi/2$ and b/a = 0.35, Table 3.7 suggests strongly that the IRH fails. The EPM can be applied in a simple fashion by assuming that L = 1 with $O_1 = T$. It is convenient to write equation (3.18) in the form

$$U(\rho,\varphi) = \sum_{q=0}^{M_1-1} D_q^{(1)} J_q(k\tau) \begin{matrix}\cos\\ \sin\end{matrix}(q\psi) + \sum_{q=0}^{M_2-1} D_q^{(2)} Y_q(k\tau) \begin{matrix}\cos\\ \sin\end{matrix}(q\psi) \qquad (3.20)$$

where cos and sin respectively apply to modes with even and odd symmetry about $\psi = 0$. Because of this symmetry the appropriate boundary condition only needs to be satisfied explicitly on $\hat{C}$, which is that part of C for which $\psi > 0$. Refer to Figure 3.8. The boundary condition is satisfied at N_1 points on that part of $\hat{C}$ for which $\tau = b$, and at N_2 points on the rest of $\hat{C}$, where $(N_1+N_2) = (M_1+M_2)$. Table 3.9 compares the results obtained with the EPM, for the lowest order even E-mode,

with the result obtained with the null field method. The value of ka obtained with the EPM, for the lowest order even E-mode, is 3.22. The result obtained with the null field method is 3.20 which agrees to better than 1%. It is interesting to compare the EPM with the SPM. For M equal to 11, 12, 13 and 14 the SPM gives values for ka of 2.61, 2.92, 2.71 and 2.62 respectively. There is no definite numerical convergence, but the wavenumber oscillates within about 20% of the accurate value. Figure 3.15 shows (for M = 12) where the SPM and EPM wavefunctions go to zero. The EPM values follow C very closely, but the SPM values bear no relation to C. For the EPM results quoted above, $\{Z_{\ell,q}\} \notin \mathcal{A}$ so that point matching had to be carried out on all of $\hat{C}$. The effect of using sets of functions belonging to $\mathcal{A}$ is considered next. First, L = 2 is taken with O_1 = T, O_2 = R and C_{12} the part shown dotted in Figure 3.8 of the circle of radius b centred at R. Γ_1 is the circle τ = b, and Γ_2 is in two parts: the circle of radius a centred at R and the semi-infinite straight lines meeting at R and parallel to the directions $\varphi = \pm \eta/2$. The wavefunction in Λ_1 is taken to be

$$U(\rho,\varphi) = \sum_{q=0}^{M_1} D_q[J_q(k\tau) - d_q Y_q(k\tau)] \begin{matrix}\cos\\ \sin\end{matrix}(n\psi), \qquad P \in \Lambda_1 \qquad (3.21)$$

where d_q is given by equation (3.16) and cos and sin apply respectively to H-modes and E-modes. In Λ_2 the wavefunction is written as a sum of M_2 wavefunctions

having the form of the R.H.S. of eqn (A1). The appropriate boundary conditions are then satisfied identically on all C and point matching only had to be carried out on C_{12}. But $\Gamma_1 \in \bar{\mathcal{L}}$ and $\Gamma_2 \in \bar{\mathcal{L}}$, and the extra constraint on the wavefunction is very severe. Values for ka of 1.79, 2.56, 3.18 and 3.39 are obtained (with $M_1 = 3$ and $M_2 = 4$). The third of these is close to the accurate value, but the others are spurious. The fourth is close to the value 3.376 appropriate to the sector waveguide (b = 0). To reduce the severity of the extra constraint, L = 1 is taken with $O_1 = T$. The wavefunction is represented by the R.H.S. of (3.21). Hence $\{Z_{1,q}\} \in \mathcal{A}$ (on Γ_1) where Γ_1 is the circle $\tau = b$. Note that it is still true that $\Gamma_1 \in \bar{\mathcal{L}}$. With $M_1 = 8$, values for ka of 2.56 and 3.23 are obtained so that only one spurious wavenumber remained and the correct one, 3.23, is accurate to 1%.

3.5.1.3 Meinke waveguide

Fig. 3.16 shows the Meinke waveguide, first studied by Meinke et al. (1963), and the ridge waveguide. The dashed lines in Fig. 3.16 are the reflections of C in the line y = 0.

The two semicircular indentations in Figure 3.16 (a) ensure the failure of the IRH. The shape of C suggests L = 2 with the rectangular coordinates of O_1 and O_2 being (0, 0) and (0, d) respectively. Λ_1 and Λ_2 are symmetrical about the line y = d/2, $|x| < a/2$ which is taken for C_{12}. Take $\{Z_{1,q}\} \in \mathcal{A}$ (on Γ_1) where Γ_1 is in two parts: the circle $\tau = b$ and the straight line

$\phi = 0, \pi$. The symmetry of the waveguide ensures that $\Gamma_1 \in \mathcal{L}$. The wavefunction in Λ_1 is taken to have the same form as the R.H.S. of equation (3.21). Point matching is only necessary on the parts of C for which $|x| = a/2$ and on C_{12}. Table 3.10 shows the values given by the EPM for the cutoff wavenumbers of the four lowest order H-modes, compared with the values obtained by Bulley and Davies (1969) who used a variational (Rayleigh-Ritz) method. The agreement is to within 0.1% for the first three modes.

3.5.1.4 Ridge waveguide

The wavefunction is necessarily singular at the points O_1 and O_2 of Figure 3.16(b) so that the IRH fails. The shape of C suggests L = 2 with O_1 and O_2 positioned as shown in Figure 3.16(b). Λ_1 and Λ_2 are symmetrical about the line $x = 0$, $d < y < b$ which is taken for C_{12}. Take $\{Z_{1,q}\} \in \mathcal{A}$ (on Γ_1) where Γ_1 consists of the two semi-infinite straight lines $\phi = 0$ and $\phi = 3\pi/2$. The symmetry of the waveguide ensures that $\Gamma_1 \in \mathcal{L}$. To satisfy the edge conditions (Jones 1964, chap. 9.2)

$$U(\rho,\varphi) = \sum_{q=0}^{M_1} D_q \, J_{2q/3}(k\tau) \begin{matrix}\cos\\ \sin\end{matrix}(2q\phi/3), \quad P \in \Lambda_1 \tag{3.22}$$

where cos and sin apply respectively to H-modes and E-modes. U has the correct singular behaviour (Jones 1964, sec. 9.2) at O_1. This has already been noticed by Davies and Nagenthiram (1971) who have shown that accurate results can thereby be obtained. A similar approach has been used by Bolle and Fye (1971) to

compute accurately the scattering from quadrilateral cylinders. Agreement to better than 0.1% with the results reported by Beaubien and Wexler (1970) and Davies and Muilwyk (1966) have been obtained (Table 3.11). The results for the E-modes (Table 3.11) by the EPM predict a mode (ka = 7.003) which is not present in Beaubien and Wexler's results. This mode does not seem to be spurious and an inspection of Fig. 19 in Beaubien and Wexler's paper indicates that a mode in between the modes of their Figs 19(a) and 19(c) is missing.

The ridge waveguide illustrates the necessity of making L large enough to accommodate all singularities of the wavefunction. Table 3.12 compares cutoff wavenumbers got from the EPM (with L = 2 as described above) and from Pyle (1966) who used a transverse resonance method. For $0.4 < d/b < 0.8$ the agreement is very close, but for small values of d/b the agreement is poor. The reason for this is as follows.

Note that the R.H.S. of equation (3.22) is not valid for $\tau > W$ because V is singular at O_2. The dimensions of the ridge waveguide to which Table 3.12 applies are such that $\tau < W$ for all parts of Ω_- to the left of x = 0, except when $d/b < 0.038$ and $d/b > 0.962$. However, consider the reflection (shown dashed in Figure 3.16(b)) of C in the line y = 0. By symmetry, the analytic continuation of U is singular at O_3 and O_4. So, the R.H.S. of equation (3.22) is not valid for $\tau > 2d$. This means that for the EPM to give very

accurate results, with L = 2, then d/b must not be less than 0.41, which explains the disagreement between the EPM and Pyle (1966) for low values of d/b. Since the wavefunction is small near the corners with rectangular coordinates (-a/2,0) and (-a/2,b), the disagreement only becomes marked when d/b is appreciably less than 0.41. By considering the reflection of C in y = b it follows that L = 2 is theoretically insufficient for d/b > 0.59. But, as d/b increases the wavefunction becomes increasingly concentrated between the ridge and the top wall of the waveguide, which is why there is fair agreement between the EPM and Pyle for d/b > 0.6. However, to obtain very accurate results with the EPM for both small and large values of d/b, it is necessary to make L = 4.

3.6 CONCLUSIONS

If the IRH is valid, the SPM gives the resonant frequencies and the wavefunctions accurately. If C is symmetrical about two perpendicular axes then the APM gives accurate results.

If the IRH fails, the SPM is liable to give spurious results, although it gives the correct resonant frequencies of almost any cross-sectional shape to an accuracy of at least 20%. However, even if a particular resonant frequency is given with reasonable accuracy, when the IRH fails the SPM wavefunction (field strength) is always meaningless.

The validity of the IRH can be gauged by inspection of C. If there are sharp corners which do not satisfy condition (3.9) and which cannot be arranged to lie on the circle of radius r_+ (see Figure 3.6), then the IRH certainly fails. If C possesses strongly concave parts, when viewed from outside, then the final paragraph of section 3.4.2.1 on the effect of concave curvature of C gives the condition governing the probable failure of the IRH.

If it is required to obtain resonant frequencies accurate to 1% or better then it is unsafe to use the SPM or CPM if there is any suspicion of the IRH failing. The EPM can be used and give accurate results, provided both that L is large enough and that, if the set of functions used for representing the wavefunction in each Λ_ℓ belongs to $\mathcal{A}$ (on some Γ_ℓ), $\Gamma_\ell \notin \bar{\mathcal{L}}$.

Two tests may be employed to obtain indications of the accuracy of the results obtained using a point-matching method for a particular problem. Inaccurate results occur if the computed cutoff wavenumbers exhibit large oscillations (about 10%) with increasing M. An indication of the accuracy can also be obtained by an examination of the computed wavefunctions. If the computed wavefunction satisfies approximately (within a tolerable error) the imposed boundary condition at points other than the matching-points on C, then confidence can be placed on the results obtained.

The point-matching methods require determinants of order about 8-12 to obtain cutoff wavenumbers accurate

to 0.1%. The computation of each cutoff wavenumber requires a search routine (e.g. 'regula falsi' method (Abramowitz and Stegun 1965, formula 3.9.3)) and involves the evaluation of about 15 determinants. The storage requirements for the APM, SPM and EPM are approximately 9, 13 and 16 K bytes respectively. The CPU time (IBM 360/44 with 8-byte words) for evaluating a single determinant is about 0.35, 1.5 and 2.3 seconds for the APM, SPM and EPM respectively.

Table 3.1: Point-matching formulas, E-modes. The computed cutoff wavenumbers are those values of k which bring to zero the determinant formed from the $d_{mn}(k)$. L is the total length of the curve C. (r_n, θ_n) are the coordinates corresponding to C_n for the isolated points on C.

Method	$d_{mn}(k)$		
	General. Take $\lvert Det(d_{mn})\rvert$. $0 \leqslant C_n < L$. $1 \leqslant n \leqslant 2N+1$	One-fold symmetry (about $\varphi = 0$). $0 \leqslant C_n < L/2$. $1 \leqslant n \leqslant N+1$	Two-fold symmetry (about $\varphi = 0$ and $\varphi = \pi/2$). $0 \leqslant C_n < L/4$. $1 \leqslant n \leqslant N+1$
Complete point-matching $\sum_n F_n\, d_{mn} = 0$	$J_m(kr_n)\ \exp(-jm\theta_n)$	$J_m(kr_n)\ \begin{matrix}\cos\\ \sin\end{matrix}(m\theta_n)$, Even / Odd	$J_{2m}(kr_n)\ \begin{matrix}\cos\\ \sin\end{matrix}(2m\theta_n)$, Even-even / Odd-odd $J_{2m+1}(kr_n)\ \begin{matrix}\cos\\ \sin\end{matrix}([2m+1]\theta_n)$, Even-odd / Odd-even
Straightforward point-matching $\sum_m A_m\, d_{mn} = 0$	$-N \leqslant m \leqslant N$	$0 \leqslant m \leqslant N$	$0 \leqslant m \leqslant N$
Alternative point-matching $\sum_n F_n\, d_{mn} = 0$	$\exp(jkr_n\cos(\psi_m - \theta_n))$ $1 \leqslant m \leqslant 2N+1$ $0 \leqslant \psi_m < 2\pi$	$\exp(jkr_n\cos\psi_m\cos\theta_n)\ \begin{matrix}\cos\\ \sin\end{matrix}$ $(kr_n \sin\psi_m \sin\theta_n)$, Even / Odd $1 \leqslant m \leqslant N+1$, $0 \leqslant \psi_m < \pi$	$\cos(kr_n\cos\psi_m\cos\theta_n)\ \begin{matrix}\cos\\ \sin\end{matrix}$ $(kr_n\sin\psi_m\sin\theta_n)$, Even-even / Odd-even $\sin(kr_n\cos\psi_m\cos\theta_n)\ \begin{matrix}\cos\\ \sin\end{matrix}$ $(kr_n\sin\psi_m\sin\theta_n)$, Even-odd / Odd-odd $1 \leqslant m \leqslant N+1$, $0 \leqslant \psi_m < \pi/2$

Table 3.2: Point-matching formulas, H-modes. Notation as given in Table 3.1. See Fig. 1.1 for definition of α_n.

Method	$d_{mn}(k)$		
	General. Take $\lvert\mathrm{Det}(d_{mn})\rvert$. $0 \leqslant C_n < L$ $1 \leqslant n \leqslant 2N+1$	One-fold symmetry (about $\varphi = 0$). $0 \leqslant C_n < L/2$. $1 \leqslant n \leqslant N+1$	Two-fold symmetry (about $\varphi = 0$ and $\varphi = \pi/2$). $0 \leqslant C_n < L/4$. $1 \leqslant n \leqslant N+1$.
Complete point-matching $\sum_n G_n d_{mn} = 0$	$[J_{m-1}(kr_n)\ \exp(j\alpha_n)$ $-J_{m+1}(kr_n)\exp(-j\alpha_n)]$	$[J_{m-1}(kr_n)\begin{matrix}\cos\\ \sin\end{matrix}(\alpha_n - m\theta_n)$ $\mp J_{m+1}(kr_n)\begin{matrix}\cos\\ \sin\end{matrix}(\alpha_n + m\theta_n)]$, Even Odd	$[J_{2m-1}(kr_n)\begin{matrix}\cos\\ \sin\end{matrix}(\alpha_n - 2m\theta_n)$ $\mp J_{2m+1}(kr_n)\begin{matrix}\cos\\ \sin\end{matrix}(\alpha_n + 2m\theta_n)]$, Even-even Odd-odd
Straightforward point-marching $\sum_m A_m d_{mn} = 0$	$\exp(-jm\theta_n)$ $-N \leqslant m \leqslant N$	$0 \leqslant m \leqslant N$	$[J_{2m}(kr_n)\begin{matrix}\cos\\ \sin\end{matrix}(\alpha_n - [2m+1]\theta_n)$ $\mp J_{2m+2}(kr_n)\begin{matrix}\cos\\ \sin\end{matrix}(\alpha_n + [2m+1]\theta_n)]$, Even-odd Odd-even $0 \leqslant m \leqslant N$
Alternative point-matching $\sum_n G_n d_{mn} = 0$. $R = kr_n\cos\varphi_m\cos\theta_n$ $S = kr_n\sin\varphi_m\sin\theta_n$ $X = \cos\varphi_m\cos(\alpha_n - \theta_n)$ $Y = \cos\varphi_m\sin(\alpha_n - \theta_n)$	$\exp(jkr_n\cos(\varphi_m - \theta_n))$ $\cdot\cos(\alpha_n - \theta_n + \varphi_m))$ $1 \leqslant m \leqslant 2N+1$ $0 \leqslant \varphi_m < 2\pi$	$\exp(jR)\begin{matrix}\cos\\ \sin\end{matrix}(S)$ $\cdot\cos(\alpha_m - \theta_n + \varphi_m)$, Even Odd $1 \leqslant m \leqslant N+1$, $0 \leqslant \varphi_m < \pi$	$[X\sin(R)\begin{matrix}\cos\\ \sin\end{matrix}(S) \mp Y\cos(R)\begin{matrix}\sin\\ \cos\end{matrix}(S)]$, Even-even Odd-even $[X\cos(R)\begin{matrix}\cos\\ \sin\end{matrix}(S) \pm Y\sin(R)\begin{matrix}\sin\\ \cos\end{matrix}(S)]$, Even-odd Odd-odd $1 \leqslant m \leqslant N+1$, $0 \leqslant \varphi_m < \pi/2$

Table 3.3: First four cutoff wavenumbers of E-modes in rectangular waveguide (Figure 2.2). b/a = 0.5. Comparison of CPM and APM with M = 10 in both cases, and $\phi_m = m\pi/M$ in the APM. "Exact" values are those given (to 3 or 4 significant figures) by the standard theory (Jordan and Balmain 1968, chap.8).

Method	d/a	ka			
exact	-	7.02	8.89	11.33	12.95
CPM	0	7.02	8.88	11.33	12.94
	0.05	7.02	8.88	11.32	12.94
	0.1	7.02	8.88	11.32	12.94
APM	0	7.02	8.88	11.33	12.94
	0.05	7.20	9.42	12.34	13.02
	0.1	7.34	10.00	13.26	13.12

Table 3.4: Cutoff wavenumber of E_{11} mode in a rectangular waveguide (a/b = 2.25) by the CPM and APM. $\phi_m = m\pi/(2M)$ in the APM. Exact ka = 7.735275.

M	CPM	APM
4	7.73456	7.73451
5	7.735277	7.735279
6	7.735275	7.735275
7	7.735275	7.735275

Table 3.5: Cutoff wavenumbers of H-modes in rectangular waveguide, b/a = 1/2 (Fig. 2.2) by CPM with M = 8.

Symmetry of wavefunction about $\varphi = 0$ and $\varphi = \pi/2$	ka					
Even-even	Mode	20	40,02	22	42	60
	Exact	6.2832	12.5664	14.0496	17.7715	18.8496
	Computed	6.283	12.566	14.050	17.772	18.850
Even-odd	Mode	10	30	12	50,23	
	Exact	3.1416	9.4248	12.9531	15.7080	
	Computed	3.142	9.425	12.953	15.708	
Odd-odd	Mode	11	31	51	13	
	Exact	7.0248	11.3272	16.9180	19.1096	
	Computed	7.025	11.327	16.918	19.110	
Odd-even	Mode	01	21	41	03	60,23
	Exact	6.2832	8.8858	14.0496	18.8496	19.8692
	Computed	6.283	8.886	14.050	18.850	19.867, 19.869

Table 3.6: Cutoff wavenumbers by CPM (and SPM) for the E and H modes in a sector waveguide ($\beta = 3\pi/2$).

Mode	Exact ka	CPM		
		M = 8	9	10
E-modes	5.136	5.136	5.136	5.136
	7.588	7.588	7.588	7.588
	8.417	8.417	8.417	8.417
	9.936	9.936	9.936	9.936
H-modes	3.054	3.054	3.054	3.054
	3.832	3.832	3.832	3.832
	5.318	5.317	5.318	5.318
	6.706	6.706	6.706	6.706
	7.016	7.016	7.016	7.016
	7.501	7.510	7.501	7.501
	9.282	9.306	9.279	9.284
	9.647	9.617	9.666	9.642
	9.970	9.966	9.970	9.969

Table 3.7: Numerical convergence of R.H.S. of equation (3.8) for the lowest order E-mode in the rounded sector waveguide with $\eta = 3\pi/2$, b = 0.35a, RO = 0.15a, $\varphi = 3\pi/4$, ka (determined using null field method) = 3.201519.

ρ/a	$V(\rho,\varphi)$ from null field method	value of R.H.S. of equation (3.8)			
		M = 2	4	6	8
0.1	0.843	0.841	0.843	0.843	0.843
0.2	0.658	0.644	0.654	0.658	0.658
0.3	0.477	0.422	0.455	0.479	0.478
0.4	0.329	0.194	0.268	0.346	0.337
0.5	0.226	-0.026	0.110	0.307	0.266
0.6	0.158	-0.220	-0.001	0.411	0.271
0.7	0.112	-0.376	-0.059	0.706	0.308
0.8	0.077	-0.484	-0.057	1.230	0.264

Table 3.8: Cutoff wavenumbers by SPM for E- and H-modes in sector waveguide. $\eta = 3\pi/2$. * denotes wavefunctions analytic at S. "Exact" values found from equations (A3).

Wavefunction symmetry about $\varphi = 0$	ka for E-modes				ka for H-modes			
	exact	SPM			exact	SPM		
		M = 8	9	10		M= 8	9	10
even			2.26		2.258	2.09		
	3.376	3.31	3.26	3.24	3.823	3.76	3.43	3.36
	5.136*	5.136	5.136	5.136	3.832*	3.832	3.832	3.832
	6.530	6.25	6.34	6.40	5.318*	5.318	5.318	5.318
	6.786	6.80	6.87	6.90	5.800	6.08		
	8.379	7.64			6.779		6.33	6.78
	8.417*	8.415	8.417	8.417	7.016*	7.016	7.016	7.016
					7.584	7.85	7.21	7.31
odd					1.401			2.61
				2.66	3.054*	3.054	3.054	3.054
	4.275	4.64			4.576	4.49	4.60	4.60
	5.970	5.61	5.62	5.68	4.851			
	7.491				6.051		6.06	6.07
	7.588*	7.593	7.588	7.588	6.706*	6.706	6.706	6.706

Table 3.9: Cutoff wavenumber by EPM of lowest order even E-mode in rounded sector waveguide. $\eta = 3\pi/2$, $b/a = 0.35$. Accurate value obtained from the null field method.

method	ka	N_1	N_2	M_1	M_2
accurate	3.20	-	-	-	-
EPM	3.22	3	9	6	6
	3.22	3	11	7	7
	3.22	4	10	7	7
	3.22	6	10	8	8

Table 3.10: Cutoff wavenumbers by EPM for four lowest order H-modes in Meinke waveguide. a/d = 1.29, b/d = 0.3. Order of determinant = 8.

method	ka			
EPM	2.268	4.516	4.566	6.172
Bulley and Davies (1969)	2.267	4.518	4.570	6.189

Table 3.11: Cutoff wavenumbers by EPM for E- and H-modes in ridge waveguide (Fig. 3.16(b)), a : b : w : d = 4 : 2 : 2 : 1. Order of determinant = 12.

Mode	ka			
	EPM	Beaubien and Wexler (1970)	Davies and Muilwyk(1966)	Bulley and Davies(1969)
E-modes	6.067	6.071		
	6.210	6.214	6.212	
	7.003	-		
	7.797	7.795	7.796	
	8.323	8.323		
H-modes	1.125	1.121		1.131
	2.423	2.423		2.463
	3.228	3.227		3.244
	3.760	3.759		3.762

Table 3.12: Cutoff wavenumbers by EPM and Pyle (1966) for lowest order H-mode in ridge waveguide, b/a = 0.45, W/a = 0.5. Order of determinant = 12.

d/b	0.05	0.1	0.2	0.3	0.4	0.5	0.6	0.7	0.8	0.9
ka from EPM	1.017	1.201	1.527	1.804	2.049	2.275	2.486	2.682	2.858	3.004
ka from Pyle(1966)	0.820	1.111	1.499	1.793	2.045	2.275	2.487	2.685	2.864	3.018

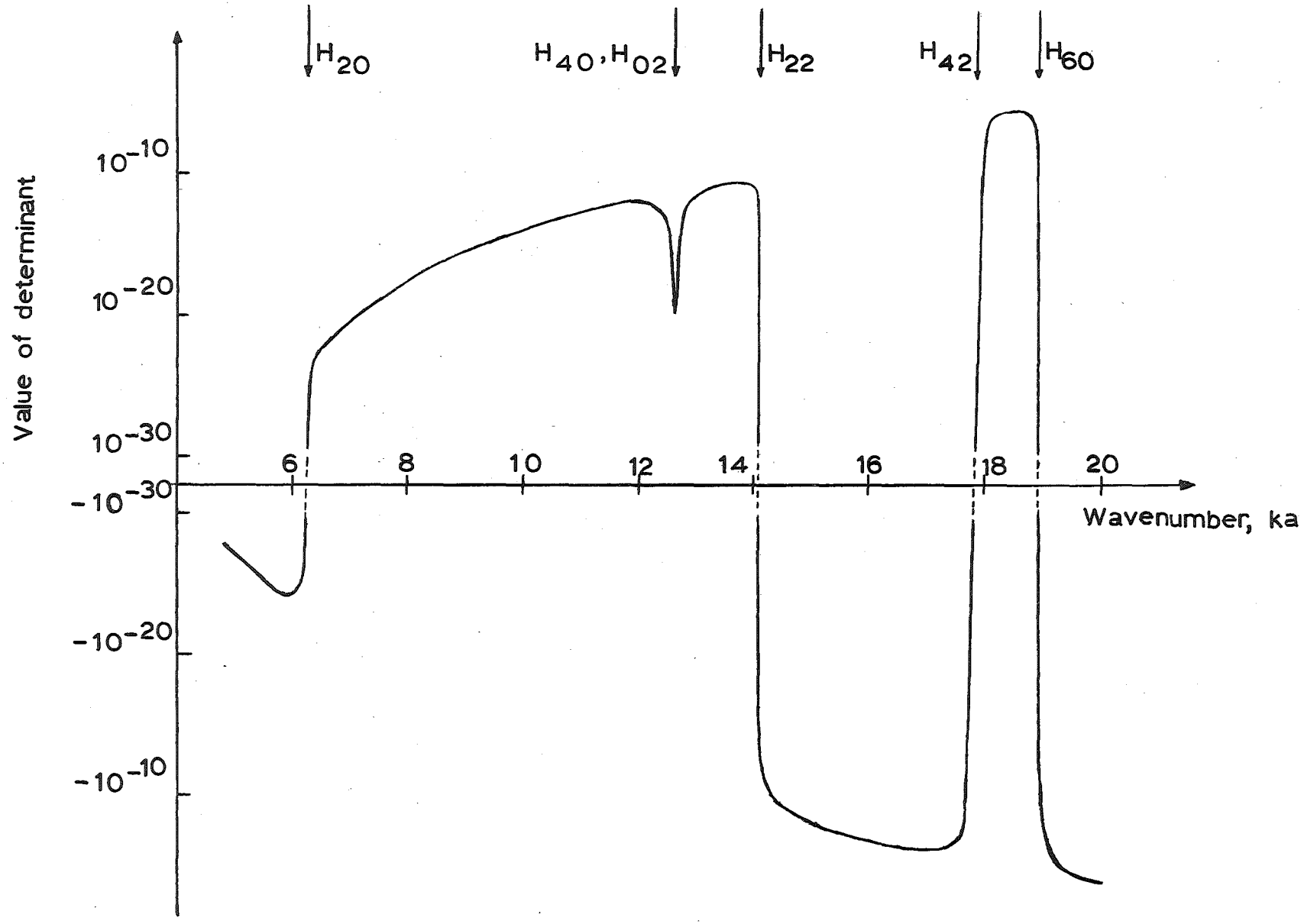

Fig. 3.1: Behaviour of determinant value for the CPM (and SPM) with M = 8 for the H-modes with even symmetry about both $\varphi = 0$ and $\varphi = \pi/2$ in a rectangular waveguide (b/a = 1/2).

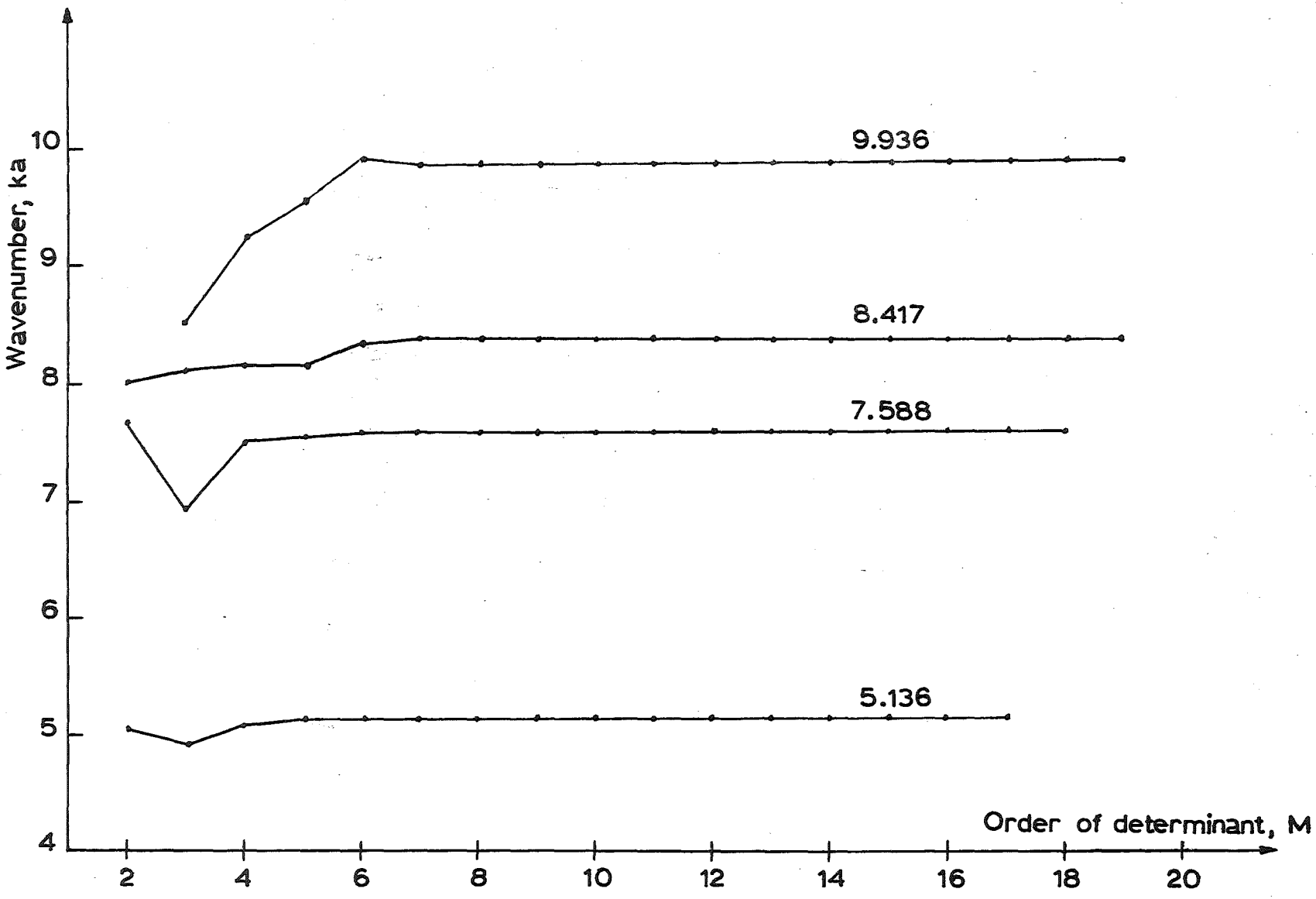

Fig. 3.2: Computed cutoff wavenumbers by CPM (and SPM) for E-modes in a sector waveguide with $\beta = 3\pi/2$ (Fig. 2.1).

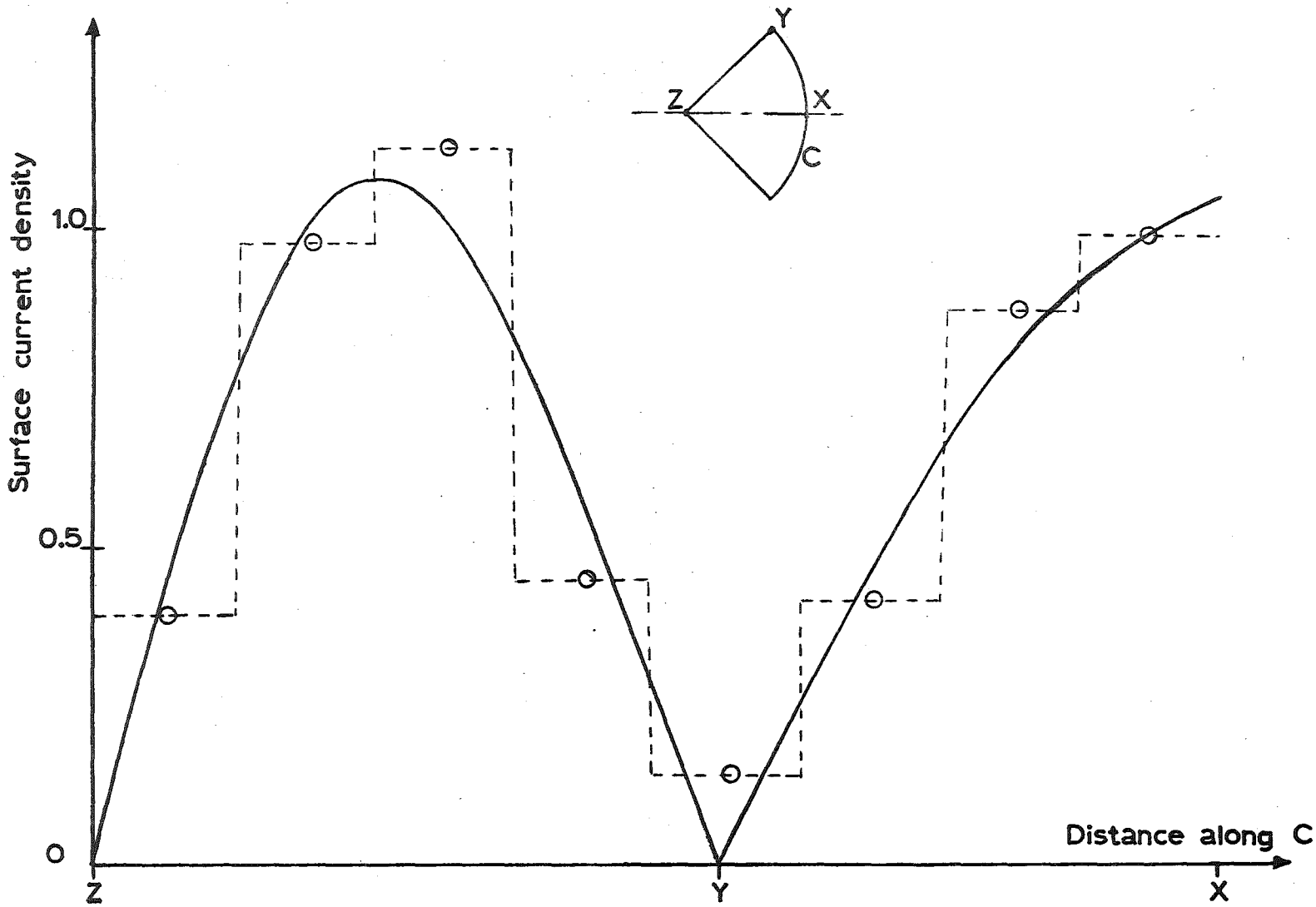

Fig. 3.3: Computed surface current density using CPM (with M = 8) for lowest order E-mode in sector waveguide ($\beta = 3\pi/2$).

Full line denotes surface current density computed from exact expression, equations (B8) and (B9).

O computed F_n at the matching points (normalised to 1.0 at point closest to X). The dash line shows the corresponding step functions.

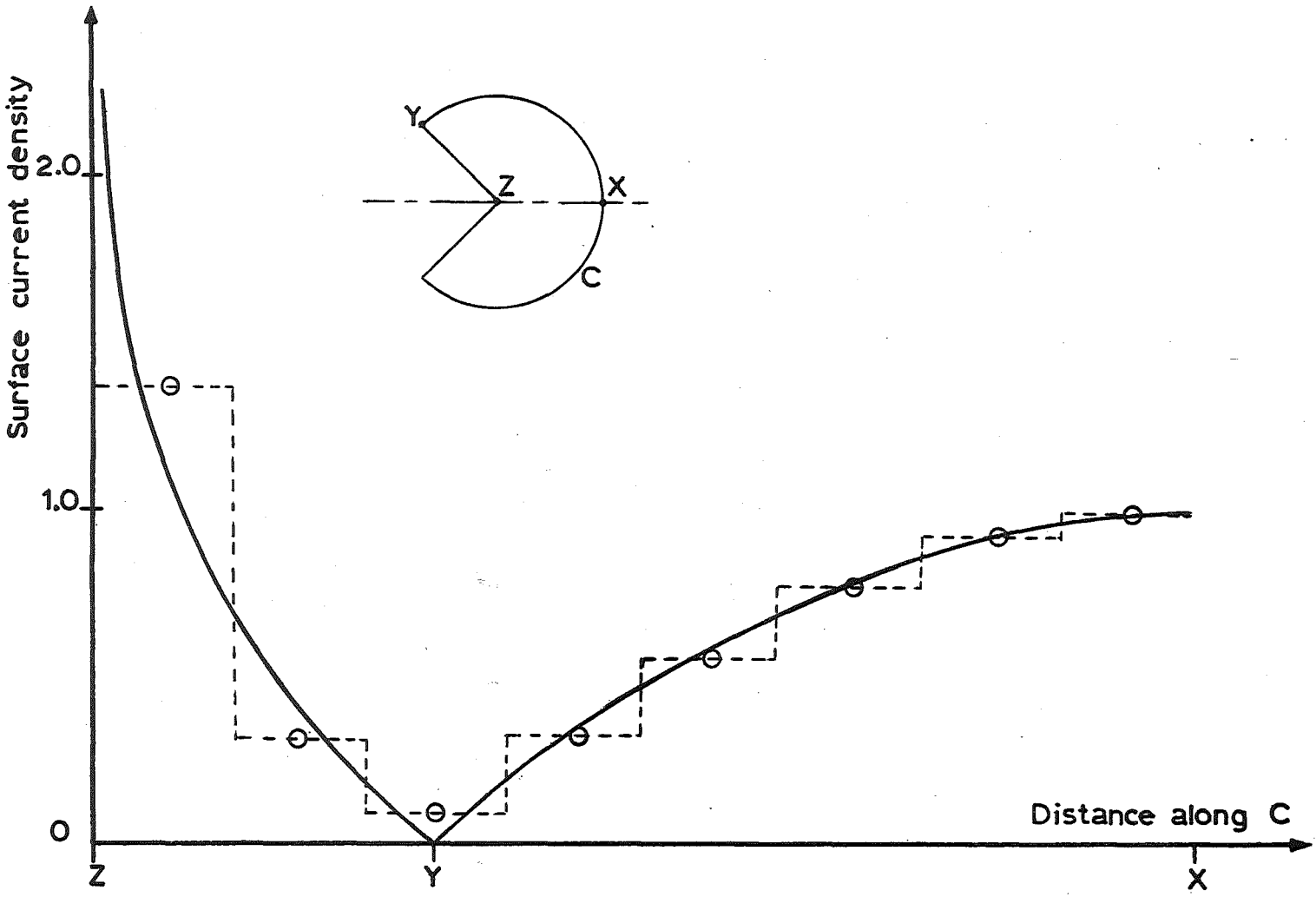

Fig. 3.4: Computed surface current density using CPM (with M = 8) for lowest order E-mode in sector waveguide ($\beta = \pi/2$).
Full line denotes surface current density computed from exact expression, equations (B8) and (B9).
O computed F_n at the matching points (normalised to 1.0 at point closest to X).
The dashed lines show the corresponding step functions.

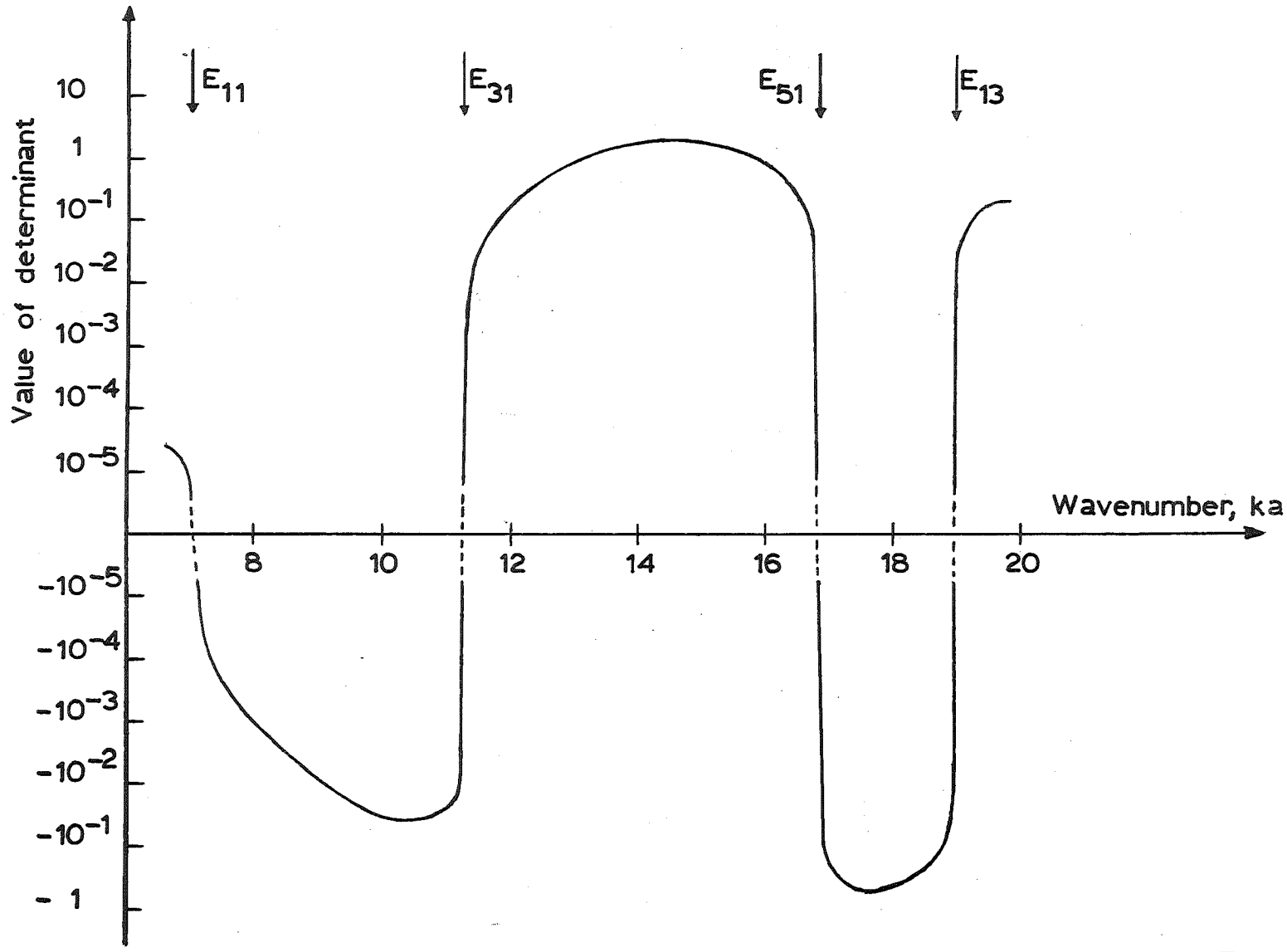

Fig. 3.5: Behaviour of determinant value for the APM with M = 5 for the E-modes with even symmetry about both $\varphi = 0$ and $\varphi = \pi/2$ in a rectangular waveguide (b/a = 1/2).

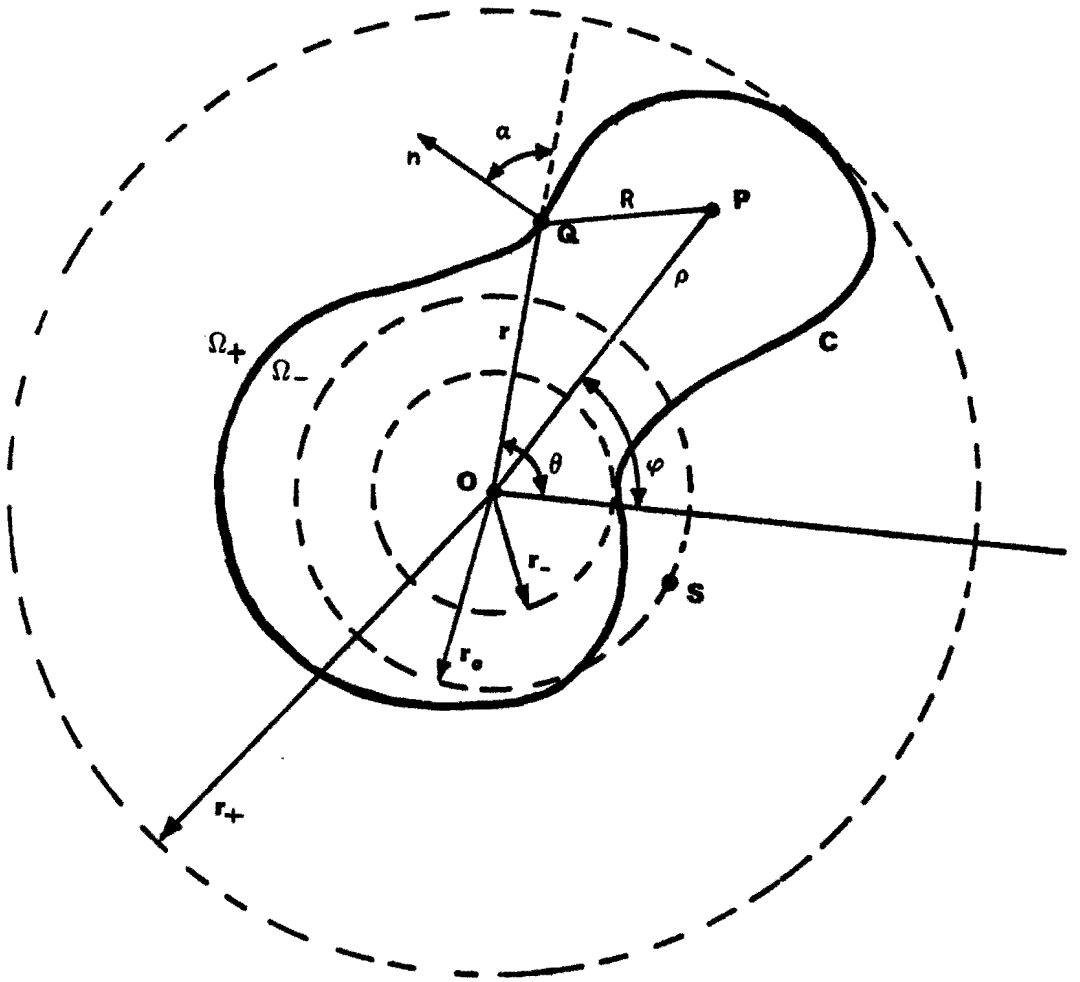

Figure 3.6 Waveguide cross-section and coordinate system.

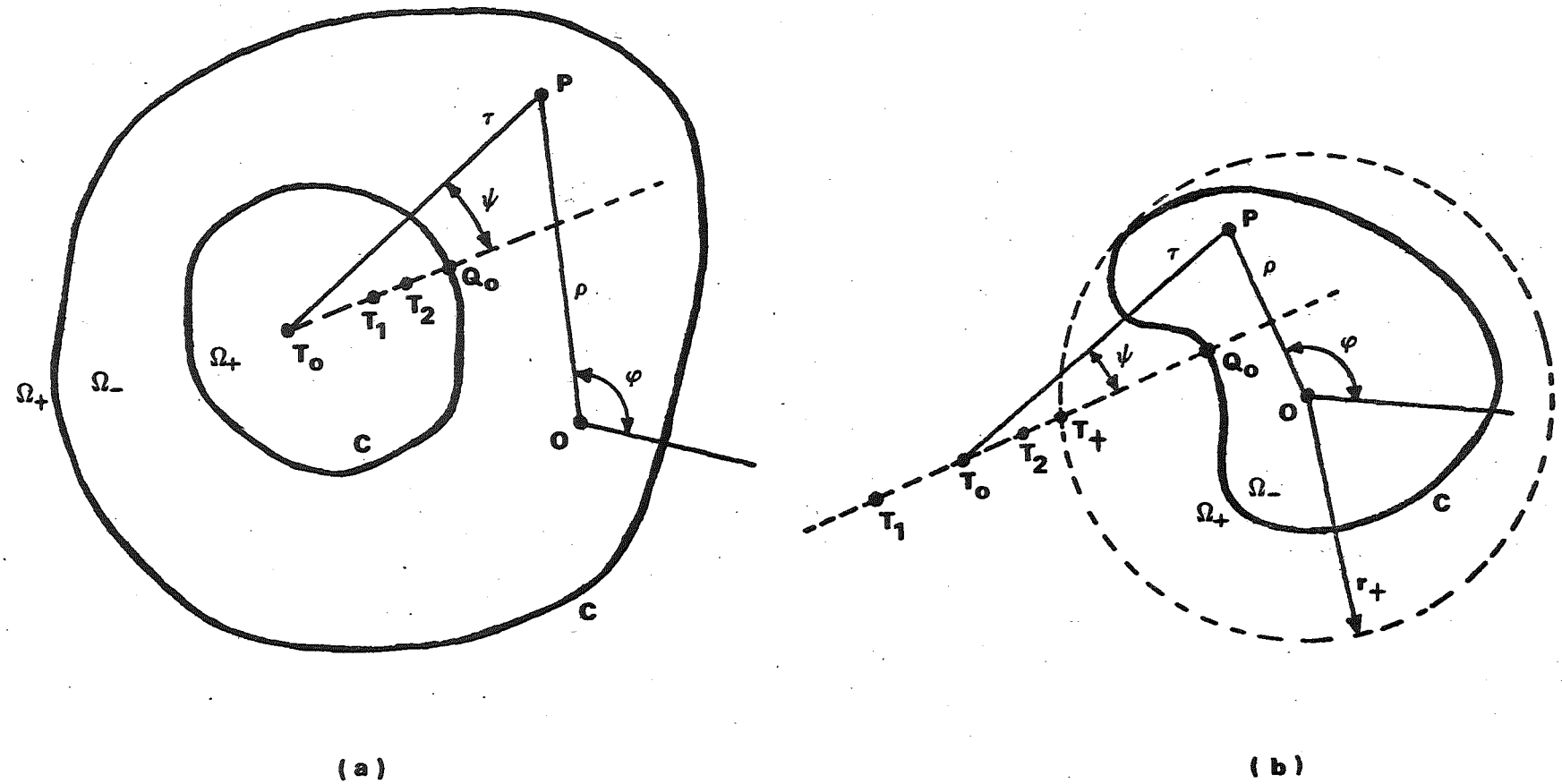

(a) (b)

Figure 3.7 Waveguides with walls having nonconvex curved parts.

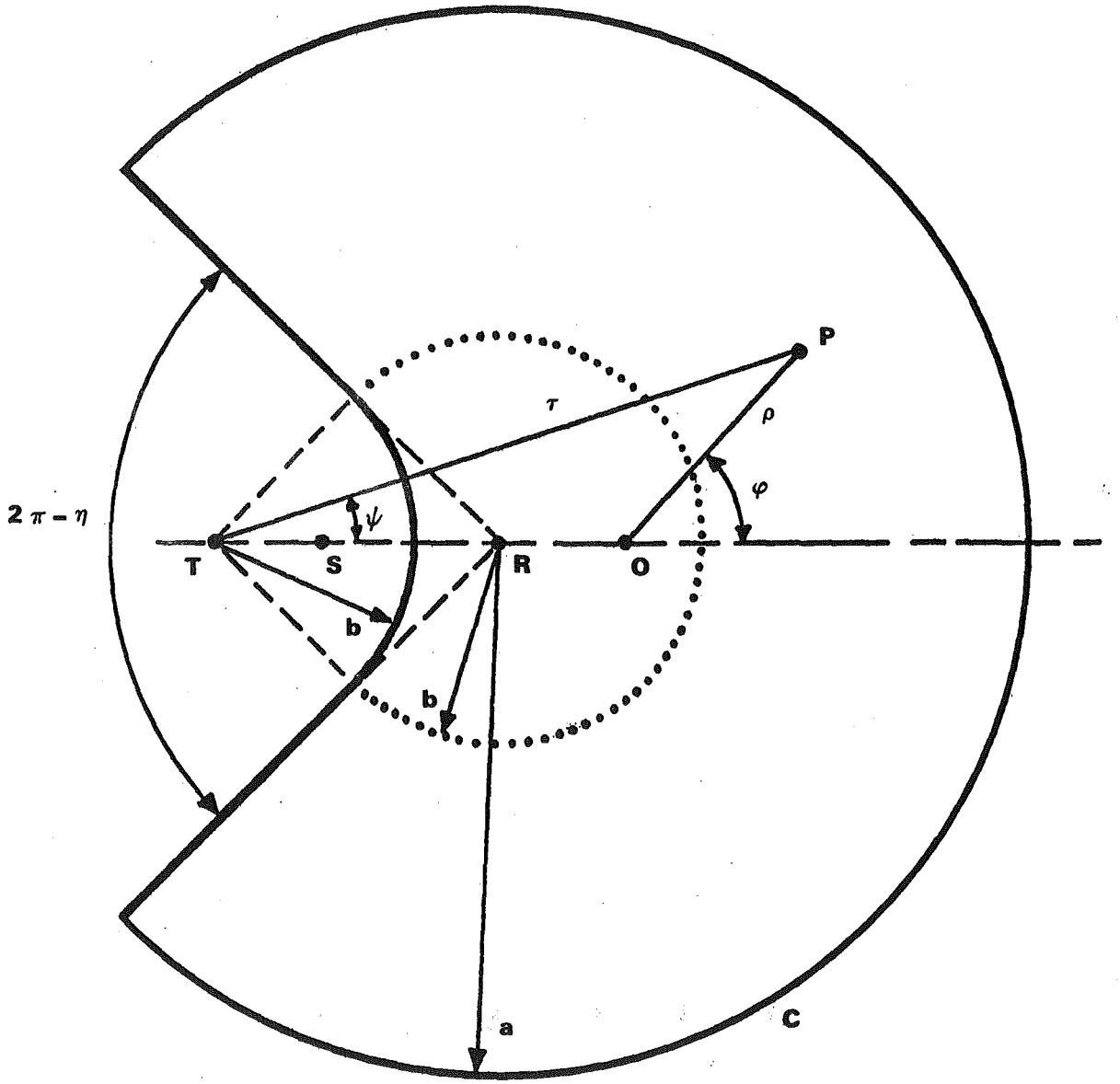

Figure 3.8 Rounded sector waveguide.

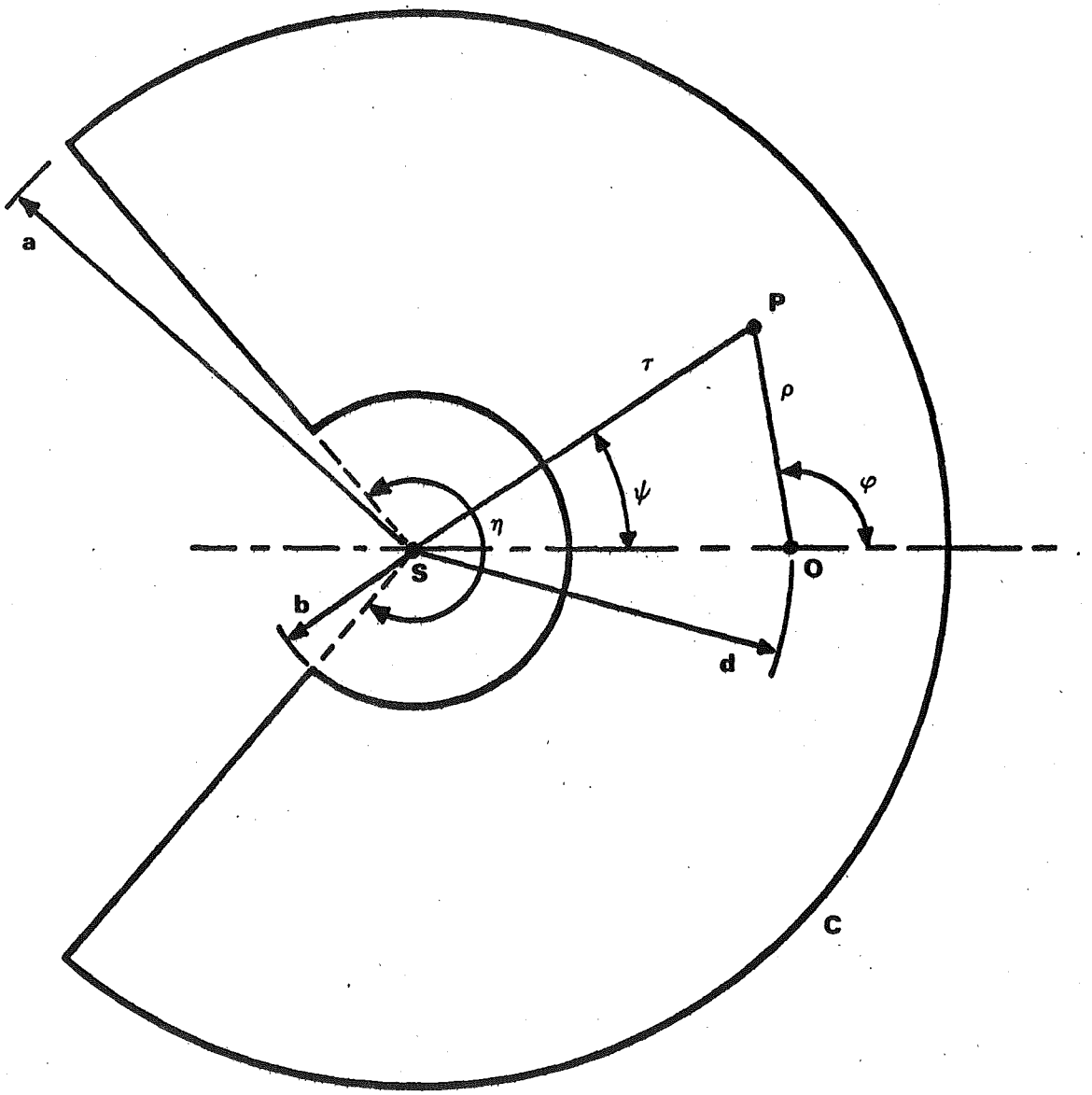

Figure 3.9 Segment waveguide. $\beta = 2\pi - \eta$.

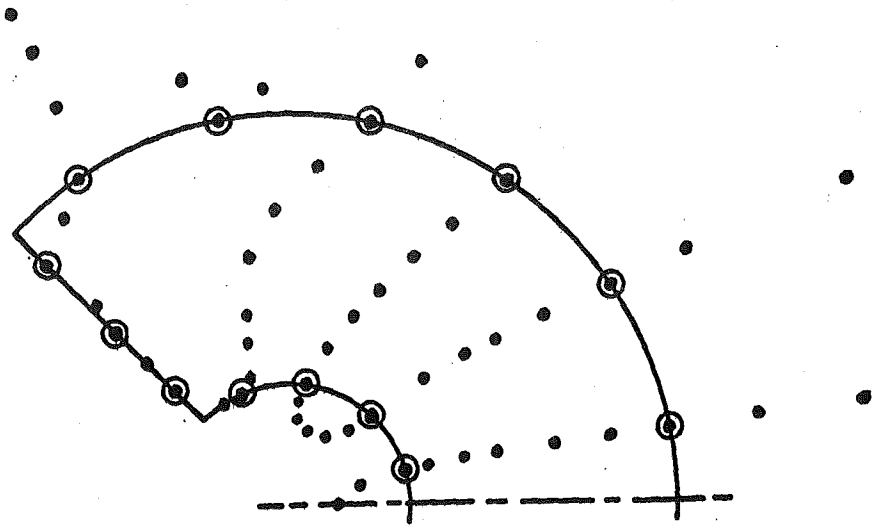

(a)

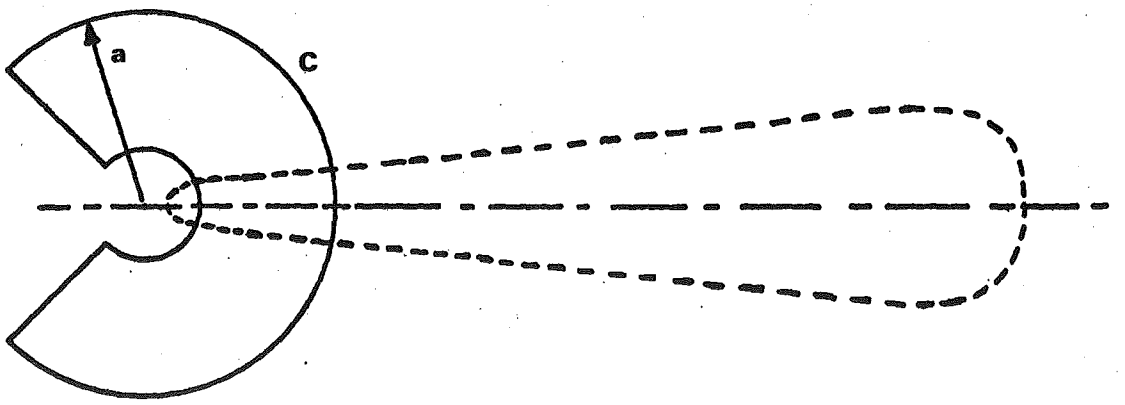

(b)

Figure 3.10 Lowest E-mode in segment waveguide.

$\eta = 3\pi/2$, b/a = 0.3, d/a = 0.5.

full line denotes C

O positions of members of $\{r_n, \theta_n\}$

• points on curves where R.H.S. of equation (3.8) is zero.

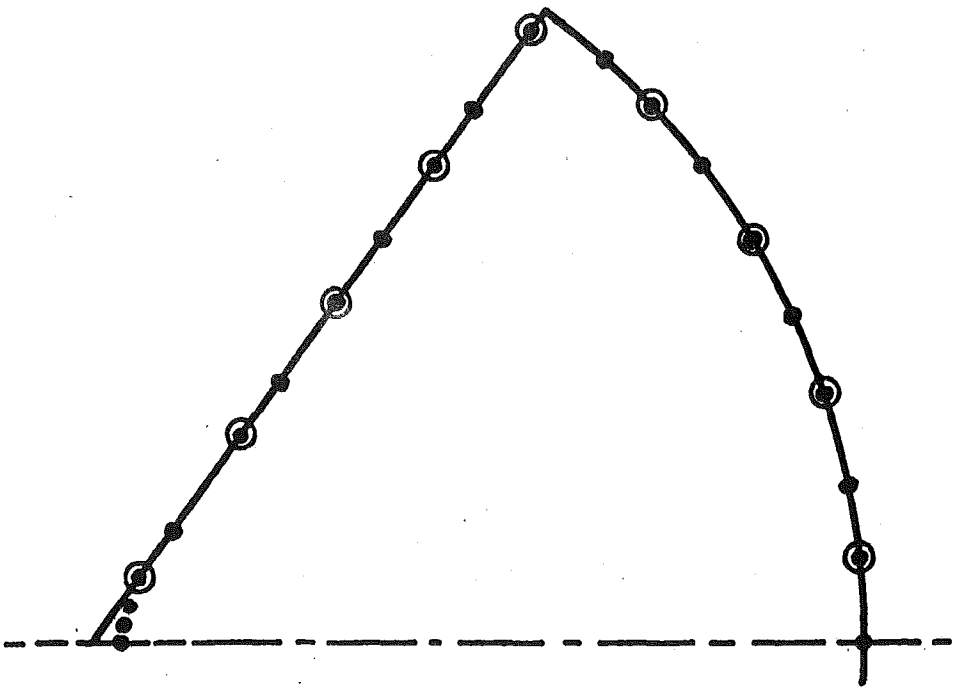

Figure 3.11 Lowest E-mode in sector waveguide.

$\eta = 109^{\circ}$.

full line denotes C

O positions of members of $\{r_n, \theta_n\}$

• points where R.H.S. of equation (3.8) is zero.

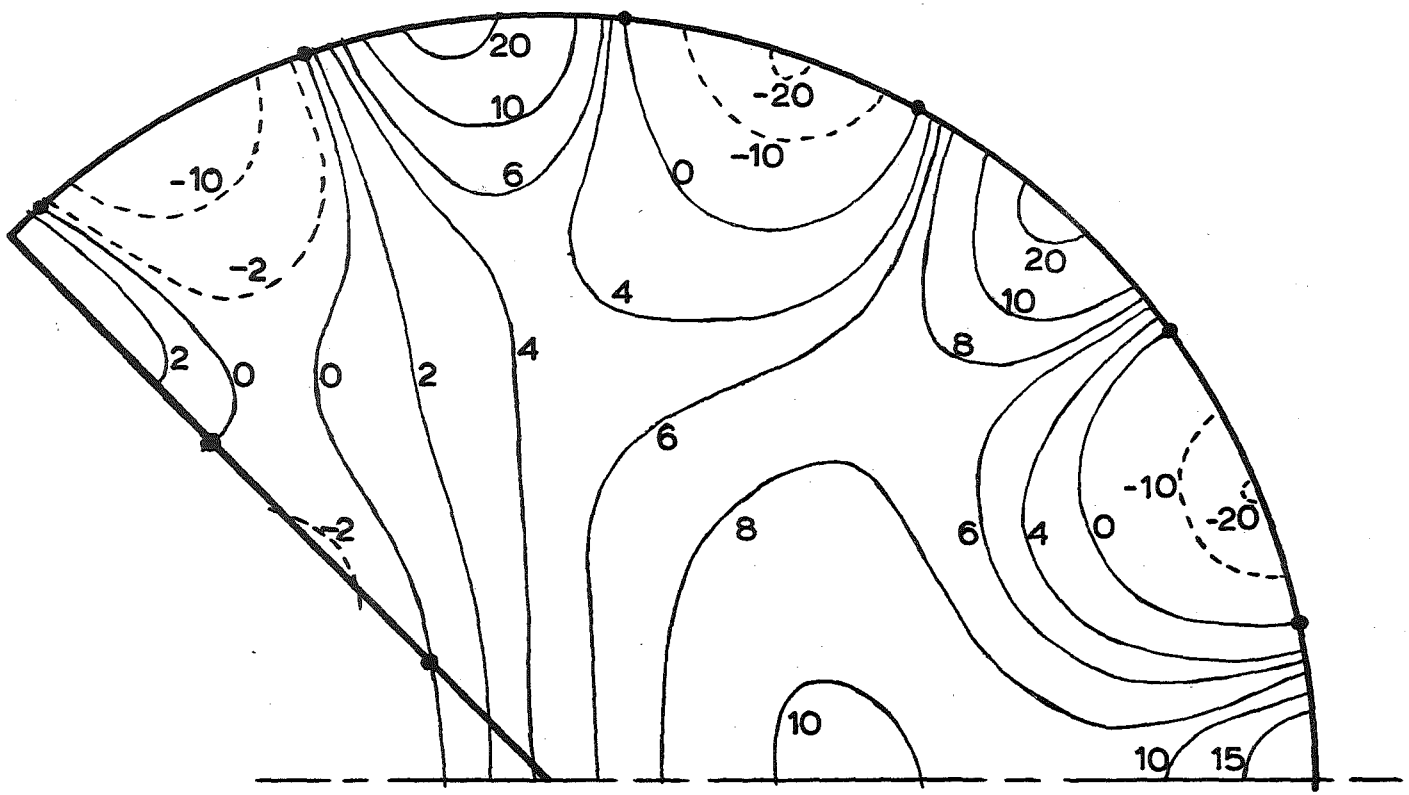

Fig. 3.12: Field plot for lowest E-mode in sector waveguide ($\eta = 3\pi/2$) by SPM. Arbitrary units. The IRH is not valid.
• positions of members of $\{r_n, \theta_n\}$.

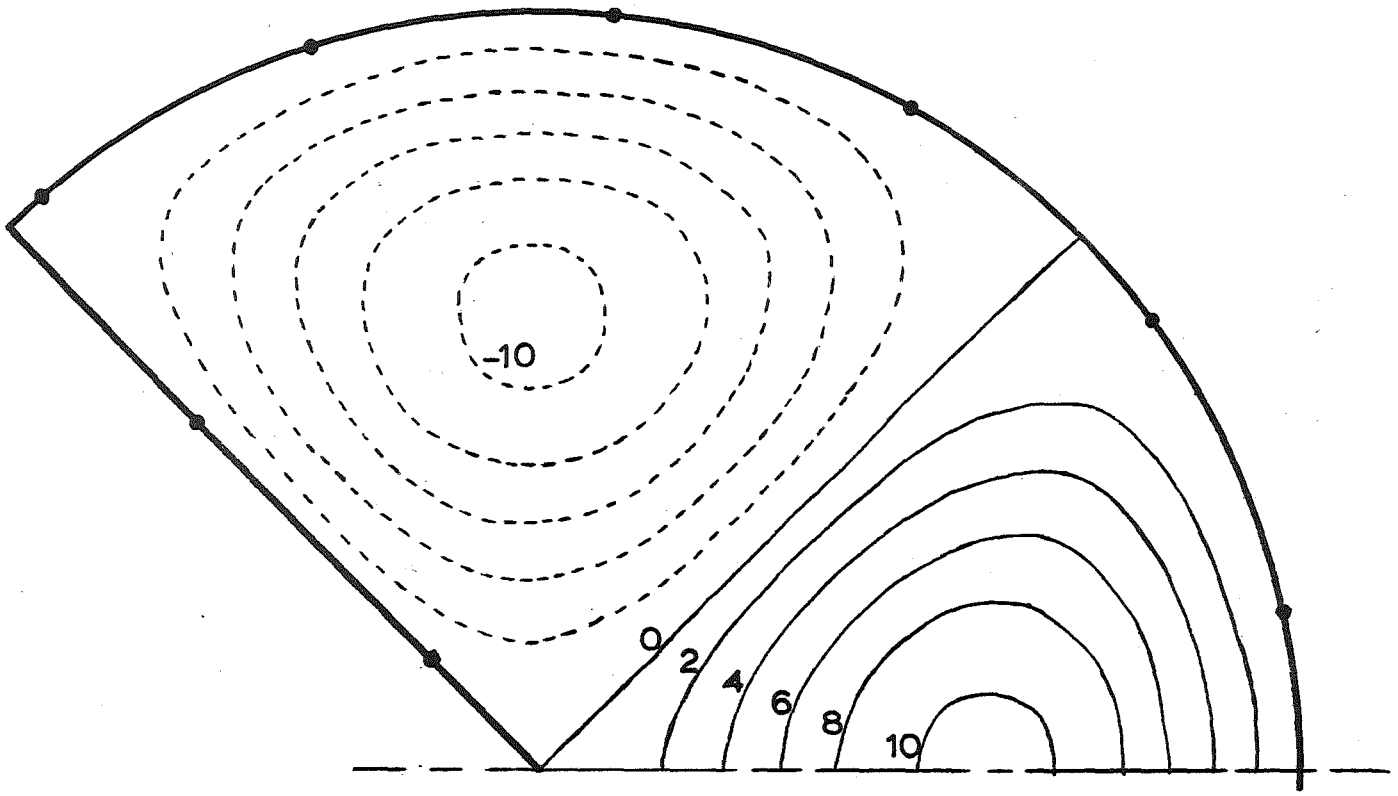

Fig. 3.13: Field plot for second lowest E-mode in sector waveguide ($\eta = 3\pi/2$) by SPM. Arbitrary units. IRH holds.
• position of members of $\{r_n, \theta_n\}$.

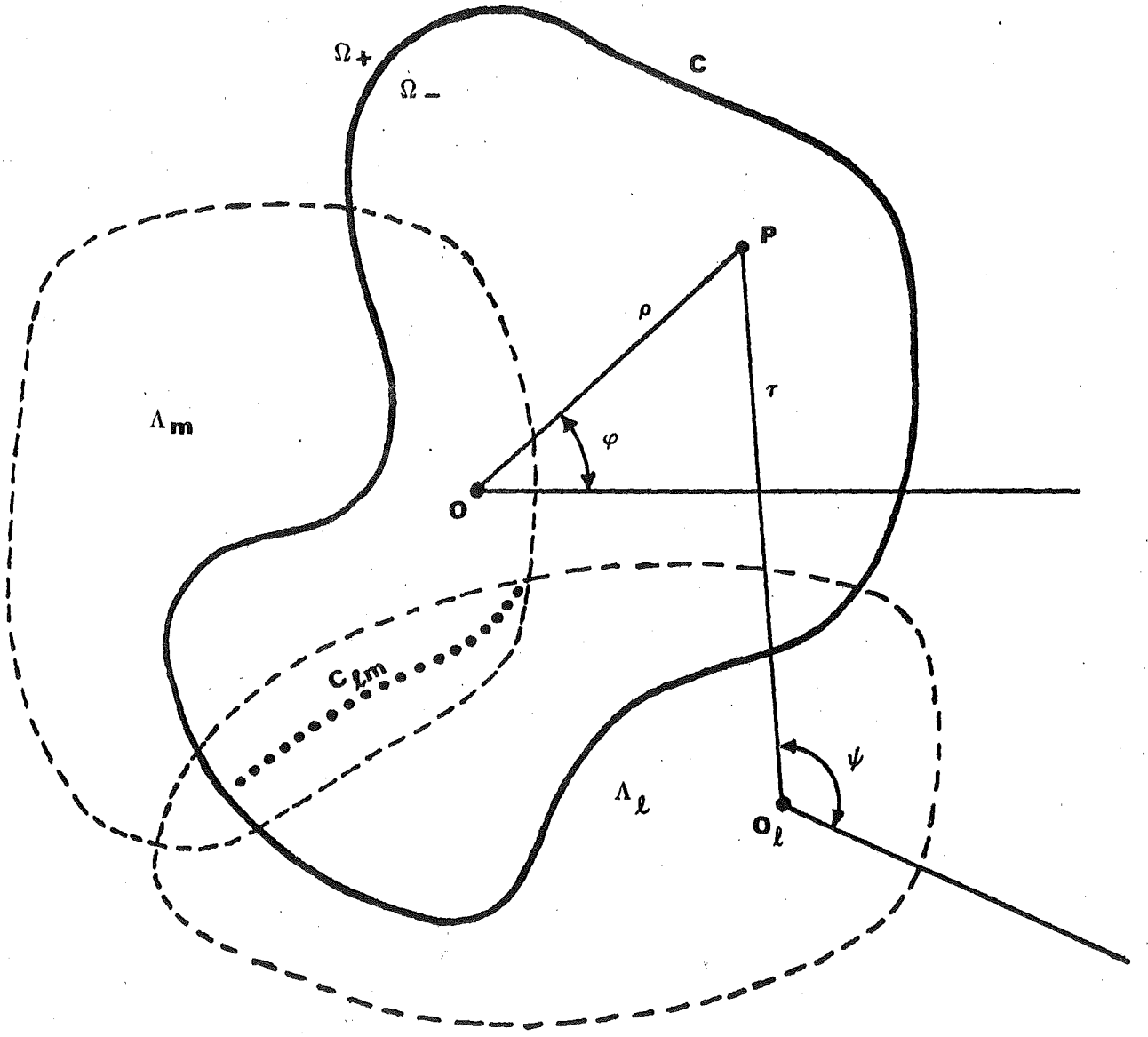

Figure 3.14 Coordinates for EPM.

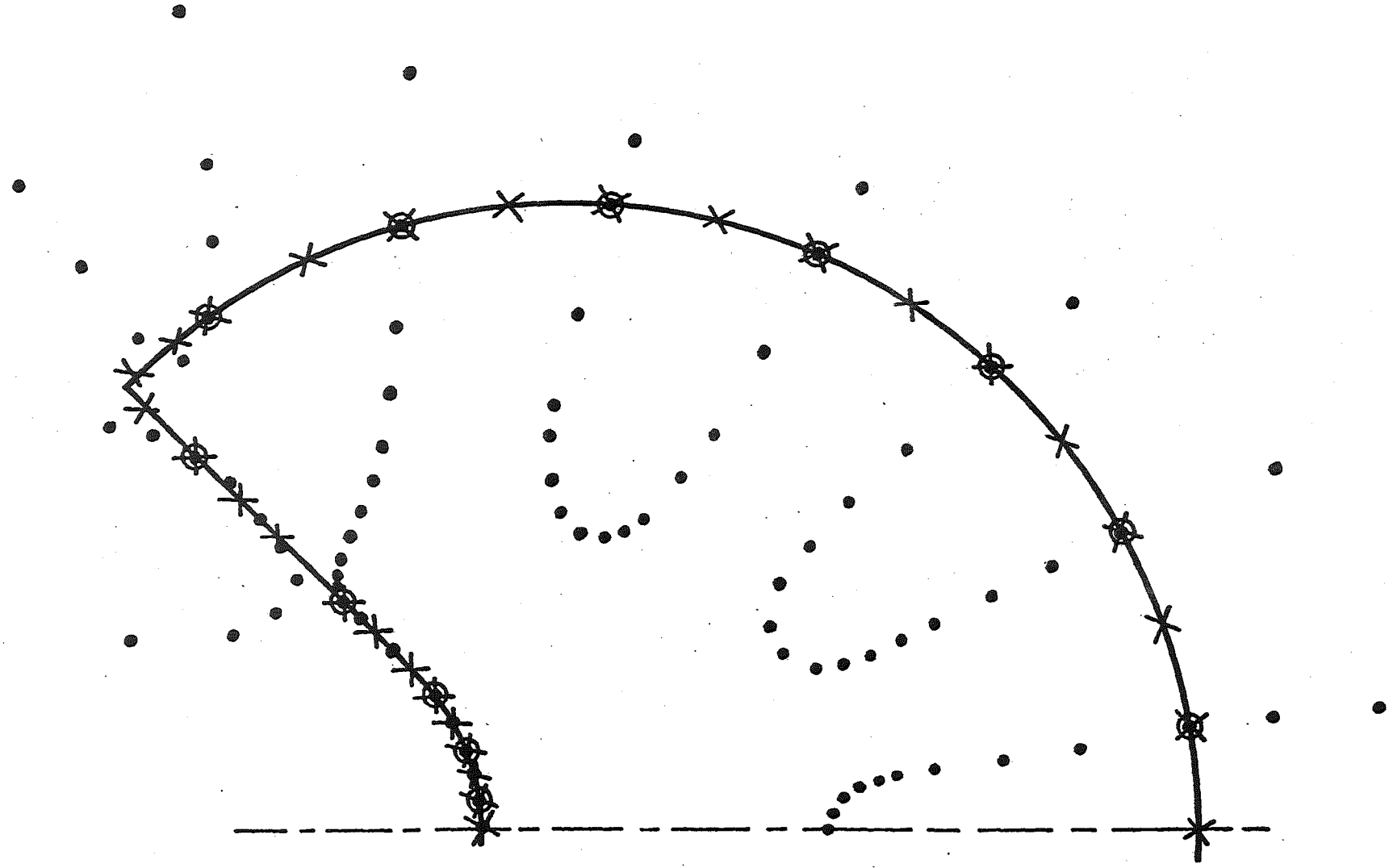

Figure 3.15 Lowest E-mode in rounded sector waveguide. $\eta = 3\pi/2$, b/a = 0.35
full line denotes C
- ○ matching points
- • points on curves where SPM wavefuntion is zero
- × points on curve where EPM wavefuntion is zero

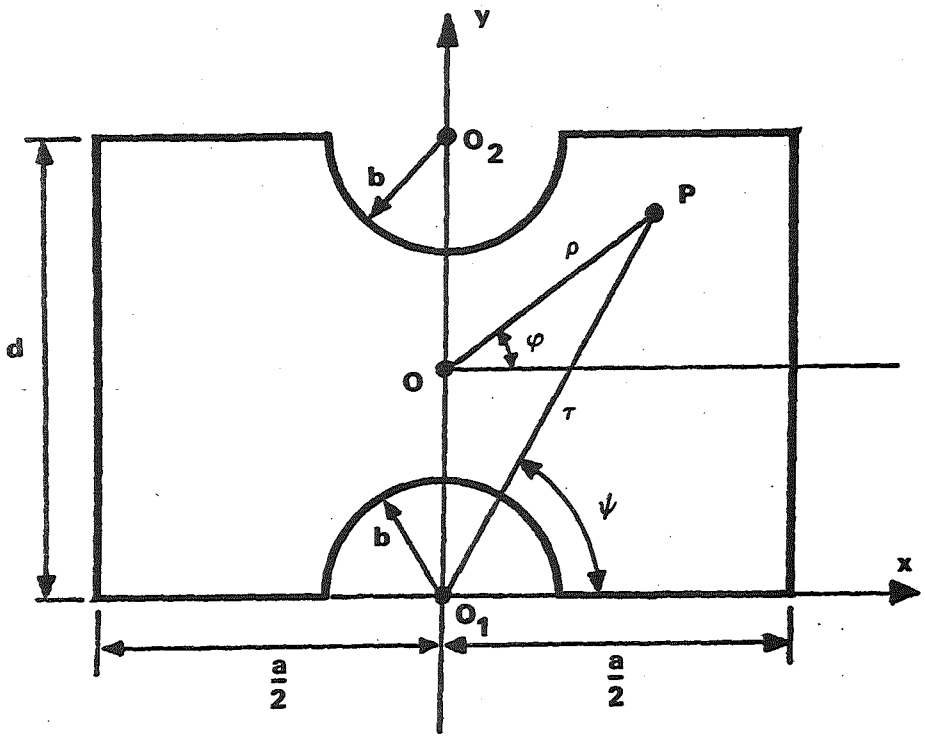

(a)

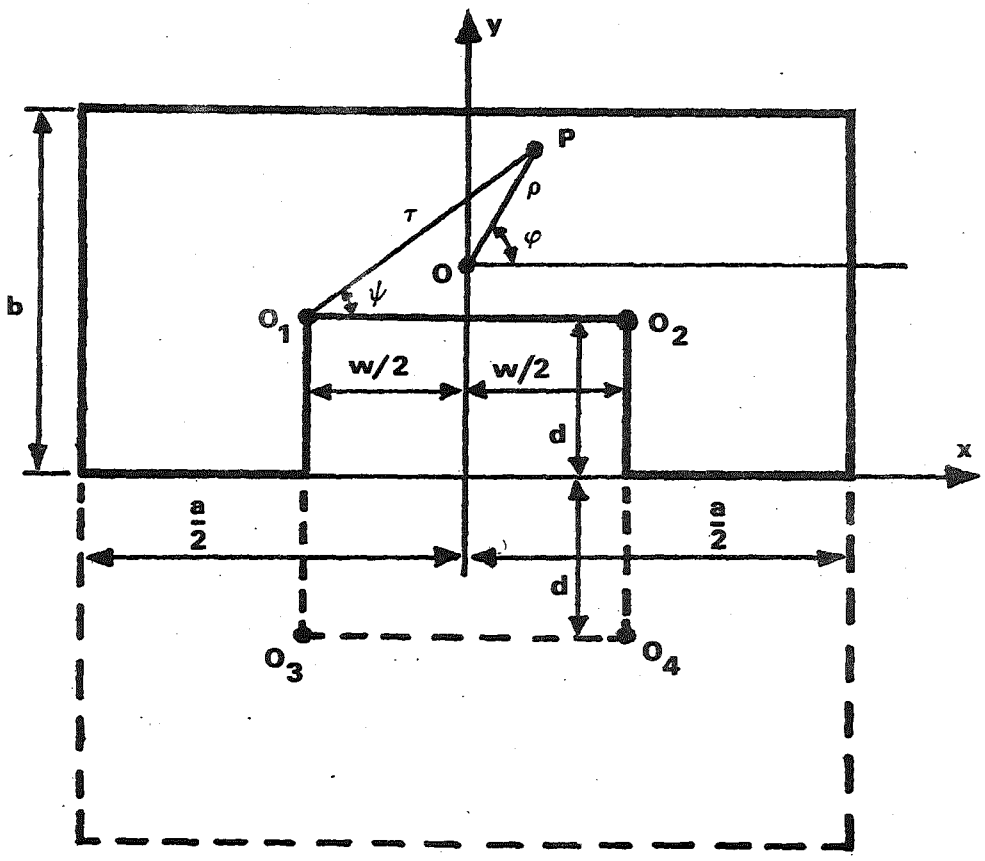

(b)

Figure 3.16 (a) Meinke waveguide

(b) Ridge waveguide.

PART 2: Polarization Source Formulation and Dielectric Loaded Waveguides

CHAPTER 4: POLARIZATION SOURCE FORMULATION

Infinity's taken
by everyone
as a figure-of-eight
written sideways on.

But all of a sudden
I now apprehend
that eight is infinity
standing on end.
Piet Hein

A formulation (which is part of a general polarization source formulation (Bates 1970)) for the diffraction of a time-harmonic electromagnetic field by dielectric and perfectly conducting bodies is presented. The general solution to this diffraction problem is given as a single integral equation which is used in the next chapter.

4.1 INTRODUCTION

In the polarization source formulation, all diffracting bodies are treated as sources of fields which travel undisturbed throughout space, thereby being straightforwardly calculable. The field is expressed exactly in terms of an integral equation over the parts of space occupied by the diffracting bodies. The name "polarization source formulation" is used because the method uses the concept of the polarization of the medium, an idea much employed with conservative fields (Jordan and Balmain 1968, secs 9.08 and 9.11). The formulation for the diffraction of a time-harmonic field by dielectric and perfectly conducting bodies is

presented in the following sections. The formulation is part of a general formulation (for bodies exhibiting arbitrary variations of permittivity, permeability and conductivity) developed by Bates (1970) and is given here for completeness as the formulation is used in chapter 5 to derive formulas for the cutoff characteristics of arbitrary waveguides loaded with circular dielectric tubes or rods.

4.2 BASIC FORMALISM

It is convenient to combine the electric and magnetic intensities, $\vec{E}$ and $\vec{H}$ respectively, into the vector column matrix $\vec{f}$:

$$\vec{f} = \begin{bmatrix} \vec{E} \\ \vec{H} \end{bmatrix}. \tag{4.1}$$

In any diffraction problem the total field $\vec{f}$ can be split up into an incident (or given) field $\vec{f}_0$ and a field $\vec{f}_p$ reradiated (or scattered) from inhomogeneities in the medium:

$$\vec{f} = \vec{f}_0 + \vec{f}_p. \tag{4.2}$$

In the polarization source formulation of electromagnetism, all reflecting, refracting and diffracting bodies are treated as perturbations of a uniform free space in which the speed c of electromagnetic waves is constant. The free space values of the permittivity ε and the permeability μ respectively are denoted by ε_0 and μ_0 and $c = (\varepsilon_0 \mu_0)^{-\frac{1}{2}}$.

In this underlying free space $\vec{f}_0$ and $\vec{f}_p$ travel everywhere with the speed c, which means that they can be expressed in terms of the usual "retarded" integral over their sources (Jones 1964, sec. 1.16). There is a source for $\vec{f}_p$ at each point in space where the medium differs from free space. Such sources are called polarization sources because the amplitude of the source density at each point, besides being a function of the departure of the medium from free space at that point, is also proportional to the total field there, i.e. the field "polarizes" the medium.

Provided discontinuous media (which are discussed in sec. 4.3) are excluded, the vector wave equations for $\vec{E}$ and $\vec{H}$, which are obtained from Maxwell's equations (1.1) by standard procedures (Jones 1964, chap. 1), can be written as

$$\nabla^2\vec{f} - c^{-2}\ddot{\vec{f}} = -\vec{w} \; ; \tag{4.3}$$

$$\vec{w} = \begin{bmatrix} c^{-2}\ddot{\vec{E}} - \nabla(\mu\times\dot{\vec{H}} + \dot{\mu}\times\vec{H}) - \nabla(\nabla\cdot\vec{E}) - (\mu\frac{\partial}{\partial t} + \dot{\mu})(\dot{\vec{D}} + \vec{J}) \\ c^{-2}\ddot{\vec{H}} + \nabla(\varepsilon\times\dot{\vec{E}} + \dot{\varepsilon}\times\vec{E}) - \nabla(\nabla\cdot\vec{H}) + (\varepsilon\frac{\partial}{\partial t} + \dot{\varepsilon})(-\dot{\vec{B}}) + \nabla\times\vec{J} \end{bmatrix} \tag{4.4}$$

where the vector column matrix $\vec{w}$, which depends linearly on $\vec{f}$, is called the polarization source density and where each superscript dot denotes a partial differentiation with respect to time t.

All space is denoted by v. The sources of $\vec{f}_0$ are taken to lie in the volume(s) v_0 separate from the volume(s) v_p containing the polarization sources. All of v, apart from v_0, is denoted by $\bar{v}_0$. So, throughout $\bar{v}_0$,

$$\nabla^2 \vec{f}_0 - c^{-2} \ddot{\vec{f}}_0 = 0 \tag{4.5}$$

which means that $\vec{f}$ can be replaced by $\vec{f}_p$ on the left hand side (but only on the left hand side) of eqn (4.3).

4.2.1 Monochromatic Fields

Denote by v_d the parts of v_p within which the constitutive parameters ε and μ are continuous and differentiable. The media are assumed to be lossless with the conductivity $g = 0$. Denote by $\vec{f}_d$ the part of $\vec{f}_p$ originating from v_d. It is convenient to restrict consideration for the moment to sources in v_d. Abrupt boundaries and perfect conductors are considered in the next section.

For monochromatic fields of angular frequency ω, it is convenient to use complex representations of fields and sources, with the time factor $\exp(j\omega t)$ suppressed. In monochromatic analyses the term $\partial/\partial t$ is replaced by $j\omega$ and the constitutive parameters are required to be time invariant ($\dot{\varepsilon} = \ddot{\varepsilon} = \dot{\mu} = \ddot{\mu} = 0$).

Using the above arguments, $\vec{w}$ (eqn (4.4)) can be written as

$$\vec{w} = \Omega \vec{f} \tag{4.6}$$

where Ω is a square matrix, the elements of which are found to be

$$\left.\begin{aligned} \Omega_{11} &= (\mu\varepsilon c^2 - 1)k^2 - \text{grad div} \\ \Omega_{12} &= -j\omega(\nabla\mu) \times \\ \Omega_{21} &= j\omega(\nabla\varepsilon) \times \\ \Omega_{22} &= (\mu\varepsilon c^2 - 1)k^2 - \text{grad div} \end{aligned}\right\} \tag{4.7}$$

k is the free space propagation constant (or wavenumber) and is given by

$$k = \omega/c. \tag{4.8}$$

Taking $\vec{\rho}$ as the radius vector of an arbitrary point P in $\bar{v}_0$ and $\vec{r}$ as the radius vector of an arbitrary point T in v_p, as in Fig. 4.1; the usual retarded integral solution of eqn (4.3) for monochromatic fields, with $\vec{f}$ replaced by $\vec{f}_d$ on the left hand side, is (Jones 1964, sec. 1.16)

$$\vec{f}_d(\vec{\rho}) = (4\pi)^{-1} \iiint_{v_d} R^{-1} \vec{w}(\vec{r}) \exp(-jkR)\, dv \tag{4.9}$$

where R is the distance between P and T, and $\vec{w}$ is given by eqns (4.6) and (4.7).

The Maxwell equations (eqn (1.1)) for div $\vec{D}$ and div $\vec{B}$, with q = 0, give

$$\left.\begin{aligned} \nabla\cdot\vec{E} &= -(\vec{E}\cdot\nabla\varepsilon)/\varepsilon \\ \nabla\cdot\vec{H} &= -(\vec{H}\cdot\nabla\mu)/\mu \end{aligned}\right\} \tag{4.10}$$

Eqn (4.10) can be substituted directly into the "grad div" terms in eqn (4.7). Consequently

$$\text{grad div} = -(\nabla)\ \gamma^{-1}(\nabla\gamma). \tag{4.11}$$

where γ is ε and μ respectively in the expressions for Ω_{11} and Ω_{22}.

4.3 ABRUPT BOUNDARIES AND PERFECT CONDUCTORS

4.3.1 Preliminaries

No electromagnetic formalism is realistic, from a practical computational point of view, unless it can

handle in a straightforward manner abrupt boundaries between different media. For instance, the boundary layer between air and a sheet of glass is effectively infinitesimally thin at all usable radio frequencies. Similarly, there are few radio engineering applications in which the losses in metallic conductors are not either negligible or computable by some straightforward perturbation technique. The assumption of perfect conductivity is a practical one, and it simplifies computations.

Consider the surface(s) σ coinciding with abrupt boundaries between parts of v_d. Denote by $\vec{f}_\sigma$ the field radiated by any polarization sources on σ. Also, consider the surface(s) s of perfect conductors and denote by $\vec{f}_s$ the field radiated by charges and currents in s. So the combined field reradiated from v_p is

$$\vec{f}_p = \vec{f}_d + \vec{f}_\sigma + \vec{f}_s \tag{4.12}$$

and, using set theoretic notation, the combined region containing polarization sources is

$$v_p = v_d \cup \sigma \cup s. \tag{4.13}$$

Fig. 4.2 shows arbitrary points Ψ on σ and Q on s. The coordinate ν is normal to σ at Ψ and to s at Q. The coordinate τ is any coordinate lying in the plane tangent to either σ at Ψ or s at Q. The surfaces σ_α and σ_β are both distant Δ (where Δ is a sufficiently small spatial interval) from σ, and the surface s_a is distant Δ from s, the distances measured along the coordinate ν. The surfaces σ_α, σ_β and σ are parallel, and the surfaces

s_a and s are parallel, in the sense that the coordinate ν intersects σ_α, σ_β and s_a perpendicularly. Denote by v_Δ the volume of a rectangular parallelepiped having sides of unity, unity and 2Δ. The size of Δ depends upon the wavelength of $\vec{f}_0$ and upon the spatial variations of the constitutive parameters and is sufficiently small so that $\vec{f}v_\Delta$ and $\vec{w}v_\Delta$ are negligible in regions where the constitutive parameters are well behaved.

Recalling the definition of Δ it is seen that the conventional boundary conditions between two different media are (Jones 1964, sec. 1.27)

$$\begin{bmatrix} \varepsilon_\alpha & 0 \\ 0 & \mu_\alpha \end{bmatrix} \vec{f}_\alpha \cdot \hat{\nu} = \begin{bmatrix} \varepsilon_\beta & 0 \\ 0 & \mu_\beta \end{bmatrix} \vec{f}_\beta \cdot \hat{\nu} \; ; \tag{4.14}$$

$$\vec{f}_\alpha \times \hat{\nu} = \vec{f}_\beta \times \hat{\nu} \tag{4.15}$$

where a superscript $\hat{}$ denotes a unit vector and subscripts α and β denote quantities on σ_α and σ_β respectively.

Denote by $\vec{K}$ and q_s respectively the surface current density and surface charge density on s. The conventional boundary conditions at a perfect conductor are (Jones 1964, sec. 1.27)

$$\begin{bmatrix} \varepsilon_a \hat{\nu} \cdot & 0 \\ 0 & \hat{\nu} \times \end{bmatrix} \vec{f}_a = \begin{bmatrix} q_s \\ \vec{K} \end{bmatrix} \tag{4.16}$$

where a subscript a denotes a quantity on s_a. Conservation of charge requires that

$$\nabla_s \cdot \vec{K} + j\omega q_s = 0 \qquad (4.17)$$

where ∇_s operates only in the plane tangent to s at Q. Note that combining eqns (4.16) and (4.17) gives

$$\hat{\nu} \cdot (\nabla_s \times \vec{H}_a) = j\omega\varepsilon_a \hat{\nu} \cdot \vec{E}_a \qquad (4.18)$$

which agrees with Maxwell's equations, so that eqns (4.16) and (4.17) are equivalent.

In many integral equation formulations of diffraction, careful limiting procedures (Richmond 1965, 1966; Mei and van Bladel 1963; Andreasen 1965) are needed for developing expressions suitable for computing fields on σ and s. This applies to the polarization source formulation, and in the present treatment the formulas for $\vec{f}_\sigma$ cannot be used on surfaces closer to σ than σ_α and σ_β, and the formulas for $\vec{f}_s$ cannot be used on surfaces closer to s than s_a. However, since Δ is small in the senses defined earlier this is of no account computationally.

4.3.2 Abrupt Boundaries

When deriving formulas for $\vec{f}_\sigma$ it is convenient to think of the constitutive parameters as varying smoothly in a thin layer (the interval $-\Delta < \nu < \Delta$) enclosing σ, as depicted in Fig. 4.3 in which γ represents either of the constitutive parameters, ε or μ. It is consistent with this assumption and with eqn (4.15) to postulate that

$$\partial(\vec{f} \times \hat{\nu})/\partial\nu = 0, \qquad -\Delta < \nu < \Delta. \qquad (4.19)$$

Since Δ is negligible compared with any wavelength of interest, the interval $-\Delta < \nu < \Delta$ is equivalent to an abrupt boundary. The values of γ, $\partial\gamma/\partial\nu$ and $\partial\gamma/\partial\tau$ at $\nu = \pm\Delta$ are identical with the corresponding values on the surfaces of the two media which are abruptly separated by σ. So, the surface sources on σ can be obtained from the formulas already derived for $\vec{w}$, using suitable limiting procedures. Denote by $\vec{w}_\sigma$ the functional form of $\vec{w}$ within $-\Delta < \nu < \Delta$.

The surface source density $\vec{\eta}$ on σ is given by

$$\vec{\eta} = \int_{-\Delta}^{\Delta} \vec{w}_\sigma \, d\nu. \tag{4.20}$$

On account of the properties of Δ defined in section 4.3.1, the right hand side of eqn (4.20) is zero unless $\vec{w}_\sigma$ has parts which are not well behaved. Although $\partial\gamma/\partial\nu$ varies smoothly within $-\Delta < \nu < \Delta$ it does so too rapidly (in the actual neighbourhood of σ) to be considered well behaved in the aforementioned sense. So the only terms in $\vec{w}$ which can contribute to $\vec{\eta}$ are those involving differentials with respect to ν. Recall the connection between $\vec{w}$ and Ω, defined by eqn (4.6). Consider the "grad div" term in Ω_{11}. If ∇_σ is the gradient operator in the plane tangent to σ at Ψ then

$$\int_{-\Delta}^{\Delta} \text{grad div } \vec{E} \, d\nu \approx \int_{-\Delta}^{\Delta} (\nabla_\sigma(\partial E_\nu/\partial\nu) + \Diamond \, \partial(\nabla\cdot\vec{E})/\partial\nu) \, d\nu$$

$$= \int_{\nu=-\Delta}^{\nu=\Delta} (d\nabla_\sigma E_\nu + \Diamond \, d\nabla\cdot\vec{E}) = \nabla_\sigma(E_{\nu\alpha} - E_{\nu\beta}) + \Diamond\nabla\cdot(\vec{E}_\alpha - \vec{E}_\beta) \tag{4.21}$$

Eqns (4.14) and (4.15) permit eqn (4.21) to be simplified to

$$\int_{-\Delta}^{\Delta} \text{grad div } \vec{E}\, d\nu = \nabla((1-(\varepsilon_\alpha/\varepsilon_\beta))E_{\nu\alpha}). \qquad (4.22)$$

Now consider Ω_{12}. Use of eqn (4.19) shows that

$$\int_{-\Delta}^{\Delta} -(\nabla\mu) \times \vec{H}\, d\nu \approx \int_{-\Delta}^{\Delta} (\vec{H} \times \hat{\nu})(\partial\mu/\partial\nu)\, d\nu = (\mu_\alpha-\mu_\beta)(\vec{H}_\alpha \times \hat{\nu}). \qquad (4.23)$$

There are similar manipulations involving Ω_{21} and Ω_{22}. Write

$$\vec{\eta} = \Lambda \vec{f}_\alpha \qquad (4.24)$$

where the elements of the square matrix Λ are given by

$$\left.\begin{aligned} \Lambda_{11} &= -(\nabla_\sigma)(1-(\varepsilon_\alpha/\varepsilon_\beta))\ \hat{\nu}\cdot \\ \Lambda_{12} &= -j\omega(\mu_\alpha-\mu_\beta)\ \hat{\nu}\times \\ \Lambda_{21} &= j\omega(\varepsilon_\alpha-\varepsilon_\beta)\ \hat{\nu}\times \\ \Lambda_{22} &= -(\nabla_\sigma)(1-(\mu_\alpha/\mu_\beta))\hat{\nu}\cdot \end{aligned}\right\} \qquad (4.25)$$

The reradiations from these surface sources can be written as

$$\vec{f}_\sigma(\vec{\rho}) = (4\pi)^{-1} \iint_\sigma R^{-1}\, \vec{\eta}(\vec{r})\, \exp(-jkR)\, d\sigma \qquad (4.26)$$

where R is the distance between Ψ and P.

4.3.3 Perfect Conductors

Although $\partial\gamma/\partial\nu$ is arbitrarily large on σ, both γ and $\vec{f}$ are finite there, which permits $\vec{\eta}$ to be evaluated in the above comparatively simple manner. However, the volume current and charge densities, $\vec{J}$ and q respectively, are infinite on s, although (where δ denotes the Dirac delta function) $\vec{K} = \vec{J}/\delta(\nu)$ and $q_s = q/\delta(\nu)$ are finite on s. Consequently, there is no limit of $\vec{w}$

giving a simple source density on s which can be postulated as the seat of $\vec{f}_s$. Multipole sources must be included (Jones 1964, sec. 11.1). However, it is more convenient to introduce the vector and scalar potentials, $\vec{A}$ and V respectively, given by

$$\vec{A}(\vec{\rho}) = \mu_0(4\pi)^{-1} \iint_S R^{-1} \vec{K}(\vec{r}) \exp(-jkR)\, ds \; ; \quad (4.27)$$

$$V(\vec{\rho}) = (4\pi\varepsilon_0)^{-1} \iint_S R^{-1} q_s(\vec{r}) \exp(-jkR)\, ds \quad (4.28)$$

where R is the distance between Q and P. At any point P in v, apart from all points on s,

$$\vec{f}_s = \begin{bmatrix} -j\omega\vec{A} - \nabla V \\ \mu_0^{-1}\nabla \times \vec{A} \end{bmatrix} . \quad (4.29)$$

4.4 PIECEWISE CONSTANT MEDIA

In piecewise constant media, the volume v_d can be divided into regions in each of which the constitutive parameters ε and μ are constant. The regions are separated from each other and from free space by abrupt boundaries.

The field reradiated from v_d is given by eqn (4.9) where $\vec{w}$ is given by eqn (4.6) with the elements of Ω (see eqn (4.7)) having, on account of the medium being piecewise constant, the simple forms:

$$\Omega_{11} = \Omega_{22} = (\mu\varepsilon c^2 - 1)k^2; \quad \Omega_{12} = \Omega_{21} = 0. \quad (4.30)$$

Both $\vec{f}_\sigma$ and $\vec{f}_s$, as defined respectively by eqns (4.24) to (4.26) and eqns (4.27) to (4.29), remain unchanged.

Recall that the symbol $\vec{f}$ on the right hand side of eqns (4.6) and (4.24) is the total field, defined by eqn (4.2). So, invoking eqn (4.12), an integral equation of the second kind for $\vec{f}$ has the form:

$$\vec{f} = \vec{f}_0 + \vec{E} \tag{4.31}$$

where $\vec{E}$ is the sum of the right hand sides of eqns (4.9), (4.26) and (4.29).

A useful physical interpretation of eqn (4.31) is that it gives $\vec{f}$ in terms of its reaction (this is the physical meaning of $\vec{E}$) upon the medium. Accurate solutions are only obtained if the reaction of $\vec{f}$ is found on (effectively) <u>all</u> of v_p.

Eqn (4.31) is used in the next chapter to analyse waveguides loaded with dielectric tubes. By using a representation for the field in the dielectric region which satisfies the physics of the problem, computationally convenient formulas are obtained for the cutoff characteristics of the dielectric loaded waveguides.

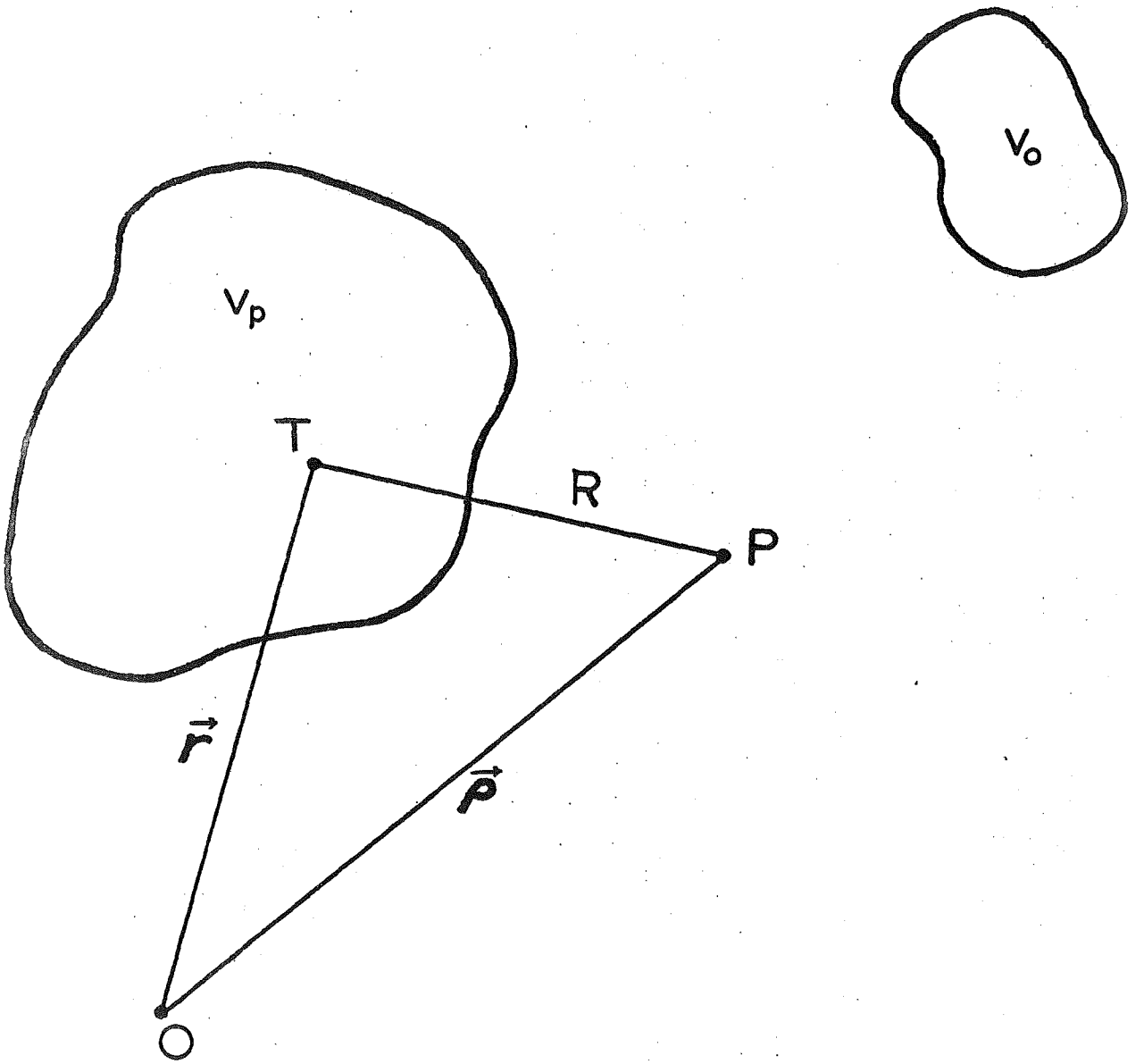

Fig. 4.1 Space and coordinates; v = all space,
$\bar{v}_o$ = complement of v_o in v

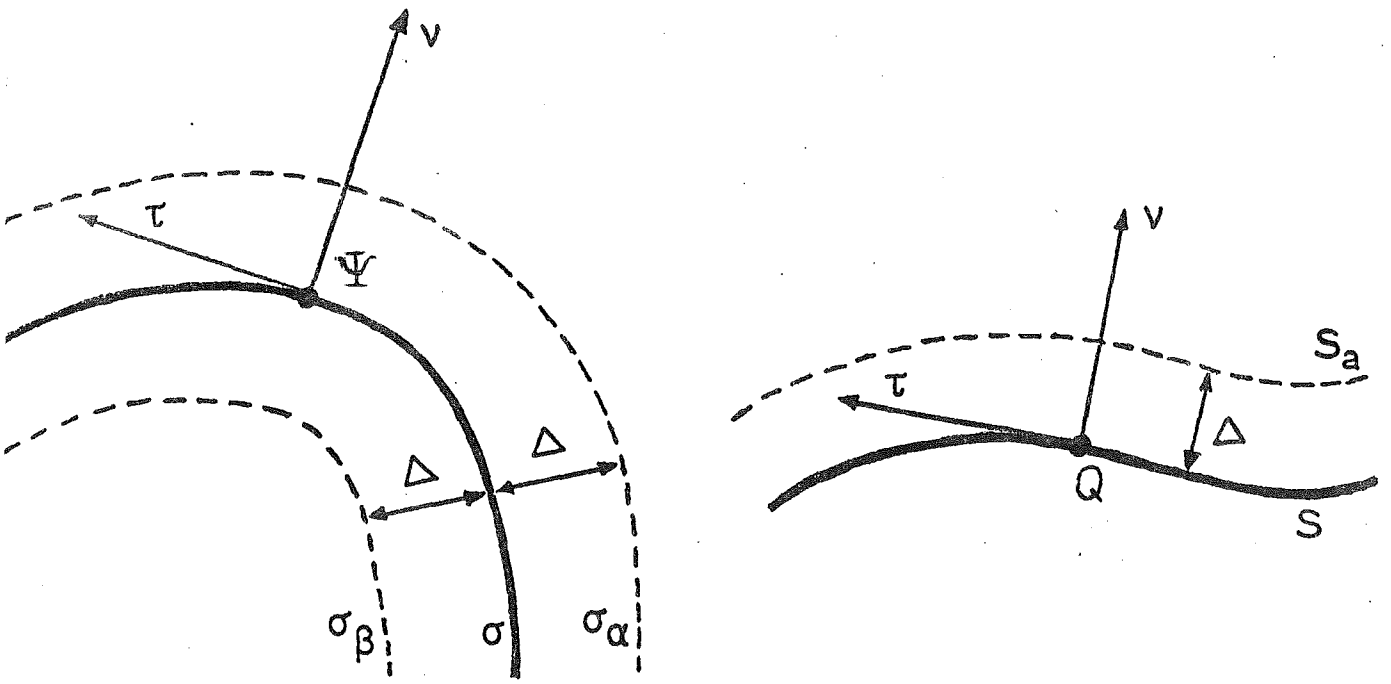

Fig. 4.2 Surfaces σ_α, σ_β and s_a for abrupt boundaries and perfect conductors

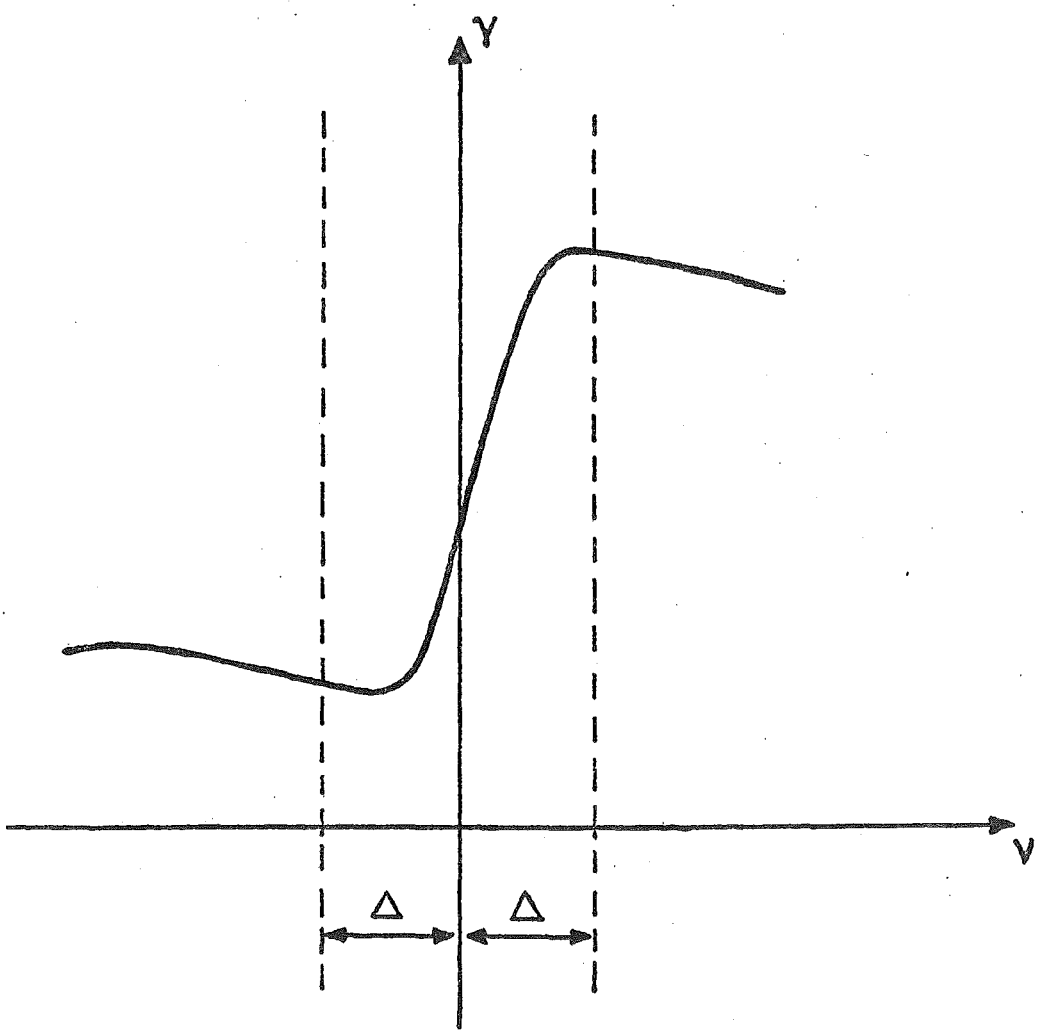

Fig. 4.3 Behaviour of γ in the region $|\nu| < \Delta$

CHAPTER 5: DIELECTRIC LOADED WAVEGUIDES

A number will find
fulfilment enough
in knowing its mind
and doing its stuff.
Piet Hein

Computationally convenient formulas for the cutoff characteristics of hollow, conducting waveguides of arbitrary cross-section loaded with dielectric tubes are presented in this chapter. Numerical results are presented for a square waveguide loaded with a solid dielectric rod. Experimental results are also reported.

5.1 INTRODUCTION

The polarization source formulation given in chapter 4 is specialized to the two-dimensional case. A representation for the field in the dielectric region which satisfies the physics of the problem is used in the polarization source integral equation (eqn (4.31)) and this, together with the extended boundary condition, is employed to obtain formulas for the cutoff characteristics of uniform waveguides of arbitrary cross-section loaded with circularly cylindrical dielectric tubes or rods. These formulas are line integral equations for the surface current density on the waveguide wall alone and are a computationally significant addition to the literature on dielectric loaded waveguides (Clarricoats 1961; Chatterjee and Chatterjee 1965; Schlosser and Unger 1966; Baier 1969;

Csendes and Silvester 1970). The numerical solution for the cutoff characteristics involves the solution of a homogeneous set of equations obtained by representing the unknown surface current density by an expansion set. The computer implementation is straightforward and only small determinant orders (about 10) are necessary. It is relatively simpler than the finite element method (Csendes and Silvester 1970, 1971; Ahmed and Daly 1969a) and variational methods (Baier 1969, 1970; English 1971a,b). All these techniques need a definition of the field within the whole waveguide region and require large matrix sizes (about 100). It should be mentioned however that most of the methods described in the above references are applicable to the propagating as well as the cutoff condition.

5.2 UNIFORM WAVEGUIDES AT CUTOFF

Consider a uniform, metal-walled, inhomogeneously-filled waveguide supporting a mode at cutoff. Provided the wall is perfectly conducting and the medium inside the waveguide is lossless (usually satisfactory assumptions for calculating cutoff characteristics when standard metallic waveguides are loaded with commonly used dielectric materials) the field in the waveguide is self supporting, so that

$$\vec{f} = \vec{f}_p \; ; \quad \vec{f}_0 = 0. \tag{5.1}$$

At cutoff, the guide wavelength is infinite and the waveguide field only exhibits two-dimensional variations.

5.2.1 Two-Dimensional Polarization Source Formalism

Erect Cartesian coordinates (x, y, z) with origin at O. Set the z-axis parallel to the waveguide axis. Denote the intersections of σ, s and v_d with the xy-plane by Γ, C and D respectively. Take P, T, Ψ and Q to lie in the xy-plane. Let the polar coordinates of P and Q be (ρ,φ) and (r,θ) respectively, as in Fig. 5.1. Since

$$\partial\vec{f}/\partial z = \partial\vec{K}/\partial z = \partial q_s/\partial z \equiv 0 \qquad (5.2)$$

it follows that the z-integration over the polarization sources can be done analytically. This results in the term $\exp(-jkR)/(\pi R)$ being replaced by $-jH_0^{(2)}(kR)$ (Jones 1964, sec. 1.34), which means that eqns (4.9), (4.26), (4.27) and (4.28) become , respectively

$$\vec{f}_d(\rho) = \vec{f}_d(\rho,\varphi) = (-j/4) \iint_D \vec{w}(r,\theta)\, H_0^{(2)}(kR)\, r\,d\theta\,dr\ ; \qquad (5.3)$$

$$\vec{f}_\sigma(\rho,\varphi) = (-j/4) \int_\Gamma \vec{\eta}(r,\theta)\, H_0^{(2)}(kR)\, d\Gamma; \qquad (5.4)$$

$$\vec{A}(\rho,\varphi) = (-j\mu_0/4) \int_C \vec{K}(r,\theta)\, H_0^{(2)}(kR)\, dC\ ; \qquad (5.5)$$

$$V(\rho,\varphi) = (-j/(4\varepsilon_0)) \int_C q_s(r,\theta)\, H_0^{(2)}(kR)\, dC, \qquad (5.6)$$

where $H_0^{(2)}$ denotes the Hankel function of the second kind of zero order and eqns (4.30), (4.25), (4.29) and (4.31) still apply.

5.2.2 Derivation of Formulas

5.2.2.1 Preliminaries

In the derivation of the formulas for the cutoff characteristics the extended boundary condition (see sec. 2.2) is employed. Computationally convenient

formulas are obtained mainly because of the addition theorem for Bessel functions (Watson 1968, chap. 11), which gives (refer to Fig. 5.1)

$$H_0^{(2)}(kR) = \sum_{m=-\infty}^{\infty} H_m^{(2)}(k\rho)\, J_m(kr)\, \exp(jm(\varphi-\theta)), \quad \rho \geqslant r \tag{5.7}$$

where $H_m^{(2)}$ and J_m denote the Hankel function of the second kind and the Bessel function of the first kind, both of order m. When $\rho < r$, $H^{(2)}$ and J are interchanged in eqn (5.7). Use has also to be made of standard Wronskian relations for Bessel functions (Watson 1968, sec. 3.63) and the standard indefinite integral (Watson 1968, sec. 5.11)

$$\int^{\alpha} t\, \mathcal{C}_\mu(\zeta k t)\, \mathcal{D}_\mu(kt)\, dt$$

$$= \frac{\alpha}{(\zeta^2-1)k} \left[\zeta\, \mathcal{C}_{\mu+1}(\zeta k\alpha)\mathcal{D}_\mu(k\alpha) - \mathcal{C}_\mu(\zeta k\alpha)\mathcal{D}_{\mu+1}(k\alpha)\right], \tag{5.8}$$

where $\mathcal{C}$ and $\mathcal{D}$ are any two Bessel functions. It is convenient to define (refer to eqn (5.8))

$$z_\mu(\mathcal{C},\mathcal{D},\alpha) = \left[\zeta\, \mathcal{C}_{\mu+1}(\zeta k\alpha)\mathcal{D}_\mu(k\alpha) - \mathcal{C}_\mu(\zeta k\alpha)\mathcal{D}_{\mu+1}(k\alpha)\right] \tag{5.9}$$

Fig. 5.2 shows a waveguide, with a wall of arbitrary shape, loaded with a dielectric tube having the constitutive parameters

$$\varepsilon = \zeta^2 \varepsilon_0 \; ; \quad \mu = \mu_0 \; , \tag{5.10}$$

where it is convenient to write ζ^2 for the relative dielectric constant (ζ is the refractive index of the dielectric). The dielectric is assumed lossless with no conductivity. The origin O of coordinates is taken

on the axis of the tube, which has inner and outer radii of a and b respectively.

5.2.2.2 E-modes at cutoff

Propagating modes in dielectric loaded waveguides are hybrid EH-modes, as these are required in general to satisfy the boundary conditions at the surface of the dielectric; but they separate into pure E-modes and pure H-modes at cutoff (Clarricoats 1961). First consider E-modes for which, at cutoff, the only components of $\vec{E}$ and $\vec{K}$ are in the z-direction. Eqns (4.17) and (5.2) show that there is no surface charge density, making it convenient to write

$$\vec{E}(\vec{\rho}) = \hat{z}\, E(\rho,\varphi) \; ; \quad \vec{K}(\vec{r}) = \hat{z}\, F(C) \; ; \quad q_s = 0 \tag{5.11}$$

Eqns (4.24) and (4.25) show that there is no contribution to the total $\vec{E}$ field from $\vec{\eta}$ since $\hat{\nu}\cdot\vec{E} = 0$, from eqn (5.11), and $\mu_\alpha = \mu_\beta$, from eqn (5.10), making Λ_{11} and Λ_{12} respectively ineffective. Eqn (5.11) shows that there is no contribution to $\vec{E}$ from eqn (4.28). Consequently, the only contributions to $\vec{E}$ come from $\vec{f}_d$, given by eqn (5.3) (with $\vec{w}$ given by eqns (4.6) and (4.30), and $\vec{f}_s$ given by substituting eqn (5.5) into eqn (4.29). It follows by straightforward manipulations that

$$E(\rho,\varphi) = -j((\zeta^2-1)k^2/4) \int_a^b \int_0^{2\pi} E(r,\theta)\, H_0^{(2)}(kR)\, r\,d\theta\,dr$$

$$- (\omega\mu_0/4) \int_C F(C)\, H_0^{(2)}(kR)\, dC. \tag{5.12}$$

Note (from inspection of Fig. 5.2) that the domain of

integration in the first term on the right hand side of eqn (5.12) corresponds to D, which appears in eqn (5.3). Within D where the refractive index is ζ, a general expression for $E(\rho,\varphi)$ satisfying Maxwell's equations identically is

$$E(\rho,\varphi) = \sum_{n=-\infty}^{\infty} [A_n J_n(\zeta k\rho) + B_n Y_n(\zeta k\rho)] \exp(jn\varphi),$$

$$a < \rho < b, \quad 0 \leqslant \varphi < 2\pi \qquad (5.13)$$

where the A_n and B_n are constants and Y_n denotes the Bessel function of the second kind of order n.

5.2.2.2.1 Reaction of the field in the dielectric regior

To obtain the reaction of the field upon the polarization sources in D, eqns (5.12) and (5.13) are combined and analysed for values of ρ and φ in D. Note that after eqn (5.13) has been substituted into it, the left hand side of eqn (5.12) has the form of a trigonometrical Fourier series in φ, the coefficients of which can be abstracted in the usual way because φ exists for $0 \leqslant \varphi < 2\pi$ for all values of r in D. If eqns (5.7) and (5.13) are substituted into the right hand side of eqn (5.12) it can be expressed as a similar Fourier series. Use has to be made of the standard indefinite integral (eqn (5.8)) and Wronskian relations for Bessel functions (Watson 1964, sec. 3.63). It should also be noted (from inspection of Fig. 5.2) that the largest value of r in D is less than the least value of r on C. Thus eqn (5.12) becomes

$$\sum_{m=-\infty}^{\infty} J_m(k\rho)\exp(jm\varphi)(-j\pi k/2)\{[b\,Z_m(J,J,b) - a\,Z_m(J,J,a) - jb\,Z_m(J,Y,b)]A_m + [b\,Z_m(Y,J,b) - a\,Z_m(Y,J,a) - jb\,Z_m(Y,Y,b)]B_m - \frac{\omega\mu_0}{4}\int_C F(C)\,H_m^{(2)}(kr)\exp(-jm\theta)\,dC\}$$

$$+ \sum_{m=-\infty}^{\infty} Y_m(k\rho)\exp(jm\varphi)(\pi ka/2)[Z_m(J,J,a)A_m + Z_m(Y,J,a)B_m] = 0, \qquad (5.14)$$

where Z_m is defined by eqn (5.9). Equating Fourier coefficients on both sides of eqn (5.14) gives the conditions

$$(j\pi k/2)[bZ_m(J,J,b) - aZ_m(J,J,a) - jbZ_m(J,Y,b)]A_m + (j\pi k/2)[bZ_m(Y,J,b) - aZ_m(Y,J,a) - jbZ_m(Y,Y,b)]B_m + \frac{\omega\mu_0}{4}\int_C F(C)\,H_m^{(2)}(kR)\exp(-jm\theta)\,dC = 0\ ; \qquad (5.15)$$

$$Z_m(J,J,a)\,A_m + Z_m(Y,J,a)\,B_m = 0. \qquad (5.16)$$

5.2.2.2.2 Extended boundary condition

The reaction of the field upon the currents in C is obtained from the extended boundary condition that $E(\rho,\varphi)$ must be zero outside C. Further, for ρ greater than the largest value of r on C, the coefficients of the trigonometrical Fourier series for $E(\rho,\varphi)$ are all zero, since φ exists for $0 \leqslant \varphi < 2\pi$. This is the advantage of the extended boundary condition, since it is not clear how the usual boundary condition could lead to this simplification. This application of the extended boundary condition to equation (5.12) gives, using eqn (5.7),

$$-j((\zeta^2-1)k^2/4) \int_a^b\int_a^{2\pi} E(r,\theta)\ J_m(kr)\ \exp(-jm\theta)\ rd\theta dr$$

$$- (\omega\mu_0/4) \int_C F(C)\ J_m(kr)\ \exp(-jm\theta)\ dC = 0 \qquad (5.17)$$

for all integers m in $-\infty < m < \infty$. By substituting eqn (5.13) into eqn (5.17) and using eqns (5.8) and (5.9), we obtain

$$(j\pi k/2)[bZ_m(J,J,b) - aZ_m(J,J,a)]A_m$$

$$+ (j\pi k/2)[bZ_m(Y,J,b) - aZ_m(Y,J,a)]B_m$$

$$+ \frac{\omega\mu_0}{4} \int_C F(C)\ J_m(kr)\ \exp(-jm\theta)\ dC = 0,$$

$$-\infty < m < \infty. \qquad (5.18)$$

5.2.2.2.3 E-mode cutoff formulas

Combining the results obtained (eqns (5.15), (5.16) and (5.18)) by the procedures outlined in the two previous sections gives

$$\int_C F(C)[\xi_m(ka,kb,\zeta)J_m(kr) + \eta_m(ka,kb,\zeta)Y_m(kr)]$$

$$\exp(-jm\theta)\ dC = 0 \qquad (5.19)$$

for all integers m in $-\infty < m < \infty$, where

$$\xi(ka,kb,\zeta) = \zeta\ J_{m+1}(\zeta kb)\ Y_m(kb) - J_m(\zeta kb)\ Y_{m+1}(kb)$$

$$- [\zeta\ Y_{m+1}(\zeta kb)Y_m(kb) - Y_m(\zeta kb)Y_{m+1}(kb)]\tau_m(ka,\zeta); \qquad (5.20)$$

$$\eta_m(ka,kb,\zeta) = -\zeta\ J_{m+1}(\zeta kb)J_m(kb) + J_m(\zeta kb)J_{m+1}(kb)$$

$$+ [\zeta\ Y_{m+1}(\zeta kb)J_m(kb) - Y_m(\zeta kb)J_{m+1}(kb)]\tau_m(ka,\zeta); \qquad (5.21)$$

$$\tau_m(ka,\zeta) = \frac{\zeta\, J_{m+1}(\zeta ka)\, J_m(ka) - J_m(\zeta ka)\, J_{m+1}(ka)}{\zeta\, Y_{m+1}(\zeta ka)\, J_m(ka) - Y_m(\zeta ka)\, J_{m+1}(ka)}. \tag{5.22}$$

The significant thing about eqn (5.19) is that it is an integral equation for the surface current alone. The field in the dielectric (characterized by the A_n and B_n of eqn (5.13)) has been eliminated.

When the dielectric tube becomes a rod then a = 0 and the formulas are simplified since $\tau_m(0,z) = 0$. When there is no dielectric tube, eqn (5.19) reduces to

$$\int_C F(C)\, J_m(kr)\, \exp(-jm\theta)\, dC = 0, \quad \zeta = 1 \tag{5.23}$$

which is the formula originally derived for E-modes at cutoff in hollow waveguides (Bates 1969b; also sec. 2.2.1, eqn (2.3)). For a circular waveguide of radius c, loaded with a coaxial dielectric tube, the cutoff condition (from eqn (5.19)) is

$$\xi_m(ka,kb,\zeta)\, J_m(kc) + \eta_m(ka,kb,\zeta)\, Y_m(kc) = 0, \tag{5.24}$$

which agrees with the expression given by Tsandoulas and Ince (1971).

5.2.3 H-modes at Cutoff

5.2.3.1 Derivation of formulas

For an H-mode at cutoff

$$\vec{H}(\vec{\rho}) = \hat{z}\, H(\rho,\varphi); \quad \vec{K}(\vec{r}) = \hat{C}\, G(C); \quad q_s = (j/\omega)\, \partial G/\partial C \tag{5.25}$$

where $\hat{C}$ is the unit vector along C, the symbol G is used to denote the surface current density directed along C as in previous analyses (Bates 1968, 1969b; also chapter 2) and the expression for q_s is obtained

from eqn (4.17).

Note that $\vec{f}_\sigma$ contributes to $H(\rho,\varphi)$ because Λ_{21}, as given by eqn (4.25), is different from zero when $\varepsilon_\alpha \neq \varepsilon_\beta$, as is the case for the dielectric tube. Apart from this difference, the analysis proceeds similarly to that for E-modes.

Using eqn (5.25), eqn (4.31) gives

$$H(\rho,\varphi) = -j((\zeta^2-1)k^2/4) \int_a^b \int_0^{2\pi} H(r,\theta) H_0^{(2)}(kR)\, r\,d\theta\,dr$$

$$- j((\zeta^2-1)/(4\zeta^2)) \int_\Gamma \partial H(r,\theta)/\partial\nu \; H_0^{(2)}(kR)\, d\Gamma$$

$$+ j/4 \int_C G(C)[(\sin\alpha/r)\partial/\partial\theta - \cos\alpha\,\partial/\partial r] H_0^{(2)}(kR)\, dC. \quad (5.26)$$

The field $H_z(\rho,\varphi)$ within D is again represented by the right hand side of eqn (5.13). This is substituted in eqn (5.26); and the extraction of the Fourier coefficients from the consideration of the reaction of the field upon the polarization sources in D gives the conditions, (equivalent to eqns (5.15) and (5.16) for E-modes)

$$\{[bZ_m(J,J,b) - aZ_m(J,J,a) - jbZ_m(J,Y,b)]$$

$$+ (\zeta-1/\zeta)[bJ'_m(\zeta kb)J_m(kb) - aJ'_m(\zeta ka)J_m(ka)$$

$$- jbJ'_m(\zeta kb)Y_m(kb)]\}A_m$$

$$+ \{[bZ_m(Y,J,b) - aZ_m(Y,J,a) - jbZ_m(Y,Y,b)]$$

$$+ (\zeta-1/\zeta)[bY'_m(\zeta kb)J_m(kb) - aY'_m(\zeta ka)J_m(ka)$$

$$- jbY'_m(\zeta kb)Y_m(kb)]\}\ B_m$$

$$+ 1/(4\pi) \int_C G(C)[H^{(2)}_{m-1}(kR)\ \exp(j\alpha)$$

$$- H^{(2)}_{m+1}(kR)\ \exp(-j\alpha)]\ \exp(-jm\theta)\ dC = 0; \qquad (5.27)$$

$$[Z_m(J,J,a) + (\zeta-1/\zeta)\ J'_m(\zeta ka)\ J_m(ka)]\ A_m$$

$$+ [Z_m(Y,J,a) + (\zeta-1/\zeta)\ Y'_m(\zeta ka)\ J_m(ka)]\ B_m = 0, \qquad (5.28)$$

for all integers m in $-\infty < m < \infty$.

Application of the extended boundary condition to eqn (5.26) gives (equivalent to eqn (5.18))

$$\{[bZ_m(J,J,b) - aZ_m(J,J,a)]$$

$$+ (\zeta-1/\zeta)[bJ'_m(\zeta kb)\ J_m(kb) - aJ'_m(\zeta ka)\ J_m(ka)]\}\ A_m$$

$$+ \{[bZ_m(Y,J,b) - aZ_m(Y,J,a)]$$

$$+ (\zeta-1/\zeta)[bY'_m(\zeta kb)\ J_m(kb) - aY'_m(\zeta ka)\ J_m(ka)]\}\ B_m$$

$$+ 1/(4\pi) \int_C G(C)[J_{m-1}(kr)\ \exp(j\alpha)$$

$$- J_{m+1}(kr)\ \exp(-j\alpha)]\ \exp(-jm\theta)\ dC = 0,$$

$$-\infty < m < \infty. \qquad (5.29)$$

5.2.3.2 H-mode cutoff formulas

The results obtained in eqns (5.27) to (5.29) are combined in the same way as has already been done (sec. 5.2.2.2) for E-modes. The result is (refer to Fig. 5.2 for the meaning of α)

$$\int_C G(C)[\bar{\xi}_m(ka,kb,\zeta)(J_{m-1}(kr)\ \exp(j\alpha) - J_{m+1}(kr)\ \exp(-j\alpha)) + \bar{\eta}_m(ka,kb,\zeta)(Y_{m-1}(kr)\ \exp(j\alpha) - Y_{m+1}(kr)\ \exp(-j\alpha))]\ \exp(-jm\theta)\ dC = 0\ ; \qquad -\infty < m < \infty, \tag{5.30}$$

$$\bar{\xi}_m(ka,kb,\zeta) = \zeta\ J_m(\zeta kb)\ Y'_m(kb) - J'_m(\zeta kb)\ Y_m(kb) - [\zeta\ Y_m(\zeta kb)\ Y'_m(kb) - Y'_m(\zeta kb)\ Y_m(kb)]\ \bar{\tau}_m(ka,\zeta); \tag{5.31}$$

$$\bar{\eta}_m(ka,kb,\zeta) = -\zeta\ J_m(\zeta kb)\ J'_m(kb) - J'_m(\zeta kb)\ J_m(kb) + [\zeta\ Y_m(\zeta kb)\ J'_m(kb) - Y'_m(\zeta kb)\ J_m(kb)]\ \bar{\tau}_m(ka,\zeta); \tag{5.32}$$

$$\bar{\tau}_m(ka,\zeta) = \frac{\zeta\ J_m(\zeta ka)\ J'_m(ka) - J'_m(\zeta ka)\ J_m(ka)}{\zeta\ Y_m(\zeta ka)\ J'_m(ka) - Y'_m(\zeta ka)\ J_m(ka)}\ , \tag{5.33}$$

where the superscript dash denotes differentiation with respect to the argument.

5.3 SQUARE WAVEGUIDE LOADED WITH DIELECTRIC ROD

5.3.1 Numerical Results

A square waveguide loaded with a dielectric rod (Fig. 5.3) has been examined to test the practical computational value of eqns (5.19) and (5.30).

From a computational viewpoint, eqns (5.19) and (5.30) are almost as convenient as eqns (2.3) and (2.4) for empty waveguides, the only significant added

complication being that both Bessel functions, of the first and second kinds, must be computed at each point on C. The factors $\xi_m(ka,kb,\zeta)$ and $\eta_m(ka,kb,\zeta)$ (and $\bar{\xi}_m$ and $\bar{\eta}_m$) only vary with m (for a given dielectric loaded waveguide) so that they add little to the computation time.

As with eqns (2.3) and (2.4), the surface current density F(C) in eqn (5.19) (and G(C) in eqn (5.30)) can be expressed approximately in the form

$$F(C) = \sum_{n=0}^{N} F_n \Phi_n(C) \qquad (5.34)$$

where the F_n are constants and the $\Phi_n(C)$ are members of a set of functions. The results of chapter 3 show that, for the square waveguide considered here, accurate results are given with $\Phi_n = \delta(C-C_n)$. This representation is used here and Table 5.1 shows the cutoff wavenumbers, computed to four significant figures (with N not exceeding 8 for any of the modes considered), for three values of the dielectric constant of the rod. Table 5.2 shows the dependence upon N of kW, when ε_r = 2.30, for the final E-mode considered in Table 5.1. Note the smoothness of the numerical convergence. Table 5.3 gives the cutoff wavenumbers, computed to four significant figures, with ε_r = 2.25 for three values of N (7, 8 and 9). It is seen that results accurate to much better than 0.1% are already obtained with N = 7.

5.3.2 Experimental Results

Since apparently accurate results were obtained with such small values of N it was thought to be worthwhile checking the computations with experiments. Transmission-type resonant cavity measurements (Barlow and Cullen 1950, chap. 3) were made at frequencies between 0.5 and 1.2 GHz on a rectangular cavity (30.48 x 30.48 x 45.82 cm^3) provided with small probes, the size of which could be varied, at either end (Fig. 5.4 depicts the experimental set up). The size of the probes was decreased until the error in the measurement of the resonant frequencies of the empty cavity was less than that due to manufacturing tolerances (< 0.15%). For the frequency range used the cavity had a Q factor (Barlow and Cullen 1950, chap. 3) of about 600. The cavity was loaded with a rod (it was too expensive to fit a tube) of paraffin wax (Cerese wax 132°) having a nominal relative dielectric constant ε_r of 2.25. No accurate means of determining ε_r (Barlow and Cullen 1950, chap. 9) were available, nor could it be determined if the wax was electromagnetically homogeneous. This is why computations for three values of ε_r were made. Table 5.1 shows that there is gratifying agreement between computation and experiment for $\varepsilon_r = 2.30$. The errors are comparable with other comparisons of theory and observation by resonant cavity measurements (Meinke et al. 1963, Baier 1969).

5.4 DISCUSSION

The computational convenience of eqns (5.19) and (5.30) is such that the cutoff characteristics of arbitrary waveguides loaded with circular dielectric tubes or rods can be computed as easily as those of empty waveguides. The compactness of the equations is lost if the cross section of the dielectric is arbitrary. However, there cannot be many practical applications of dielectric loaded waveguides for which there is much advantage in using dielectric cylinders of other than annular or circular cross section.

Table 5.1 Computed and measured cutoff wavenumbers of dielectric loaded square waveguide. b/W = 0.161, $\varepsilon_r = \zeta^2$ = relative dielectric constant of rod.

d/W	Mode	kW			
		Measured	Computed		
			ε_r = 2.25	2.30	2.35
0.0	H-modes	2.865	2.963	2.958	2.954
		4.410	4.410	4.409	4.408
	E-modes	3.746	3.764	3.741	3.719
		6.664	6.686	6.671	6.655
0.206	H-modes	2.904	2.987	2.982	2.980
		2.895	2.990	2.986	2.982
		4.328	4.351	4.349	4.347
	E-modes	3.888	3.906	3.886	3.866
		6.215	6.236	6.214	6.194

Table 5.2: Dependence upon N of the computed wavenumber of the second E-mode in a square waveguide loaded with a dielectric rod (Fig. 5.3), for d/W = 0.206 and ε_r = 2.30.

N	kW
5	6.191
6	6.208
7	6.215
8	6.214
9	6.214

Table 5.3: Computed cutoff wavenumbers of dielectric loaded square waveguide for three values of N. b/W = 0.161, ε_r = 2.25.

d/W	Mode	kW		
		N= 7	8	9
0.0	H-modes	2.963 4.409	2.963 4.410	2.963 4.410
	E-modes	3.764 6.686	3.764 6.686	3.764 6.686
0.206	H-modes	2.987 2.990 4.355	2.987 2.990 4.351	2.986 2.990 4.351
	E-modes	3.906 6.236	3.906 6.236	3.906 6.235
0.372	E-modes	4.196 6.030	4.198 6.034	

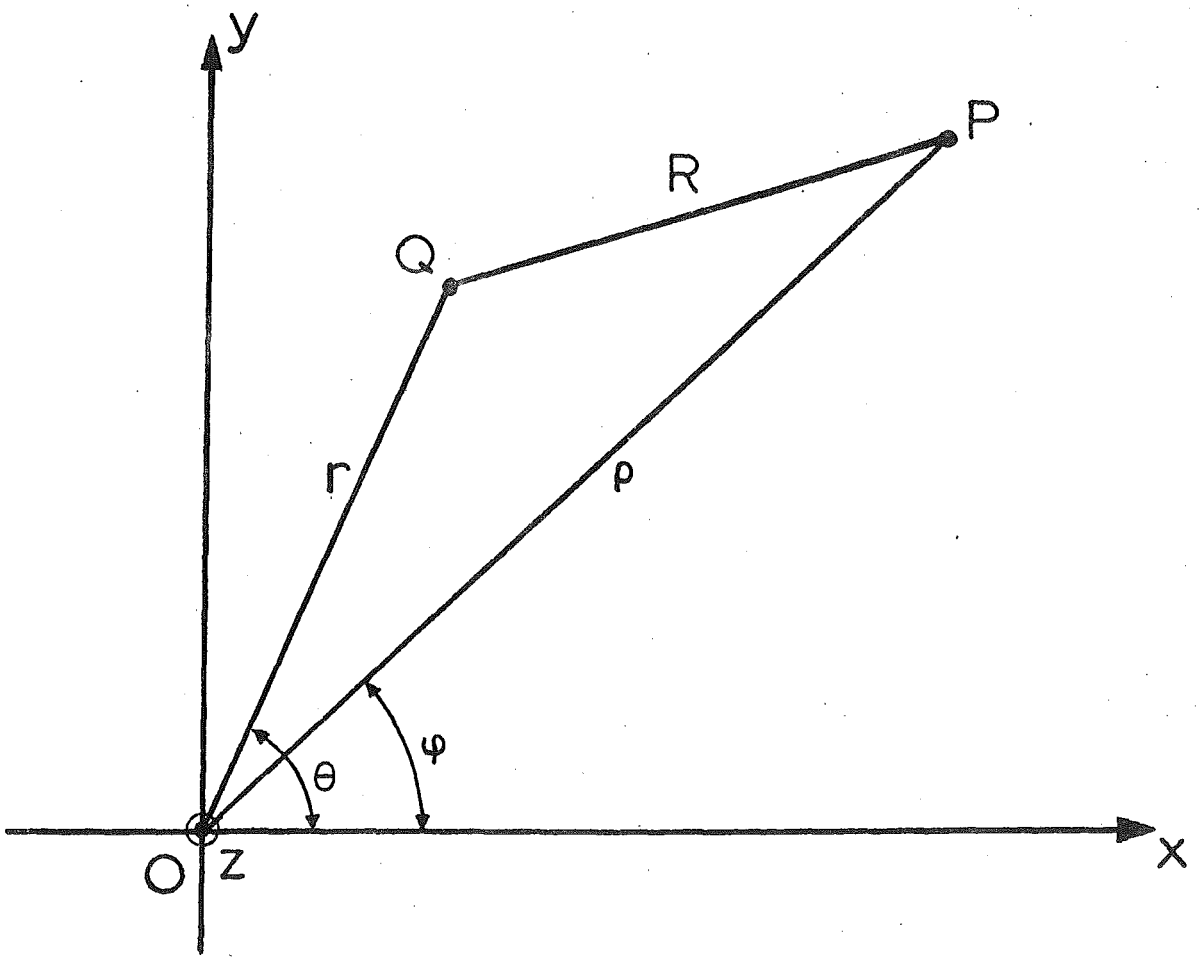

Fig. 5.1 Coordinates in the xy-plane; z-axis perpendicular to paper.

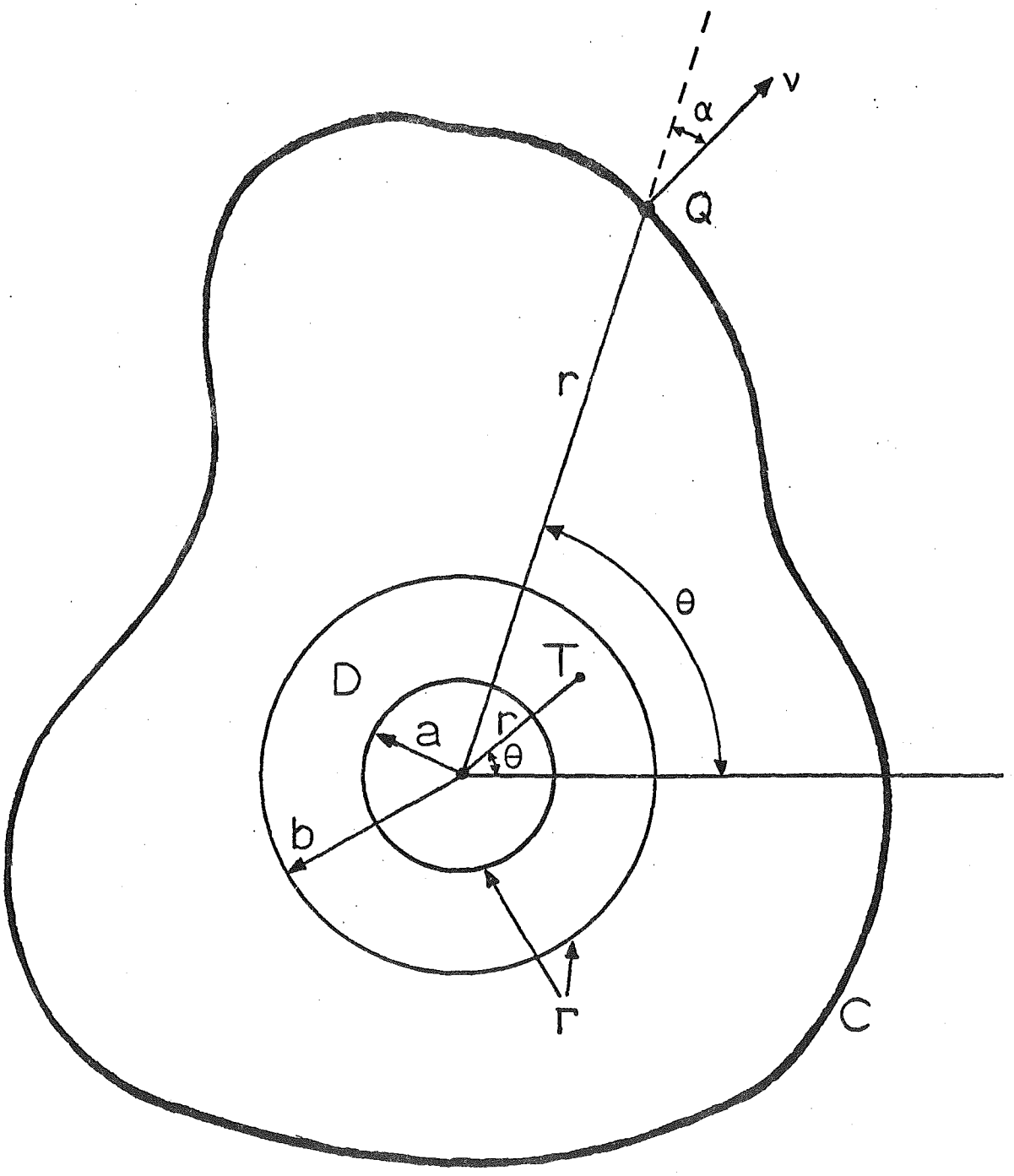

Fig. 5.2 Waveguide of arbitrary cross-section loaded with dielectric tube

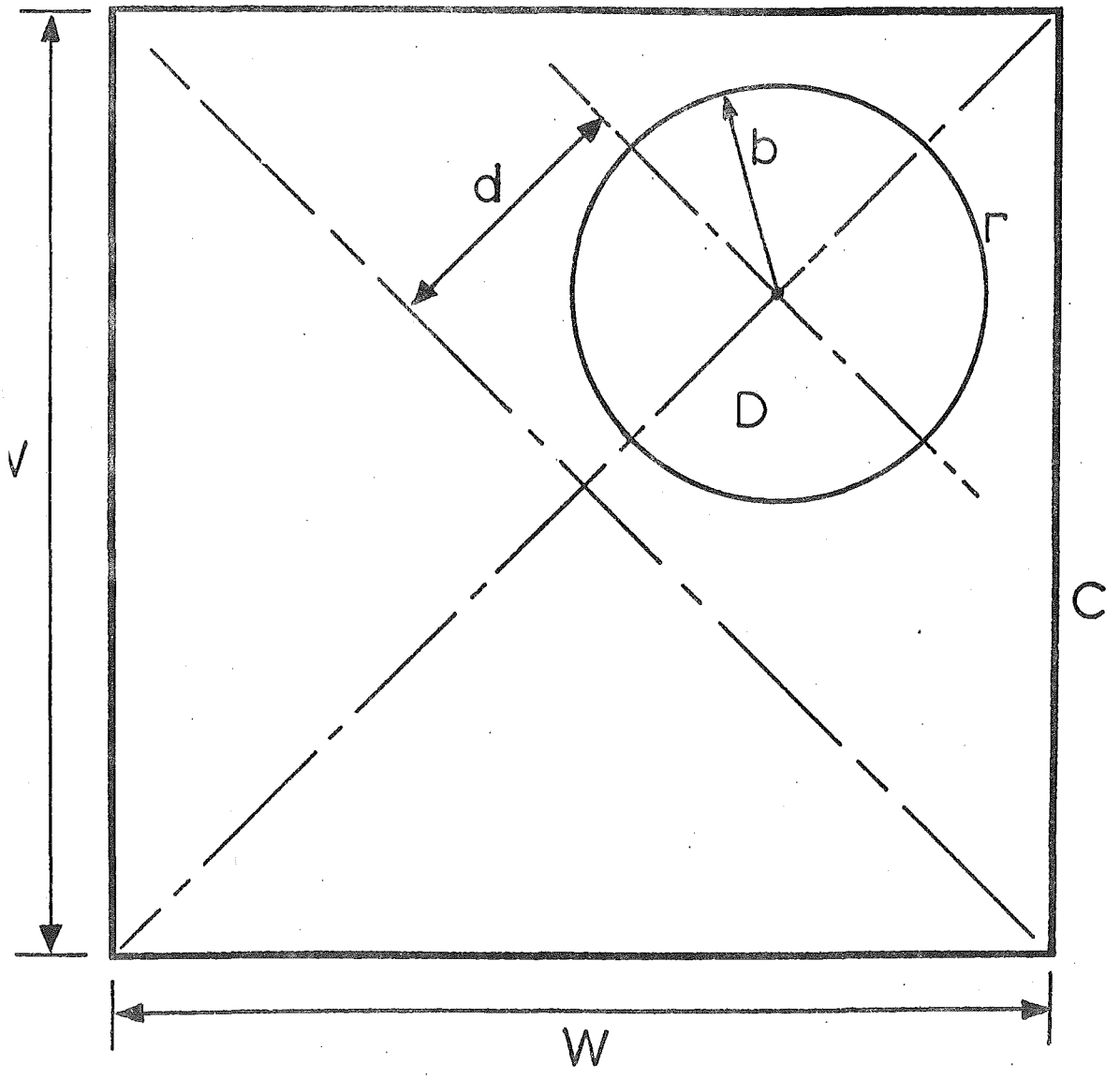

Fig. 5.3 Square waveguide loaded with dielectric rod

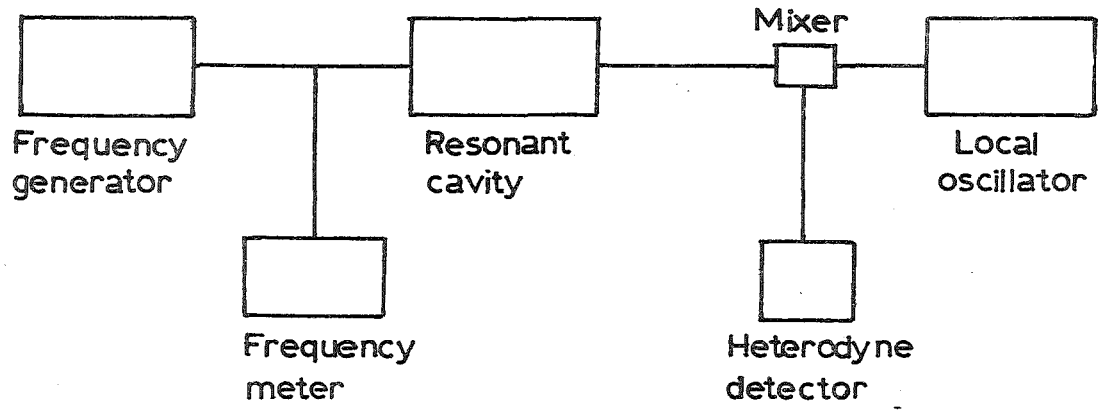

Fig. 5.4: Resonant cavity measurements

PART 3: Azimuthal Surface Wave

CHAPTER 6: AZIMUTHAL SURFACE WAVE - GENERAL EXTERNAL FIELD

> ' 'Tis so', said the Duchess: 'and the moral of that is - "Oh, 'tis love, 'tis love, that makes the world go round".'
>
> Lewis Carroll

The literature on surface waves contains several comparatively simple analyses of the effect of curvature of the guiding surface. It is shown here that these are not generally suitable for obtaining accurate estimates of the variation of attenuation with curvature. The general external field for any circular cylindrical guiding surface is considered and universal tables for the surface impedance are given. These tables can be used to obtain the propagation characteristics of any particular guiding surface.

6.1 INTRODUCTION

Surface waves are waves that are associated with an interface between two different media, there being a recognizable surface which supports and guides the waves (Barlow 1959; Barlow and Brown 1962). The guiding of surface waves by plane or single-wire structures has been much studied (Gouban 1950, 1951; Barlow and Cullen 1953; Harvey 1960; Barlow and Brown 1962; King and Wiltse 1962; Amemiya 1965; Yabe and Kakukawa 1968; Lee and Jones 1971). There have also been studies (Elliott 1955; Barlow and Brown 1962, chap.

7; Horiuchi 1953) of the azimuthal surface wave which is the wave associated with guiding structures which are bent into circular arcs in the direction of propagation.

In this chapter and chapter 7, the TM wave (Elliott 1955) for an azimuthal guiding surface is considered. This is the dominant wave and it is of great theoretical interest since there exist exact and comparatively simple expressions for its fields. The analytic form of the field outside the guiding surface is independent of the exact nature of the surface. This external field is introduced in sec. 6.2.

Previous studies of the azimuthal surface wave include a qualitative approach to the propagation and cutoff of the wave (Lawson 1966) and a first order approximation to the propagation characteristics (Elliott 1955). These are discussed briefly in section 6.3. In particular, a critical evaluation is given of a well known method of attenuation calculation by power balance (Barlow and Brown 1962, chap. 7). The essential simplicity of this method is attractive but it is shown here to be tautological. This chapter and chapter 7 give a convenient method of computing accurately the attenuation and phase constants of azimuthal surface waves.

In many calculations involving the propagation of surface waves around bends, the guiding surface is characterised by a surface impedance which is assumed to be independent of curvature (Wait and Spies 1968).

This is a reasonable approximation in certain cases but there does not seem to have been any systematic attempt to gauge the approximation quantitatively. In this chapter a set of universal tables is presented (section 6.4) which will allow the approximation to be evaluated comparatively simply in any particular case by the method described in chapter 7, where the dielectric clad cylinder is considered.

In many situations the important consideration is the variation of attenuation with curvature of the guiding surface. There has been no detailed consideration of how this is affected by assuming the surface impedance to be independent of curvature. The approach described in this and the next chapters allows the variation of attenuation with curvature to be evaluated in any particular case.

To obtain the surface impedance for the universal tables in section 6.4, it was necessary to compute an expression containing Hankel functions of complex order. The technique which was used is described in Appendix C.

The results of chapters 6 and 7 have been published (Bates and Ng 1971).

6.2 PRELIMINARIES

Consider a monochromatic (angular frequency ω) wave, exhibiting no variation in the z-direction; guided by the surface of radius R, shown in Fig. 6.1. Restrict consideration to the transverse magnetic (TM) wave, and to the fields in the region $\rho > R$. Thus, with the factor $\exp(j\omega t)$ understood, (Barlow and Brown 1962, chap. 7):

$$H_z = H_\nu^{(2)}(k\rho)\exp(-j\nu\varphi), \tag{6.1}$$

$$E_\rho = -\frac{\zeta_0 \nu}{k\rho} H_z, \tag{6.2}$$

$$E_\varphi = j\zeta_0 \frac{H_\nu^{(2)'}(k\rho)}{H_\nu^{(2)}(k\rho)} H_z, \tag{6.3}$$

$$\nu = (\beta - j\alpha)R, \quad k = \omega(\mu_0\varepsilon_0)^{\frac{1}{2}}, \tag{6.4}$$

where (ρ, φ, z) are the cylindrical polar coordinates, $H_\nu^{(2)}(x)$ is the Hankel function of the second kind of order ν and argument x, a prime denotes differentiation with respect to the argument, ζ_0 is the intrinsic impedance of free space and $(\beta - j\alpha)$ is the surface wave propagation constant (α and β are both real).

The surface impedance at $\rho = R$ is denoted by ζ_1 and is given by

$$\zeta_1 = \xi_1 + j\eta_1 = -\left.\frac{E_\varphi}{H_z}\right|_{\rho=R} = -j\zeta_0 \frac{H_\nu^{(2)'}(kR)}{H_\nu^{(2)}(kR)}. \tag{6.5}$$

The components of the complex Poynting vector in the ρ and φ directions, denoted by P_ρ and P_φ respectively, are given by

$$P_\rho = E_\varphi H_z^* = j\zeta_0 H_\nu^{(2)'}(k\rho) H_{\nu*}^{(1)}(k\rho) \exp(-2\alpha R\varphi), \quad (6.6)$$

$$P_\varphi = -E_\rho H_z^* = \frac{\zeta_0 \nu}{k\rho} H_\nu^{(2)}(k\rho) H_{\nu*}^{(1)}(k\rho) \exp(-2\alpha R\varphi), \quad (6.7)$$

where $H_\nu^{(1)}(x)$ is the Hankel function of the first kind of order ν and argument x and the asterisk denotes the complex conjugate.

The evaluation of the expression for ζ_1, equation (6.5) is discussed in Appendix C and a set of universal tables of ζ_1/ζ_0 is given in section 6.4.

6.3 ATTENUATION CALCULATION BY POWER BALANCE

Azimuthal surface waves have been the subject of some previous studies (Elliott 1955; Barlow and Brown 1962; Horiuchi 1953, Lawson 1966). A survey of surface wave guiding structures is given by Harvey (1960).

Lawson (1966) gives a qualitative discussion of propagation along curved paths and estimates the conditions under which leakage or radiation of the field is significant. The leakage is considered in relation to the behaviour of the Hankel functions.

A first order calculation of the propagation characteristics of azimuthal surface waves on circular cylinders, suitable for small attenuation constants, has been given by Elliott (1955). In the solution of the propagation characteristics from the field equations, the attenuation constant is first assumed to be zero and then the attenuation constant is evaluated by a perturbation calculation.

Horiuchi (1953) uses a perturbation of the rectangular coordinates in the analysis of the azimuthal TE

wave on a dielectric clad cylinder. The analysis is applicable only to small curvatures.

Previous studies of the propagation characteristics of azimuthal surface waves have hence been either qualitative or only valid for small curvatures. If accurate quantitative results are required, a detailed investigation such as that given in section 6.4 and chapter 7, must be undertaken. It is found that in general the attenuation constant is not so small that it can be neglected to first order, as in Elliott's (1955) calculations.

Refer to Fig. 6.1 and consider the space outside the guiding surface of radius R. Denote by $S_\varphi(\varphi)$ the total power, in watts, flowing in the φ-direction. Also, denote by $S_\rho(r,\varphi)$ the radial power, in watts per radian, flowing at any radius r. Because power must be conserved in any physical system, and because the space outside $\rho = R$ is assumed free (and therefore lossless), any changes in S_φ with φ must be made up by power flowing across the guiding surface and by power radiating away at infinity. This gives the power balance:

$$S_\varphi(\varphi) - S_\varphi(\varphi+d\varphi) = [S_\rho(\infty,\varphi) - S_\rho(R,\varphi)]\, d\varphi \qquad (6.8)$$

Barlow and Brown (1962, sec. 7.3) obtained an approximate power balance from the following two assumptions, which seem reasonable for most curved surface waveguides. They assumed first that most of the power guided by the surface would exist outside the surface, and second that the power flowing radially across the

surface would all be radiated away at infinity. So, they asserted that

$$S_\varphi(\varphi) - S_\varphi(\varphi+d\varphi) \approx S_\rho(R,\varphi)\, d\varphi. \tag{6.9}$$

In terms of the Poynting vector components, introduced in section 6.2, the radial power flow is given by

$$S_\rho(r,\varphi) = \mathcal{R}e\, rP_\rho \tag{6.10}$$

and the circumferential power flow is given by

$$S_\varphi(\varphi) = \mathcal{R}e\left[\int_R^\infty P_\varphi\, d\rho\right], \tag{6.11}$$

where $\mathcal{R}e$ denotes "the real part of". After substituting from equation (6.7), the integral in equation (6.11) can be evaluated immediately (Watson 1968, p. 135). On using equations (6.6) and (6.10), equation (6.11) can be written as

$$2\alpha R\, S_\varphi(\varphi) = \frac{2\zeta_0}{\pi k} \exp(-2\alpha R\varphi) \exp(\pi\alpha R) - S_\rho(R,\varphi). \tag{6.12}$$

At first sight it seems reasonable to expect that if equation (6.12) is combined with either of the power balance equations, (6.8) or (6.9), then an equation for α will result. This equation can be expected to be transcendental, so that it will only be possible to solve it numerically, unless simplifying assumptions can be made. Barlow and Brown (1962) made such assumptions and, after using equation (6.9), obtained a plausible expression for α. Unfortunately, this expression cannot be even approximately valid, because equation (6.8) is merely equation (6.12) multiplied by

$d\varphi$, as the following reasoning shows. The left hand side of equation (6.8) is $(-\partial S_{\varphi}(\varphi)/\partial\varphi)d\varphi$, which is by definition identical with $2\alpha R S_{\varphi}(\varphi)d\varphi$ because $2\alpha R$ is the power attenuation constant of the wave. Also, as $\rho \to \infty$, the Hankel functions in equation (6.6) transform into the exponentials in equation (6.12). Thus, an expression for α cannot be obtained from the power balance.

6.4 UNIVERSAL TABLES

In this section the external field is considered. The field equations have been given in section 6.2. The surface impedance is given by equation (6.5). The argument and the modulus of the order of the Hankel functions are of the same order (Barlow and Brown 1962, chap. 7), that is,

$$kR = O(|\nu|), \tag{6.13}$$

which is the most inconvenient case for numerical computation. Appendix C describes the method which was employed to compute the expression (6.5) for the surface impedance.

The external case is important because it is the same for any type of circular cylindrical guiding surface. It is therefore useful to construct universal tables, for the external case, of surface impedance versus λ/R, for various values of phase constant β and attenuation constant α; where λ is the wavelength and R is the radius of curvature of the guiding surface. The results are given in Table 6.1 which is drawn up for various sets of values of β/k and for various fixed

values of α/k. The normalised surface impedance $(\zeta_1/\zeta_0) = (\xi_1 + j\eta_1)/\zeta_0$ is given as the complex number pair $(\xi_1/\zeta_0, \eta_1/\zeta_0)$ and is listed as a function of λ/R.

Fig. 6.2 is a typical plot of a family of curves for ζ_1/ζ_0. For any particular curve there is a value of λ/R at which the value of ξ_1/ζ_0 changes from positive to negative. This represents the transition between the case where net power flows into the guiding structure and that where net power flows out through the guiding surface. The value of the imaginary part η_1/ζ_0 also changes at certain values of the parameters from an inductive, positive value to a capacitive, negative value when the guiding structure can no longer support the TM wave.

The use of Table 6.1 to obtain the propagation constants of the azimuthal surface wave guided by a dielectric clad cylinder is considered in chapter 7.

β/k = 1.00

λ/R	α/k = 0.0		0.02		0.04	
0.0	0.0	0.0	-0.142 00	-0.141 00	-0.202 00	-0.198 00
0.01	-0.929 -01	0.539 -01	-0.879 -01	-0.142 00	-0.192 00	-0.198 00
0.02	-0.117 00	0.682 -01	-0.740 -01	-0.701 -01	-0.169 00	-0.217 00
0.03	-0.134 00	0.783 -01	-0.897 -01	-0.327 -01	-0.119 00	-0.193 00
0.04	-0.147 00	0.864 -01	-0.105 00	-0.960 -02	-0.102 00	-0.150 00
0.05	-0.159 00	0.933 -01	-0.118 00	0.698 -02	-0.102 00	-0.116 00
0.06	-0.169 00	0.993 -01	-0.130 00	0.200 -01	-0.107 00	-0.893 -01
0.07	-0.178 00	0.105 00	-0.141 00	0.307 -01	-0.115 00	-0.684 -01
0.08	-0.186 00	0.110 00	-0.150 00	0.399 -01	-0.123 00	-0.514 -01
0.09	-0.193 00	0.114 00	-0.159 00	0.479 -01	-0.131 00	-0.371 -01
0.10	-0.200 00	0.119 00	-0.167 00	0.551 -01	-0.139 00	-0.248 -01
0.11	-0.207 00	0.123 00	-0.174 00	0.617 -01	-0.146 00	-0.141 -01
0.12	-0.213 00	0.127 00	-0.181 00	0.676 -01	-0.153 00	-0.449 -02
0.13	-0.218 00	0.130 00	-0.188 00	0.732 -01	-0.160 00	0.413 -02
0.14	-0.224 00	0.134 00	-0.194 00	0.784 -01	-0.167 00	0.120 -01
0.15	-0.229 00	0.137 00	-0.200 00	0.832 -01	-0.173 00	0.192 -01
0.16	-0.234 00	0.140 00	-0.205 00	0.878 -01	-0.179 00	0.259 -01
0.17	-0.239 00	0.143 00	-0.210 00	0.921 -01	-0.184 00	0.321 -01
0.18	-0.243 00	0.146 00	-0.215 00	0.963 -01	-0.190 00	0.380 -01
0.19	-0.248 00	0.149 00	-0.220 00	0.100 00	-0.195 00	0.435 -01
0.20	-0.252 00	0.152 00	-0.225 00	0.104 00	-0.200 00	0.487 -01
0.30	-0.289 00	0.176 00	-0.265 00	0.135 00	-0.242 00	0.898 -01
0.40	-0.318 00	0.196 00	-0.296 00	0.160 00	-0.275 00	0.120 00
0.50	-0.342 00	0.214 00	-0.322 00	0.180 00	-0.302 00	0.144 00
0.60	-0.363 00	0.229 00	-0.344 00	0.198 00	-0.325 00	0.165 00
0.70	-0.383 00	0.243 00	-0.364 00	0.214 00	-0.346 00	0.183 00
0.80	-0.400 00	0.257 00	-0.382 00	0.229 00	-0.365 00	0.200 00
0.90	-0.416 00	0.269 00	-0.399 00	0.243 00	-0.382 00	0.215 00
1.00	-0.431 00	0.281 00	-0.414 00	0.256 00	-0.398 00	0.229 00
1.50	-0.493 00	0.333 00	-0.478 00	0.312 00	-0.464 00	0.290 00
2.00	-0.542 00	0.378 00	-0.529 00	0.359 00	-0.515 00	0.340 00
3.00	-0.620 00	0.457 00	-0.608 00	0.441 00	-0.596 00	0.425 00
4.00	-0.682 00	0.526 00	-0.671 00	0.512 00	-0.660 00	0.498 00
5.00	-0.734 00	0.590 00	-0.724 00	0.578 00	-0.714 00	0.565 00

$\beta/k = 1.00$

λ/R	$\alpha/k = 0.06$		0.08		0.10	
0.0	-0.249 00	-0.241 00	-0.289 00	-0.277 00	-0.324 00	-0.308 00
0.01	-0.242 00	-0.241 00	-0.283 00	-0.277 00	-0.320 00	-0.309 00
0.02	-0.236 00	-0.241 00	-0.278 00	-0.277 00	-0.316 00	-0.308 00
0.03	-0.229 00	-0.255 00	-0.274 00	-0.277 00	-0.312 00	-0.309 00
0.04	-0.196 00	-0.265 00	-0.273 00	-0.284 00	-0.308 00	-0.308 00
0.05	-0.160 00	-0.249 00	-0.259 00	-0.298 00	-0.308 00	-0.310 00
0.06	-0.138 00	-0.221 00	-0.232 00	-0.304 00	-0.304 00	-0.320 00
0.07	-0.127 00	-0.192 00	-0.203 00	-0.297 00	-0.291 00	-0.332 00
0.08	-0.124 00	-0.166 00	-0.180 00	-0.280 00	-0.271 00	-0.338 00
0.09	-0.125 00	-0.144 00	-0.163 00	-0.259 00	-0.247 00	-0.337 00
0.10	-0.128 00	-0.125 00	-0.153 00	-0.237 00	-0.224 00	-0.328 00
0.11	-0.132 00	-0.108 00	-0.147 00	-0.216 00	-0.205 00	-0.315 00
0.12	-0.137 00	-0.931 -01	-0.144 00	-0.196 00	-0.190 00	-0.298 00
0.13	-0.142 00	-0.799 -01	-0.144 00	-0.179 00	-0.179 00	-0.281 00
0.14	-0.147 00	-0.681 -01	-0.145 00	-0.162 00	-0.172 00	-0.263 00
0.15	-0.153 00	-0.574 -01	-0.147 00	-0.148 00	-0.167 00	-0.246 00
0.16	-0.158 00	-0.477 -01	-0.150 00	-0.134 00	-0.163 00	-0.230 00
0.17	-0.163 00	-0.387 -01	-0.153 00	-0.122 00	-0.162 00	-0.214 00
0.18	-0.168 00	-0.304 -01	-0.156 00	-0.110 00	-0.162 00	-0.200 00
0.19	-0.173 00	-0.227 -01	-0.160 00	-0.997 -01	-0.162 00	-0.187 00
0.20	-0.178 00	-0.155 -01	-0.164 00	-0.899 -01	-0.163 00	-0.174 00
0.30	-0.221 00	0.387 -01	-0.203 00	-0.187 -01	-0.190 00	-0.829 -01
0.40	-0.255 00	0.758 -01	-0.237 00	0.275 -01	-0.221 00	-0.258 -01
0.50	-0.283 00	0.105 00	-0.265 00	0.620 -01	-0.249 00	0.156 -01
0.60	-0.307 00	0.129 00	-0.290 00	0.901 -01	-0.274 00	0.484 -01
0.70	-0.329 00	0.150 00	-0.312 00	0.114 00	-0.297 00	0.758 -01
0.80	-0.348 00	0.168 00	-0.332 00	0.135 00	-0.317 00	0.995 -01
0.90	-0.366 00	0.185 00	-0.350 00	0.154 00	-0.335 00	0.121 00
1.00	-0.382 00	0.201 00	-0.367 00	0.171 00	-0.352 00	0.140 00
1.50	-0.449 00	0.266 00	-0.436 00	0.242 00	-0.422 00	0.217 00
2.00	-0.502 00	0.320 00	-0.489 00	0.298 00	-0.477 00	0.277 00
3.00	-0.584 00	0.408 00	-0.573 00	0.391 00	-0.562 00	0.373 00
4.00	-0.649 00	0.484 00	-0.639 00	0.469 00	-0.628 00	0.454 00
5.00	-0.704 00	0.553 00	-0.694 00	0.540 00	-0.684 00	0.526 00

$\beta/k = 1.05$

λ/R	$\alpha/k = 0.0$		0.02		0.04	
0.0	0.0	0.320 00	0.644 -01	0.326 00	0.123 00	0.341 CC
0.01	-0.571 -06	0.312 00	0.676 -01	0.319 00	0.127 00	0.336 CC
0.02	-0.411 -03	0.301 00	0.729 -01	0.313 00	0.132 00	0.327 CC
0.03	-0.358 -02	0.289 00	0.848 -01	0.298 CO	0.130 00	0.351 CC
0.04	-0.104 -01	0.277 00	0.879 -01	0.272 00	0.196 00	0.350 CO
0.05	-0.196 -01	0.267 00	0.790 -01	0.248 00	0.232 00	0.282 CC
0.06	-0.298 -01	0.259 00	0.641 -01	0.229 00	0.217 00	0.219 CO
0.07	-0.402 -01	0.253 00	0.475 -01	0.216 00	0.185 00	0.180 CO
0.08	-0.505 -01	0.248 00	0.311 -01	0.207 00	0.152 00	0.157 CC
0.09	-0.604 -01	0.245 00	0.157 -01	0.201 00	0.123 00	0.145 CC
0.10	-0.699 -01	0.242 00	0.140 -02	0.197 00	0.976 -01	0.138 CO
0.11	-0.789 -01	0.241 00	-0.118 -01	0.194 00	0.754 -01	0.134 CO
0.12	-0.874 -01	0.240 00	-0.241 -01	0.193 00	0.558 -01	0.133 CO
0.13	-0.955 -01	0.239 00	-0.355 -01	0.192 00	0.385 -01	0.132 CO
0.14	-0.103 00	0.238 00	-0.460 -01	0.192 00	0.229 -01	0.133 CO
0.15	-0.111 00	0.238 00	-0.559 -01	0.192 00	0.877 -02	0.134 CO
0.16	-0.118 00	0.238 00	-0.652 -01	0.192 00	-0.412 -02	0.135 CO
0.17	-0.124 00	0.239 00	-0.739 -01	0.193 00	-0.160 -01	0.137 CC
0.18	-0.131 00	0.239 00	-0.821 -01	0.194 00	-0.269 -01	0.139 CO
0.19	-0.137 00	0.240 00	-0.900 -01	0.195 00	-0.371 -01	0.141 CO
0.20	-0.143 00	0.240 00	-0.974 -01	0.196 00	-0.467 -01	0.143 OC
0.30	-0.193 00	0.250 00	-0.157 00	0.210 00	-0.119 00	0.165 CO
0.40	-0.230 00	0.261 00	-0.200 00	0.225 00	-0.168 00	0.185 00
0.50	-0.261 00	0.273 00	-0.234 00	0.240 00	-0.206 00	0.203 00
0.60	-0.288 00	0.285 00	-0.263 00	0.253 00	-0.237 00	0.219 00
0.70	-0.311 00	0.296 00	-0.288 00	0.266 00	-0.264 00	0.234 CO
0.80	-0.332 00	0.306 00	-0.310 00	0.278 00	-0.288 00	0.248 CC
0.90	-0.351 00	0.317 00	-0.330 00	0.290 00	-0.309 00	0.262 CO
1.00	-0.368 00	0.327 00	-0.348 00	0.301 00	-0.328 00	0.274 CO
1.50	-0.440 00	0.373 00	-0.423 00	0.351 00	-0.406 00	0.329 CO
2.00	-0.495 00	0.415 00	-0.480 00	0.395 00	-0.465 00	0.375 CO
3.00	-0.581 00	0.488 00	-0.568 00	0.472 00	-0.554 00	0.456 CC
4.00	-0.648 00	0.555 00	-0.636 00	0.541 00	-0.624 00	0.527 CC
5.00	-0.704 00	0.617 00	-0.693 00	0.605 00	-0.682 00	0.592 CO

$\beta/_k$ = 1.05

λ/R	α/k = 0.06		0.08		0.10	
0.0	0.175 00	0.360 00	0.221 00	0.381 00	0.262 00	0.4C1 CO
0.01	0.178 00	0.358 00	0.286 00	0.276 00	-0.277 00	-0.389 CO
0.02	0.158 00	0.369 00	0.625 00	0.728 00	-0.124 00	-0.465 CO
0.03	0.182 00	0.272 00	0.547 -01	0.120 01	-0.709 -01	-0.285 CC
0.04	0.499 -01	0.403 00	0.195 00	0.215 -01	-0.573 00	-0.932 CO
0.05	0.240 00	0.629 00	-0.138 00	0.210 00	0.700 -01	-0.291 CC
0.06	0.541 00	0.431 00	-0.489 00	0.650 00	-0.170 00	-0.725 -C1
0.07	0.496 00	0.187 00	0.405 00	0.291 01	-0.475 00	0.214 -C1
0.08	0.391 00	0.912 -01	0.160 01	-0.928 -01	-0.104 01	-0.648 -C1
0.09	0.309 00	0.569 -01	0.822 00	-0.234 00	-0.166 01	-0.147 C1
0.10	0.248 00	0.451 -01	0.552 00	-0.195 00	0.343 00	-0.182 01
0.11	0.202 00	0.423 -01	0.414 00	-0.157 00	0.587 00	-0.966 CO
0.12	0.165 00	0.434 -01	0.328 00	-0.127 00	0.496 00	-0.623 CO
0.13	0.135 00	0.465 -01	0.267 00	-0.103 00	0.409 00	-0.456 CC
0.14	0.110 00	0.504 -01	0.222 00	-0.842 -01	0.341 00	-0.358 CO
0.15	0.878 -01	0.546 -01	0.186 00	-0.680 -01	0.289 00	-0.293 CO
0.16	0.687 -01	0.591 -01	0.156 00	-0.540 -01	0.247 00	-0.246 CO
0.17	0.518 -01	0.635 -01	0.131 00	-0.418 -01	0.213 00	-0.211 00
0.18	0.365 -01	0.679 -01	0.109 00	-0.310 -01	0.184 00	-0.182 CO
0.19	0.227 -01	0.722 -01	0.899 -01	-0.213 -01	0.159 00	-0.159 CO
0.20	0.101 -01	0.764 -01	0.729 -01	-0.124 -01	0.137 00	-0.139 00
0.30	-0.791 -01	0.112 00	-0.379 -01	0.491 -01	0.317 -02	-0.277 -C1
0.40	-0.136 00	0.140 00	-0.103 00	0.881 -01	-0.701 -01	0.285 -01
0.50	-0.178 00	0.163 00	-0.149 00	0.118 00	-0.121 00	0.673 -C1
0.60	-0.212 00	0.182 00	-0.186 00	0.142 00	-0.161 00	0.975 -01
0.70	-0.241 00	0.200 00	-0.217 00	0.163 00	-0.194 00	0.123 CO
0.80	-0.266 00	0.216 00	-0.244 00	0.182 00	-0.222 00	0.144 CO
0.90	-0.288 00	0.231 00	-0.267 00	0.199 00	-0.247 00	0.164 CO
1.00	-0.308 00	0.245 00	-0.289 00	0.214 00	-0.269 00	0.181 CO
1.50	-0.389 00	0.305 00	-0.372 00	0.279 00	-0.356 00	0.253 CO
2.00	-0.450 00	0.354 00	-0.435 00	0.333 00	-0.420 00	0.310 CO
3.00	-0.541 00	0.439 00	-0.529 00	0.421 00	-0.516 00	0.403 CO
4.00	-0.612 00	0.512 00	-0.601 00	0.497 00	-0.589 00	0.481 CO
5.00	-0.671 00	0.579 00	-0.660 00	0.565 00	-0.649 00	0.551 00

β/k = 1.10

λ/R	α/k = 0.0		0.02		0.04	
0.0	0.0	0.458 00	0.478 -01	0.460 00	0.944 -01	0.466 00
0.01	-0.293 -16	0.454 00	0.486 -01	0.457 00	0.958 -01	0.463 00
0.02	-0.362 -08	0.450 00	0.495 -01	0.453 00	0.974 -01	0.460 00
0.03	-0.179 -05	0.446 00	0.506 -01	0.449 00	0.992 -01	0.456 00
0.04	-0.397 -04	0.441 00	0.519 -01	0.444 00	0.101 00	0.453 00
0.05	-0.253 -03	0.436 00	0.537 -01	0.439 00	0.104 00	0.450 00
0.06	-0.867 -03	0.430 00	0.557 -01	0.433 00	0.108 00	0.446 00
0.07	-0.208 -02	0.424 00	0.573 -01	0.426 00	0.114 00	0.441 00
0.08	-0.399 -02	0.418 00	0.579 -01	0.418 00	0.121 00	0.433 00
0.09	-0.661 -02	0.411 00	0.572 -01	0.409 00	0.126 00	0.421 00
0.10	-0.988 -02	0.405 00	0.552 -01	0.400 00	0.128 00	0.408 00
0.11	-0.137 -01	0.399 00	0.520 -01	0.391 00	0.128 00	0.395 00
0.12	-0.180 -01	0.394 00	0.478 -01	0.383 00	0.126 00	0.381 00
0.13	-0.226 -01	0.389 00	0.429 -01	0.375 00	0.121 00	0.369 00
0.14	-0.275 -01	0.384 00	0.373 -01	0.368 00	0.115 00	0.357 00
0.15	-0.325 -01	0.380 00	0.313 -01	0.361 00	0.108 00	0.347 00
0.16	-0.377 -01	0.376 00	0.250 -01	0.355 00	0.101 00	0.337 00
0.17	-0.430 -01	0.373 00	0.186 -01	0.350 00	0.925 -01	0.329 00
0.18	-0.483 -01	0.369 00	0.120 -01	0.346 00	0.841 -01	0.322 00
0.19	-0.536 -01	0.367 00	0.545 -02	0.342 00	0.756 -01	0.316 00
0.20	-0.589 -01	0.364 00	-0.111 -02	0.338 00	0.671 -01	0.311 00
0.30	-0.108 00	0.350 00	-0.614 -01	0.319 00	-0.899 -02	0.284 00
0.40	-0.150 00	0.347 00	-0.110 00	0.316 00	-0.673 -01	0.281 00
0.50	-0.185 00	0.349 00	-0.150 00	0.319 00	-0.113 00	0.286 00
0.60	-0.215 00	0.354 00	-0.184 00	0.325 00	-0.151 00	0.293 00
0.70	-0.241 00	0.360 00	-0.213 00	0.332 00	-0.183 00	0.302 00
0.80	-0.265 00	0.367 00	-0.238 00	0.340 00	-0.211 00	0.311 00
0.90	-0.287 00	0.374 00	-0.261 00	0.348 00	-0.236 00	0.320 00
1.00	-0.306 00	0.382 00	-0.282 00	0.356 00	-0.258 00	0.329 00
1.50	-0.386 00	0.419 00	-0.367 00	0.397 00	-0.347 00	0.374 00
2.00	-0.448 00	0.455 00	-0.430 00	0.436 00	-0.413 00	0.416 00
3.00	-0.541 00	0.524 00	-0.526 00	0.507 00	-0.512 00	0.490 00
4.00	-0.613 00	0.587 00	-0.600 00	0.572 00	-0.587 00	0.558 00
5.00	-0.673 00	0.646 00	-0.661 00	0.633 00	-0.649 00	0.620 00

$\beta/k = 1.10$

λ/R	$\alpha/k = 0.06$		0.08		0.10	
0.0	0.139 00	0.475 00	0.181 00	0.486 00	0.221 00	0.499 CC
0.01	0.141 00	0.472 00	0.183 00	0.484 CC	0.223 00	0.497 CO
0.02	0.143 00	0.470 00	0.185 00	0.482 CC	0.225 CC	0.495 CO
0.03	0.145 00	0.467 00	0.187 00	0.480 00	0.227 00	0.493 CC
0.04	0.147 00	0.464 00	0.190 00	0.478 00	0.229 00	0.489 CO
0.05	0.148 00	0.461 00	0.194 00	0.473 00	0.230 00	0.485 CC
0.06	0.149 00	0.462 00	0.190 00	0.467 00	0.252 00	0.484 CC
0.07	0.156 00	0.465 00	0.181 00	0.474 00	0.234 00	0.454 CO
0.08	0.170 00	0.465 00	0.183 00	0.492 00	0.195 00	0.461 CC
0.09	0.186 00	0.458 00	0.203 00	0.511 00	0.171 00	0.502 CO
0.10	0.201 00	0.444 00	0.237 00	0.517 CO	0.181 00	0.560 CO
0.11	0.211 00	0.425 00	0.274 00	0.506 00	0.228 00	0.612 CO
0.12	0.216 00	0.404 00	0.306 00	0.480 00	0.306 00	0.634 CC
0.13	0.216 00	0.382 00	0.326 00	0.444 00	0.390 00	0.616 00
0.14	0.212 00	0.362 00	0.334 00	0.407 00	0.457 00	0.562 CC
0.15	0.205 00	0.343 00	0.333 00	0.371 00	0.495 00	0.491 CO
0.16	0.196 00	0.327 00	0.324 00	0.339 00	0.505 00	0.420 CC
0.17	0.186 00	0.313 00	0.311 00	0.311 00	0.496 CO	0.357 CO
0.18	0.174 00	0.301 00	0.296 00	0.289 00	0.476 00	0.306 CO
0.19	0.163 00	0.291 00	0.279 00	0.270 00	0.450 00	0.265 CC
0.20	0.151 00	0.282 00	0.262 00	0.255 00	0.423 00	0.234 CO
0.30	0.507 -01	0.245 00	0.121 00	0.198 00	0.205 00	0.140 CC
0.40	-0.207 -01	0.242 00	0.306 -01	0.197 00	0.877 -01	0.143 CO
0.50	-0.742 -01	0.248 00	-0.326 -01	0.207 00	0.118 -01	0.159 CO
0.60	-0.117 00	0.258 00	-0.812 -01	0.219 00	-0.439 -01	0.176 CO
0.70	-0.152 00	0.268 00	-0.121 00	0.232 00	-0.881 -01	0.192 CO
0.80	-0.183 00	0.279 00	-0.154 00	0.245 00	-0.125 00	0.208 CO
0.90	-0.210 00	0.290 00	-0.183 00	0.258 00	-0.156 00	0.223 CO
1.00	-0.234 00	0.301 00	-0.209 00	0.270 00	-0.184 00	0.237 CO
1.50	-0.327 00	0.350 00	-0.308 00	0.325 00	-0.288 00	0.298 CO
2.00	-0.396 00	0.394 00	-0.379 00	0.372 00	-0.362 00	0.349 CO
3.00	-0.497 00	0.473 00	-0.483 00	0.455 00	-0.469 00	0.436 CO
4.00	-0.574 00	0.542 00	-0.561 00	0.527 00	-0.549 00	0.511 CO
5.00	-0.637 00	0.607 00	-0.625 00	0.593 00	-0.614 00	0.578 CC

$\beta/k = 1.15$

λ/R	$\alpha/k = 0.0$		0.02		0.04	
0.0	0.0	0.568 00	0.404 -01	0.569 00	0.804 -01	0.572 00
0.01	-0.120 -29	0.565 00	0.408 -01	0.567 00	0.811 -01	0.570 00
0.02	-0.621 -15	0.563 00	0.412 -01	0.564 00	0.818 -01	0.567 00
0.03	-0.721 -10	0.560 00	0.416 -01	0.561 00	0.826 -01	0.565 00
0.04	-0.213 -07	0.557 00	0.420 -01	0.559 00	0.834 -01	0.563 00
0.05	-0.646 -06	0.555 00	0.425 -01	0.556 00	0.843 -01	0.560 00
0.06	-0.627 -05	0.552 00	0.431 -01	0.553 00	0.852 -01	0.557 00
0.07	-0.317 -04	0.548 00	0.437 -01	0.550 00	0.864 -01	0.555 00
0.08	-0.107 -03	0.545 00	0.444 -01	0.547 00	0.877 -01	0.552 00
0.09	-0.274 -03	0.542 00	0.452 -01	0.543 00	0.894 -01	0.549 00
0.10	-0.582 -03	0.538 00	0.459 -01	0.539 00	0.913 -01	0.546 00
0.11	-0.108 -02	0.534 00	0.465 -01	0.535 00	0.934 -01	0.542 00
0.12	-0.179 -02	0.530 00	0.469 -01	0.531 00	0.954 -01	0.537 00
0.13	-0.276 -02	0.526 00	0.469 -01	0.526 00	0.973 -01	0.532 00
0.14	-0.399 -02	0.522 00	0.467 -01	0.521 00	0.988 -01	0.526 00
0.15	-0.548 -02	0.517 00	0.460 -01	0.516 00	0.998 -01	0.520 00
0.16	-0.724 -02	0.513 00	0.450 -01	0.510 00	0.100 00	0.514 00
0.17	-0.924 -02	0.509 00	0.435 -01	0.505 00	0.100 00	0.507 00
0.18	-0.115 -01	0.505 00	0.417 -01	0.500 00	0.993 -01	0.500 00
0.19	-0.139 -01	0.501 00	0.395 -01	0.494 00	0.979 -01	0.493 00
0.20	-0.165 -01	0.497 00	0.371 -01	0.489 00	0.960 -01	0.486 00
0.30	-0.492 -01	0.467 00	0.149 -02	0.450 00	0.581 -01	0.433 00
0.40	-0.848 -01	0.450 00	-0.395 -01	0.428 00	0.103 -01	0.404 00
0.50	-0.118 00	0.441 00	-0.778 -01	0.417 00	-0.341 -01	0.391 00
0.60	-0.149 00	0.438 00	-0.112 00	0.412 00	-0.732 -01	0.385 00
0.70	-0.177 00	0.437 00	-0.143 00	0.412 00	-0.108 00	0.385 00
0.80	-0.202 00	0.439 00	-0.171 00	0.414 00	-0.138 00	0.387 00
0.90	-0.225 00	0.441 00	-0.196 00	0.417 00	-0.166 00	0.391 00
1.00	-0.246 00	0.445 00	-0.219 00	0.421 00	-0.190 00	0.396 00
1.50	-0.333 00	0.471 00	-0.311 00	0.450 00	-0.289 00	0.427 00
2.00	-0.400 00	0.501 00	-0.380 00	0.482 00	-0.361 00	0.461 00
3.00	-0.500 00	0.562 00	-0.484 00	0.545 00	-0.468 00	0.528 00
4.00	-0.577 00	0.621 00	-0.563 00	0.606 00	-0.549 00	0.591 00
5.00	-0.641 00	0.677 00	-0.628 00	0.664 00	-0.615 00	0.651 00

$\beta / k = 1.15$

λ / R	$\alpha / k = 0.06$		0.08		0.10	
0.0	0.120 00	0.577 00	0.158 00	0.584 00	0.194 00	0.592 00
0.01	0.120 00	0.575 00	0.159 00	0.582 00	0.196 00	0.590 00
0.02	0.121 00	0.573 00	0.160 00	0.580 00	0.197 00	0.589 00
0.03	0.122 00	0.571 00	0.161 00	0.578 00	0.198 00	0.587 00
0.04	0.124 00	0.569 00	0.162 00	0.576 00	0.200 00	0.585 00
0.05	0.125 00	0.566 00	0.164 00	0.574 00	0.201 00	0.584 00
0.06	0.126 00	0.564 00	0.165 00	0.572 00	0.202 00	0.582 00
0.07	0.127 00	0.562 00	0.167 00	0.570 00	0.204 00	0.580 00
0.08	0.129 00	0.560 00	0.168 00	0.568 00	0.206 00	0.578 00
0.09	0.131 00	0.558 00	0.169 00	0.567 00	0.206 00	0.575 00
0.10	0.133 00	0.556 00	0.170 00	0.567 00	0.205 00	0.574 00
0.11	0.137 00	0.554 00	0.173 00	0.567 00	0.204 00	0.576 00
0.12	0.141 00	0.551 00	0.178 00	0.567 00	0.206 00	0.580 00
0.13	0.145 00	0.546 00	0.184 00	0.567 00	0.210 00	0.585 00
0.14	0.149 00	0.541 00	0.192 00	0.564 00	0.218 00	0.590 00
0.15	0.153 00	0.534 00	0.200 00	0.560 00	0.230 00	0.592 00
0.16	0.156 00	0.527 00	0.208 00	0.553 00	0.243 00	0.592 00
0.17	0.159 00	0.519 00	0.215 00	0.545 00	0.258 00	0.587 00
0.18	0.160 00	0.510 00	0.221 00	0.535 00	0.272 00	0.579 00
0.19	0.161 00	0.501 00	0.226 00	0.524 00	0.285 00	0.568 00
0.20	0.161 00	0.492 00	0.229 00	0.512 00	0.296 00	0.554 00
0.30	0.123 00	0.417 00	0.198 00	0.404 00	0.287 00	0.399 00
0.40	0.657 -01	0.379 00	0.129 00	0.352 00	0.202 00	0.323 00
0.50	0.135 -01	0.362 00	0.660 -01	0.331 00	0.125 00	0.296 00
0.60	-0.315 -01	0.356 00	0.135 -01	0.324 00	0.623 -01	0.288 00
0.70	-0.703 -01	0.356 00	-0.307 -01	0.324 00	0.115 -01	0.289 00
0.80	-0.104 00	0.358 00	-0.686 -01	0.327 00	-0.311 -01	0.293 00
0.90	-0.134 00	0.363 00	-0.102 00	0.333 00	-0.678 -01	0.300 00
1.00	-0.161 00	0.369 00	-0.131 00	0.339 00	-0.999 -01	0.308 00
1.50	-0.266 00	0.403 00	-0.243 00	0.378 00	-0.219 00	0.352 00
2.00	-0.342 00	0.440 00	-0.322 00	0.418 00	-0.303 00	0.395 00
3.00	-0.453 00	0.510 00	-0.437 00	0.492 00	-0.421 00	0.473 00
4.00	-0.535 00	0.576 00	-0.521 00	0.560 00	-0.508 00	0.543 00
5.00	-0.602 00	0.637 00	-0.590 00	0.623 00	-0.577 00	0.608 00

β/k = 1.20

λ/R	α/k = 0.0		0.02		0.04	
0.0	0.0	0.663 00	0.361 -01	0.664 00	0.721 -01	0.666 CC
0.01	-0.176 -45	0.661 00	0.363 -01	0.662 00	0.725 -01	0.664 CC
0.02	-0.108 -22	0.660 00	0.366 -01	0.660 00	0.729 -01	0.663 CC
0.03	-0.423 -15	0.658 00	0.368 -01	0.658 00	0.733 -01	0.661 CC
0.04	-0.265 -11	0.656 00	0.370 -01	0.657 00	0.737 -01	0.659 CC
0.05	-0.502 -09	0.654 00	0.372 -01	0.655 00	0.742 -01	0.657 CC
0.06	-0.165 -07	0.652 00	0.375 -01	0.653 00	0.747 -01	0.655 CC
0.07	-0.201 -06	0.650 00	0.378 -01	0.651 00	0.752 -01	0.653 CC
0.08	-0.130 -05	0.648 00	0.381 -01	0.648 00	0.757 -01	0.651 CC
0.09	-0.557 -05	0.645 00	0.384 -01	0.646 00	0.763 -01	0.649 CC
0.10	-0.178 -04	0.643 00	0.387 -01	0.644 00	0.770 -01	0.647 CC
0.11	-0.461 -04	0.641 00	0.391 -01	0.642 00	0.777 -01	0.645 CC
0.12	-0.102 -03	0.638 00	0.395 -01	0.639 00	0.785 -01	0.643 CC
0.13	-0.199 -03	0.636 00	0.399 -01	0.637 00	0.794 -01	0.640 CC
0.14	-0.352 -03	0.633 00	0.402 -01	0.634 00	0.804 -01	0.638 CC
0.15	-0.578 -03	0.630 00	0.406 -01	0.631 00	0.814 -01	0.635 CC
0.16	-0.892 -03	0.627 00	0.408 -01	0.628 00	0.824 -01	0.632 CC
0.17	-0.131 -02	0.625 00	0.410 -01	0.625 00	0.833 -01	0.629 CC
0.18	-0.183 -02	0.622 00	0.411 -01	0.622 00	0.842 -01	0.625 CC
0.19	-0.248 -02	0.619 00	0.410 -01	0.618 00	0.850 -01	0.622 CC
0.20	-0.325 -02	0.615 00	0.407 -01	0.615 00	0.856 -01	0.618 CC
0.30	-0.179 -01	0.585 00	0.291 -01	0.578 00	0.793 -01	0.574 CC
0.40	-0.413 -01	0.560 00	0.457 -02	0.548 00	0.542 -01	0.536 CC
0.50	-0.681 -01	0.543 00	-0.249 -01	0.526 00	0.216 -01	0.509 CC
0.60	-0.951 -01	0.531 00	-0.550 -01	0.512 00	-0.121 -01	0.492 CC
0.70	-0.121 00	0.524 00	-0.839 -01	0.503 00	-0.443 -01	0.482 CC
0.80	-0.146 00	0.520 00	-0.111 00	0.498 00	-0.743 -01	0.476 CC
0.90	-0.169 00	0.518 00	-0.136 00	0.496 00	-0.102 00	0.473 CC
1.00	-0.191 00	0.517 00	-0.160 00	0.496 CC	-0.128 00	0.473 CC
1.50	-0.282 00	0.530 00	-0.257 00	0.509 00	-0.232 00	0.487 CC
2.00	-0.352 00	0.552 00	-0.331 00	0.532 00	-0.310 00	0.513 CC
3.00	-0.460 00	0.604 00	-0.442 00	0.587 00	-0.425 00	0.570 CC
4.00	-0.541 00	0.657 00	-0.526 00	0.643 00	-0.511 00	0.628 CC
5.00	-0.608 00	0.711 00	-0.594 00	0.698 00	-0.581 00	0.684 CC

β/k = 1.20

λ/R	α/k = 0.06		0.08		0.10	
0.0	0.108 00	0.669 00	0.142 00	0.674 00	0.177 00	0.679 00
0.01	0.108 00	0.668 00	0.143 00	0.672 00	0.177 00	0.678 00
0.02	0.109 00	0.666 00	0.144 00	0.671 00	0.178 00	0.676 00
0.03	0.109 00	0.664 00	0.145 00	0.669 00	0.179 00	0.675 00
0.04	0.110 00	0.663 00	0.145 00	0.667 00	0.180 00	0.673 00
0.05	0.111 00	0.661 00	0.146 00	0.666 00	0.181 00	0.672 00
0.06	0.111 00	0.659 00	0.147 00	0.664 00	0.182 00	0.670 00
0.07	0.112 00	0.657 00	0.148 00	0.663 00	0.183 00	0.669 00
0.08	0.113 00	0.655 00	0.149 00	0.661 00	0.184 00	0.668 00
0.09	0.113 00	0.654 00	0.150 00	0.659 00	0.185 00	0.666 00
0.10	0.114 00	0.652 00	0.151 00	0.658 00	0.186 00	0.664 00
0.11	0.115 00	0.650 00	0.152 00	0.656 00	0.187 00	0.663 00
0.12	0.116 00	0.648 00	0.153 00	0.655 00	0.188 00	0.662 00
0.13	0.118 00	0.646 00	0.154 00	0.653 00	0.189 00	0.661 00
0.14	0.119 00	0.644 00	0.156 00	0.652 00	0.190 00	0.660 00
0.15	0.121 00	0.642 00	0.157 00	0.651 00	0.191 00	0.660 00
0.16	0.123 00	0.639 00	0.160 00	0.649 00	0.193 00	0.659 00
0.17	0.124 00	0.636 00	0.162 00	0.647 00	0.196 00	0.659 00
0.18	0.126 00	0.633 00	0.165 00	0.645 00	0.200 00	0.659 00
0.19	0.128 00	0.630 00	0.169 00	0.642 00	0.204 00	0.657 00
0.20	0.130 00	0.626 00	0.172 00	0.639 00	0.208 00	0.656 00
0.30	0.133 00	0.574 00	0.190 00	0.581 00	0.250 00	0.597 00
0.40	0.109 00	0.526 00	0.169 00	0.518 00	0.235 00	0.516 00
0.50	0.723 -01	0.492 00	0.128 00	0.475 00	0.190 00	0.459 00
0.60	0.342 -01	0.471 00	0.845 -01	0.449 00	0.140 00	0.426 00
0.70	-0.209 -02	0.459 00	0.433 -01	0.434 00	0.924 -01	0.408 00
0.80	-0.355 -01	0.452 00	0.566 -02	0.426 00	0.497 -01	0.399 00
0.90	-0.662 -01	0.449 00	-0.284 -01	0.423 00	0.116 -01	0.395 00
1.00	-0.942 -01	0.449 00	-0.593 -01	0.423 00	-0.226 -01	0.395 00
1.50	-0.206 00	0.465 00	-0.180 00	0.441 00	-0.153 00	0.415 00
2.00	-0.288 00	0.492 00	-0.266 00	0.470 00	-0.244 00	0.447 00
3.00	-0.407 00	0.552 00	-0.390 00	0.534 00	-0.372 00	0.515 00
4.00	-0.496 00	0.612 00	-0.481 00	0.596 00	-0.466 00	0.579 00
5.00	-0.567 00	0.670 00	-0.553 00	0.655 00	-0.540 00	0.641 00

$\beta/k = 1.25$

λ/R	$\alpha/k = 0.0$		0.02		0.04	
0.0	0.0	0.750 00	0.333 -01	0.750 00	0.665 -01	0.752 00
0.02	-0.126 -31	0.747 00	0.336 -01	0.748 00	0.670 -01	0.749 00
0.03	-0.491 -21	0.746 00	0.337 -01	0.746 00	0.673 -01	0.748 00
0.04	-0.967 -16	0.744 00	0.338 -01	0.745 00	0.675 -01	0.746 00
0.05	-0.145 -12	0.743 00	0.340 -01	0.743 00	0.678 -01	0.745 00
0.06	-0.190 -10	0.741 00	0.341 -01	0.742 00	0.681 -01	0.743 00
0.07	-0.618 -09	0.740 00	0.343 -01	0.740 00	0.684 -01	0.742 00
0.08	-0.841 -08	0.738 00	0.345 -01	0.739 00	0.687 -01	0.740 00
0.09	-0.641 -07	0.736 00	0.346 -01	0.737 00	0.691 -01	0.739 00
0.10	-0.325 -06	0.735 00	0.348 -01	0.735 00	0.694 -01	0.737 00
0.11	-0.123 -05	0.733 00	0.350 -01	0.734 00	0.698 -01	0.736 00
0.12	-0.370 -05	0.731 00	0.352 -01	0.732 00	0.702 -01	0.734 00
0.13	-0.944 -05	0.730 00	0.354 -01	0.730 00	0.706 -01	0.732 00
0.14	-0.210 -04	0.728 00	0.356 -01	0.728 00	0.710 -01	0.731 00
0.15	-0.421 -04	0.726 00	0.359 -01	0.727 00	0.715 -01	0.729 00
0.16	-0.773 -04	0.724 00	0.361 -01	0.725 00	0.720 -01	0.727 00
0.17	-0.132 -03	0.722 00	0.363 -01	0.723 00	0.725 -01	0.725 00
0.18	-0.212 -03	0.720 00	0.366 -01	0.721 00	0.731 -01	0.723 00
0.19	-0.325 -03	0.718 00	0.368 -01	0.719 00	0.737 -01	0.721 00
0.20	-0.476 -03	0.716 00	0.370 -01	0.716 00	0.743 -01	0.719 00
0.30	-0.528 -02	0.692 00	0.356 -01	0.690 00	0.775 -01	0.691 00
0.40	-0.173 -01	0.668 00	0.252 -01	0.662 00	0.700 -01	0.659 00
0.50	-0.349 -01	0.647 00	0.735 -02	0.637 00	0.523 -01	0.629 00
0.60	-0.556 -01	0.630 00	-0.147 -01	0.617 00	0.288 -01	0.605 00
0.70	-0.775 -01	0.617 00	-0.385 -01	0.602 00	0.294 -02	0.587 00
0.80	-0.996 -01	0.608 00	-0.624 -01	0.591 00	-0.232 -01	0.574 00
0.90	-0.121 00	0.601 00	-0.858 -01	0.583 00	-0.488 -01	0.565 00
1.00	-0.142 00	0.597 00	-0.108 00	0.578 00	-0.733 -01	0.559 00
1.50	-0.233 00	0.594 00	-0.206 00	0.575 00	-0.178 00	0.555 00
2.00	-0.306 00	0.607 00	-0.283 00	0.589 00	-0.260 00	0.569 00
3.00	-0.419 00	0.649 00	-0.400 00	0.632 00	-0.381 00	0.615 00
4.00	-0.505 00	0.697 00	-0.489 00	0.682 00	-0.472 00	0.667 00
5.00	-0.575 00	0.746 00	-0.561 00	0.733 00	-0.546 00	0.719 00

$\beta / k = 1.25$

λ / R	$\alpha / k = 0.06$		0.08		0.10	
0.0	0.994 -01	0.754 00	0.132 00	0.757 00	0.164 00	0.761 00
0.02	0.100 00	0.751 00	0.133 00	0.755 00	0.165 00	0.759 00
0.03	0.101 00	0.750 00	0.133 00	0.753 00	0.166 00	0.758 00
0.04	0.101 00	0.749 00	0.134 00	0.752 00	0.166 00	0.756 00
0.05	0.101 00	0.747 00	0.134 00	0.751 00	0.167 00	0.755 00
0.06	0.102 00	0.746 00	0.135 00	0.749 00	0.168 00	0.754 00
0.07	0.102 00	0.744 00	0.136 00	0.748 00	0.168 00	0.753 00
0.08	0.103 00	0.743 00	0.136 00	0.747 00	0.169 00	0.751 00
0.09	0.103 00	0.742 00	0.137 00	0.745 00	0.170 00	0.750 00
0.10	0.104 00	0.740 00	0.137 00	0.744 00	0.170 00	0.749 00
0.11	0.104 00	0.739 00	0.138 00	0.743 00	0.171 00	0.747 00
0.12	0.105 00	0.737 00	0.139 00	0.741 00	0.172 00	0.746 00
0.13	0.105 00	0.735 00	0.139 00	0.740 00	0.173 00	0.745 00
0.14	0.106 00	0.734 00	0.140 00	0.738 00	0.173 00	0.744 00
0.15	0.107 00	0.732 00	0.141 00	0.737 00	0.174 00	0.742 00
0.16	0.107 00	0.731 00	0.142 00	0.736 00	0.175 00	0.741 00
0.17	0.108 00	0.729 00	0.142 00	0.734 00	0.176 00	0.740 00
0.18	0.109 00	0.727 00	0.144 00	0.733 00	0.177 00	0.739 00
0.19	0.110 00	0.725 00	0.145 00	0.731 00	0.178 00	0.738 00
0.20	0.111 00	0.723 00	0.146 00	0.730 00	0.179 00	0.737 00
0.30	0.120 00	0.696 00	0.162 00	0.704 00	0.203 00	0.716 00
0.40	0.117 00	0.658 00	0.166 00	0.660 00	0.217 00	0.668 00
0.50	0.100 00	0.621 00	0.152 00	0.617 00	0.207 00	0.615 00
0.60	0.753 -01	0.593 00	0.125 00	0.581 00	0.180 00	0.572 00
0.70	0.471 -01	0.571 00	0.944 -01	0.556 00	0.146 00	0.540 00
0.80	0.183 -01	0.556 00	0.625 -01	0.538 00	0.110 00	0.518 00
0.90	-0.979 -02	0.546 00	0.315 -01	0.525 00	0.755 -01	0.504 00
1.00	-0.366 -01	0.539 00	0.206 -02	0.517 00	0.429 -01	0.495 00
1.50	-0.150 00	0.533 00	-0.120 00	0.511 00	-0.898 -01	0.488 00
2.00	-0.236 00	0.549 00	-0.211 00	0.528 00	-0.186 00	0.506 00
3.00	-0.362 00	0.598 00	-0.343 00	0.579 00	-0.324 00	0.560 00
4.00	-0.456 00	0.651 00	-0.440 00	0.635 00	-0.423 00	0.618 00
5.00	-0.531 00	0.705 00	-0.517 00	0.691 00	-0.502 00	0.676 00

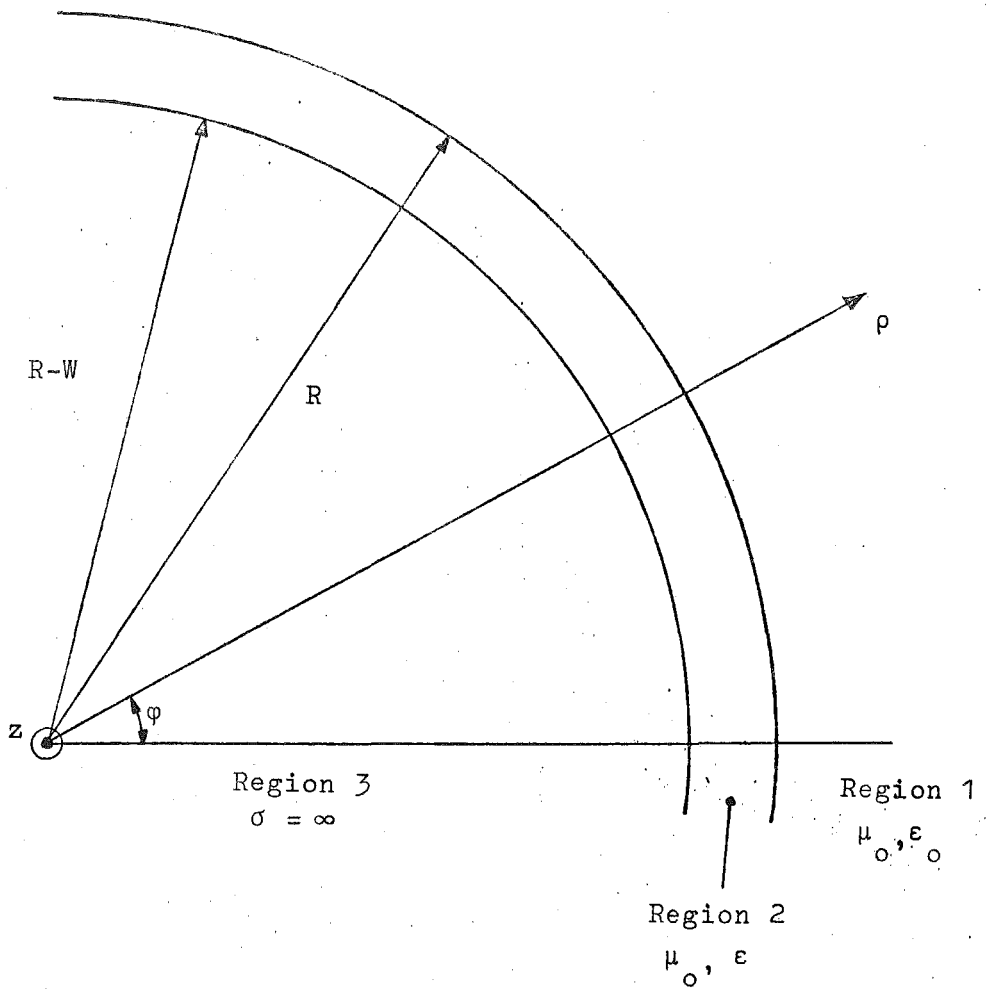

Fig.6.1 The azimuthal guiding structure.

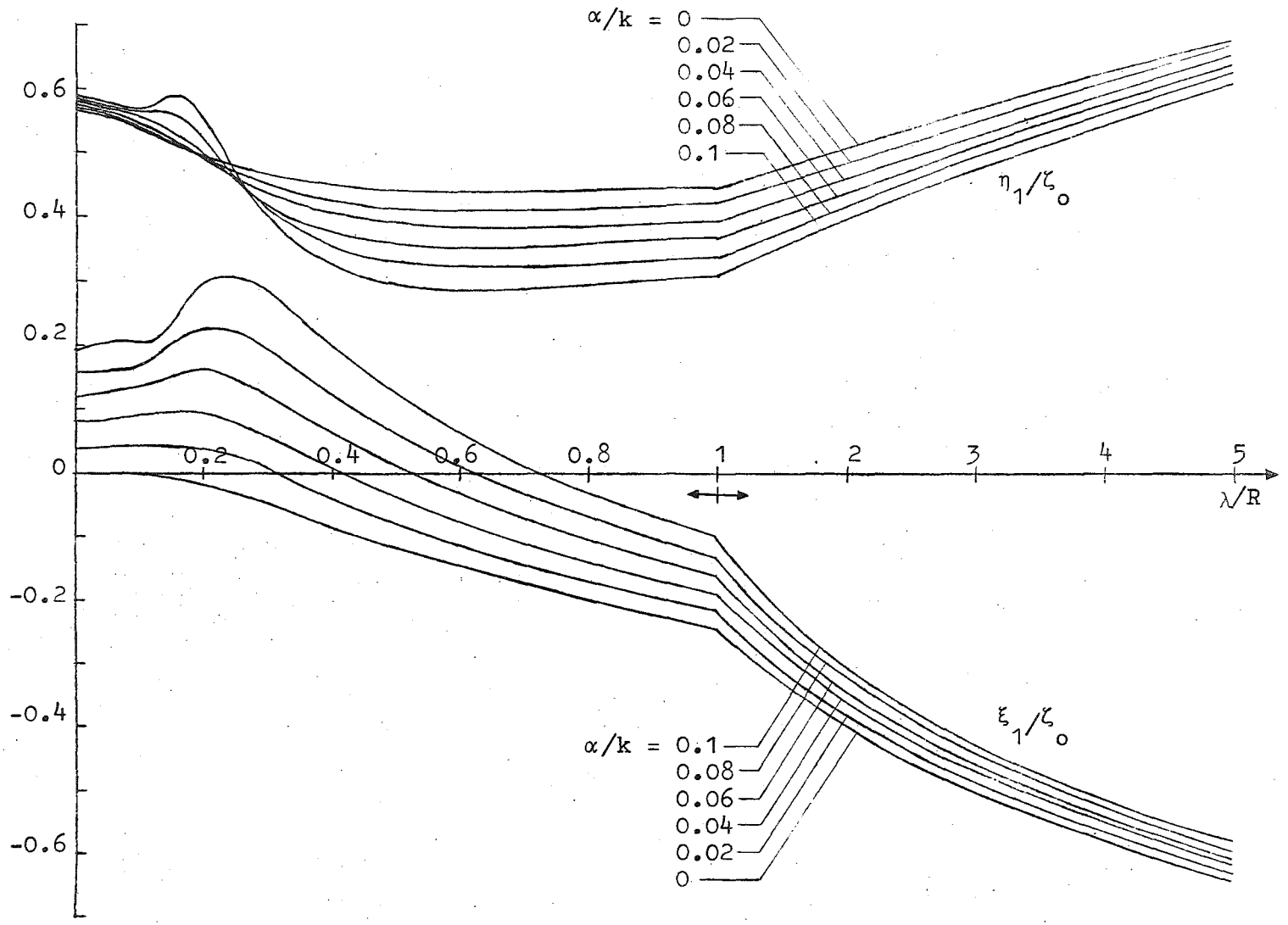

Table 6.2: Normalised surface impedance, ζ_1/ζ_0 for external field, $\beta/k = 1.15$.

CHAPTER 7: DIELECTRIC CLAD CYLINDER

My notion was that you had been
(Before she had this fit)
An obstacle that cam between
Him, and ourselves, and it.
Lewis Carroll

The guiding of an azimuthal surface wave by a dielectric clad cylinder is considered. The propagation characteristics of the guiding surface are obtained by matching the surface impedance of the external region to that of the guiding region.

7.1 INTRODUCTION

Results for the general external field of an azimuthal surface wave have been given in chapter 6 in the form of universal tables. These tables can be used to obtain the propagation characteristics of any particular guiding surface. The particular case of a dielectric clad circular cylinder (Elliott 1955) is considered here; and results for the behaviour of the propagation characteristics as a function of the curvature of the guiding surface are given. The techniques used to obtain computationally convenient expressions for the surface impedance are discussed.

7.2 PRELIMINARIES

The application of the universal tables to the particular case of a dielectric clad circular cylindrical (Elliott 1955) guiding surface (Fig. 6.1) is considered in this section. Fig. 6.1 is taken to represent a

perfectly conducting cylinder of radius (R-W) coated with a dielectric of thickness W. The fields present are the external field in the region $\rho > R$ and the internal field in the dielectric region. Equations (6.1) to (6.5) describe the TM wave for the external region.

For the dielectric region (region 2 in Fig. 6.1) we have, for the TM wave,

$$H_z = [AH_\nu^{(1)}(nk\rho) + BH_\nu^{(2)}(nk\rho)] \exp(-j\nu\varphi), \tag{7.1}$$

$$E_\rho = - \frac{\zeta_0 \nu}{k\rho n^2} H_z, \tag{7.2}$$

$$E_\varphi = \frac{jnk}{\omega\varepsilon} [AH_\nu^{(1)'}(nk\rho) + BH_\nu^{(2)'}(nk\rho)] \exp(-j\nu\varphi), \tag{7.3}$$

where $n = (\varepsilon/\varepsilon_0)^{\frac{1}{2}}$ is the refractive index of the dielectric and A and B are constants. The boundary condition at $\rho = (R-W)$ is

$$\left.\frac{\partial H_z}{\partial \rho}\right|_{\rho = R-W} = 0. \tag{7.4}$$

Using equation (7.1), equation (7.4) becomes

$$A\, H_\nu^{(1)'}(nk[R-W]) + B\, H_\nu^{(2)'}(nk[R-W]) = 0. \tag{7.5}$$

The surface impedance for the internal field is given by

$$\zeta_2 = \xi_2 + j\eta_2 = - \left.\frac{E_\varphi}{H_z}\right|_{\rho=R}, \tag{7.6}$$

and from equations (7.1), (7.3), (7.5) and (7.6),

$$\zeta_2 = -\frac{j\zeta_0}{n}$$

$$\times \frac{H_\nu^{(1)'}(nkR)\, H_\nu^{(2)'}(nk[R-W]) - H_\nu^{(1)'}(nk[R-W])\, H_\nu^{(2)'}(nkR)}{H_\nu^{(1)}(nkR)\, H_\nu^{(2)'}(nk[R-W]) - H_\nu^{(1)'}(nk[R-W])\, H_\nu^{(2)}(nkR)} . \tag{7.7}$$

7.3 COMPUTATION OF SURFACE IMPEDANCE

In general, it will be simpler to compute the surface impedance expression for region 2 than for region 1, because in region 2 condition (6.13) no longer applies. However, the Hankel functions are again of complex order and the computation still requires care.

Equation (7.7) can be put into a more convenient form for computation. Using the Addition Theorem for Bessel functions (Watson 1968, p.145), equation (7.7) becomes

$$\zeta_2 = -\frac{j\zeta_0}{n}$$

$$\times \frac{\sum_{p=1}^{\infty} [(H_\nu^{(1)'} H_{\nu+p}^{(2)'} - H_{\nu+p}^{(1)'} H_\nu^{(2)'}) + (-1)^p (H_\nu^{(1)'} H_{\nu-p}^{(2)'} - H_{\nu-p}^{(1)'} H_\nu^{(2)'})] J_p(nkW)}{\frac{-4jJ_0(nkW)}{\pi nkR} + \sum_{p=1}^{\infty} [(H_\nu^{(1)} H_{\nu+p}^{(2)'} - H_{\nu+p}^{(1)'} H_\nu^{(2)}) + (-1)^p (H_\nu^{(1)} H_{\nu-p}^{(2)'} - H_{\nu-p}^{(1)'} H_\nu^{(2)})] J_p(nkW)} \tag{7.8}$$

where the argument for the Hankel functions is (nkR). Equation (7.8) is further transformed by the use of Wronskian relations (Watson 1968, p.76) and Lommel polynomials (Watson 1968, pp 294-299) to give

$$\zeta_2 = -\frac{j\zeta_0}{n}\left\{\frac{\sum_{p=1}^{\infty} J_p(nkw)\left[\frac{\nu}{nkR}\,C(p,\nu,nkR) + D(p,\nu,nkR)\right]}{-2J_0(nkW) + \sum_{p=1}^{\infty} J_p(nkW)\,E(p,\nu,nkR)}\right\}; \tag{7.9}$$

where

$$C(p,\nu,nkR) = R_{p,\nu+1}(nkR) - R_{p-2,\nu+1}(nkR) + R_{p,1-\nu}(nkR) - R_{p-2,1-\nu}(nkR), \tag{7.10}$$

$$D(p,\nu,nkR) = R_{p-1,\nu}(nkR) - R_{p+1,\nu}(nkR) + R_{p-1,2-\nu}(nkR) - R_{p-3,2-\nu}(nkR), \tag{7.11}$$

$$E(p,\nu,nkR) = -R_{p,\nu+1}(nkR) + R_{p-2,\nu+1}(nkR) - R_{p,1-\nu}(nkR) + R_{p-2,1-\nu}(nkR). \tag{7.12}$$

$R_{p,\nu}$ is a Lommel polynomial. Equation (7.9) is convenient for computation because each $R_{p,\nu}$ is a polynomial of finite order.

Typical graphs of the variation of ζ_2/ζ_0 with λ/R for sets of values of β/k with α/k constant and for sets of values of α/k with β/k constant are given in Fig. 7.1. From the figure it is seen that for any curve, the value of η_2/ζ_0 changes from positive (inductive case) to negative (capacitive case) at a particular value of λ/R. This cross-over value of λ/R drops rapidly as β/k increases (for a fixed α/k). The limiting value of β/k is equal to the value of the refractive index n, because $\beta < nk$ for a guided surface wave. From the family of curves for various values of α/k and with β/k constant, it is seen that a small

change in the value of α/k can cause a marked change in ξ_2/ζ_0, but only a small change in η_2/ζ_0.

7.4 PROPAGATION CHARACTERISTICS

To obtain the actual propagation characteristics of any guiding surface, the surface impedance of the external region (region 1) will have to be matched to that of the guiding region. For the dielectric clad cylinder ζ_1 must be matched to ζ_2, for fixed values of n and λ/W and for any particular λ/R. The values of α/k and β/k must be found so that

$$\zeta_1 = \zeta_2 \tag{7.13}$$

is satisfied. Let

$$\zeta = \zeta_1 = \zeta_2 = \xi + j\eta \tag{7.14}$$

for the matched case. The results are given in Figs 7.2 and 7.3 for various values of n and λ/W. From Figs 7.2 and 7.3 it is seen that the attenuation constant α and the real part of ζ/ζ_0 increases with λ/R, showing that the losses increase with curvature. The imaginary part of the surface impedance decreases with curvature.

Define T, the trapping factor as

$$T = \left|\frac{\eta}{\xi}\right| \tag{7.15}$$

which gives an effective measure of the guiding capability of a surface waveguide. T ranges from ∞ when the attenuation is zero, to 0 when the wave is no longer guided along the surface. The plots of T in

Figs 7.2 and 7.3 show that the trapping factor decreases rapidly with curvature. For a fixed λ/W and any fixed λ/R, T increases with n, the refractive index of the dielectric (Fig. 7.2); while for a fixed n and any particular λ/R, T increases with the thickness of the dielectric layer W (Fig. 7.3). This is in accord with the well known fact (Barlow and Brown 1962) that a dielectric coating with a high refractive index provides better trapping, and hence better guiding with smaller losses, than one with a low refractive index coating. Similarly, the trapping tends to increase with increased thickness of the coating.

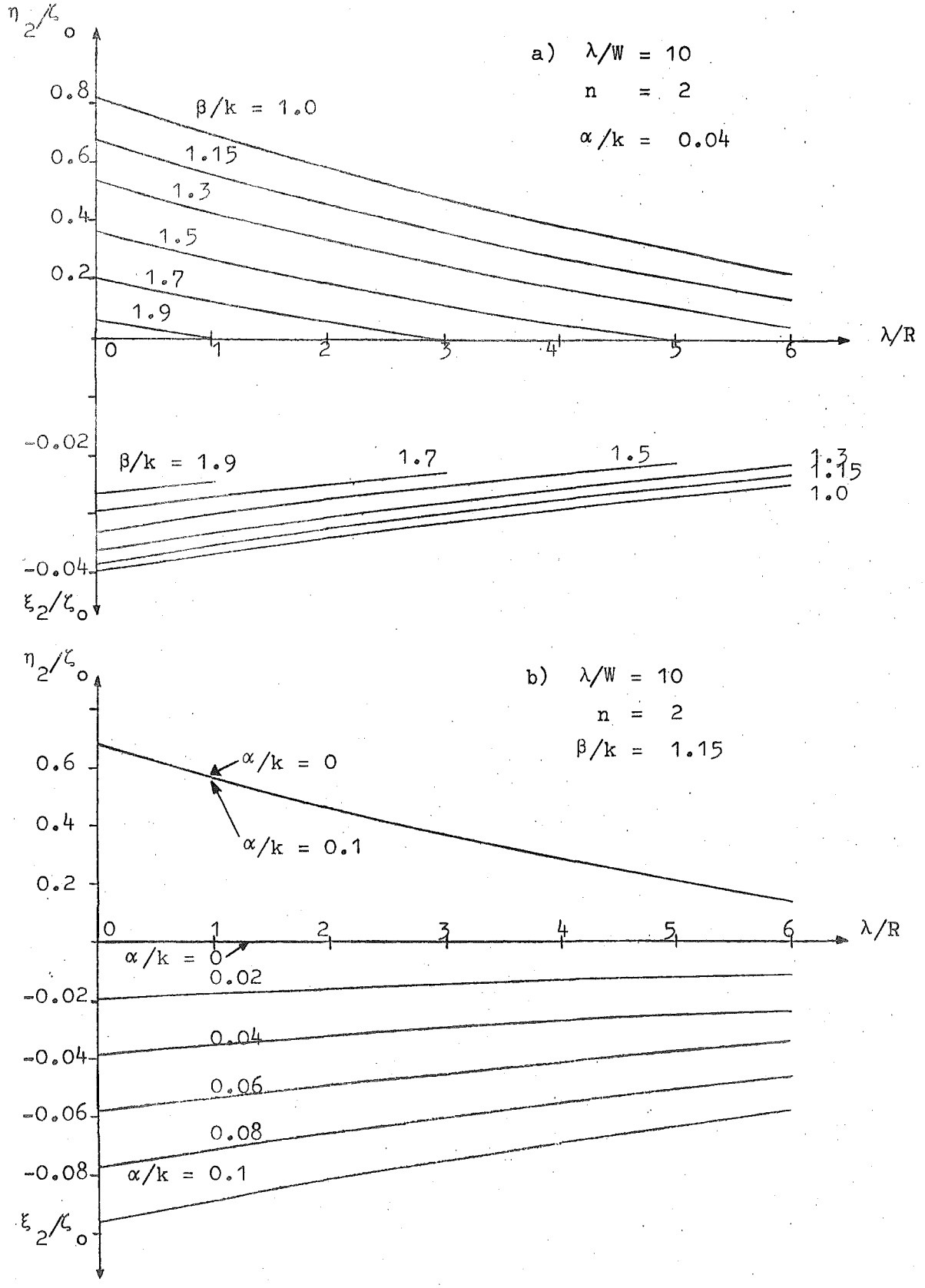

Fig. 7.1 Normalised surface impedance, ζ_2/ζ_o for internal field of dielectric clad cylinder.

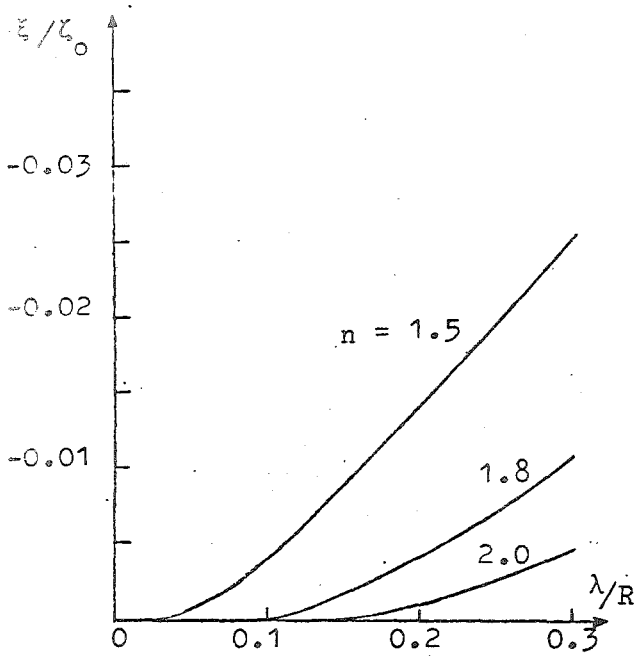

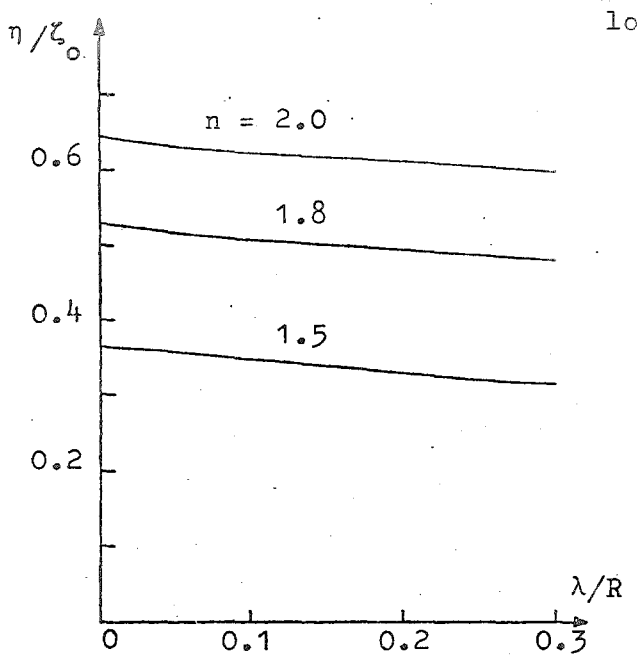

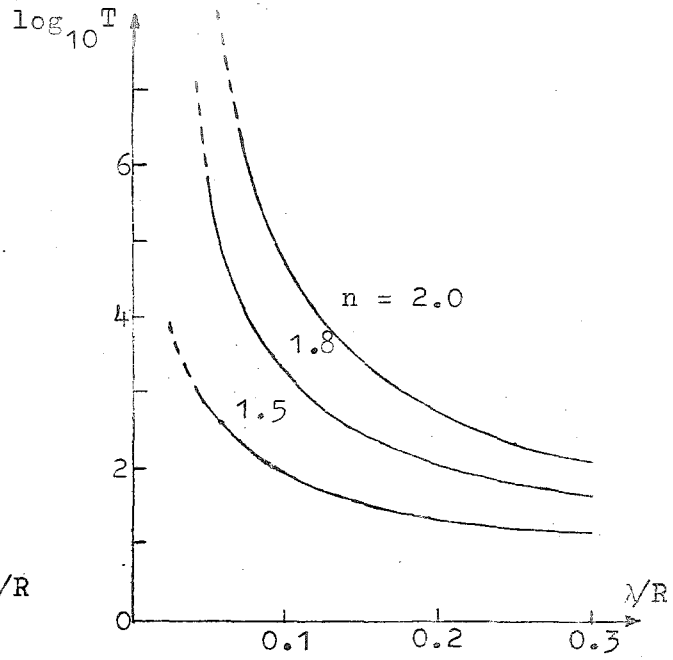

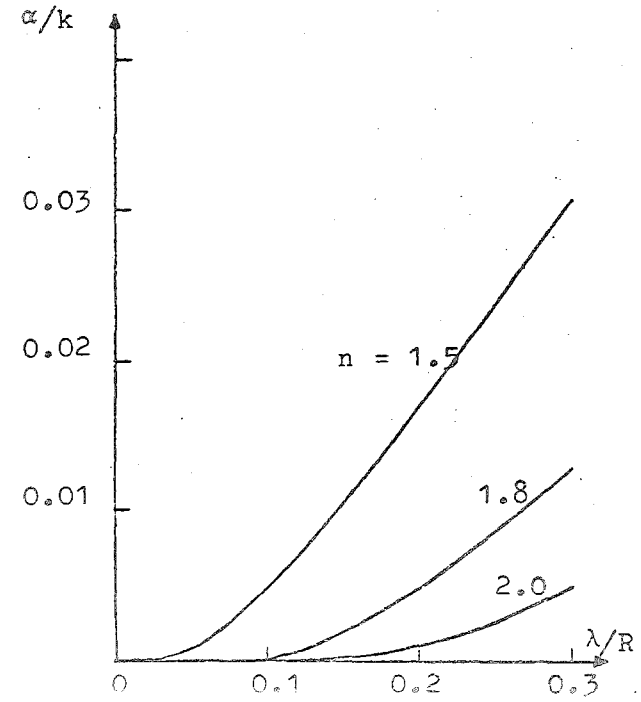

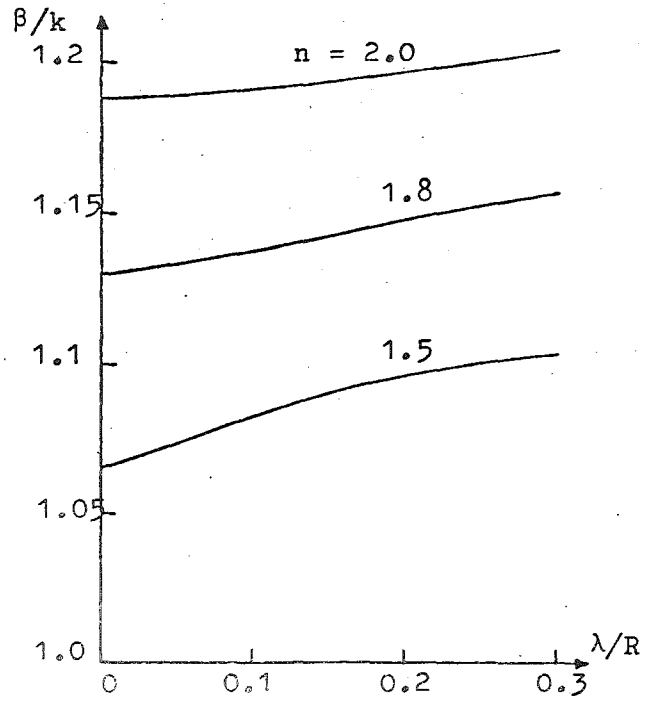

Fig. 7.2

Propagation characteristics of dielectric clad cylinder with $\lambda/W = 10$.

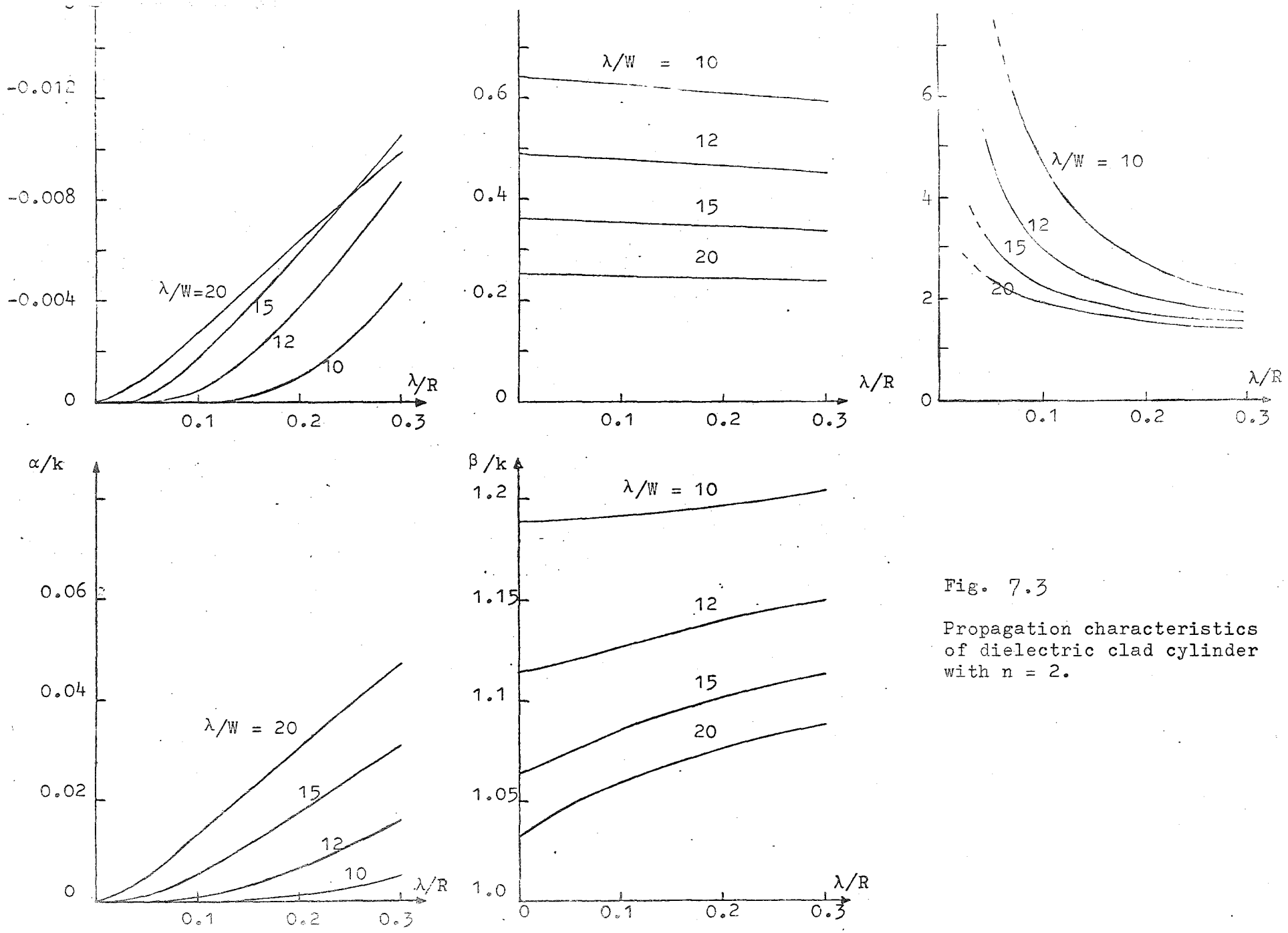

Fig. 7.3

Propagation characteristics of dielectric clad cylinder with n = 2.

PART 4: Conclusions and Suggestions for Further Research

CHAPTER 8: CONCLUSIONS AND SUGGESTIONS FOR FURTHER RESEARCH

We shall have to evolve
problem-solvers galore -
Since each problem they solve
creates ten problems more.
Piet Hein

8.1 CONCLUSIONS

The numerical solutions of three types of guiding structures have been considered in this thesis.

An investigation into the numerical solution of the hollow waveguide problem by the null field method shows that the method is comparable, in accuracy and computational facility, with other general numerical methods. A significant advantage of the null field method is the small determinant orders (about 8 to 10) needed to give results accurate to 0.1%. Cross-sections with reentrant corners are straightforwardly handled by using representations for the surface current densities which satisfy the required analytical behaviour at the corners.

The complete point-matching method is shown to give accurate results (to 0.1%) only for convex shapes. A detailed investigation of the straightforward point-matching method, together with its relation to the internal Rayleigh hypothesis which is introduced, shows that it is liable to give erroneous wavefunctions for reentrant shapes. This behaviour led to the development of an extended point-matching method which is shown to

be capable of handling cases for which the straightforward point-matching method fails. Accurate results using the extended point-matching method are obtained for the ridge waveguide and Meinke waveguide.

Point-matching methods are simple computational techniques and where applicable produce accurate results (about 0.1%) with small determinant orders (about 8 to 12).

In Part 2, formulas for the cutoff characteristics of waveguides of arbitrary cross-section loaded with dielectric tubes are presented. The significant thing about the derivation given in chapter 5 is that the field in the dielectric is eliminated and formulas are obtained that are line integral equations for the surface current densities on the waveguide wall alone. These formulas are almost as convenient as the null field equations for hollow waveguides. The computational convenience of the formulas is illustrated by results for a square waveguide loaded with a dielectric rod. As with the null field method, results accurate to 0.1% are obtained with small determinant orders (about 9).

An exact analysis of the azimuthal surface wave is presented in Part 3, in which no simplifying assumptions are made about the attenuation. Universal tables are given for the general external field and these are used to obtain accurately the behaviour of the propagation characteristics of a dielectric clad cylindrical guiding surface.

8.2 SUGGESTIONS FOR FURTHER RESEARCH

Many methods are now available for the numerical solution of the hollow waveguide problem (chapter 1). As yet however, there is no comprehensive comparison of the methods on a single computer. This would be a worthwhile task for a research group with suitable facilities. The production of a standard program package for waveguide analysis would be a very useful contribution. Such a program package would probably contain several methods so that a user can have the option of comparing results from various methods in a doubtful situation.

The analytic continuation method of Mittra and Wilton (1969), proposed in section 1.2.5.3 as another means (in addition to extended point-matching) of extending the usefulness of straightforward point-matching, is as yet untested and an investigation could usefully be made into this.

In chapter 5, results have been given for the cut-off characteristics of dielectric loaded waveguides. This study can be extended to the general propagating case by using an integral formulation which can again be obtained from the polarization source formulation (Bates 1970).

The study of the azimuthal surface wave can be looked upon as a prelude to the more difficult task of analysing the behaviour of bent Goubau lines. Some experimental results are available (Sato et al. 1964; Goubau and Sharp 1957; Thorley 1969) but at present only a few simple, approximate analyses of this aspect are available (Barlow 1966; Sato et al. 1964).

APPENDICES

APPENDIX A: SEGMENT AND SECTOR WAVEGUIDES

Figure 3.9 shows the segment waveguide. The wavefunction for a particular mode is

$$U(\rho,\varphi) = [J_{q\mu}(k\tau) - B_q Y_{q\mu}(k\tau)] \begin{matrix}\sin\\ \cos\end{matrix}(q\mu[\phi-(\eta/2)]),$$

$$\mu = \pi/\eta \qquad \text{(A1)}$$

where q is an integer and sin and cos apply to the E-mode and H-mode respectively, and

$$\left.\begin{aligned} B_q &= J_{q\mu}(kb)/Y_{q\mu}(kb) = J_{q\mu}(ka)/Y_{q\mu}(ka), \quad \text{E-mode;} \\ B_q &= J'_{q\mu}(kb)/Y'_{q\mu}(kb) = J'_{q\mu}(ka)/Y'_{q\mu}(ka), \quad \text{H-mode} \end{aligned}\right\} \qquad \text{(A2)}$$

where the dash denotes differentiation with respect to the argument. The cutoff wavenumbers are those values of k which satisfy either of the conditions (A2).

When b = 0 in Fig. 3.9, the segment waveguide becomes the sector waveguide for which the wavefunction is given by equation (A1) with $B_q = 0$. The cutoff wavenumbers k satisfy

$$\left.\begin{aligned} J_{q\mu}(ka) &= 0, \quad \text{E-mode;} \\ J'_{q\mu}(ka) &= 0, \quad \text{H-mode.} \end{aligned}\right\} \qquad \text{(A3)}$$

APPENDIX B: SURFACE CURRENT DENSITIES

B1 Reentrant Corner

Fig. B1 shows a reentrant corner of C with exterior angle β. For an E-mode in the waveguide the field in the neighbourhood of the corner can be represented by

$$E_z = \sum_{n=1}^{\infty} a_n J_{n\nu}(k\rho) \sin(n\nu\varphi), \tag{B1}$$

where $\nu = \pi/(2\pi-\beta)$. The z-directed component of the surface current density (only component) is obtained from $\hat{n} \times \vec{H}$ where $\hat{n}$ is the inward normal at any point on C. Thus, using the Maxwell's equations (1.1),

$$\begin{aligned} F(C) &= \hat{n} \times \hat{\rho}\, H_\rho\big|_{\varphi=0,(2\pi-\beta)} \\ &= \hat{n} \times \hat{\rho}\, \frac{j\omega\varepsilon_0}{k^2} \left(\frac{1}{\rho} \frac{\partial E_z}{\partial \varphi}\right)\Bigg|_{\varphi=0,(2\pi-\beta)} \end{aligned} \tag{B2}$$

From (B2), the exact surface current density on C in the vicinity of the corner (Fig. B1) can therefore be represented by

$$F(C) = \sum_{n=1}^{\infty} A_n J_{n\nu}(kr)/r, \quad \text{along OA;}$$

$$F(C) = \sum_{n=1}^{\infty} (-1)^{n+1} A_n J_{n\nu}(kr)/r, \quad \text{along OB,} \tag{B3}$$

where the A_n are constants and r is the distance measured from O along OA or OB.

For an H-mode, the surface current density is directed along the curve C. A representation

$$H_z = \sum_{n=0}^{\infty} a_n J_{n\nu}(k\rho) \cos n\nu\varphi \tag{B4}$$

may be used to represent the field in the neighbourhood of O. From eqn (B4) the exact surface current density representations

$$G(C) = \sum_{n=0}^{\infty} A_n J_{n\nu}(kr), \quad \text{along OA;} \tag{B5}$$

$$G(C) = \sum_{n=0}^{\infty} (-1)^{n+1} A_n J_{n\nu}(kr), \quad \text{along OB,} \tag{B6}$$

are obtained.

B2 Sector Waveguide

The field at cutoff for the lowest order E-mode in the sector waveguide (Figs 2.1 and B1) can be represented exactly by (from eqn (A1) of Appendix A)

$$E_z = J_\mu(k\tau) \sin(\mu[\phi-\eta/2]), \quad \mu = \pi/\eta. \tag{B7}$$

The cutoff wavenumber is the lowest positive value of k, other than zero, which satisfies eqn (A3) with q = 1. From (B7) and using derivations as in eqn (B2) the surface current density on the waveguide wall is given by

$$F(C) = A \left|J'_\mu(ka)\right| \sin(\mu[\phi-\eta/2]), \text{ along the curved part;} \tag{B8}$$

$$F(C) = -A \frac{\mu}{k\tau} J_\mu(k\tau), \text{ along the straight parts,} \tag{B9}$$

where A is a constant proportionality factor.

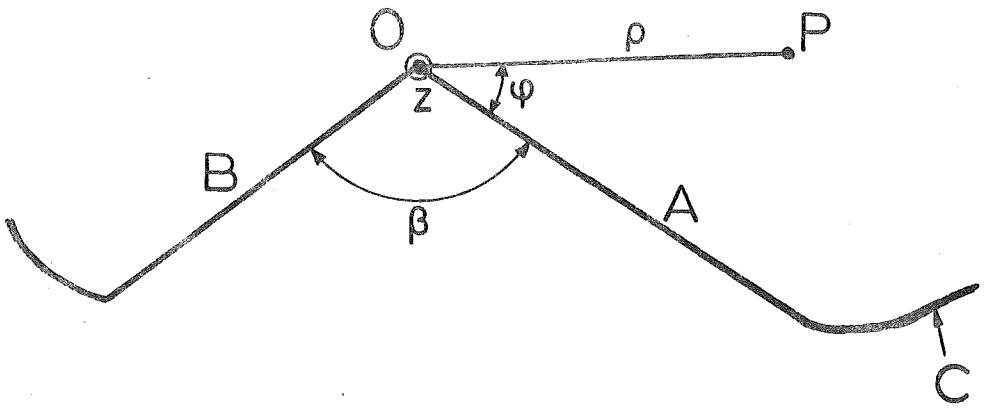

Fig. B1: Reentrant corner and coordinate system.

APPENDIX C: COMPUTATION OF HANKEL FUNCTIONS OF COMPLEX ORDER

The expression (6.5) for ζ_1 is difficult to compute as it stands. It has been found possible, however, to obtain two convenient forms of expression (6.5). The first enables ζ_1 to be computed for λ/R greater than about 0.1, while the second, asymptotic form enables ζ_1 to be computed when λ/R is small.

C1 Expression for $\lambda/R > 0.1$

Equation (6.5) can be expressed as

$$\frac{j\zeta_1}{\zeta_0} = \frac{\frac{1}{2}[J_\nu^2(kR) + Y_\nu^2(kR)]' - \frac{j2}{\pi kR}}{J_\nu^2(kR) + Y_\nu^2(kR)} . \qquad (C1)$$

Now, equation (C1) is expanded as (Watson 1968, p.444)

$$\frac{j\zeta_1}{\zeta_0} = -\frac{\frac{8}{\pi^2}\int_0^\infty K_1(2kR \sinh t) \sinh t \cosh 2\nu t\,dt + \frac{j2}{\pi kR}}{\frac{8}{\pi^2}\int_0^\infty K_1(2kR \sinh t)\, 2kR \cosh t \frac{\sinh 2\nu t}{2\nu}\, dt} , \qquad (C2)$$

where $K_1(x)$ is a modified Bessel function of order 1 and argument x. Hence,

$$\frac{j\zeta_1}{\zeta_0} = \frac{(\frac{\beta}{k} - j\frac{\alpha}{k})\,(A - \frac{\pi}{4kR} + jB)}{C - jD} , \qquad (C3)$$

where

$$\left.\begin{aligned} A &= \int_0^\infty K_1(2kR\sinh t) \sinh t \sinh 2R\beta t \sin 2R\alpha t\, dt, \\ B &= \int_0^\infty K_1(2kR\sinh t) \sinh t \cosh 2R\beta t \cos 2R\alpha t\, dt, \end{aligned}\right\}$$

$$C = \int_0^\infty K_1(2kR \sinh t) \cosh t \sinh 2R\beta t \cos 2R\alpha t \, dt,$$
$$D = \int_0^\infty K_1(2kR \sinh t) \cosh t \cosh 2R\beta t \sin 2R\alpha t \, dt. \quad \text{(C4)}$$

Note that for $\alpha = 0$, $A = D = 0$. The integrals in equation (C4) are truncated to an upper limit ϕ, where the value of ϕ is chosen as the limit of t for which $K_1(2kR \sinh t)$ can be generated in a computer. Choose

$$2kR \sinh \phi = 160. \quad \text{(C5)}$$

The integrals, from 0 to ϕ, were performed numerically, accurate to three significant figures, by the Extended Simpson's Rule (Abramowitz and Stegun 1965, p.886).

The error involved in the truncation of the integrals to the upper limit of ϕ can be estimated. Consider the integral, D. The error involved in integrating from 0 to ϕ is

$$\varepsilon = \left| \int_\phi^\infty K_1(2kR \sinh t) \cosh t \cosh 2R\beta t \sin 2R\alpha t \, dt \right|$$
$$< \int_\phi^\infty K_1(2kR \sinh t) \cosh t \cosh 2R\beta t \, dt. \quad \text{(C6)}$$

The errors involved in the truncation of the other integrals (A, B and C) are of the same order but less than that of D.

Since $\phi < t < \infty$ in equation (C6), we have, using condition (C5),

$$2kR \sinh t \geqslant 160. \quad \text{(C7)}$$

Using the large argument approximation (Watson 1968, p.202) for $K_1(2kR \sinh t)$, we have for equation (C6),

$$\varepsilon < \int_{\psi}^{\infty} \sqrt{\frac{\pi}{4kR \sinh t}}\, e^{-2kR \sinh t} \cosh t \cosh 2R\beta t \, dt,$$

$$< \int_{\psi}^{\infty} \sqrt{\frac{\pi}{2kR}}\, e^{-2kR \sinh t}\, e^{(2R\beta+\frac{1}{2})t} \, dt, \qquad (C8)$$

since

$$e^{x} > \cosh x, \qquad \frac{e^{x}}{2} > \sinh x. \qquad (C9)$$

If the condition

$$[2kR \cosh t - (2R\beta+\tfrac{1}{2})] \gg 1 \qquad (C10)$$

is satisfied for all $t \geqslant \psi$, then

$$\varepsilon < \int_{\psi}^{\infty} \sqrt{\frac{\pi}{2kR}}\, e^{-2kR\sinh t}\, e^{(2R\beta+\frac{1}{2})t} [2kR\cosh t-(2R\beta+\tfrac{1}{2})t]dt,$$

$$= \left| \sqrt{\frac{\pi}{2kR}} \left[e^{-2kR\sinh t}\, e^{(2R\beta+\frac{1}{2})t} \right]_{\psi}^{\infty} \right| \qquad (C11)$$

Hence

$$\varepsilon < \sqrt{\frac{\pi}{2kR}}\, e^{-2kR\sinh\psi}\, e^{(2R\beta+\frac{1}{2})\psi} \, . \qquad (C12)$$

Equations (C10) and (C12) provide an estimate of the error. For example, for $\beta/k = 1.0$ and $\lambda/R = 0.06$; equation (C10) is satisfied and (C12) gives $\varepsilon \approx 0.8 \times 10^{-6}$. This is the value of the integral from ψ to ∞. The value of the integral from 0 to ψ is greater than 10^{-2} in magnitude; hence the contribution of the integral (ψ to ∞) can be neglected in this case as it will not affect the three significant figures accuracy of the integral (0 to ψ). Similarly, for

$\beta/k = 1.25$ and $\lambda/R = 0.15$, $\varepsilon \approx 0.5 \times 10^{-6}$. The actual value of the integral (ψ to ∞) will be less than ε, because ε has been overestimated. The value of ε gives an estimate of the smallest value of λ/R for which (C3) can be used. This value is dependent on the value of β/k but can be taken to be about 0.1.

C2 Asymptotic Form for Small λ/R

The asymptotic form for equation (6.5) is derived by using the asymptotic forms (Watson 1968, sec. 13.7) for $[J_\nu^2(kR) + Y_\nu^2(kR)]$ and its derivative in equation (C1). From equation (C1):

$$\frac{j\zeta_1}{\zeta_0} = -\frac{j + \frac{1}{2kR}\sum_{m=0}^{\infty}\frac{\{1.3.5\ldots(2m+1)\}\ (\nu,m)}{2^m(kR)^{2m}}}{\sum_{m=0}^{\infty}\frac{\{1.3.5\ldots(2m-1)\}\ (\nu,m)}{2^m(kR)^{2m}}} \qquad \text{(C13)}$$

$$(\nu,m) = \frac{\Gamma(\nu+m+\frac{1}{2})}{m!\,\Gamma(\nu-m+\frac{1}{2})}\ , \qquad \text{(C14)}$$

and Γ denotes the gamma functions. Equation (C13) is used when λ/R is small (i.e. when kR is large).

It is found that the results of equations (C2) and (C13) agree with each other to three significant figures when $(\lambda/R) = 0.1$.

REFERENCES

Abaka, E. and Baier, W. (1969), "TE and TM modes in transmission lines with circular outer conductor and eccentric circular inner conductor", Electron. Lett., 5, 251-252.

Abramowitz, M. and Stegun, I.A. (1965), Handbook of Mathematical Functions, Dover, New York.

Ahmed, S. and Daly, P. (1969a), "Finite-element methods for inhomogeneous waveguides", Proc. IEE (London), 116, 1661-1664.

Ahmed, S. and Daly, P. (1969b), "Waveguide solutions by the finite-element method", Radio Electron. Engr., 38, 217-223.

Amemiya, Y. (1965), "Surface wave transmission lines", Electronics and Comm. in Japan, 48, No. 12, 162-176.

Andreasen, M.G. (1965), "Scattering from bodies of revolution", IEEE Trans., AP-13, 303-310.

Arlett, P.L., Bahrani, A.K. and Zienkiewicz, O.C. (1968), "Application of finite-elements to the solution of Helmholtz's equation", Proc. IEE (London), 115, 1762-1766.

Audeh, N.F. and Fuller, J.A. (1968), "A study of uniform waveguides of arbitrary cross-sections by the point-matching method", University of Alabama Research Inst., Alabama, UARI Research Report No. 56.

Baier, W. (1969), "Berechnung der grenzfrequenzen inhomogen gefüllter rechteckhohlleiter und der bei diesen frequenzen auftretended feldzustände", Arch. Elek. Ubertragung, 23, 237-241.

Baier, W. (1970), "Waves and evanescent fields in rectangular waveguides filled with a transversely inhomogeneous dielectric", IEEE Trans., MTT-18, 696-705.

Barlow, H.M. (1959), "Surface waves supported by cylindrical surfaces", IRE Trans., AP-7, S147-S158.

Barlow, H.E.M. (1964), "Waveguide survey", Electronics and Power, 10, 332-338.

Barlow, H.E.M. (1966), "Field distribution at bends in circular H_{on} and cylindrical surface waveguides", Proc. IEE (London), 113, 1913-1919.

Barlow, H.M. and Brown, J. (1962), Radio Surface Waves, OUP, London.

Barlow, H.M. and Cullen, A.L. (1950), Microwave measurements, Constable, London.

Barlow, H.M. and Cullen, A.L. (1953), "Surface waves", Proc. IEE, 108, Pt III, 329-347.

Bates, R.H.T. (1967), "The point-matching method for interior and exterior two-dimensional boundary value problems", IEEE Trans., MTT-15, 185-187.

Bates, R.H.T. (1968), "Modal expansions for electromagnetic scattering from perfectly conducting cylinders of arbitrary cross-section", Proc. IEE (London), 115, 1443-1445.

Bates, R.H.T. (1969a), "The Rayleigh hypothesis, the extended-boundary-condition and point matching", Electron. Lett., 5, 654-655.

Bates, R.H.T. (1969b), "The theory of the point-matching method for perfectly conducting waveguides and transmission lines", IEEE Trans., MTT-17, 294-301.

Bates, R.H.T. (1970), "Polarization source formulation of electromagnetism and the penetrable wedge problem", Lab. of Electromagnetic Theory, Technical Univ. of Denmark, Lyngby, Report NB52.

Bates, R.H.T. and Ng, F.L. (1971), "Contributions to the theory of the azimuthal surface wave", Alta Frequenza, 40, 658-666.

Beaubien, M.H. and Wexler, A. (1968), "An accurate finite-difference method for higher order waveguide modes", IEEE Trans., MTT-16, 1007-1017.

Beaubien, M.J. and Wexler, A. (1970), "Unequal-arm finite-difference operators in the positive-definite successive overrelaxation (PDSOR) Algorithm", IEEE Trans., MTT-18, 1132-1149.

Beaubien, M. and Wexler, A. (1971), "Higher waveguide modes by positive definite SOR", IEEE Trans., MTT-19 839-840.

Bochner, S. and Martin, W.T. (1948), General Complex Variables, Princeton University Press, Princeton.

Bolle, D.M. and Fye, D.M. (1971), "Application of point-matching method to scattering from quadrilateral cylinders", Electron. Lett., 7, 577-579.

Bulley, R.M. (1970), "Analysis of the arbitrary shaped waveguide by polynomial approximation", IEEE Trans., MTT-18, 1022-1028.

Bulley, R.M. and Davies, J.B. (1969), "Computation of approximate polynomial solutions to TE modes in an arbitrary shaped waveguide", IEEE Trans., MTT-17, 440-446.

Burrows, M.L. (1969a), "Equivalence of the Rayleigh solution and the extended-boundary-condition solution for scattering problems", Electron. Lett., 5, 277-278.

Burrows, M.L. (1969b), "Example of the generalized function validity of the Rayleigh hypothesis", Electron. Lett., 5, 694-695.

Chatterjee, S.K. and Chatterjee, R. (1965), "Dielectric loaded waveguides - a review of theoretical solutions", Radio and Electron. Engr., 30, 145-160, 195-205, 259-288, 353-364.

Chopra, I. and Durvasula, S. (1971), "Vibration of simply-supported trapezoidal plates. Part I. Symmetric trapezoids", J. Sound and Vibration, 19, 379-392.

Chopra, I. and Durvasula, S. (1972), "Vibration of simply supported trapezoidal plates. Part II. Unsymmetric trapezoids", J. Sound Vib., 20, 125-134.

Chu, L.J. (1938), "Electromagnetic waves in elliptic hollow pipes of metal", J. Appl. Phys., 9, 583-591.

Clarricoats, P.J.B. (1961), "Propagation along unbounded and bounded dielectric rods Parts 1 and 2", Proc. IEE, 108C, 170-186.

Cohn, S.B. (1947), "Properties of ridge wave guide", Proc. IRE, 35, 783-788.

Collins, J.H. and Daly, P. (1963), "Calculations for guided electromagnetic waves using finite-difference methods", J. Electr. and Control, 14, 361-380.

Collins, J.H. and Daly, P. (1964), "Orthogonal mode theory of single ridge waveguides", J. Electr. and Control, 17, 121-129.

Computers and Automation (1969), "Characteristics of general purpose digital computers", 15th Annual edition of Directory, 18, n.7, also (1970), 19, n. 6B.

Conway, H.D. (1960), "The approximate analysis of certain boundary value problems", J. Appl. Mech., 27, 275-277.

Conway, H.D. (1961), "Bending, buckling and flexural vibration of simply supported polygon plates by point matching", J. Appl. Mech., 28, 288-291.

Csendes, Z.J. and Silvester, P. (1970), "Numerical solution of dielectric loaded waveguides I, finite-element analysis", IEEE Trans., MTT-18, 1124-1131.

Csendes, Z.J. and Silvester, P. (1971), "Numerical solution of dielectric loaded waveguides: II - modal approximation theory", IEEE Trans., MTT-19, 504-509.

Cullen, A.L. and Özkan, O. (1971), "Point-matching technique for rectangular-cross-section dielectric rod", Electron. Lett., 7, 497-499.

Davies, J.B. (1972), "A review of methods for numerical solution of the hollow waveguide problem", Proc. IEE (London), 119, 33-37.

Davies, J.B. and Kretzschmar, J.G. (1972), "Analysis of hollow elliptical waveguides by polygon approximation", Proc. IEE (London), in press.

Davies, J.B. and Muilwyk, C.A. (1966), "Numerical solution of uniform hollow waveguides with boundaries of arbitrary shape", Proc. IEEE, 113, 277-284.

Davies, J.B. and Nagenthiram, P. (1971), "Irregular fields, nonconvex shapes and the point-matching method for hollow waveguides", Electron. Lett., 7, 401-404.

Davis, P.J. and Rabinowitz, P. (1967), Numerical Integration, Blaisdell, Massachusetts.

Dwight, H.B. (1948), "Tables of roots for natural frequencies in coaxial cavities", Jour. Math. Phys., 27, 84-89.

Elliott, R.S. (1955), "Azimuthal surface waves on circular cylinders", J. Appl. Phys., 26, 368-376.

English, W.J. (1971a), "Vector variational solutions of inhomogeneously loaded cylindrical waveguide structures", IEEE Trans., MTT-19, 9-18.

English, W.J. (1971b), "A computer-implemented vector variational solution of loaded rectangular waveguides", SIAM J. Appl. Math., 21, 461-469.

Fifer, S. (1961), Analogue Computation, Vol. III, McGraw-Hill, New York.

Forsythe, G.E. and Wasow, W.R. (1960), Finite-difference Methods for Partial Differential Equations, John Wiley, New York.

Fox, L. (1971), "Some experiments with singularities in linear elliptic partial differential equations", Proc. Roy. Soc. Lond., A.323, 179-190.

Fuller, J.A. and Audeh, N.F. (1969), "The point-matching solution of uniform non-symmetric waveguides", IEEE Trans., MTT-17, 114-115.

Gal'chenko, N.A. and Mikhalevksiy, V.S. (1970), "Application of Schwartz's method to the calculation of the electrical parameters of single ridge and double ridge waveguides", Radio Engrg. Electron. Phys., 15, 38-44.

Goodwin, E.T. (1961), Modern Computing Methods, HMSO, London.

Goubau, G. (1950), "Surface waves and their application to transmission lines", J. Appl. Phys., 21, 1119-1128.

Goubau, G. (1951), "Single-conductor surface-wave transmission lines", Proc. IRE, 39, 619-624.

Goubau, G. and Sharp, C.E. (1957), "Investigations with a model surface-wave transmission line", IRE Trans., AP-5, 222-227.

Green, H.E. (1965), "The numerical solution of some important transmission-line problems", IEEE Trans., MTT-13, 676-692.

Gruner, L. (1967), "Higher-order modes in rectangular coaxial waveguides", IEEE Trans., MTT-15, 483-485.

Hammersley, J.M. and Handscomb, D.C. (1964), Monte Carlo Methods, Methuen, London.

Harrington, R.F. (1961), Time-Harmonic Electromagnetic Fields, McGraw-Hill, New York,

Harrington, R.F. (1965), "On the calculation of scattering by conducting cylinders", IEEE Trans., AP-13, 812-813.

Harrington, R.F. (1967), "Matrix methods for field problems", Proc. IEEE, 55, 136-149.

Harrington, R.F. (1968), Field Computation by Moment Methods, MacMillan, New York.

Harvey, A.F. (1960), "Periodic and guiding structures at microwave frequencies", IRE Trans., MTT-8, 30-61.

Hashimoto, M. and Fujisawa, K. (1970), "Considerations on matrix methods and estimation of their errors", IEEE Trans., MTT-18, 352-359.

Hopfer, S. (1955), "The design of ridged waveguides", IRE Trans., MTT-3, 20-29.

Horiuchi, K. (1953), "Surface wave propagation over a coated conductor with small cylindrical curvature in direction of travel", J. Appl. Phys., 24, 961-962.

Horiuchi, K., Nakamura, J., Nago, A., Inada, K. and Hirai, T. (1968), "Parabolic cylinder waveguides", Electron. and Comm. in Japan, 51-B, 69-77.

Hu, A.Y. and Ishimaru, A. (1961), "The dominant cutoff wavelength of a lunar line", IRE Trans., MTT-9, 552-556.

Hu, A.Y. and Ishimaru, A. (1963), "Attenuation constant of lunar line and T-septate lunar line", IEEE Trans., MTT-11, 243-250.

Hu Wang, A.Y. (1964), "Dominant cut-off wavelength of a T-septate lunar line", Proc. IEE (London), 111, 1262-1266.

Hunter, J.D. (1972), "The surface current density on perfectly conducting polygonal cylinders", Can. J. Phys., in press.

Hunter, J.D. and Bates, R.H.T. (1970), "Computation of scattering from a class of bodies of unrestricted size", J. Engrg. Math., 4, 119-128.

Hunter, J.D. and Bates, R.H.T. (1972), "Secondary diffraction from close edges on perfectly conducting bodies", Int. J. Electronics, in press.

IBM (1968), System 360 Scientific Subroutine Package H20-0205-3, Technical Publications Dept, New York.

Imbriale, W.A. and Mittra, R. (1970), "The two-dimensional inverse scattering problem", IEEE Trans., AP-18, 633-642.

Jones, D.S. (1964), The Theory of Electromagnetism, Pergamon, New York.

Jordan, E.C. and Balmain, K.G. (1968), Electromagnetic Waves and Radiating Systems, 2nd Ed., Prentice-Hall, New Jersey.

Kantorovitch, L.V. and Krylov, V.I. (1958), Approximate Methods of Higher Analysis, P. Noordhoff, The Netherlands.

King, M.J. and Wiltse, J.C. (1962), "Surface-wave propagation on coated or uncoated metal wires at millimeter wavelengths", IRE Trans., AP-10, 246-254.

Konrad, A. and Silvester, P. (1971), "Scalar finite-element program package for two-dimensional field problems", IEEE Trans., MTT-19, 952-954.

Kretzschmar, J.G. (1970), "Wave propagation in hollow conducting elliptical waveguides", IEEE Trans., MTT-18, 547-554.

Kretzschmar, J.G. (1971), "Field configuration of the TM_{C01} mode in an elliptical waveguide", Proc. IEE (London), 118, 1187-1189.

Kron, G. (1944), "Equivalent circuit of the field equations of Maxwell", Proc. IRE, 32, 289-299.

Larsen, T. (1969), "Superelliptic broadband transition between rectangular and circular waveguides", Proc. European Microwave Conference, IEE Conference Publication No. 58, 277-280.

Laura, P.A. (1964), "On the determination of the natural frequency of a star-shaped membrane", J. Royal Aeronaut. Soc., 68, 274-275.

Laura, P.A. (1965), "Determination of cutoff frequencies of waveguides with arbitrary cross-sections by point matching", Proc. IEEE, 53, 1660-1661.

Laura, P.A. (1966a), "A simple method for the determination of cutoff frequencies of waveguides with arbitrary cross sections", Proc. IEEE, 54, 1495-1497.

Laura, P.A. (1966b), "Application of the point-matching method in waveguide problems", IEEE Trans., MTT-14, 251.

Laura, P.A. (1966c), "Conformal mapping and the determination of cutoff frequencies of waveguides with arbitrary cross section", Proc. IEEE, 54, 1078-1080.

Laura, P.A. (1967), "Calculation of eigenvalues for uniform fluid waveguides with complicated cross sections", J. Acoust. Soc. Amer., 42, 21-26.

Laura, P.A. and Faulstich, A.J., Jun. (1967), "Cutoff frequencies of uniform waveguides of regular polygonal cross sections", Proc. IEEE, 55, 410-411.

Laura, P.A., Romanelli, E. and Maurizi, M.H. (1972), "On the analysis of waveguides of doubly-connected cross-section by the method of conformal mapping", J. Sound Vib., 20, 27-38.

Lawson, J.D. (1966), "Guided surface waves and the radiation from charges moving in curved paths", Amer. Jour. Phys., 34, 601-605.

Lee, S.W. and Jones, W.R. (1971), "Surface waves on two-dimensional corrugated structures", Radio Science, 6, 811-818.

Lewin, L. (1970), "On the restricted validity of point-matching techniques", IEEE Trans., MTT-18, 1041-1047.

Mei, K.K. and van Bladel, J.G. (1963), "Scattering by perfectly conducting rectangular cylinder", IEEE Trans., AP-11, 185-192.

Meinke, H.H. (1963), "A survey on the use of conformal mapping for solving wave-field problems", in Jordan, E.C. (ed.), Symposium on Electromagnetic Theory and Antennas, Pergamon, New York, 1113-1124.

Meinke, H.H. and Baier, W. (1968), "The characteristics of waveguides with general cross-section", NTZ-Comm. Journal 7, 1-8.

Meinke, H.H., Lange, K.P. and Ruger, J.F. (1963), "TE and TM waves in waveguides of very general cross-section", Proc. IEEE, 51, 1436-1443.

Millar, R.F. (1969), "On the Rayleigh assumption in scattering by a periodic surface, Pts I and II", Proc. Camb. Phil. Soc., 65, 773-791, and (1971), 69, 217-225.

Millar, R.F. (1970), "The location of singularities of two-dimensional harmonic functions", SIAM J. Math. Anal., 1, 333-344 and 345-353.

Millar, R.F. (1971), "Singularities of two-dimensional exterior solutions of the Helmholtz equation", Proc. Camb. Phil. Soc., 69, 175-188.

Millar, R.F. and Bates, R.H.T. (1970), "On the legitimacy of an assumption underlying the point matching method", IEEE Trans., MTT-18, 325-327.

Millar, R.F. and Burrows, M.L. (1969), "Rayleigh hypothesis in scattering problems", Electron. Lett., 5, 416-418.

Mittra, R. and Wilton, D.R. (1969), "A numerical approach to the determination of electromagnetic scattering characteristics of perfect conductors", Proc. IEEE, 57, 2064-2065.

Montgomery, J.P. (1971), "On the complete eigenvalue solution of ridged waveguides", IEEE Trans., MTT-19, 547-555.

Morse, P.M. and Feshbach, H. (1953), Methods of Theoretical Physics, McGraw-Hill, New York.

Motz, H. (1946), "The treatment of singularities of partial differential equations by relaxation methods", Quart. Appl. Math., 4, 371-377.

Ng, F.L. and Bates, R.H.T. (1972), "Null field method for waveguides of arbitrary cross section", IEEE Trans., Microwave Theory Tech., in press.

Ojalvo, I.U. and Linzer, F.D. (1965), "Improved point-matching techniques", Quart. J. Mech. Appl. Math., 18, Pt. 1, 41-56.

Pontoppidan, K. (1969), "Numerical solution of waveguide problems using finite difference methods", Proc. European Microwave Conference, IEE Conference Publication No. 58, 99-102.

Pyle, J.R. (1966), "The cutoff wavelength of the TE10 mode in ridge rectangular waveguide of any aspect ratio", IEEE Trans., MTT-14, 175-183.

Pyle, J.R. and Angley, R.J. (1964), "Cutoff wavelengths of waveguides with unusual cross-sections", IEEE Trans., MTT-12, 556-557.

Rayevskiy, S.B. and Smorgonskiy, V.Ya. (1970), "Method of computation of critical frequencies of an elliptical waveguide", Radio Engng. and Electron. Physics, 15, 1702-1705.

Read, F.H. (1969), "Accurate calculations of double-aperture electrostatic immersion lenses", J. Sci. Instruments (J. Phys. E), 2, Series 2, 165-169.

Reid, J.K. and Walsh, J.E. (1965), "An elliptic eigenvalue problem for a reentrant region", J. Soc. Indust. Appl. Math., 13, 837-850.

Richards, D.J. and Wexler, A. (1972), "Finite elements within curved boundary", IEEE Trans., Microwave Theory Tech., in press.

Richmond, J.H. (1965), "Scattering by a dielectric cylinder of arbitrary cross section shape", IEEE Trans., AP-13, 334-341.

Richmond, J.H. (1966), "TE scattering by a dielectric cylinder of arbitrary cross section shape", IEEE Trans., AP-14, 460-464.

Royer, G.M. (1971), "A Monte Carlo procedure for potential theory problems", IEEE Trans., MTT-19, 813-818.

Sato, R., Chiba, J., Park, S., Iwata, S., Koide, R. and Miyamoto, S. (1964), "Losses due to bends in surface-wave transmission lines", Electronics and Comm. in Japan, 47, No.3, 50-53.

Schelkunoff, S.A. (1943), Electromagnetic Waves, D. van Nostrand, New York.

Schlosser, W. (1968), "Determination of normal modes of waveguides with arbitrary boundary", in Proc. of 3rd Colloquium on Microwave Communication, Akademiai Kiado, Budapest, 449-455.

Schlosser, W. and Unger, H.G. (1966), "Partially filled waveguides and surface waveguides of rectangular cross-section", in Advances in Microwaves vol. 1, L. Young editor, Academic Press, 319-387.

Silver, S. (1965), Microwave Antenna Theory and Design, Dover, New York.

Silvester, P. (1969a), "A general high-order finite-element waveguide analysis program", IEEE Trans., MTT-17, 204-210.

Silvester, P. (1969b), "Finite-element solution of homogeneous waveguide problems", Alta Frequeza (Numero Speciale), 38, 313-317.

Silvester, P. (1969c), "High-order finite element waveguide analysis", IEEE Trans., MTT-17, 651.

Silvester, P. (1969d), "High-order polynomial triangular finite elements for potential problems", Int. J. Engrg. Sci., 7, 849-861.

Silvester, P. (1970a), "Biharmonic operators for the waveguide proglem", IEEE Trans., MTT-18, 63-64.

Silvester, P. (1970b), "Numerical formation of finite-difference operators", IEEE Trans., MTT-18, 740-743.

Sinnott, D.H. (1968), "The computation of waveguide fields and cutoff frequencies using finite difference techniques", Aust. Defence Scientific Service, Tech. Note, Pad 158.

Sinnott, D.H. (1970), "The application of finite difference techniques to electromagnetic problems", Elect. Engng. Trans. (Australia), EE-6, 6-11.

Spielman, B.E. and Harrington, R.F. (1972), "Waveguides of arbitrary cross-section by solution of a non-linear integral eigenvalue equation", IEEE Trans., Microwave Theory Tech., in press.

Steele, C.W. (1968), "Numerical computation of electric and magnetic fields in a uniform waveguide of arbitrary cross section", J. Comput. Phys., 3, 148-153.

Thomas, D.T. (1969), "Functional approximations for solving boundary value problems by computer", IEEE Trans., MTT-17, 447-454.

Thorley, W.D. (1969), "An experimental investigation into the losses at bends in surface wave transmission lines", M.E. Thesis, University of Canterbury, New Zealand.

Tischer, F.J. (1963), "Conformal mapping in waveguide considerations", Proc. IEEE, 51, 1050-1051.

Tsandoulas, G.N. and Ince, W.J. (1971), "Modal inversion in circular waveguides - I: theory and phenomenology", IEEE Trans., MTT-19, 386-392.

Uptain, S.T. and Audeh, N.F. (1966), "Transverse resonance solution of uniform trapezoidal waveguides", IEEE Trans., MTT-14, 158.

Valenzuela, G.R. (1961), "The cutoff wavelength of composite waveguides", IRE Trans., MTT-9, 363-364.

Veselov, G.I. and Gaydar, V.I. (1970), "Analysis of a circular waveguide with an internal cross-shaped conductor", Radio Engng., 25, 147-149.

Veselov, G.I. and Platonov, N.I. (1969), "Analysis of a 'corner' waveguide", Radio Engng., 24, 124-126.

Veselov, G.I. and Semenov, S.G. (1970), "Theory of circular waveguide with eccentrically placed metallic conductor", Radio Engng. and Electron. Physics, 15, 687-690.

Vine, J. (1966), "Impedance networks" in Vitkovitch, D. (Ed.), Field Analysis: Experimental and Computational Methods, Van Nostrand, chap. 7.

Wait, J.R. and Spies, K.P. (1968), "Radio propagation over a cylindrical hill including the effect of a surmounted obstacle", IEEE Trans., AP-16, 700-705.

Wasow, W. (1951), "Random walks and the eigenvalues of elliptic differential equations", J. Res. Nat. Bur. Stand., 46, 65-73.

Waterman, P.C. (1965), "Matrix formulation of electromagnetic scattering", Proc. IEEE, 53, 805-812.

Watson, G.N. (1968), A Treatise on the Theory of Bessel Functions, 2nd ed., Cambridge, New York.

Wexler, A. (1969), "Computation of electromagnetic fields", IEEE Trans., MTT-17, 416-439.

Whinnery, J.R. and Ramo, S. (1944), "A new approach to the solution of high frequency field problems", Proc. IRE, 32, 284-288.

Whiteman, J.R. (1971), "Finite-difference techniques for a harmonic mixed boundary problem having a reentrant boundary", Proc. Roy. Soc. Lond., A.323, 271-276.

Whiting, K.B. (1968), "A treatment for boundary singularities in finite difference solutions of Laplace's equation", IEEE Trans., MTT-16, 889-891.

Williams, W., Parke, N.G., Moran, D.A., and Sherman, C.H. (1964), "Acoustic radiation from a finite cylinder", J. Acoust. Soc. Amer., 36, 2316-2322.

Yabe, H. and Kakukawa, T. (1968), "On the eigenvalue of a G-line and its strict solution", Electronics and Comm. in Japan, 51-A, 28-35.

Yee, H.Y., (1966), "On determination of cutoff frequencies of waveguides with arbitrary cross section", Proc. IEEE, 54, 64.

Yee, H.Y. and Audeh, N.F. (1965), "Uniform waveguides with arbitrary cross section considered by the point matching method", IEEE Trans., MTT-13, 847-851.

Yee, H.Y. and Audeh, N.F. (1966a), "Attenuation constants of waveguides with general cross-sections", IEEE Trans., MTT-14, 252-253.

Yee, H.Y. and Audeh, N.F. (1966b), "Cutoff frequencies of eccentric waveguides", IEEE Trans., MTT-14, 487-493.

Zagrodzinski, J. (1968), "Electromagnetic fields in parabolic waveguides and resonators", in Proc. of 3rd Colloquium on Microwave Communication, Akademiai Kiado, Budapest, 457-465.

Zienkiewicz, O.C. and Cheung, Y.K. (1967), The Finite-Element Method in Continuous Structural Mechanics, McGraw-Hill, New York.